

SURFACE FORCES APPARATUS

USER'S MANUAL

for

SFA 3 and SFA 2000

with Attachments

Updated: 1 Jan 2013

CONTENTS

Applies to
SFA3 SFA2000

Introduction to the Surface Forces Apparatus (SFA) technique	3	yes	yes
Setting up and equipping an SFA laboratory (SFA lab), Table 1: list of required items.....	5	yes	yes
Description of UNITS and PARTS of the SFA 3, the SFA 3 brochure.....	16	yes	some
Handling the SFA 3: cleaning and assembly (Basic Unit only)	51	yes	some
Original publication of the SFA 3 (in <i>J. Materials Research</i> , 1990).....	61	yes	no
Preparation of surfaces for force measurements or interferometric experiments.....	70	yes	yes
Installation of surfaces into the SFA 3.....	80	yes	some
Initial observation of surfaces with Newton's rings.....	83	yes	yes
Observation of surfaces with FECO fringes, initial measurements and calibrations	84	yes	yes
Filling the SFA chamber with liquid.....	87	yes	yes
General operating procedures	88	yes	yes
Distance, surface shape (deformations) and other measurements with FECO fringes.....	90	yes	yes
Measuring static (equilibrium) forces	102	yes	yes
Measuring dynamic (viscous, lubrication) forces interactions (with references).....	105	yes	yes
Calibrations & analyzing the results	106	yes	yes
Miscellaneous hints and troubleshooting; servicing your SFA	111	yes	yes
Syringe injection unit	117	yes	yes
Friction device.....	118	yes	some
Bimorph slider.....	122	yes	yes
Bimorph vibrator.....	133	yes	yes
Other (optional) attachments and customized modifications.....	135	yes	yes
Further info on the SFA 3 and attachments, performance specs, Table II: list of parts	138	yes	some
References to SFA technology and literature on force measurements, videos.....	144	yes	yes
Example of an actual SFA experiment	147	yes	yes
Force-measuring capabilities of SFA and AFM compared	159	yes	yes
Introduction to the SFA 2000: The SFA 2000 brochure.....	162	no	yes
Recent advances in the SFA technique (mainly SFA 2000 and attachments).....	153	no	yes
Setting up and equipping an SFA laboratory	182	yes	yes
SFA 2000 Basic Unit and Attachments	188	no	yes
SFA 2000 – how it works	211	no	yes
Assembly of the SFA 2000	212	no	yes
Using the SFA 2000 and its attachments, cleaning & maintenance	216	no	yes
Some new, recently introduced attachments or modifications	220	yes	yes

INTRODUCTION TO THE SFA TECHNIQUE

Surface Forces Apparatuses (SFAs) are research instruments for directly measuring the static and dynamic forces between surfaces, and for studying other interfacial and thin film phenomena at the molecular level. Although useful for both basic and applied research, the SFA is essentially a research tool, intended for investigations of new phenomena and the unexpected, rather than for routine measurements. To this end, SFAs have been designed to be highly versatile, allowing for improvisation and the ability to choose different measuring techniques during experiments.

What it does

The SFA measures the forces between two surfaces in vapors or liquids with a sensitivity of a few millidynes (10 nN) and a distance resolution of 1Å (0.1 nm). It can also be used to measure the refractive index of the medium between the surfaces, molecular orientations in thin films (under certain conditions), adsorption isotherms, capillary condensation, surface deformations arising from surface forces, dynamic interactions such as viscoelastic and frictional forces, and other time-dependent phenomena in real time. Though mica surfaces are the primary surfaces used for these measurements, it is possible to deposit or coat these surfaces with surfactants, lipids, polymers, proteins, metals, metal oxides, silica, etc., so as to alter the nature and chemistry of the interacting surfaces while keeping them smooth by virtue of the molecularly smooth mica substrate surface.

How it works

Figure 1 shows an assembled *basic SFA 3 apparatus* ready for use. The shapes of the interacting surfaces and the absolute separation between them are measured by analyzing the optical interference fringes produced when white light passes normally through the two surfaces, described later. The distance between the surfaces can be controlled over a range of 5 mm with a resolution of 1Å by a four-stage mechanism of increasing sensitivity. The stiffness of the *force-measuring spring* can be adjusted during experiments by moving a dove-tailed clamp along the length of the spring. This enables forces of greatly differing magnitudes to be measured. Dynamic measurements are conducted with surfaces either in normal motion by vibrating the piezoelectric crystal supporting the upper surface, or by shearing the two surfaces laterally using one of the *friction attachments* described later.

Additional features

The SFA 3 and SFA 2000 employ similar techniques to those used in earlier SFAs (the SFA Mk 1 and 2), but they are easier to operate and are generally more user-friendly. The first three stages of the four-stage distance controls allow for rapid manual or motorized control of surface separation to within 10 Å (1 nm), with the final sub Ångstrom control been done via a piezo-crystals. All four distance controls have been specially designed to produce linear displacements of the surfaces without backlash (there are no moving shafts or sliding dovetails in any of the distance control mechanisms – only springs). The SFA 3 and 2000 are also more robust, less susceptible to thermal drifts, easier to clean, and (with additional bathing cup attachments) require smaller quantities of liquid than conventional SFAs. A number of facilities that appeared as accessories in earlier models are now part of the Basic Unit, and new attachments allow for the measurement of (dynamic) friction, lubrication and viscoelastic forces over a large range of shear rates and sliding speeds, for simultaneous fluorescence and confocal imaging, (electro)chemical reactions, and other interfacial phenomena.

The SFA 3 and SFA 2000

This manual first describes the SFA 3 as well as how to set up and conduct SFA experiments in general, then the SFA 2000 and more recent advances and developments.

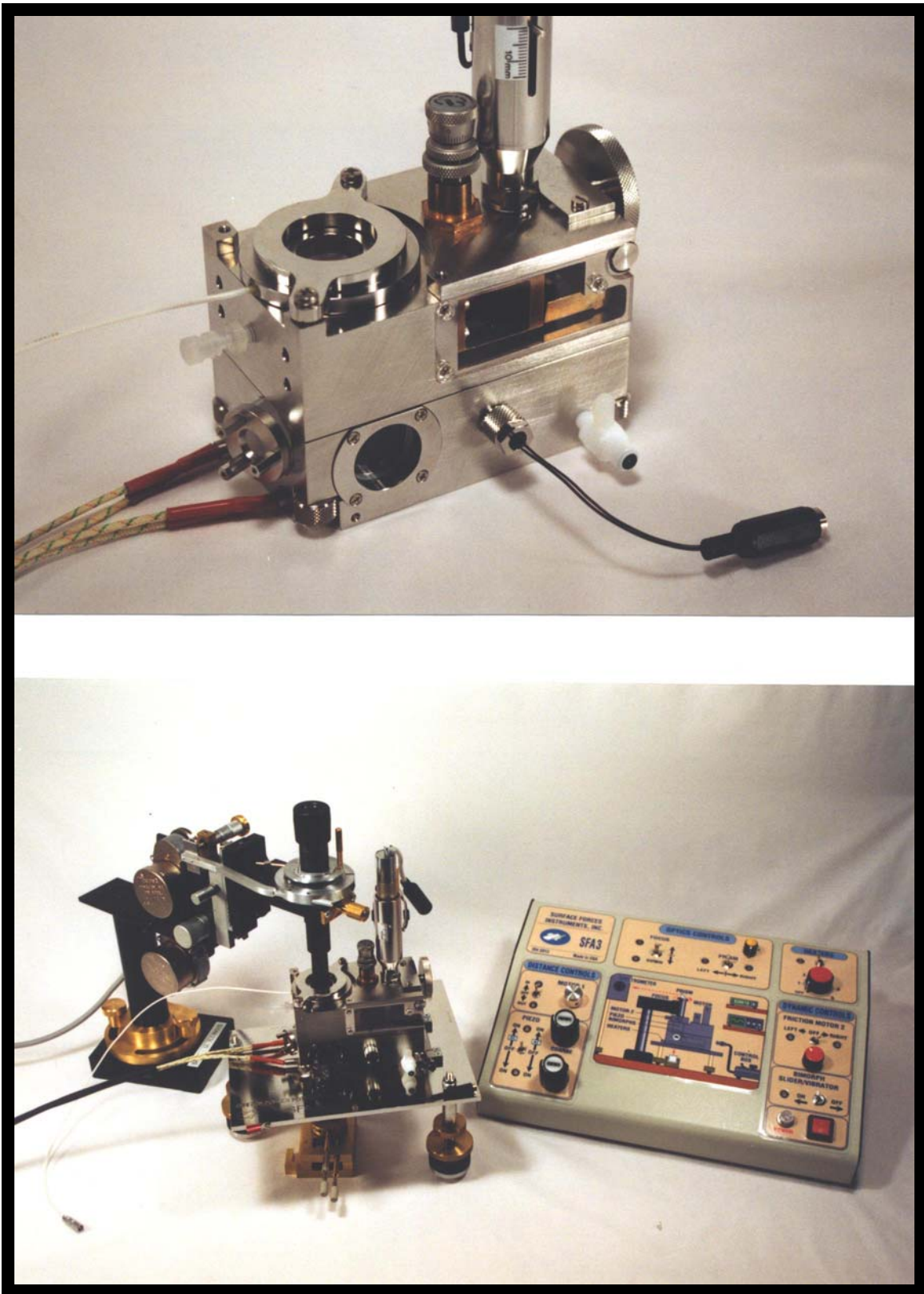


Figure 1. Surface Forces Apparatus 3 (top)
with Optics Stand, Mirror and Control Box (bottom)

SETTING UP AND EQUIPPING A SURFACE FORCES MEASUREMENT LABORATORY

This section is focused on the SFA 3, but most of it also applies to the SFA 2000.

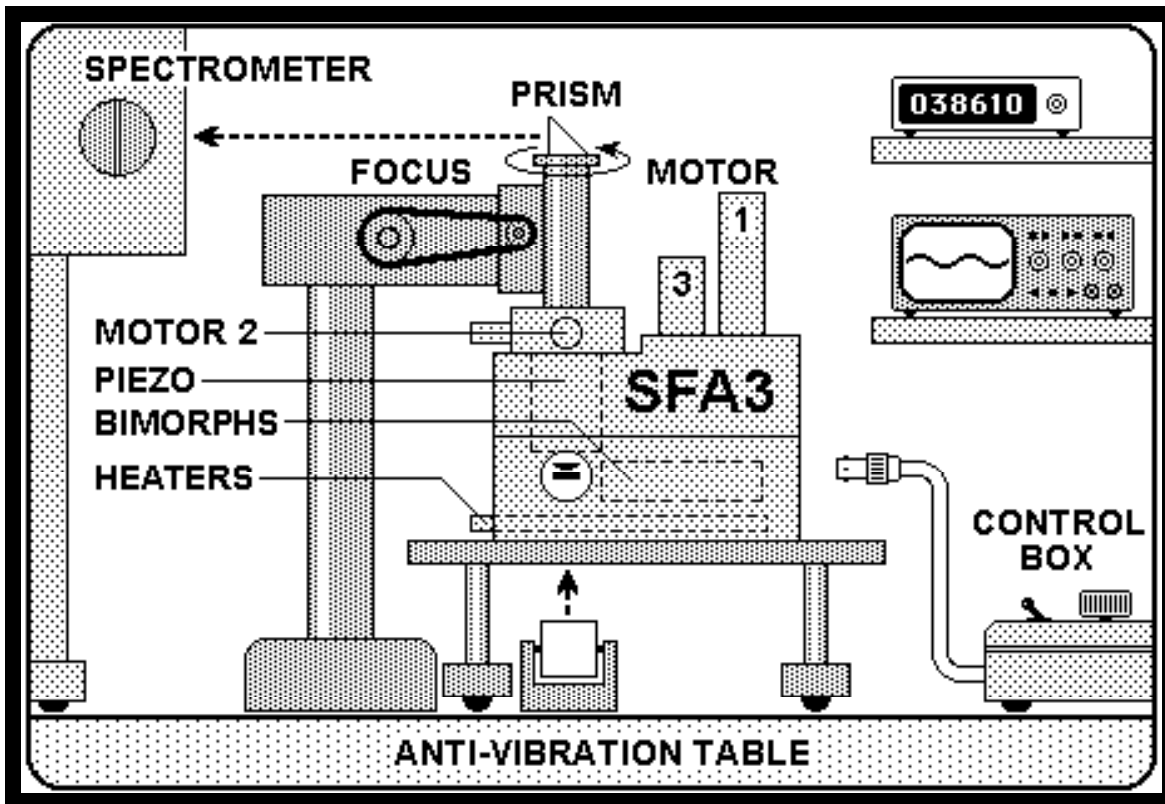


Figure 2. Schematic of an SFA 3 setup, also showing those parts that are controlled by the CONTROL BOX. Recommended horizontal distance from prism to spectrometer entrance slit: ~50 cm. Recommended vertical distance from prism to table top: ~30 cm. Similar dimensions apply to the SFA 2000.

IMPORTANT CONSIDERATIONS IN PLANNING AN SFA LABORATORY

Figure 3 shows a suitable layout for a small surface forces laboratory, indicating convenient locations for a WET LAB (for liquid purification, solvent distillation, etc.) an ASSEMBLY ROOM (for assembling and cleaning the apparatus) and one DARK ROOM (for performing experiments). Ideally, the laboratory should be located in a basement or ground floor – well away from vibration-producing machinery such as large pumps or air-conditioning units. The walls, furniture and floor should never be coated or cleaned with oil-based polishes that give off surface active contaminants into the atmosphere (these can usually be smelled if present). All laboratory surfaces, including floors and work benches, should be cleaned with warm water only. The dark room(s) should be thermostatically controllable to $\pm 0.1^{\circ}\text{C}$, if possible, and the thermostating air-conditioning or air-ducting system should not be connected to other laboratories so as not to introduce air-borne contamination into the lab atmosphere. Ideally, the air pressure of the experimental rooms should be slightly higher than of the adjoining rooms, ensuring a steady flow of (clean and thermostatted) air from that room outwards.

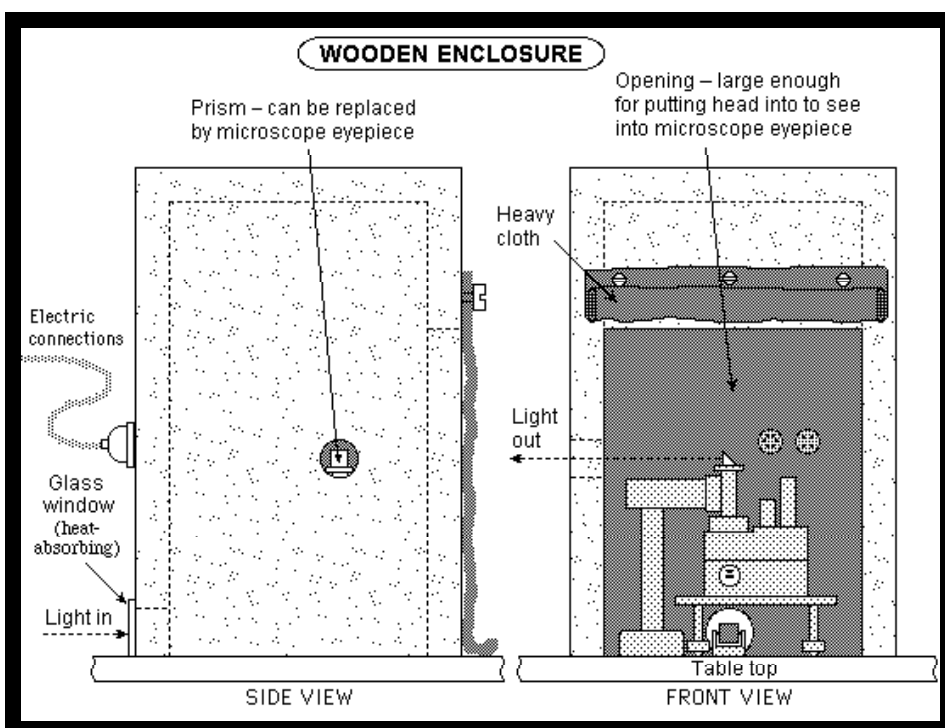
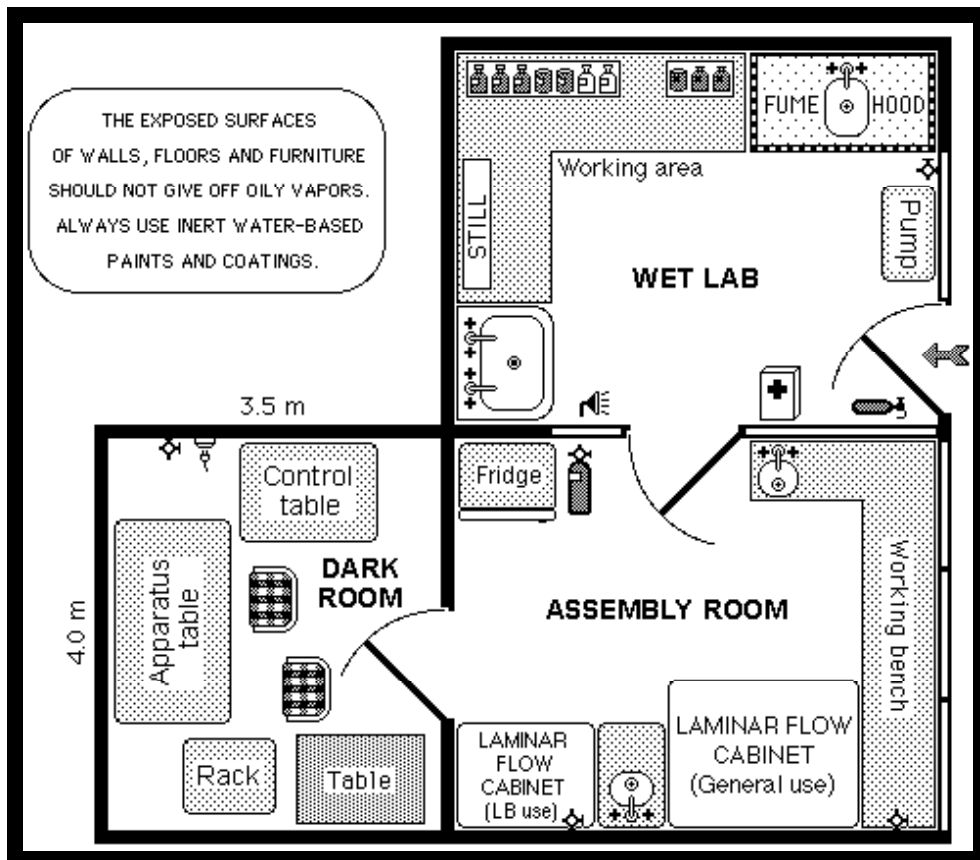


Figure 3. Top: Small self-contained surface forces laboratory. Additional experimental rooms (dark rooms) may be added at a later date. Bottom: Apparatus Housing. See pages 182-188 for further details.

Recommended laboratory hardware and fittings (see Table I on page 11 for complete list, and Table II on page 139 for further details on individual parts and components)

Your SFA3 package should arrive in a condition ready for immediate use in experiments – all necessary apparatus parts, assembly tools, electrical items and cables being provided with your unit (see lists on pages 7-10). However, a number of additional laboratory hardware items (not provided in the package) are needed for carrying out experiments. These are described in the following paragraphs (essential items are underlined). A full list of items is given in Table I below.

The following major laboratory hardware items and facilities are recommended for most routine experiments, some of which are shown in Figure 3: Work benches with sinks, tables and chairs. Storage cabinets. Clean inert gas supply outlets in each room (such as clean, dry nitrogen gas from boil off source, not cylinders). **Laminar flow cabinet(s)** for cutting mica, apparatus assembly, and for other preparations under dust-free conditions. Fume hood. Distillation units for water and solvent purification. Anti-vibration table for placing apparatus (optional, but essential for laboratories located above ground-level). Small fridge. **Evaporator** vacuum pump for silvering and surface deposition (ducted to the outside through the wall). Additional laboratory and apparatus-associated items are listed in Table I below.

Optical items (see Table I for details)

Grating **spectrometer** with 90° **prism** at entry slit on adjustable turntable, one exit port with movable reticulated eyepiece and a second exit port for normal or video camera, recommended resolution: 0.15 Å (0.015 nm), grating dispersion 32Å/mm (spare gratings of 16Å/mm and 64Å/mm optional). **White light source** – tungsten-halogen or xenon-arc lamp, with collimating lens and IR heat-absorbing filter. **Sodium lamp** and **mercury pen-ray** light sources. Rotating image dove prism. Light polarizers. Video camera-recorder system (optional for dynamic measurements).

Electronic items (see Table I for details)

General purpose 5-digit **multimeter**. High voltage power supply and/or **amplifier** for driving piezoelectric crystals and bimorphs (low voltage power supplies for driving DC motors are supplied with the Basic Unit). Other equipment and electronic devices such as function generators, amplifiers, strain-gauge bridges, frequency counters, lock-in amplifiers, chart recorders and storage scopes may be required for specialized experiments (see Table I).

Miscellaneous items (see Table I for details)

Mica cutting stage and small **hot plate** for gluing mica sheets and other substrates to silica disks. Langmuir-Blodgett trough for depositing organic layers on surfaces. Miscellaneous laboratory supplies and materials: glassware, filters, **mica** (Ruby Muscovite clear, thick large sheets, about 6"×6" square), **glues**, chemicals, etc.

SFA 3 BASIC UNIT

The SFA 3 Basic Unit consists of the following items (parts in [square brackets] are optional):

UPPER CHAMBER
LOWER CHAMBER
[VARIABLE] FORCE MEASURING SPRING
BASE
PIEZOMOUNT
OPTICS STAND
MIRROR
[FRICTION DEVICE]
[BIMORPH SLIDER]
[BIMORPH VIBRATOR]
CONTROL BOX
TOOL KIT (SEE LIST BELOW)
SUPPLY BOX (SEE LIST BELOW)
ELECTRIC CABLES (SEE LIST BELOW)

See Table I on page 11 and Table II on page 139 for further details on individual parts and components.

ASSEMBLY TOOLS (TOOL KIT)

Screw drivers, flat type – 11 sizes (mm): 1.5, 2.0, 2.5, 3.0, 4.0, 4-in-one, two large
Screw drivers, hex type, Allen keys – 9 sizes (mm): 0.9 1.3, 1.5, 2.0, 2.5, 3.0, 4.0, 0.028", 0.035"
Screw drivers, Philips type – 3 sizes: 00, 0, 1
Nut driver – 1 size: 4.0 mm, for adjusting limit switch positions on motor housings
Tweezers (1 flat tipped, 1 Teflon coated, for handling small parts and polished surfaces)
Tweezers – specially shaped, for picking up cylindrical silica disks
Forceps (stainless steel, 2 sizes: 4" and 6", for handling parts, helical springs, etc.)
Forceps (1 angled, 1 pointed, for handling platinum wire, mica and small parts)
Spatula (steel, for inserting/removing main spring of Upper Chamber)
Cleaning brushes (15) – for cleaning threaded holes with water or alcohol only
Mini wrenches (3/16" – for mirror cables, 1/8" – for micro electric connectors)
Adjustable spanner/wrench (for micrometer, motor housings, etc.)
Double-ended right angled screw driver (for bolting main spring in Upper Chamber)

SUPPLY ITEMS (SUPPLY BOX)

Base pads/kinematic mounts (three, for base legs)
Belts (two, for Optics Stand)
Eyepiece (X10 wide-angle, *Nikon CFWE 10XA*)
Force-measuring springs (4 spare)
Friction Device clamping screws (two)
Friction Device restrainer with short 3.5 mm screw
Glass disk for sealing apparatus without using piezo mount and for leak tests
Glue (some crystals of Shell EPON RESIN 1004 and 1009)
Graticule / reticule with cross-hair (for eyepiece)
Kel-F tubing with Luer connectors at ends (two)
Luer fittings (2 fem-fem, 2 male-male, 2 fem-male, 3 caps, 2 male ports, 2 female ports, 1 valve, O-rings size -003 for Luer threads, Teflon Luer filter)
Microscope tube (for use with Friction Device) with X10 objective installed
Microscope tube (normal, for use with Optics Stand) with X5 objective
Mirror control cables (3, with thumb screws, end clamps and washers)
Mirror knobs (3)
Needles (3, for cleaving mica)
O-rings (30 spare): -003, -006, -007, -008, -010, -012, -015*, -020, -222, -224, -236
Perspex window (1 spare)
Prism (1 inch, for placing on top of Optics Stand)
Screws (spares, unusual sizes only)
Self-adhesive vernier scale for motor housing (spare strip)
Silica disks (8): 3.5 mm high (2), 4.0 mm (2), 4.5 mm (1), 2.5 mm for friction device mount only (3).
Small Kel-F tipped 1.6 mm stainless steel screws (3 spare)
Spanners (two) for bellows ring clamps
Spirit level (for placing on Base)
Stand for Upper Chamber (flat base with 4 supporting legs, tapered on top)*
Syringe (50 ml, for filling SFA chamber)
Teflon bellows (1 spare)
Thermistor port
Thermistor (wired to connecting cable, plus one spare)
Thumb screws (two, brass, for Optics Stand base)
Upper Chamber stainless-steel helical spring (alternatives, with different stiffness)
Adjustable tilt clamp (1) with deformable O-rings (2) to suit
Narrow bandpass filter (for Na line)
Two 4-pin sealed electric connectors for Upper chamber

* Optional, requires separate order.

ELECTRIC CABLES AND CONNECTORS (* ITEMS SUPPLIED WITH CONTROL BOX ONLY)

Check that the Control Box and Apparatus are electrically earthed or 'grounded' before switching on. The Apparatus should be earthed via a hole on the front of the Base Plate. See comments on avoiding 'earth loops' or 'ground loops' on page 43.

Numbers refer to those marked on cables. Note: 1 metre (m) ~3 feet.

POWER

1. *POWER STATION: surge-protected, to suit local voltage supply.
2. *POWER INPUT CABLE (2 m): Three-pin chord from Station to Control Box.

OPTICS STAND

3. *OPTICS CABLE (mini-DIN, 2–3 m): 8-pin cable from Control Box Optics Output to Optics Stand. In some models, one end of this cable is already attached to the Optics Stand.

APPARATUS MOTOR 1

4. *MOTOR 1 CABLE (mini-DIN, 2 m): Six-pin cable from Control Box Output to Motor 1.
5. *ENCODER CABLE (2 m): 8-pin silver steel connector leading to two 4-pin cables each terminating in a 21-pin connector to be plugged into display counters for Motors 1 and 2.

PIEZO

6. PIEZO INPUT CABLE (1 m): Connect free end to low-voltage (± 5 –10 V) regulated DC power supply or function generator (ripple < 1 mV). Turn Piezo switch to EXT. When using internal power supply, switch to INT.
7. *PIEZO OUTPUT CABLE (BNC–BNC, 1 m): From Control Box Piezo Output to high gain DC amplifier (X50–100 TREK type, with BNC input socket).
8. *PIEZO MOUNT CABLE (BNC–BNC coax cable, 2 m): From high gain amplifier to Piezo Mount on apparatus via BNC–LEMO connector.

FRICITION DEVICE

9. FRICITION DEVICE CABLE (2 m). Connect free end to strain gauge detector/bridge, the other end to the 4-pin LEMO receptacle on the Friction Device.
10. *MOTOR 2 CABLE (mini-DIN, 2 m): Six-pin cable from Control Box Output to Motor 2.
11. *ENCODER CABLE (2 m): 8-pin silver steel connector leading to two 4-pin cables each terminating in a 21-pin connector to be plugged into display counters for Motors 1 and 2.

BIMORPH SLIDER / VIBRATOR (optional)

12. BIMORPH INPUT CABLE (1 m): Connect free end to DC power supply or function generator.
13. *BIMORPH OUTPUT CABLE (BNC–BNC, 1 m): From Bimorph Output on Control Box to low gain amplifier or directly to Bimorph Slider.
14. *BIMORPH MOUNT CABLE (BNC–LEMO coax connector, 2 m): From low gain amplifier or directly from Bimorph Output on Control Box to LEMO connector on Bimorph Slider. This cable can also be used to connect the BIMORPH VIBRATOR to a lock-in amplifier or oscilloscope.

MISCELLANEOUS

15. HEATER CABLE (2 m): Connect from Control Box Heater Output to heater rods in Lower Chamber.
16. *FUSES: Spare 0.5 and 1.0 Amp fuses for Control Box fuse holders (fast action fuses).
17. THEMISTOR: Connect thermistor leads to resistance input on multimeter (not supplied).
18. EARTHING LEAD: Single wire connection from front of Base plate to earth (ground).

TABLE I – COMPLETE LIST OF LABORATORY ITEMS REQUIRED

OPTICAL ITEMS	
EQUIPMENT ITEM	REQUIRED FOR
Grating spectrometer [Spec] 1/2 or 1/4 (0.25-0.35) meter, with adjustable width entrance slit, first exit port modified for wide-field viewing eyepiece on translation stage with manual drive encoder (travel distance: 15 mm), second exit port for video camera. Resolution of $\lambda \sim 0.15 \text{ \AA}$. Recommended dispersion: 32 $\text{\AA}/\text{mm}$ (1200 grooves/mm for $\frac{1}{2}$ meter) but x2 higher and lower dispersion gratings recommended, 550 nm blaze.	Measuring surface separations, surface shapes, thin film thickness and refractive index using FECO fringe interferometry.
Prism turntable [Newport] with 3-axis rotation/tilting controls.	For holding prism at spectrometer entrance slit.
Wide field Eyepiece 10X adjustable focus, with 10 mm X10 mm sq. grid reticle / graticule.	For mounting on translation stage at spectrometer exit port.
Display Counter with power supply.	For translation stage encoder output at spectrometer exit port.
White light source 12V, 100W Tungsten-Halogen lamp, or Xenon Arc Lamp, with focussing (collimating) lens and IR heat filter.	White light source for SFA box.
IR filter (hot or cold mirror)	For absorbing/reflecting IR light from white light source.
Dove prism in rotary holder	For rotating image from SFA box before it goes into spectrometer.
Yellow Filter (or sodium lamp)	For observing Newton's rings with white light (instead of Na lamp).
Mercury Lamp thin pen-ray type ($\sim 5 \text{ W}$)	Wavelength standard calibration (also for curing certain glues)
Stage micrometer	For calibrating lateral magnification of spectrometer output image
Calibration microscope (Micrometer eyepiece)	Calibrating springs (with XYZ stage)
Polarizer	Analyze FECO fringe polarization

VACUUM COATING UNIT

EQUIPMENT ITEM	REQUIRED FOR
Vacuum Coating Unit / Evaporator with 18" high bell jar	Deposit silver, silica, etc., on mica.
Thickness monitor	Measuring thickness of deposited films on mica (or other) surfaces.
Molybdenum or tungsten boats	For evaporating silver shot / wire
Silver shot	For evaporating 500-550Å films on mica

MICA CUTTING AND GLUING

EQUIPMENT ITEM	REQUIRED FOR
Mica cutting stage [Prior] XYZ translation stage with platinum wire, low voltage DC power supply.	For cutting thin mica sheets by melting through them (mica sheet supported on two metal blocks).
Small Hot-Plate Use with low voltage power supply. Can be constructed in-house.	For melting thermosetting glues, used for gluing mica sheets to silica disks.
Mica Thick, large sheets of Clear Ruby Muscovite	Used as substrate surfaces
Platinum wire 0.006" or 0.2 mm diameter	For melt-cutting mica
Thermosetting Glues	Gluing mica sheets for aqueous solutions
Thermosetting Glues	Gluing mica sheets for organic solvents
UV-curing Glues	Gluing mica sheets in flattened contact

ELECTRICAL ITEMS

EQUIPMENT ITEM	REQUIRED FOR
Low Voltage DC Power Supply Dual Outputs: 0 to $\pm 24V$, 5 Amp.	For 100 W lamp, mica cutting stage, and small gluing hot-plate.
Multimeter (5 digit)	AC/DC V-I-R measurements.
Voltage amplifier [Trek]	Amplify outputs from Control Centre to piezo and bimorphs.
Function Generator (FG) mHz, ramp, sine, square, triangular, sawtooth, ± 5 to ± 10 DC offset, low ripple.	For driving piezos and bimorphs, after amplifying X100 with VA.
Voltage amplifier (VA)	Amplify outputs from FG and LVPS to piezos/bimorphs
Strain Gauge Bridge	Measure friction strain gauge output
Chart Recorder	Recording friction traces
Storage O-Scope	Recording/storing fast friction transients
Multimeter (high precision)	High accuracy instr., e.g., for thermocouple
Lock-in amplifier	Measure amplitude- phase relationships in dynamic experiments

GENERAL LABORATORY SUPPLIES

EQUIPMENT ITEM	REQUIRED FOR
Pressure rinsers [Gelman] or ethanol squirt guns	For high pressure ethanol squirt cleaning of SFA parts.
Laminar Flow Cabinet or Work Station: Outward horizontal air-flow type	For cutting mica, apparatus assembly, and other preparations under dust-free conditions.
Glass Desiccators	For storing mica sheets, samples, etc.
Anti-vibration table	For placing apparatus (optional, but essential for laboratories located above ground-level).
Oil-less pumps	Aspirating liquids, evacuating desiccators.
Silica disks and windows	Replacement or spare
Miscellaneous small tools and disposable items needed for cleaning and assembly	Tool kit (provided), forceps, tweezers, glassware, filters, tubing, syringes, etc.
E - Nitrogen gas supply (from liq. nitrogen)	Purging apparatus, blow dry cleaning
E - Syringes, needles, Luer connectors, PTFE tubing	Injection filling, purging, draining SFA chambers
Water Aspirators	Aspirating chamber during cleaning/filling
Spirit level (supplied)	Leveling SFA when placed on Base Plate
Domes (transparent covers)	Covering apparatus parts
Langmuir-Blodgett Deposition Trough	Depositing organic layers on surfaces
Anti-vibration table (1 per SFA system/room)	Reducing vibrations during experiments
Balance	General purpose balances
Centrifuge	Purifying solutions of dust / particulates
Conductivity cell/pH meter	Electrodes can be inserted into SFA
Distillation Units	Purifying water and organic liquids
Drying oven	For glassware, etc.
Fridge – laboratory type	General purpose
Normal/stereo microscope	General purpose
Oil-less pumps	Aspirating liquids, evacuating desiccators

VIDEO CAMERAS / RECORDING SYSTEMS

EQUIPMENT ITEM	REQUIRED FOR
Video Camera (SIT)	Visualizing moving FECO fringes
Video Monitor	Observing FECO fringe patterns
Video Recorder with single and variable frame speed, & freeze frame capabilities	Recording moving FECO fringes
Video Micrometer	Analyzing positions of FECO fringes
Video Timer	Recording exact times of events
Other cameras	High resolution recording of fast (transient) events
Quantitative CCD, High speed, etc.	

THE SFA 3: DESCRIPTION OF UNITS AND PARTS, WITH FIGURES

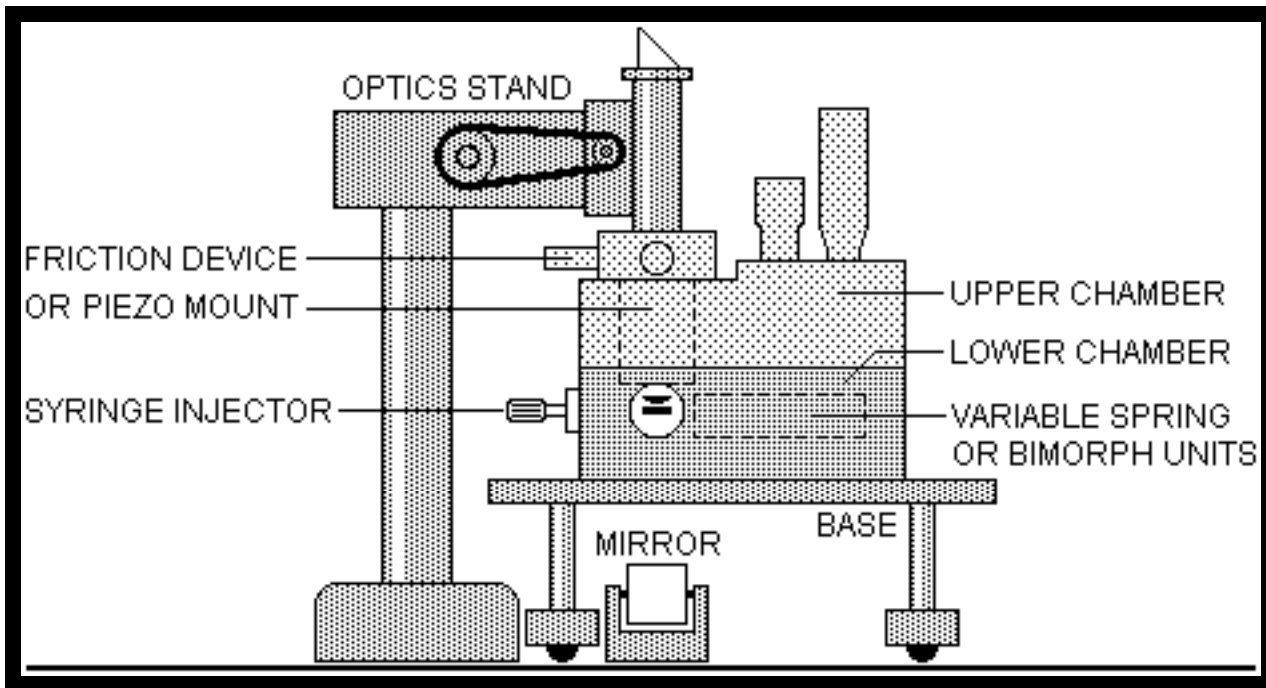


Figure 4. Units and attachments of the SFA3.

The SFA 3 is composed of the following numbered UNITS and ATTACHMENTS:

BASIC UNIT	0 – MISCELLANEOUS 1 – UPPER (CONTROL) CHAMBER 2 – LOWER (LIQUID) CHAMBER 3 – BASE AND LEGS 4 – VARIABLE SPRING 5 – PIEZO MOUNT 6 – MIRROR 7 – OPTICS STAND
ATTACHMENTS	8 – SYRINGE INJECTOR 11 – FRICTION DEVICE 12 – BIMORPH SLIDER 13 – BIMORPH VIBRATOR

Each UNIT is composed of a number of machined PARTS, usually between 10 and 30, together with special screws, electric connections and other small fittings. All of these come together to produce the final assembled apparatus. The apparatus is normally delivered fully assembled and functional, that is, UNITS 1–5 will be assembled and fitted together. UNITS 6 and 7, which are used separately from each other, will also be pre-assembled before delivery. Some parts and supply items do not belong to any obvious unit or are used in a number of different units, these have been placed in the MISCELLANEOUS UNIT category.

Table II on page 139 lists the names and numbers of all the parts and units of the SFA 3 and its attachments. This list can be folded out for referencing when reading the sections on cleaning, assembly and operations, or when referring to the figures and drawings.

The following pages contain many figures, assembly drawings and photographs of different units, key parts and supply items. Additional figures and drawings, especially of ATTACHMENTS, appear at other places in this manual, as well as in the SFA 3 brochure (pages 18-21).

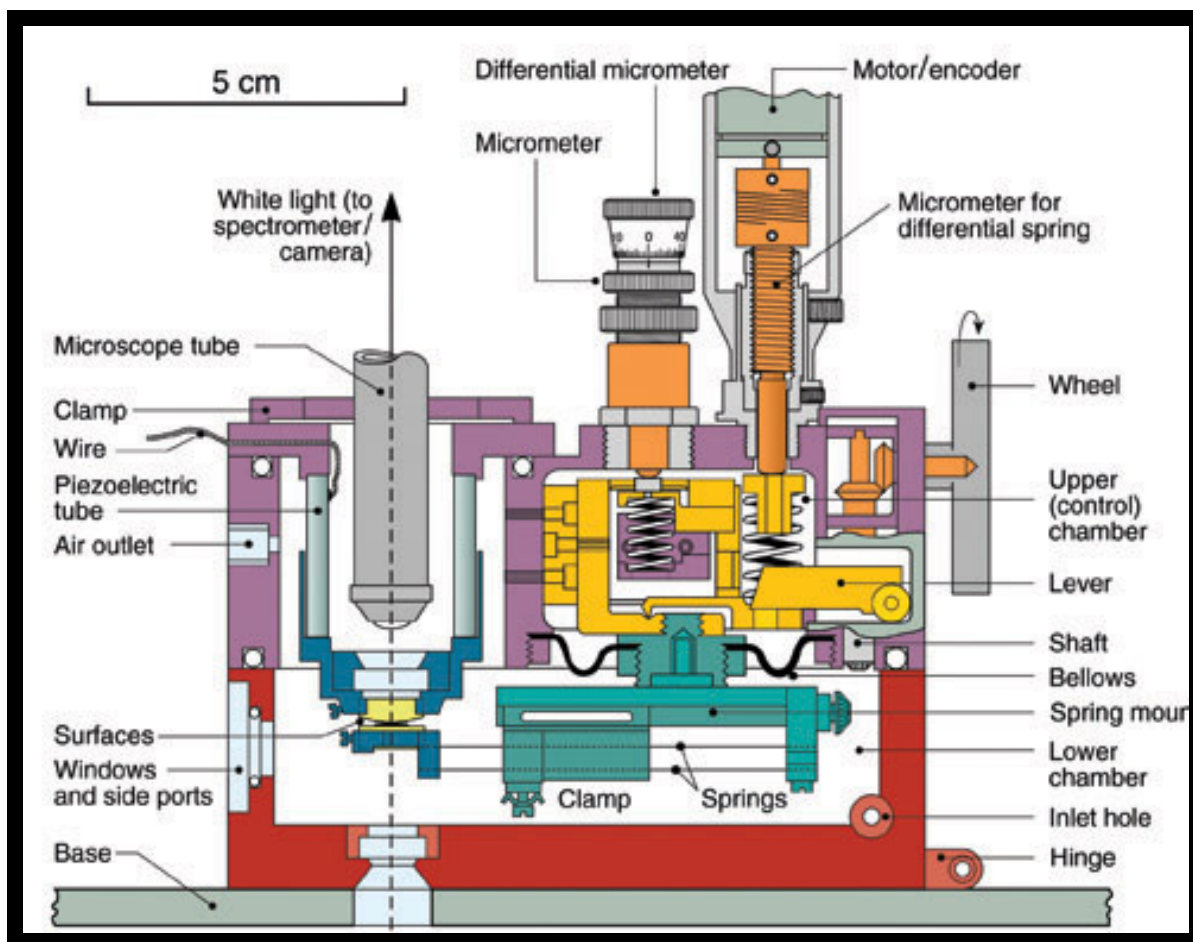
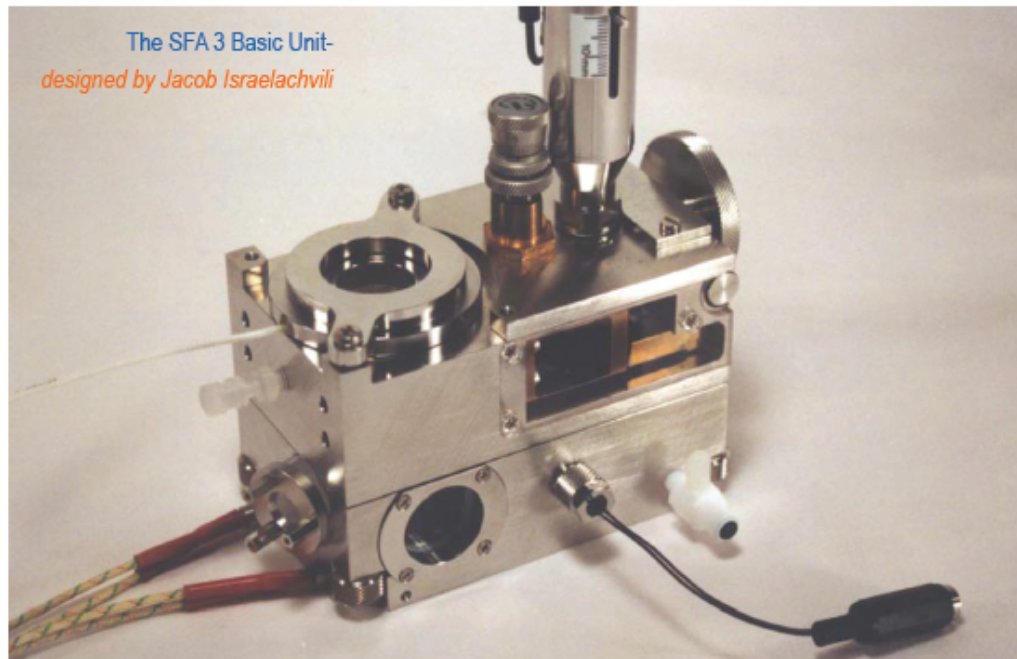


Figure 5. Assembly drawing of SFA 3 BASIC UNIT showing key parts.

A sophisticated research instrument for directly measuring static and dynamic forces between surfaces and biosurfaces and for studying other interfacial and thin film phenomena at the molecular level. Modular design with facility for expansion with new attachments and upgrades.



APPLICATIONS

Research areas and types of interactions that can be directly measured:

Dispersion science – Forces between surfaces in liquids and controlled vapors

Adhesives, lube oils – Long-range colloidal forces and short-range adhesion forces

Composite materials – Chemical reactions and interactions of metal and oxide surfaces

Detergency, food research – Forces between surfactant monolayers and bilayers

Biomaterials and biosurfaces – Forces between protein and polymer-coated surfaces

Biomedical interactions – Ligand-receptor and model biomembrane interactions

Tribology – Friction and lubrication of smooth or rough surfaces, thin film rheology

Powder technology – Capillary effects and surface deformations during interactions

Materials research – Interactions of different surface layers: metals, oxides, silica, etc.

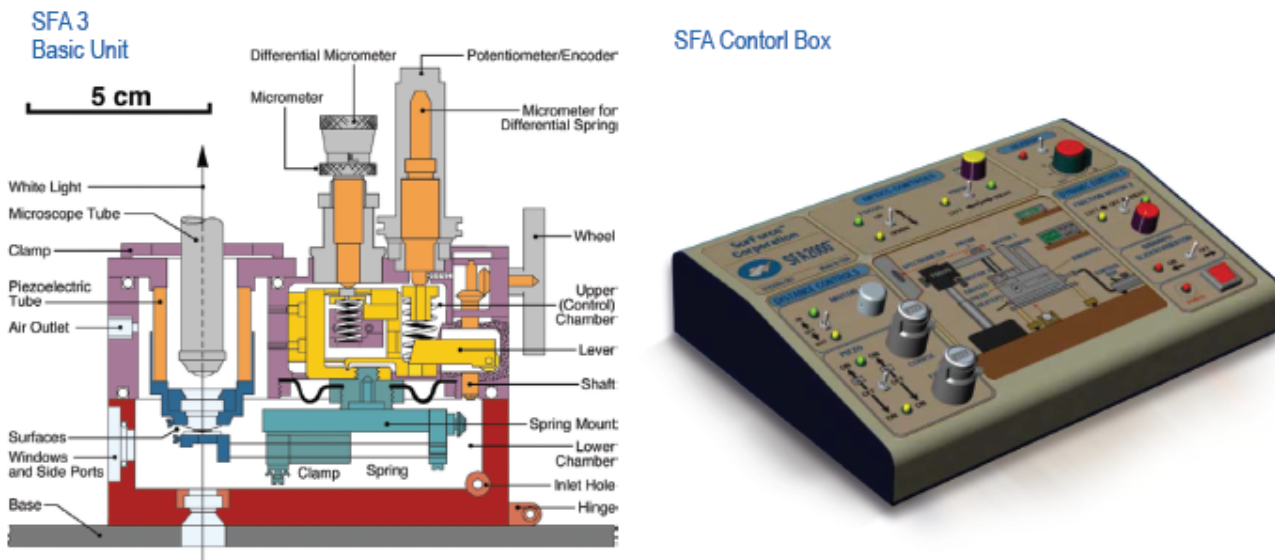
This list is not exhaustive; contact us for your specific needs.

GENERAL DESCRIPTION

The SFA measures forces between two smooth surfaces in vapors or liquids with a sensitivity of a few nN and a distance resolution of 1Å (0.1 nm). It can also measure the refractive index of the medium between the surfaces, adsorption isotherms, capillary condensation, surface deformations arising from surface forces, dynamic interactions such as viscoelastic and frictional forces, and other time-dependent phenomena in real time. The molecularly smooth surfaces of hard materials such as mica, silica or sapphire serve as suitable substrate surfaces in most measurements; these can also be coated with thick or thin layers of surfactants, lipids, polymers, metals, metal oxides, proteins, etc.

HOW IT WORKS

The figure below is a schematic drawing of the SFA ready for use for normal force measurements. The shapes of the interacting surfaces and the separation between them are measured by analyzing the optical interference fringes (known as FECO fringes) produced when white light passes through the two surfaces. The distance between the surfaces is controlled by a four-stage mechanism of increasing sensitivity from millimeters to ångstroms. The stiffness of the force-measuring spring can be adjusted during experiments to enable forces of greatly differing magnitudes to be measured. Dynamic measurements are conducted with surfaces in motion using one of the attachments described on the following pages.



USES

The SFA technique has been used to characterize and quantify the fundamental interactions between surfaces in liquids and vapors (see references below). Static interactions include van der Waals forces, electric double-layer forces, forces due to solvent structure (solvation and hydration forces), capillary forces, hydrophobic interactions, the steric forces between adsorbed polymer layers, surfactant monolayers and lipid bilayers, various adhesion forces and bio-specific "lock-and-key" type binding interactions. Dynamic and time-dependent interactions include the viscosity of liquids in ultra-thin films (nano-rheology), the slow relaxations of liquids, surfactant molecules and polymers in confined geometries, and surface deformations during the approach, separation and lateral sliding of two surfaces. More recent applications have included food technology, the friction of clutches, how geckos run on walls and ceilings, the bioadhesion of mussels, and the biolubrication of joints.

MAIN FEATURES AND ATTACHMENTS

For anyone who wants to accurately measure forces between well-defined surfaces of known geometry and separation, the SFA3 stands unrivalled as to accuracy, thermal drift and directness of measurement. Unlike some surface force-measuring instruments, such as pin-on-disk tribometers and scanning probe microscopes, the SFA3, when used with FECO optics, measures forces between surfaces of known geometry and at precisely known surface separations, both of which are measured directly at the point of interaction. Attachments to the basic unit allow for dynamic measurements to be made, for example, of friction, lubrication and viscoelastic forces over a large range of sliding speeds or shear rates. Four of these new facilities or attachments are illustrated below:

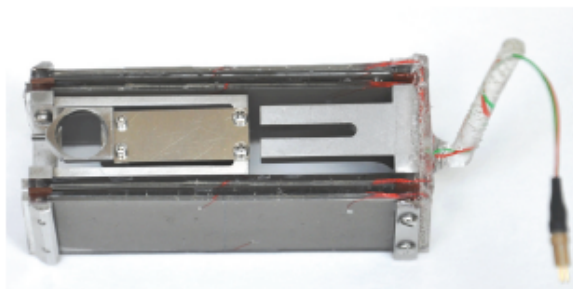
FRICITION DEVICE

For friction and lubrication studies



(EXTENDED) BIMORPH SLIDER

For high-speed shearing of thin films



BIMORPH VIBRATOR

For measuring thin-film viscosity



UNDER-WATER MOUNTS

For biological (e.g., protein) surfaces



THE SFA AND FECO OPTICAL TECHNIQUE

Recent advances in the surface forces apparatus (SFA) technique. J Israelachvili, Y Min, M Akbulut, A Alig, G Carver, W Greene, K Kristiansen, E Meyer, N Pesika, K Rosenberg and H Zeng, *Reports on Progress in Physics* (2010) 73 1-16.

Adhesion and Short-Range Forces Between Surfaces: New Apparatus for Surface Force Measurements [the SFA 3]. J. N. Israelachvili and P. M. McGuiggan, *J. Mater. Res.* (1990) 5 2223.

The extended surface forces apparatus. Part III. High-speed interferometric distance measurement. Zäch, M., J. Vanicek, and M. Heuberger, *Review of Scientific Instruments* (2003) 74 (1) 260-266.

Extending the surface force apparatus capabilities by using white light interferometry in reflection. Connor, J. N. and R.G. Horn, *Review of Scientific Instruments* (2003) 74 (11) 4601-4606.

Topographic information from multiple beam interferometry in the Surface Forces Apparatus. M. Heuberger, G. Luengo, J. Israelachvili, *Langmuir* (1997) 13 3839-3848.

High Speed Friction Measurements Using a Modified Surface Forces Apparatus. D. D. Lowrey, K. Tasaka, J. H. Kindt, X. Banquy, N. Belman, Y. Min, N. S. Pesida, G. Mordukhovich, J. N. Israelachvili. *Tribology Letters* (2011) 42 117-127.

COLLOIDAL, POLYMER AND ADHESION INTERACTIONS

Intermolecular and Surface Forces (3rd Ed). J. Israelachvili, *Elsevier & Academic Press*, 2010.

Direct measurement of depletion attraction and thin-film viscosity between lipid bilayers in aqueous polyethylene oxide solutions. T. L. Kuhl, A. D. Berman, S. W. Hui, J. N. Israelachvili, *Macromolecules* (1998) 31 8250-8257.

Debye length and double-layer forces in polyelectrolyte solutions. Rafi Tadmor, Ernesto Hernandez-Zapata, Nianhuan Chen, Phil Pincus, Jacob Israelachvili. *Macromolecules* (2002) 35 (6) 2380-2388.

Evaporation and instabilities of microscopic capillary bridges. N. Maeda et al. *PNAS* (2003) 100 (3) 803-808.

Transient Interfacial Patterns and Instabilities Associated with Liquid Film Adhesion and Spreading. Hongbo Zeng, Yu Tian, Matthew Tirrell, Jacob Israelachvili. *Langmuir* (2007) 23 6126-6135.

Role of electrochemical reactions in Pressure Solution. George W. Greene, Kai Kristiansen, Emily E. Meyer, James R. Boles and Jacob N. Israelachvili, *Geochimica et Cosmochimica Acta* (2009) 73 2862-2874.

BIOLOGICAL AND BIOMEDICAL INTERACTIONS

Design Rules for Biomolecular Adhesion: Lessons from Force Measurements. Deborah Leckband, *Annu. Rev. Chem. Biomol. Eng.* (2010) 1, 365-389.

Intermolecular forces in biology. Deborah Leckband, Jacob Israelachvili. *Quart. Revs. Biophys.* (2001) 34 (2) 105-267.

Direct Measurement of a Tethered Ligand-Receptor Interaction Potential. J.Y. Wong et al., *Science* (1997) 275 820-822.

Direct measurements of multiple adhesive alignments and unbinding trajectories between cadherin extracellular domains. Sivasankar, S., B. Gumbiner, and D. Leckband, *Biophysical Journal* (2001) 80(4) 1758-1768.

Thin film morphology and tribology of food emulsions: a study of three mayonnaise samples. S. Giasson, J. Israelachvili, H. Yoshizawa, *J. Food Science* (1997) 62 640-652.

Thin film rheology and tribology of chocolate. G. Luengo et al., *J. Food Science* (1997) 62 767-812.

Impact of polymer tether length on multiple ligand-receptor bond formation. Claus Jeppesen, Joyce Y. Wong, Tonya L. Kuhl, Jacob N. Israelachvili, Nasreen Mullah, Samuel Zalipsky, Carlos M. Marques. *Science* (2001) 293 465-468.

Adsorption, Lubrication, and Wear of Lubricin on Model Surfaces: Polymer Brush-Like Behavior of a Glycoprotein. B. Zappone, M. Ruths, G. W. Greene, G. D. Jay, J. Israelachvili. *Biophysical Journal* (2007) 92 1693-1707.

Interaction forces and adhesion of supported myelin lipid bilayers modulated by myelin basic protein. Younjin Min, Kai Kristiansen, Joan M. Boggs, Cynthia Husted, Joseph A. Zasadzinski, Jacob Israelachvili. *PNAS* (2009) 106 3154-3159.

Force Amplification Response of Actin Filaments under Compression. George W. Greene, Travers H. Anderson, Hongbo Zeng, Bruno Zappone, Jacob N. Israelachvili. *PNAS* (2009) 106 (2) 445-449.

Adaptive mechanically controlled lubrication mechanism in articular joints. W. Greene et al., *PNAS* (2011) 108 5255.

DYNAMIC, RHEOLOGICAL AND TRIBOLOGICAL INTERACTIONS

Surface Forces and Nanorheology of Molecularly Thin Films. Marina Ruths and Jacob N. Israelachvili, in *Handbook of Nanotechnology*, 3rd edition, Chapter 29, B. Bhushan, Ed., *Springer-Verlag*. (2010) 857-922.

Surface Forces and Viscosity of Water Measured Between Silica Sheets. R.G Horn et al., *Chem Phys Lett* (1989) 162 404.

Thin film rheology and tribology of confined polymer melts: contrasts with bulk properties. G. Luengo, et al., *Macromolecules* (1997) 30 2482-2494.

Triboelectrification between smooth metal surfaces coated with self-assembled monolayers (SAMs). Akbulut, M., A.R.G. Alig, and J. Israelachvili, *Journal of Physical Chemistry B* (2006) 110(44) 22271-22278.

Friction and tribochemical reactions occurring at shearing interfaces of nanothin silver films on various substrates. Akbulut, Limit cycles in dynamic adhesion and friction processes: a discussion. H. Zeng et al., *J. Adhesion* (2006) 82 933-943.

DIFFERENT SURFACES (MATERIALS) AND INTERFACING WITH OTHER TECHNIQUES

The x-ray surface forces apparatus for simultaneous x-ray diffraction and direct normal and lateral force measurements. Y. Golan et al., *Rev. Sci. Instr.* (2002) 73 (6) 2486-2488.

Interactions of Silica Surfaces. G. Vigil et al., *J. Colloid Interface Sci.* (1994) 165 367.

Contact Electrification and Adhesion between Dissimilar Materials. R.G. Horn and D.T. Smith, *Science* (1992) 256 362.

3D Force and Displacement Sensor for SFA and AFM measurements. Kai Kristiansen, Patricia McGuiggan, Greg Carver, Carl Meinhart, Jacob Israelachvili, *Langmuir* (2008); 24(4): 1541-1549.

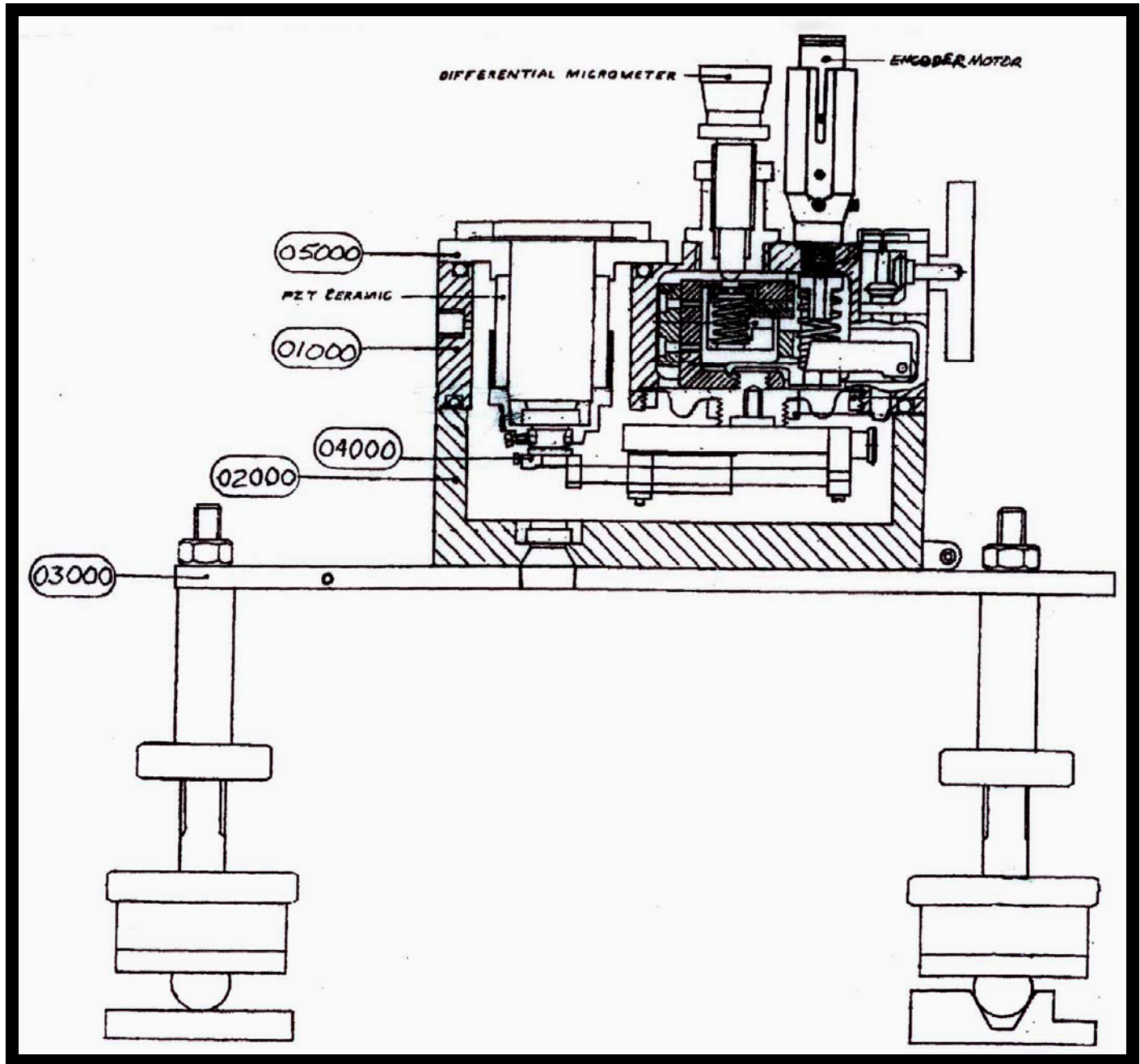


Figure 6. SUB-UNITS 1 to 5 of SFA3 BASIC UNIT.

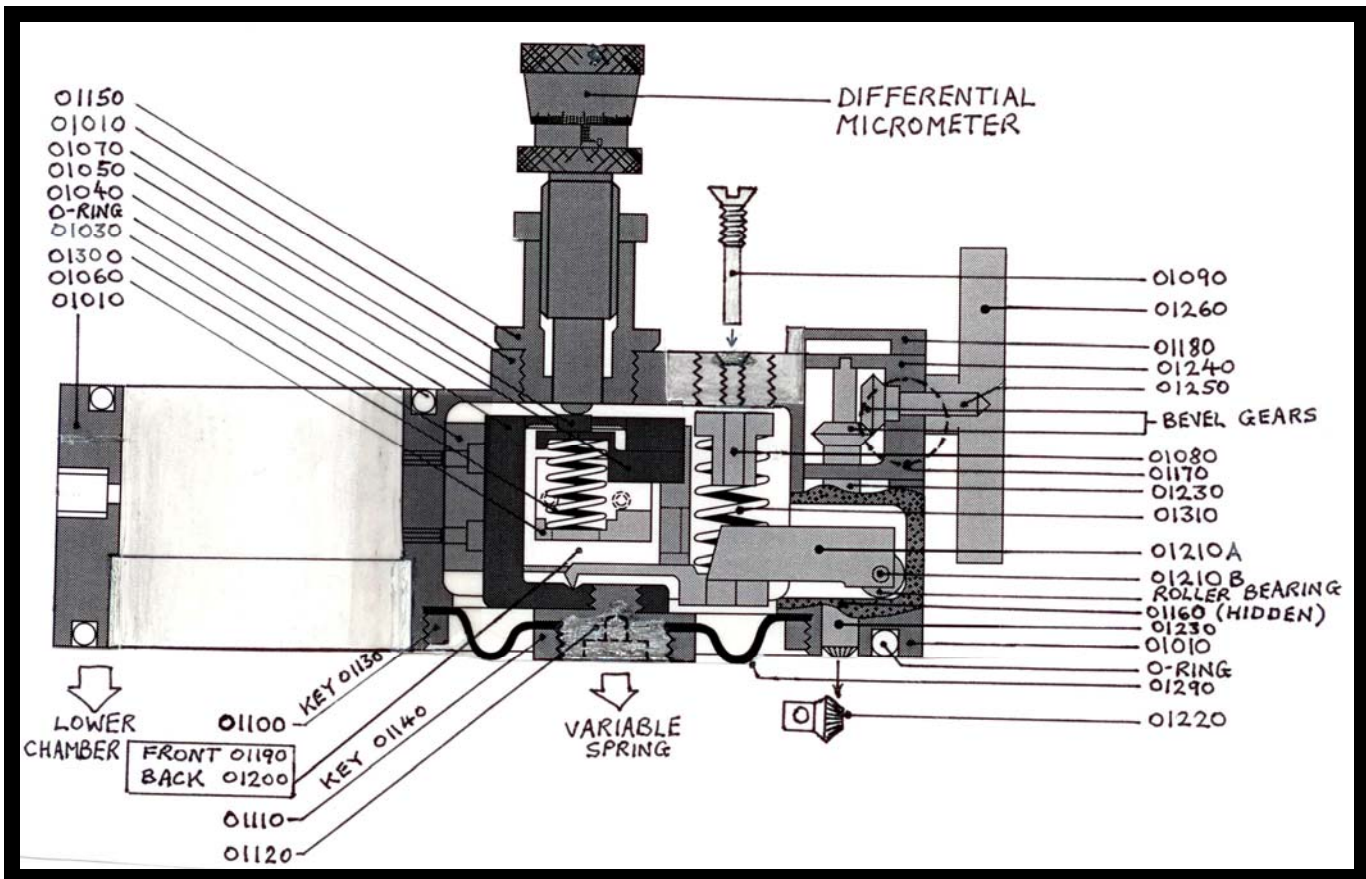


Figure 7. Assembly drawing of UPPER CHAMBER.

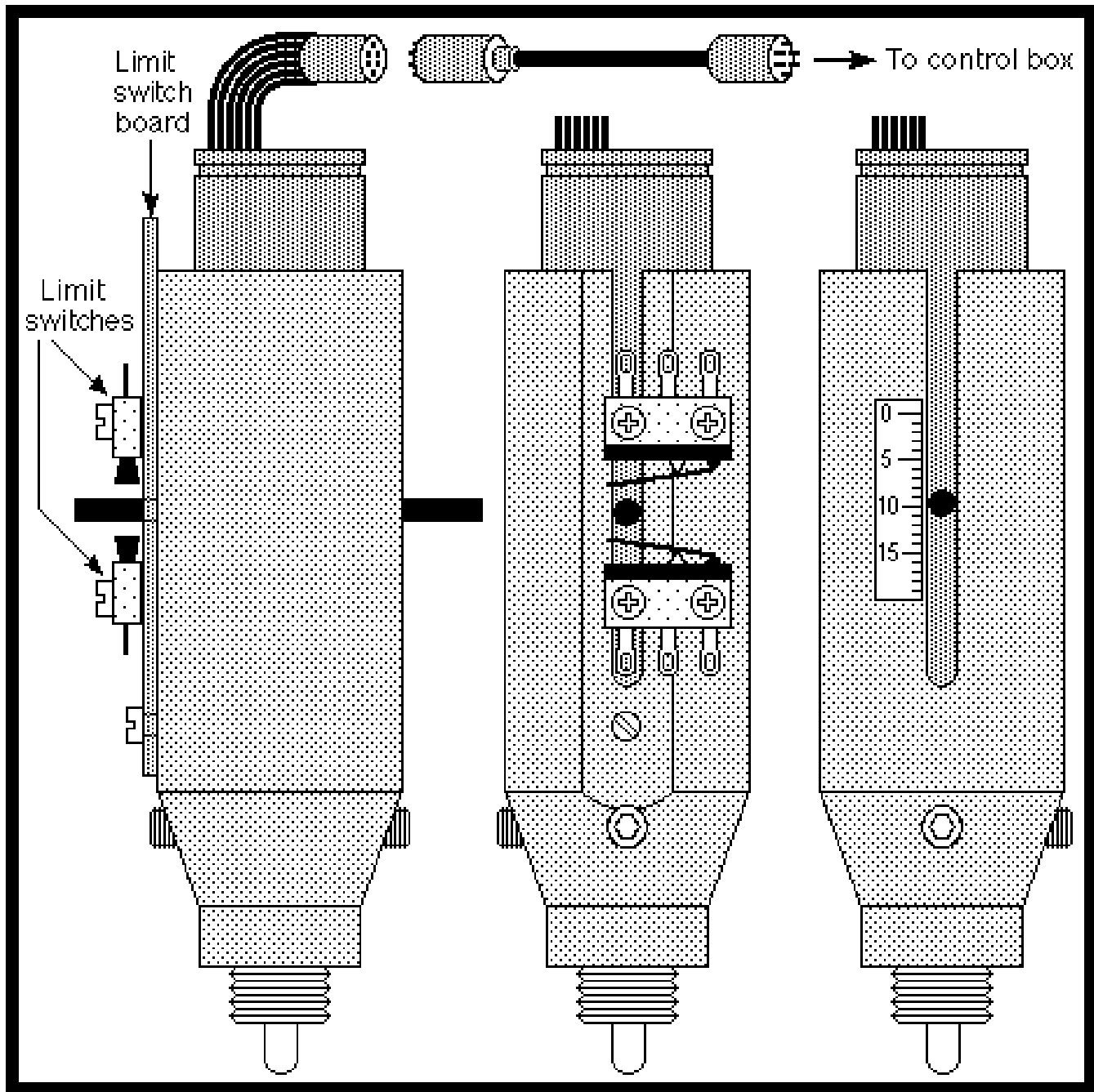


Figure 8. Assembly drawing of motor housing on UPPER CHAMBER (and FRICTION DEVICE).

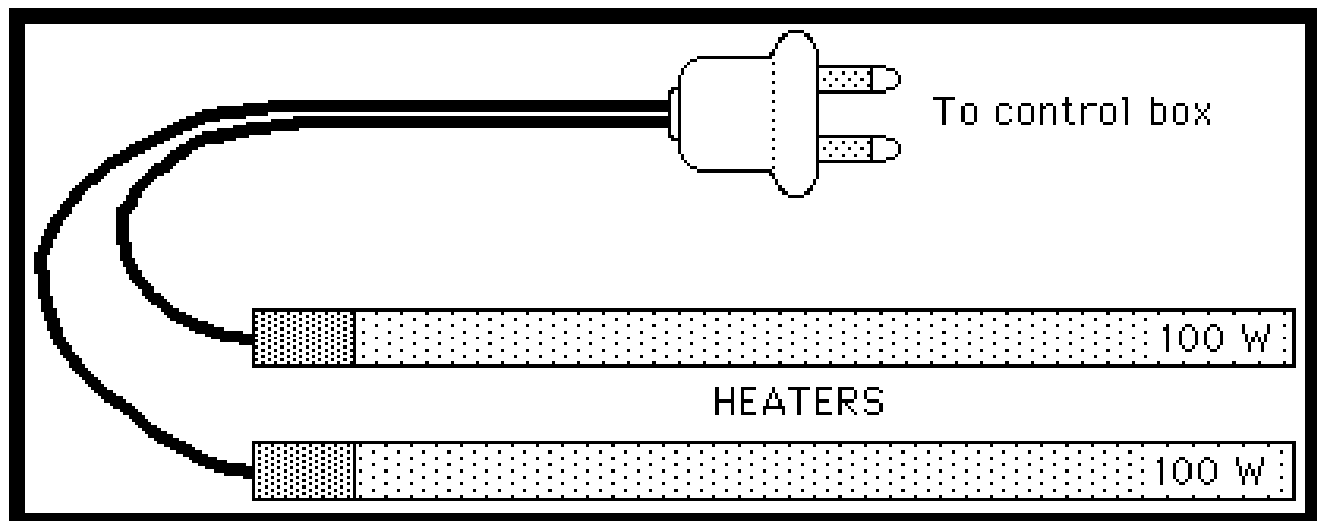
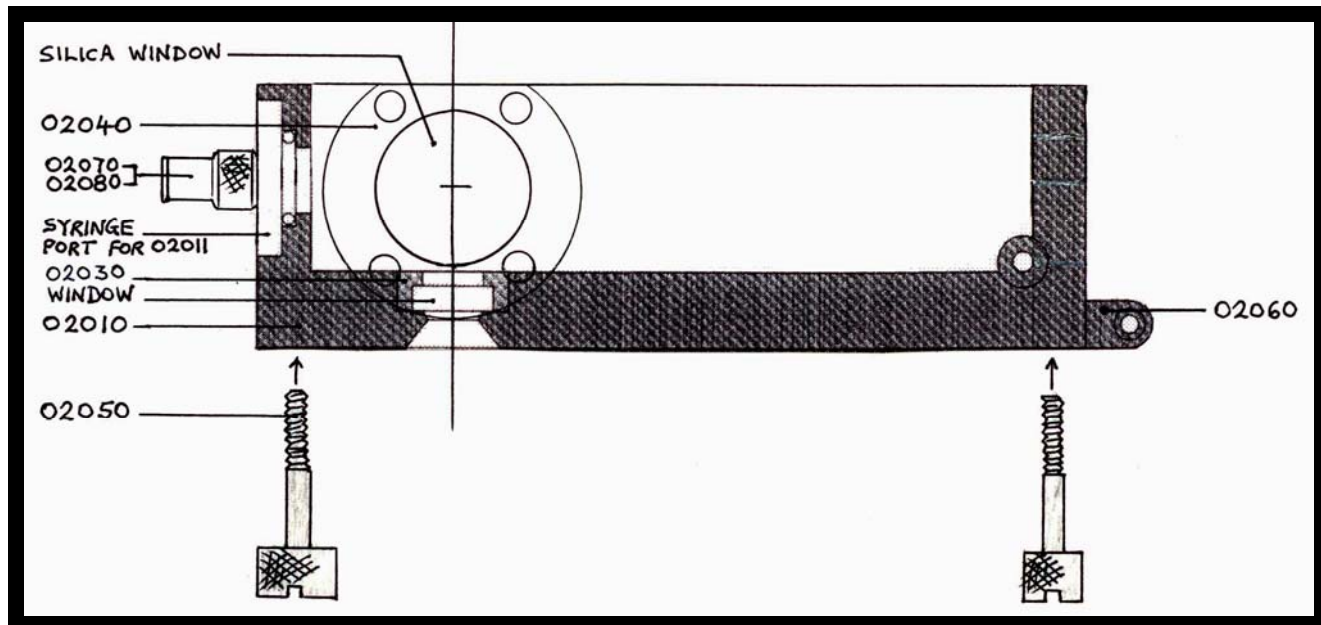


Figure 9. Assembly drawing of LOWER CHAMBER and HEATERS. Heater cables may be connected in parallel or in series, depending on local voltage.

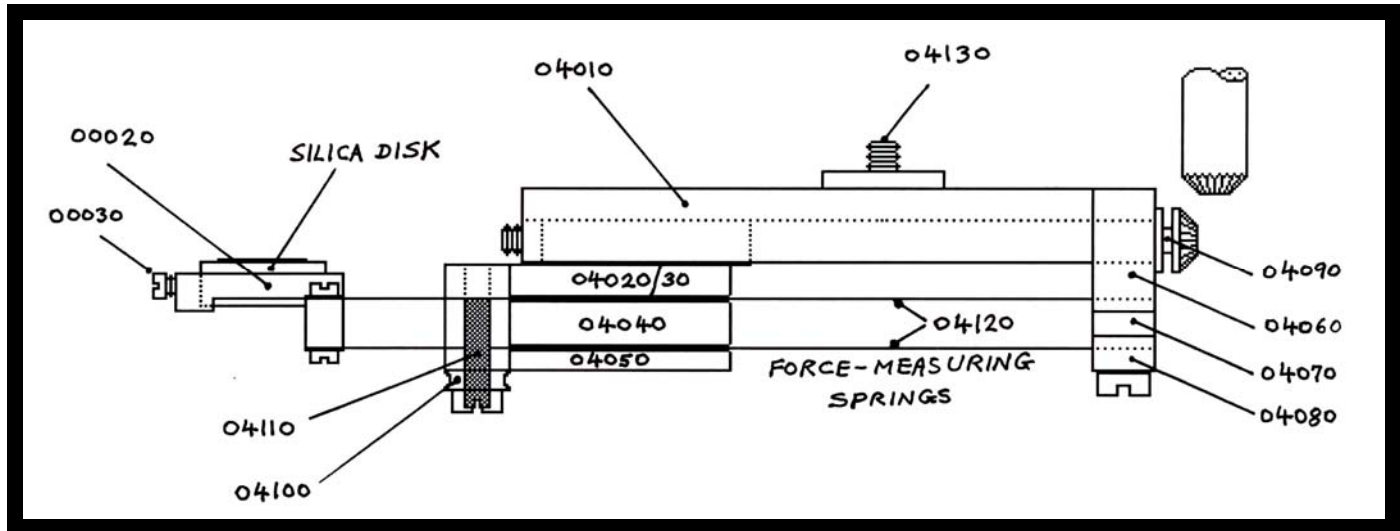


Figure 10. Assembly drawing of VARIABLE SPRING.

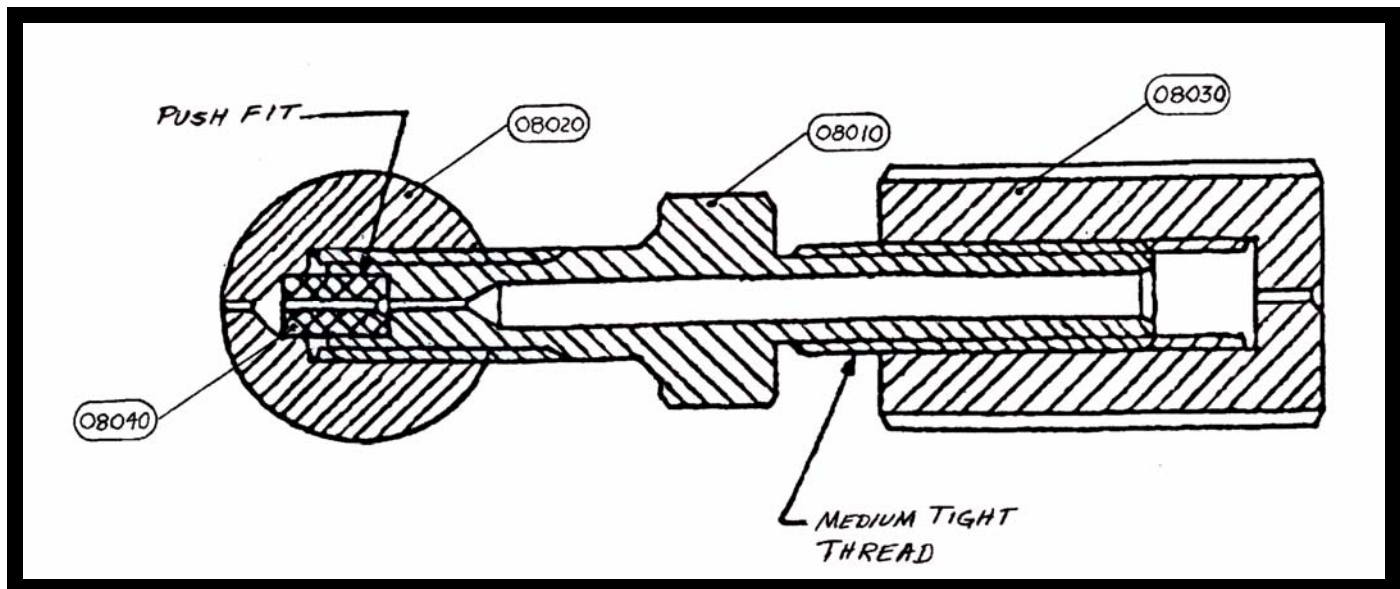


Figure 11. Assembly drawing of SYRINGE INJECTOR (alternative designs also possible).

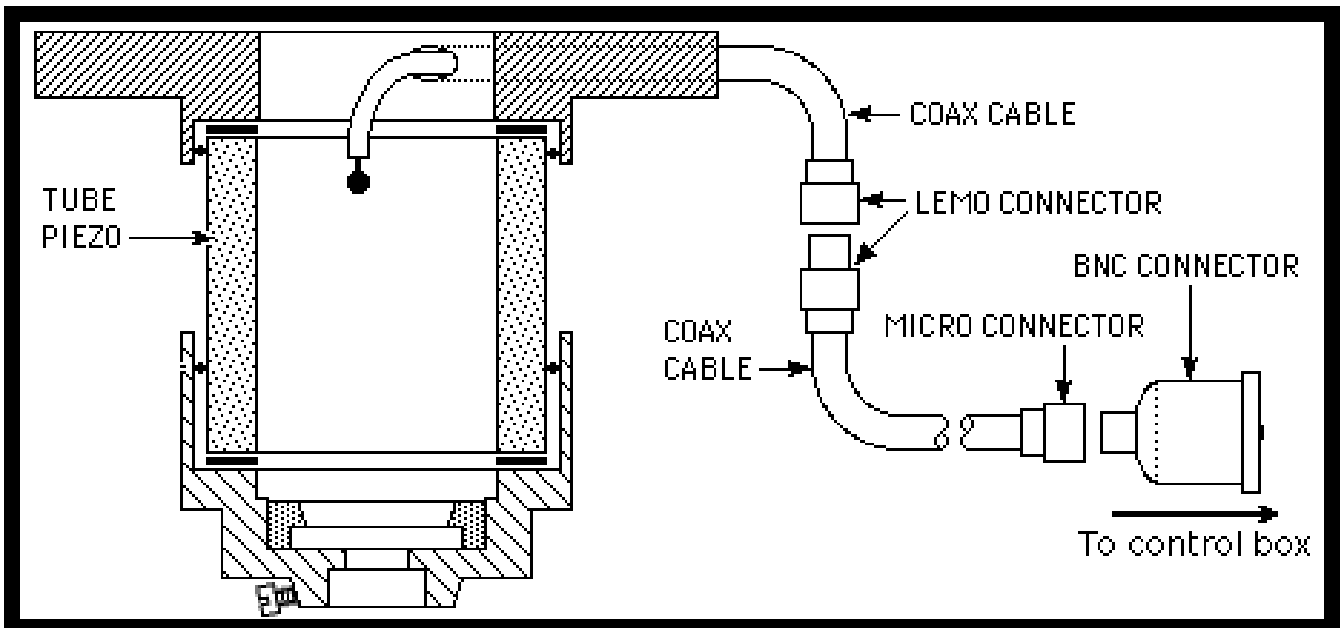


Figure 12. Assembly drawing of PIEZO MOUNT.

Note: when handling the micro-connectors, do not push or pull the thin coaxial cable – always connect and disconnect by turning and pushing or pulling the brass hex head.

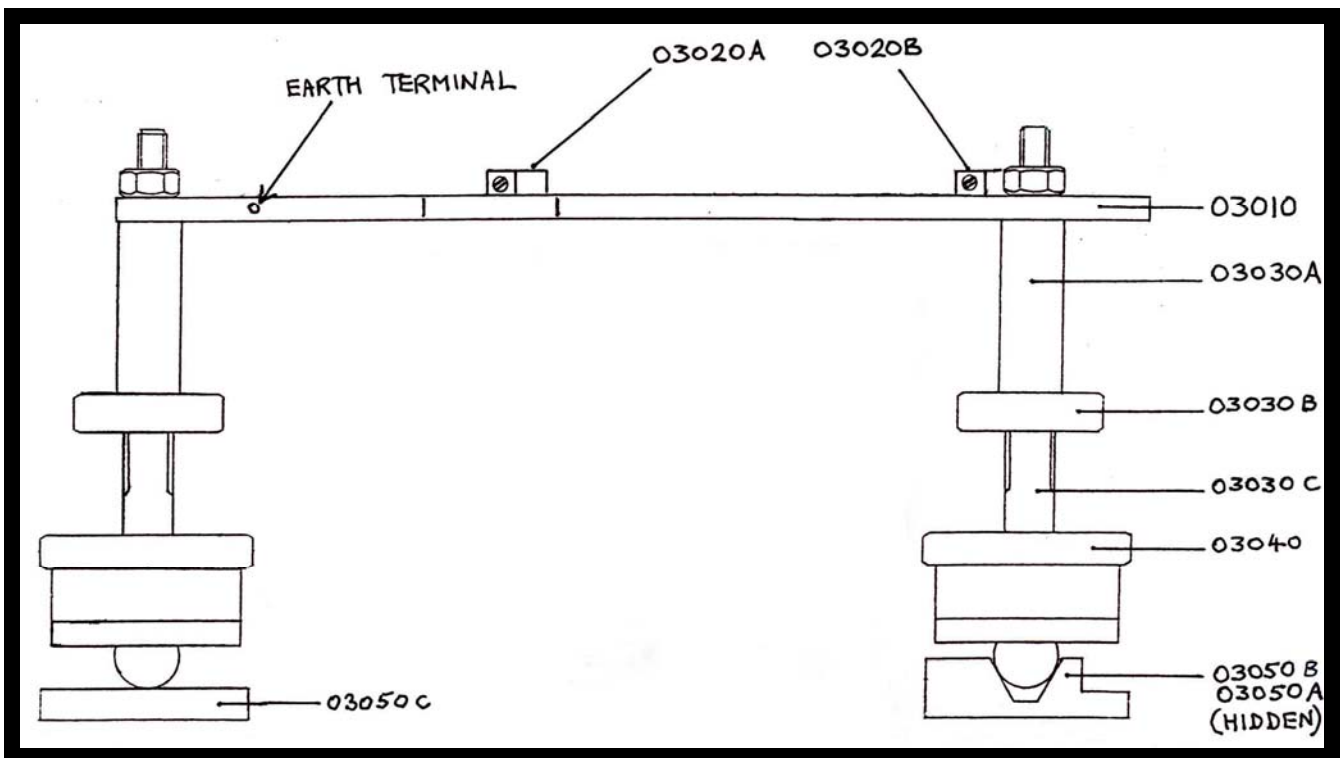


Figure 13. Assembly drawing of BASE with 3 legs.

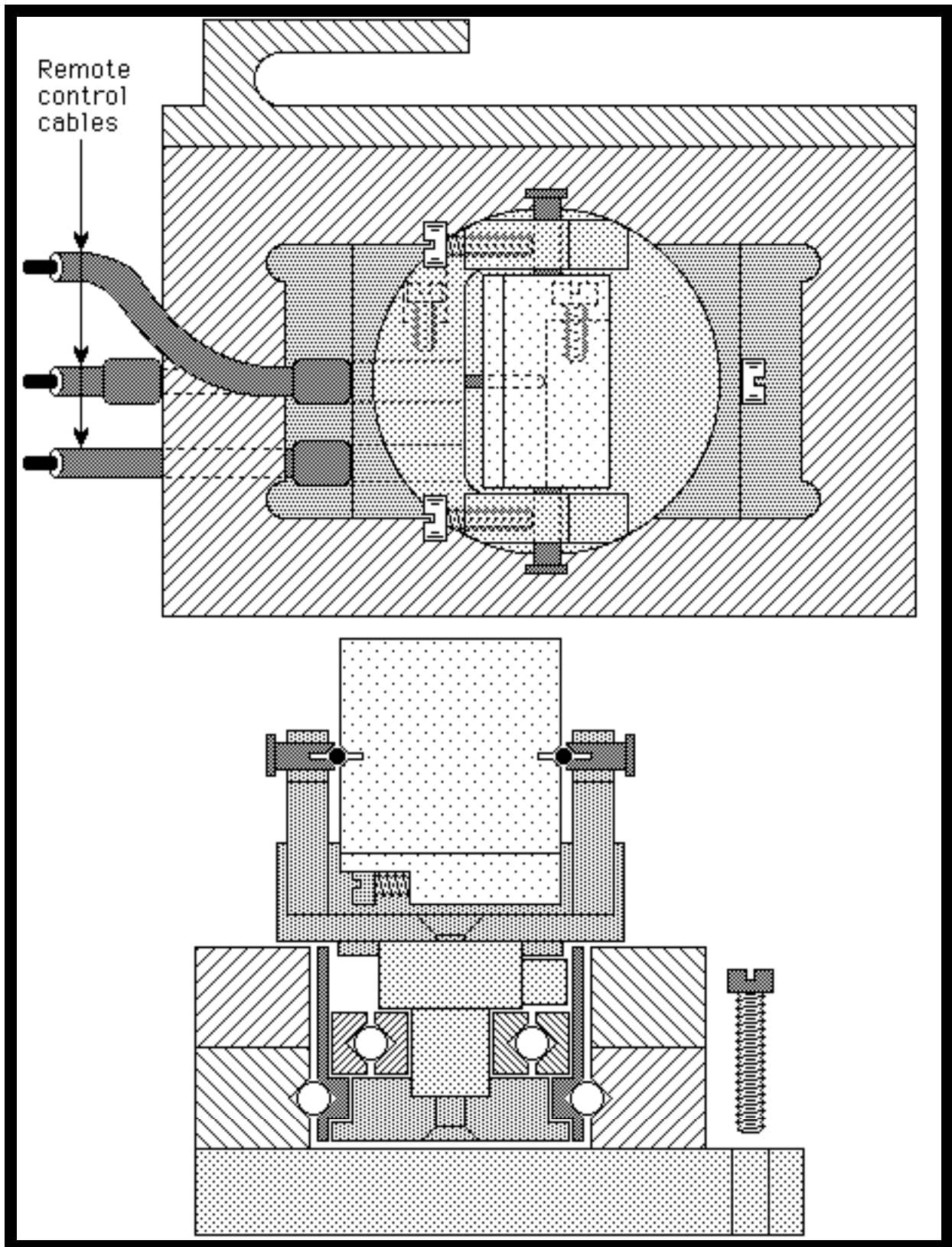


Figure 14. Assembly drawings of MIRROR (alternative design also possible).

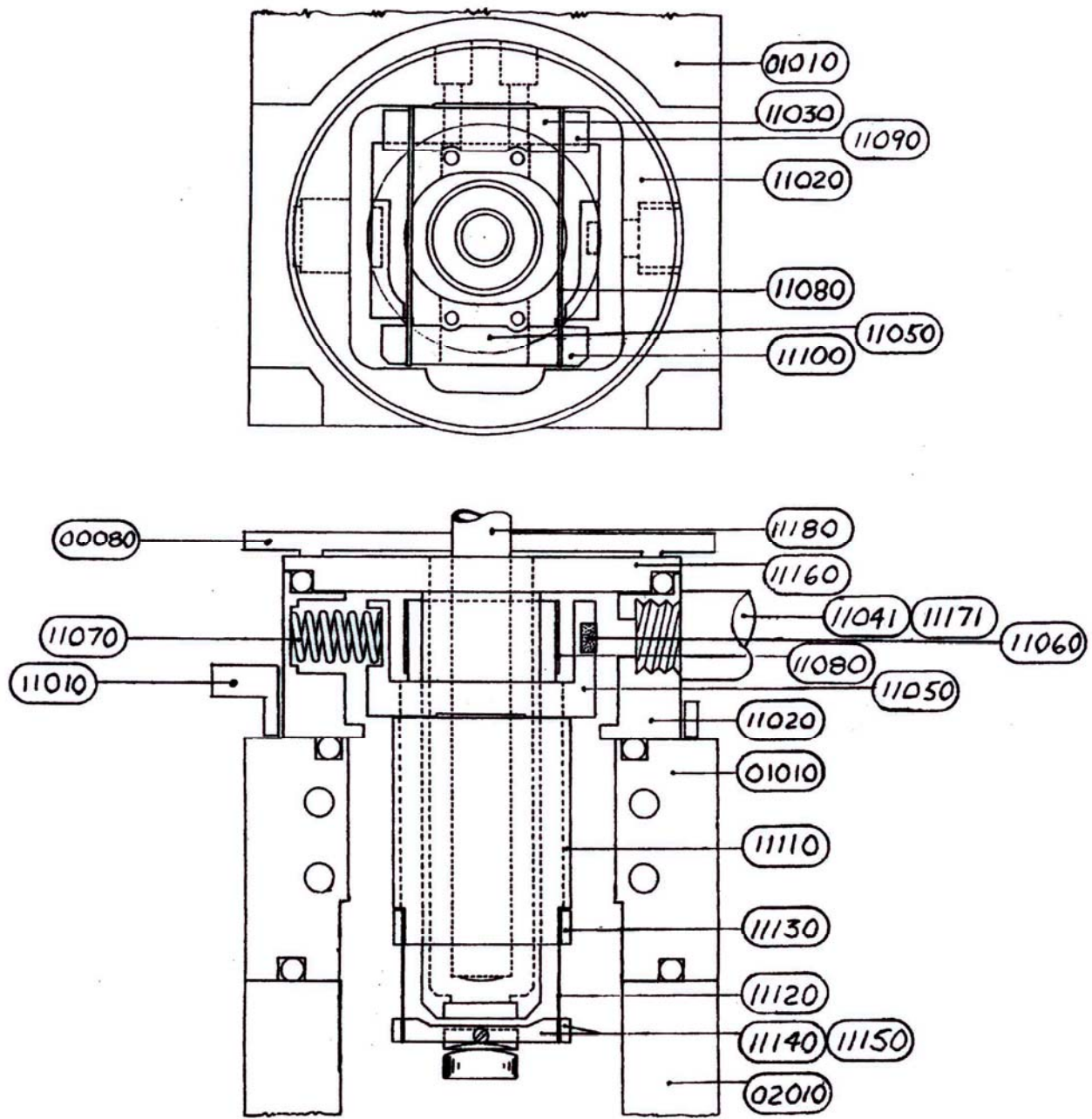


Figure 15. Assembly drawing of FRICTION DEVICE.

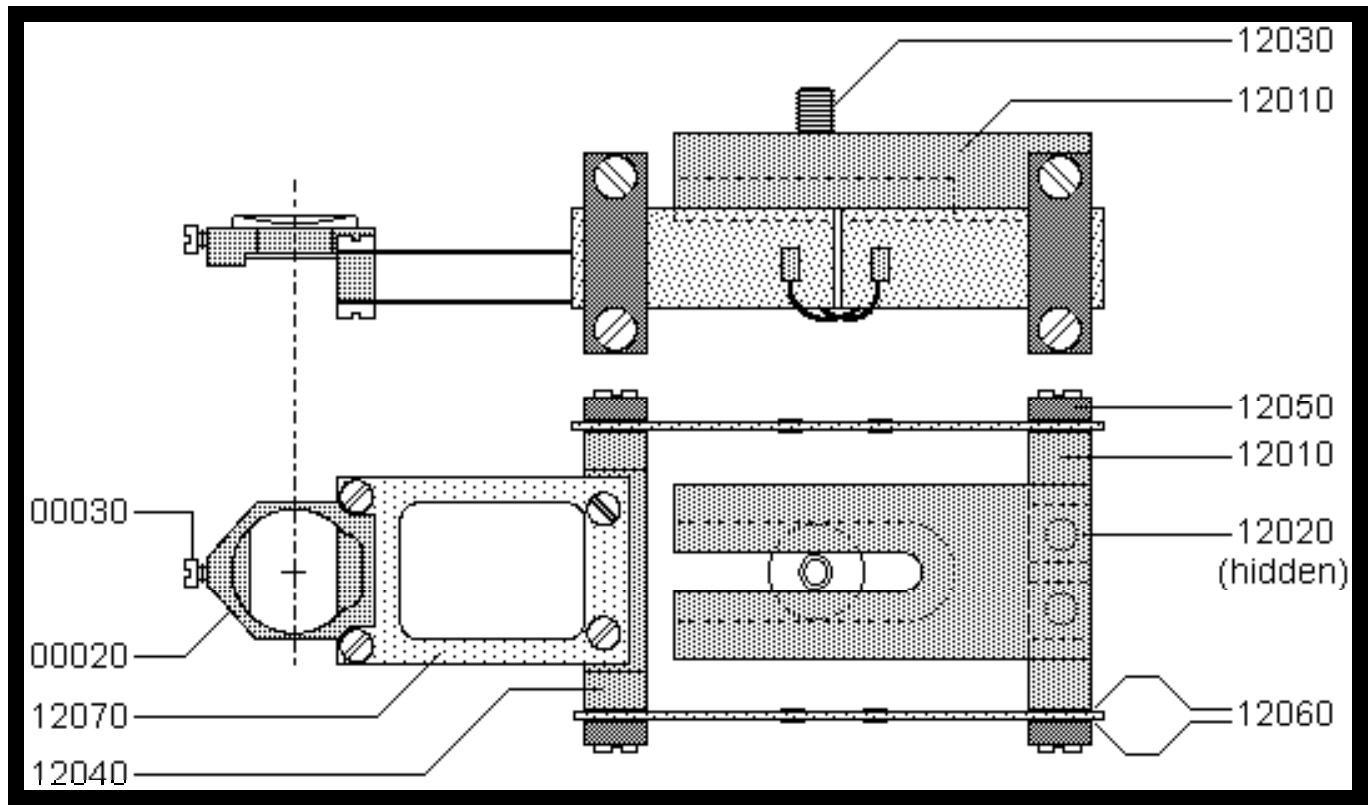


Figure 16. Assembly drawing of BIMORPH SLIDER (extended bimorph slider now available – see pages 220 and 223).

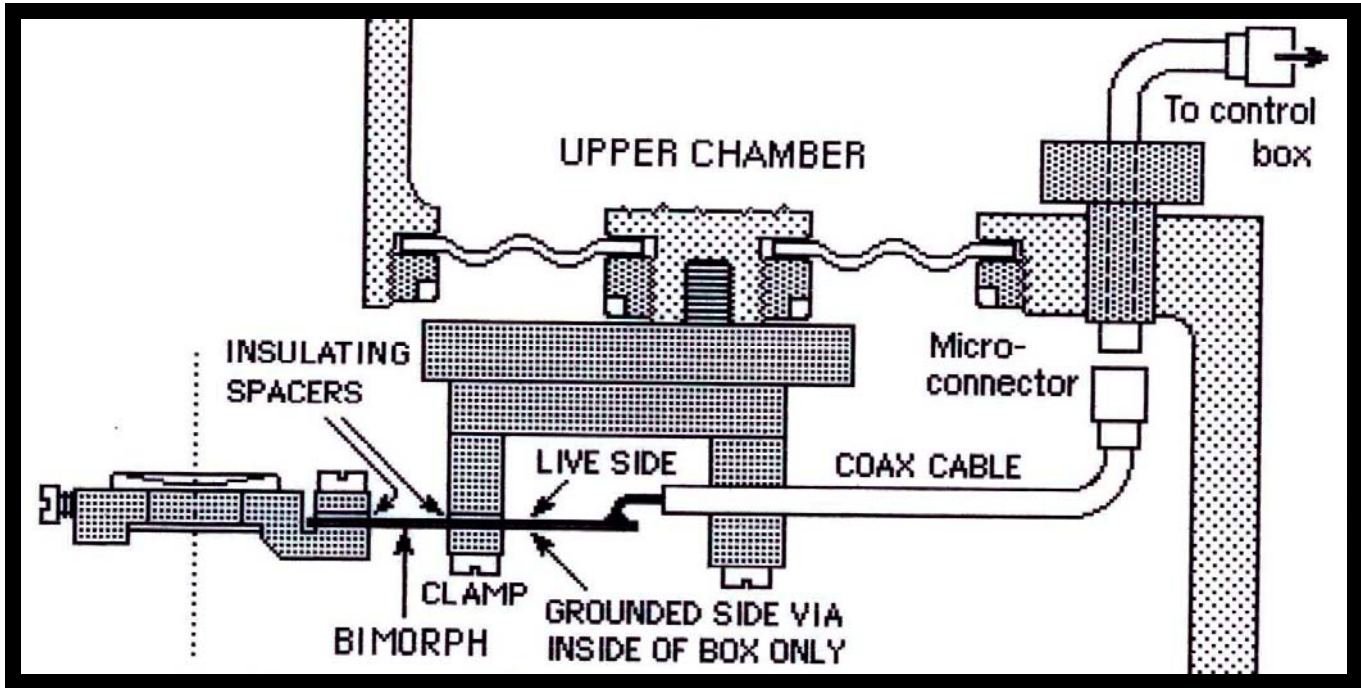
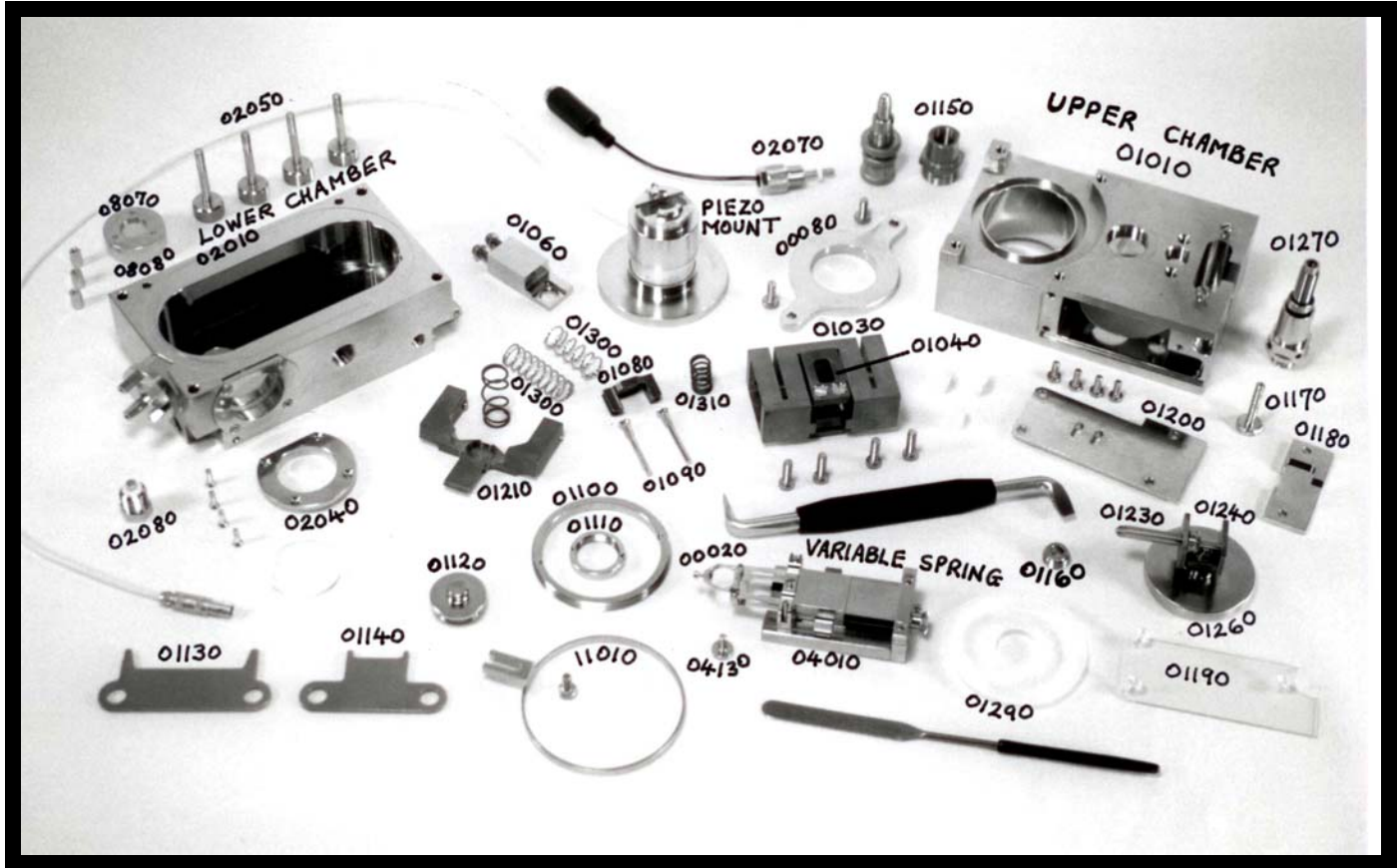
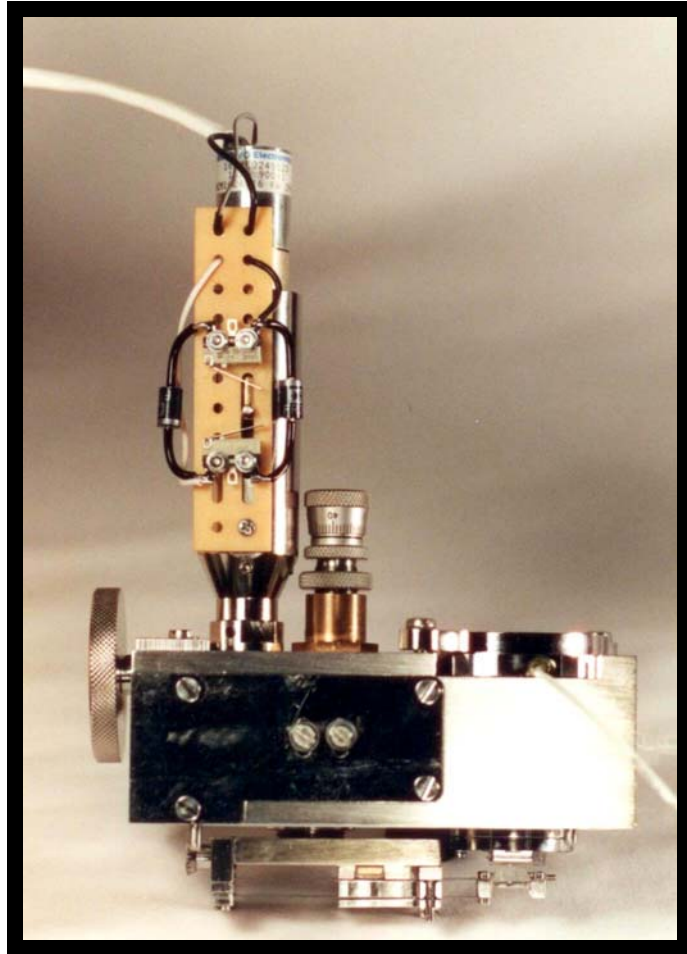
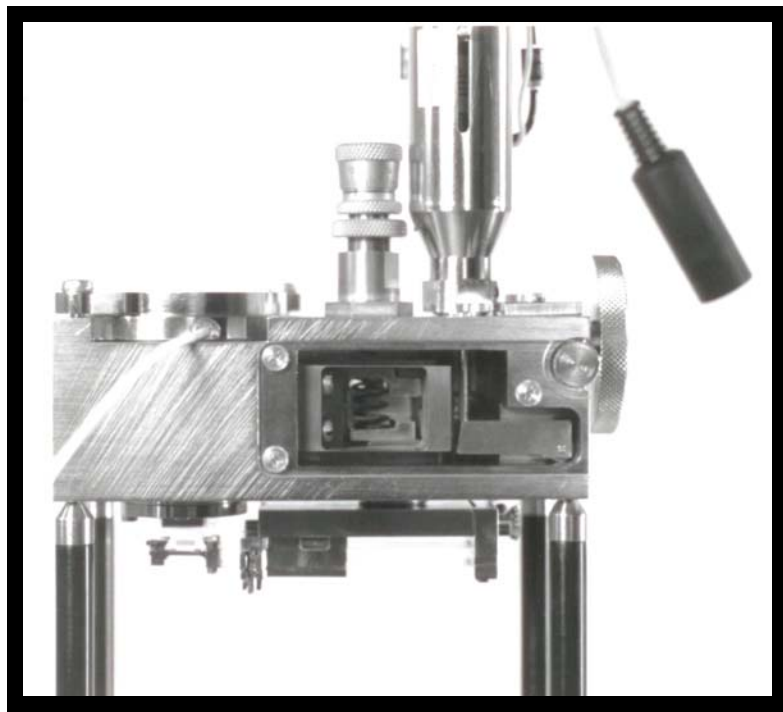


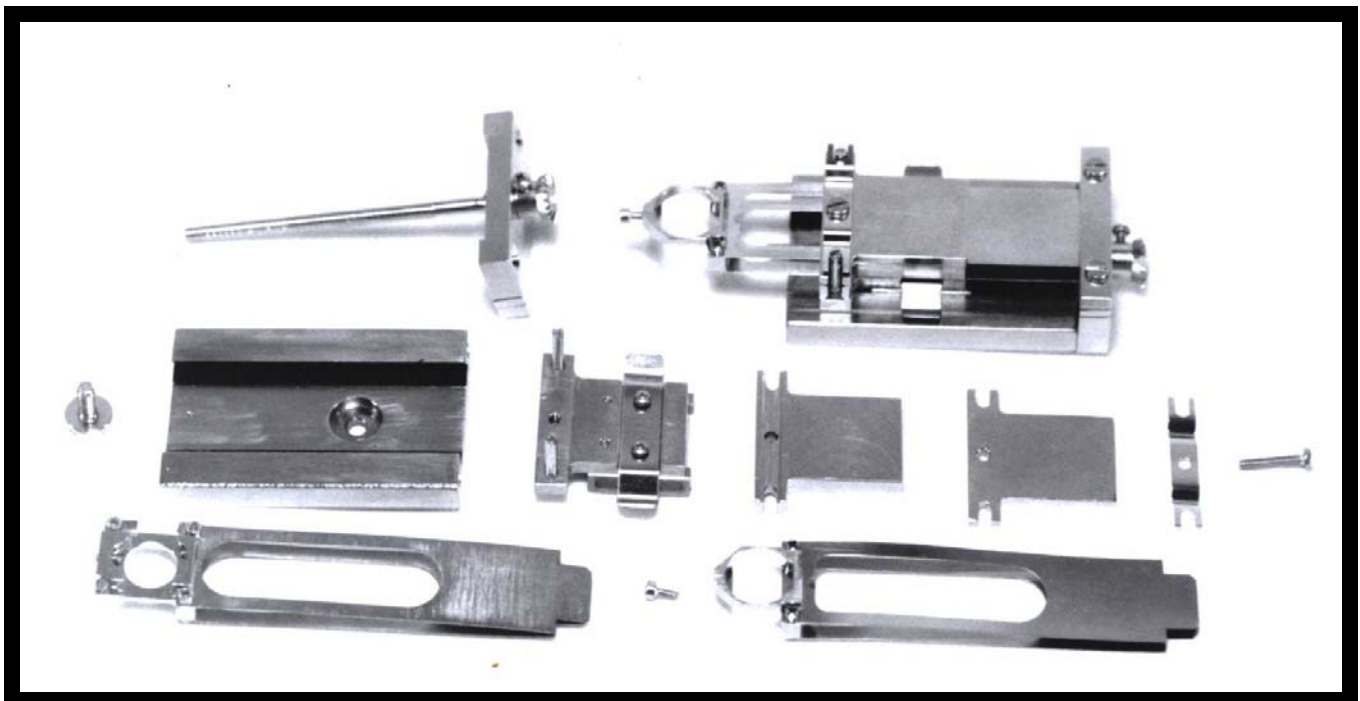
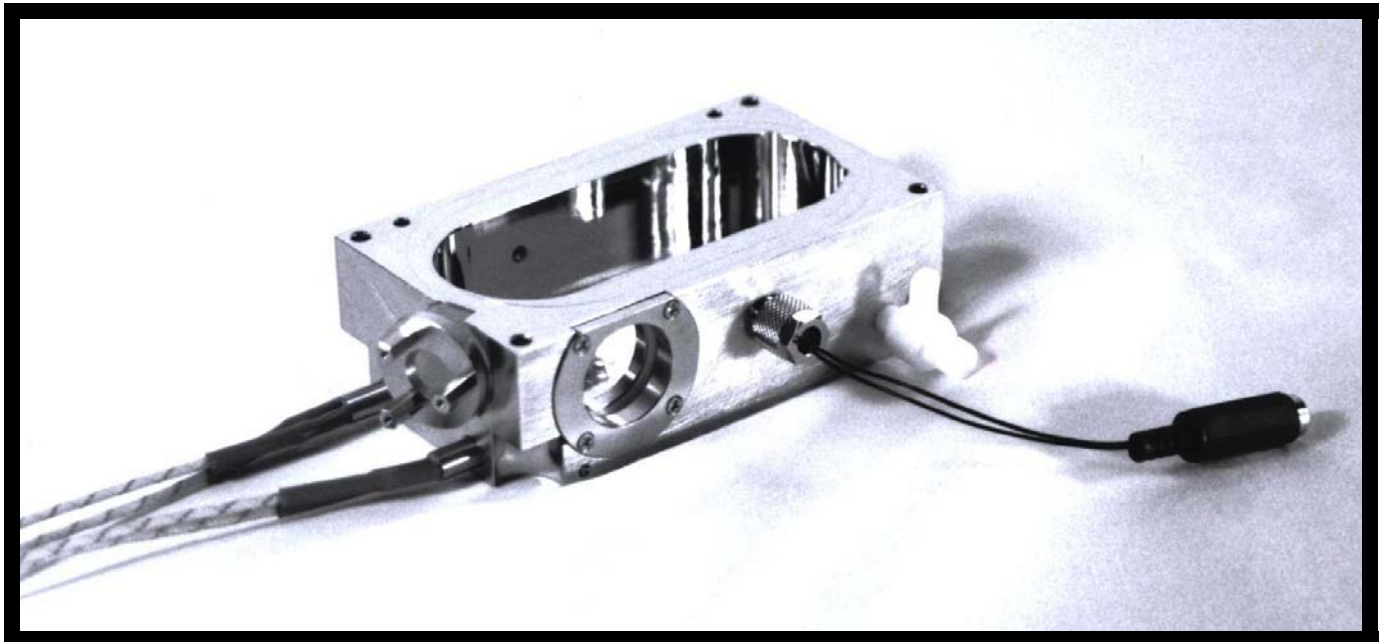
Figure 17. Assembly drawing of BIMORPH VIBRATOR.



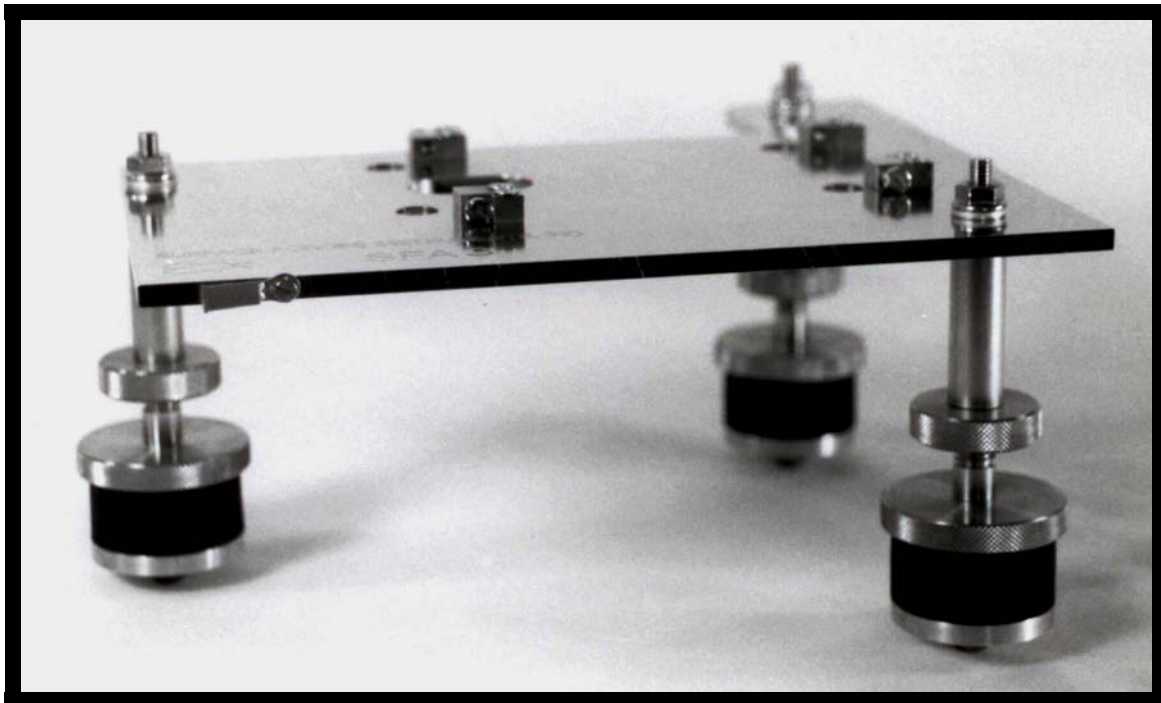
Figures 18. Photographs of dismantled BASIC UNIT showing key parts.



Figures 19. Photographs of UPPER CHAMBER.



Figures 20. Photographs of LOWER CHAMBER and VARIABLE SPRING.

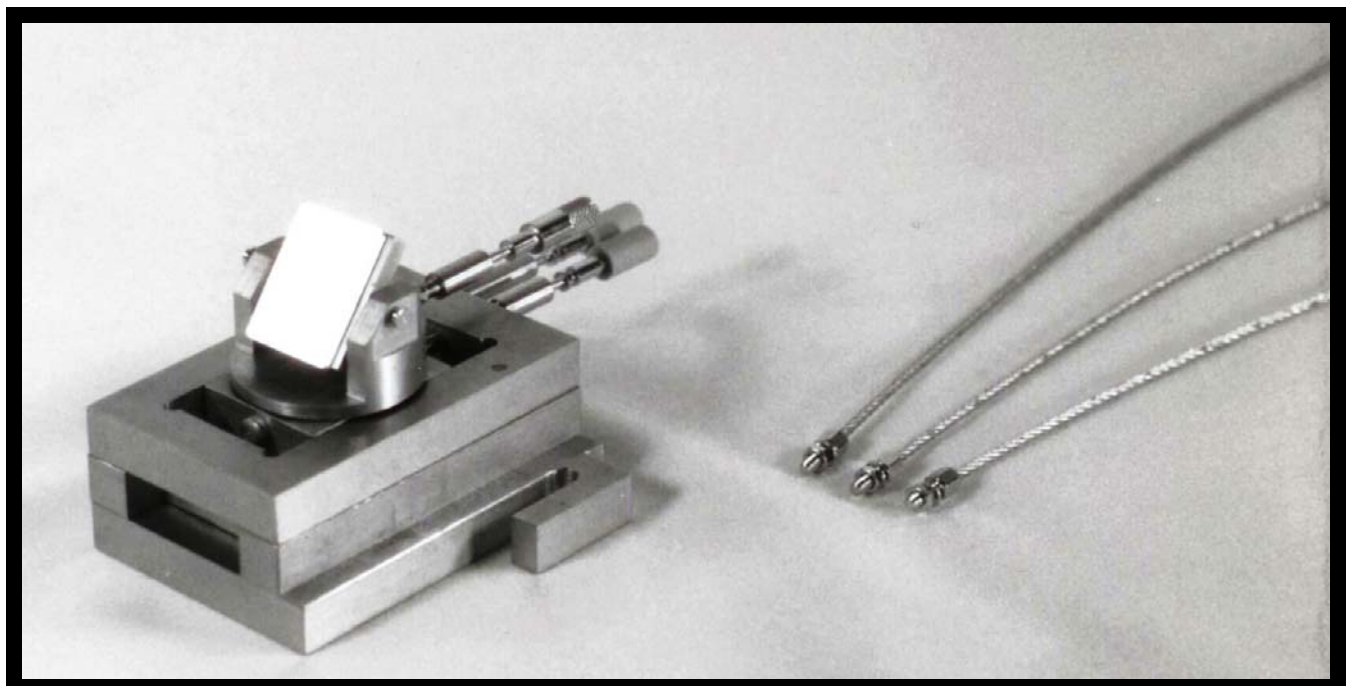


Figures 21. Photograph of BASE.

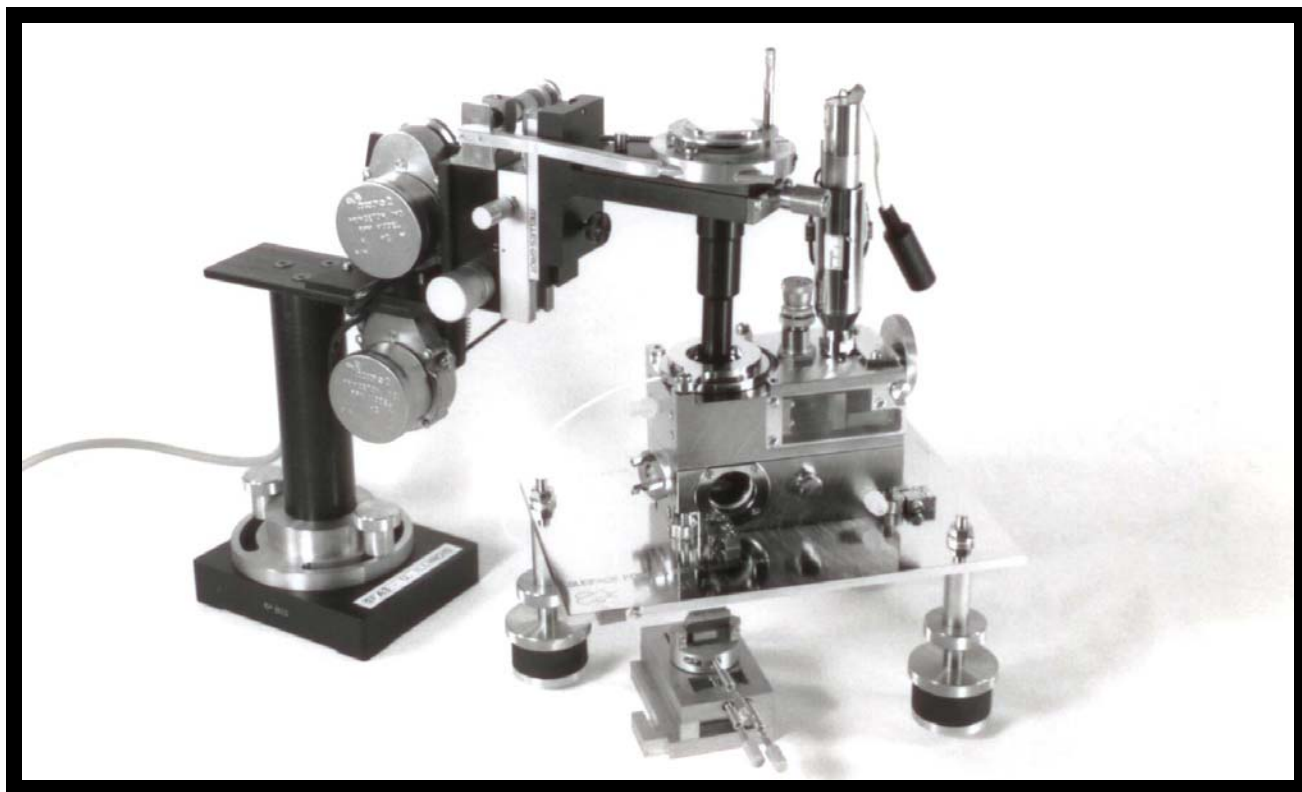
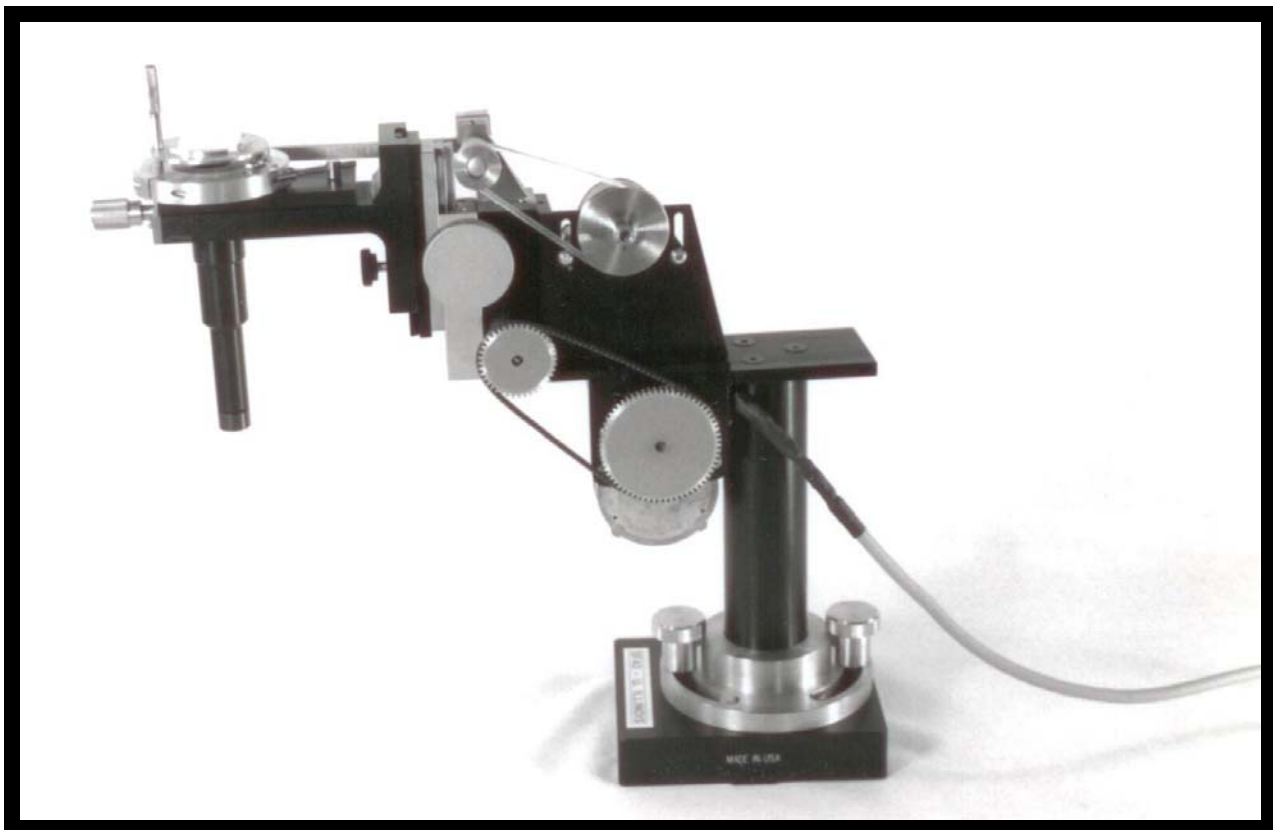
The small screw hole on the front of the base plate is for electrically connecting the apparatus to earth (ground).



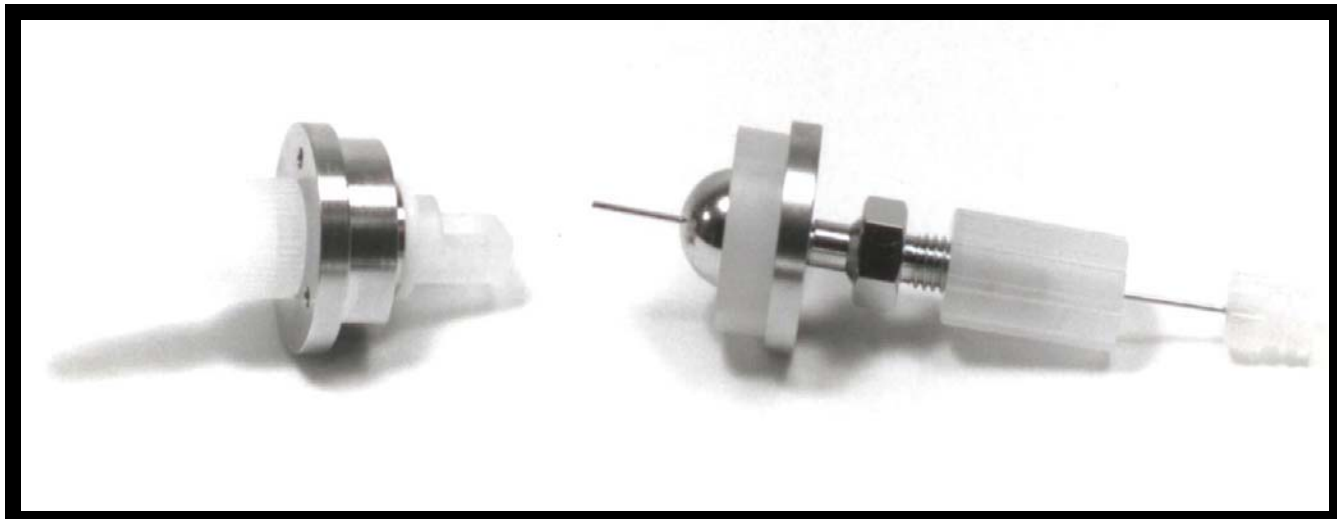
Figures 22. Photograph of PIEZO MOUNT.



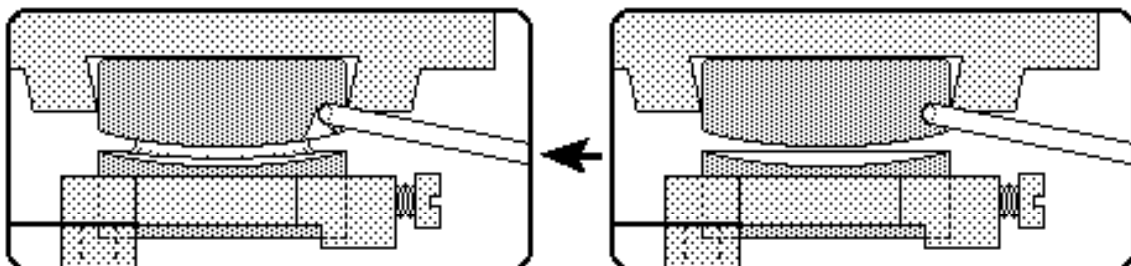
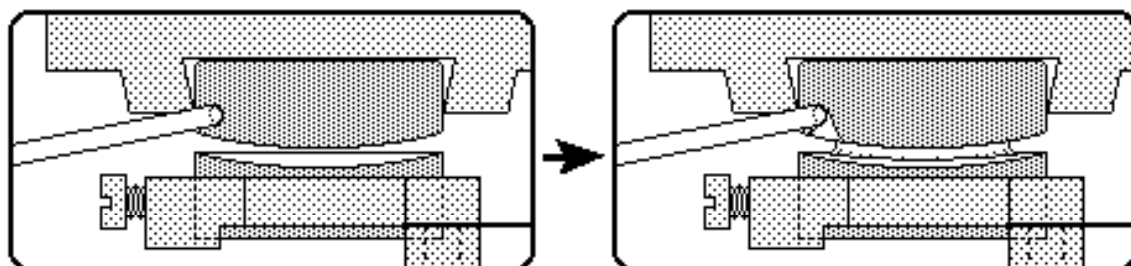
Figures 23. Photograph of MIRROR (alternative design now available and recommended).



Figures 24. Photograph of OPTICS STAND (updated and improved design now available).

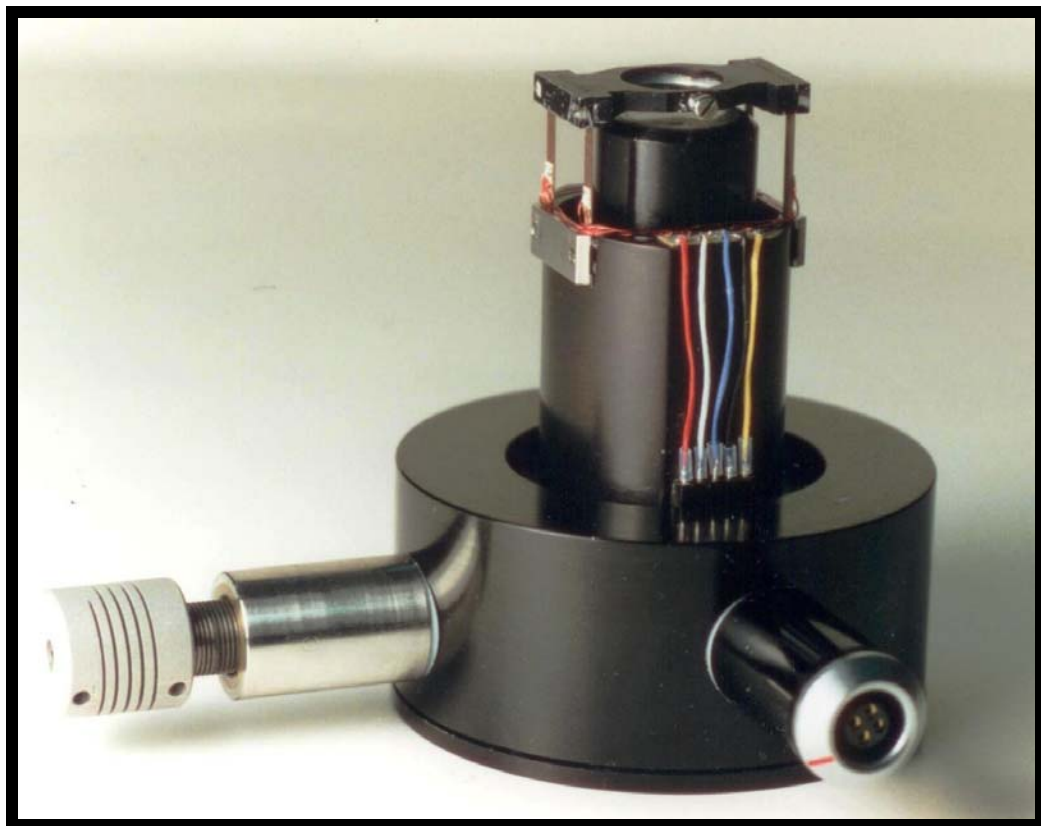


(A)

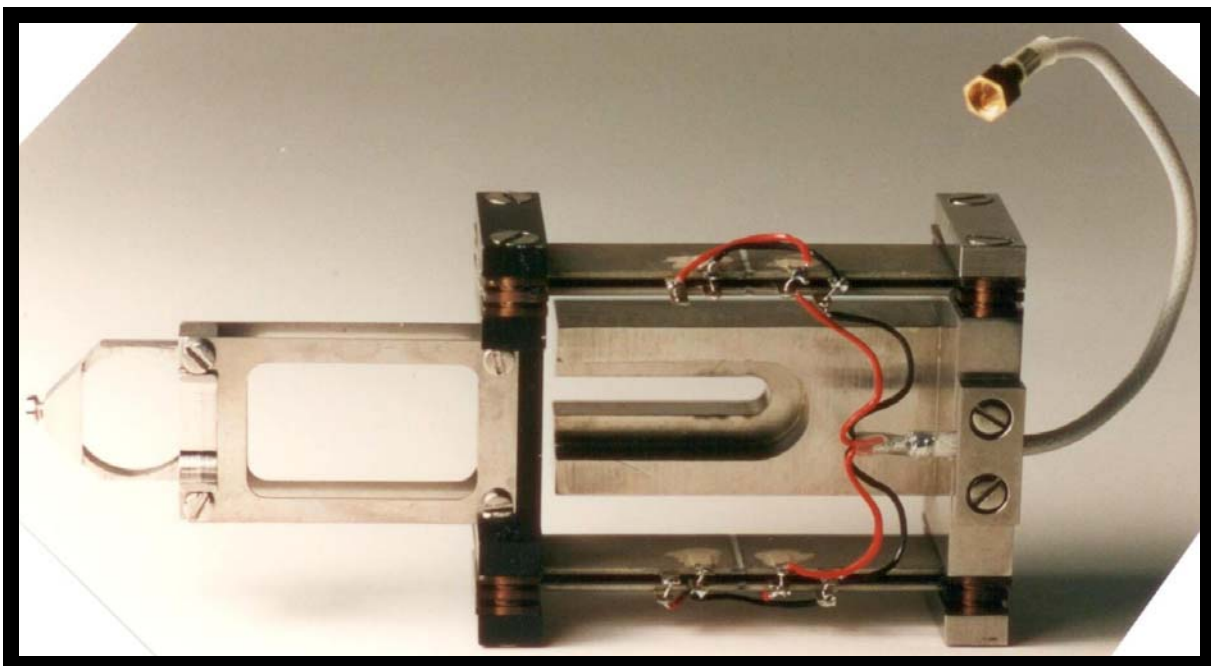
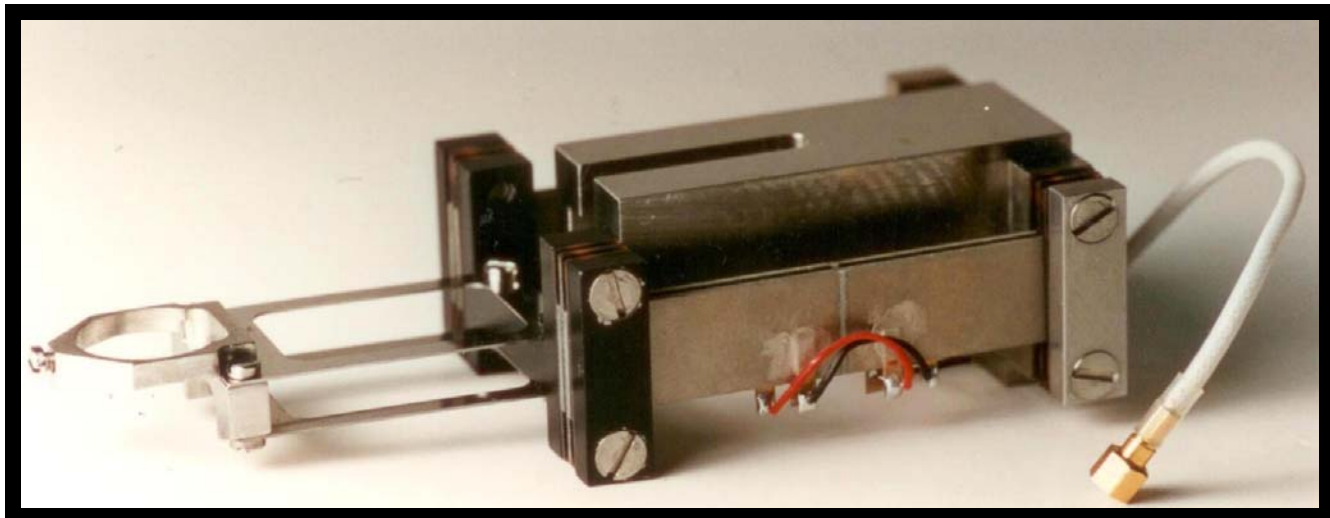


(B)

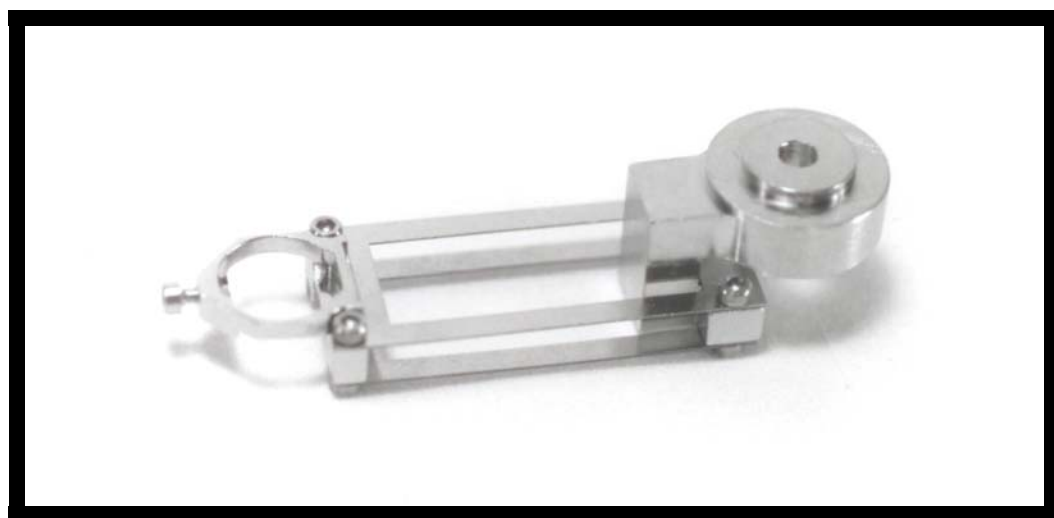
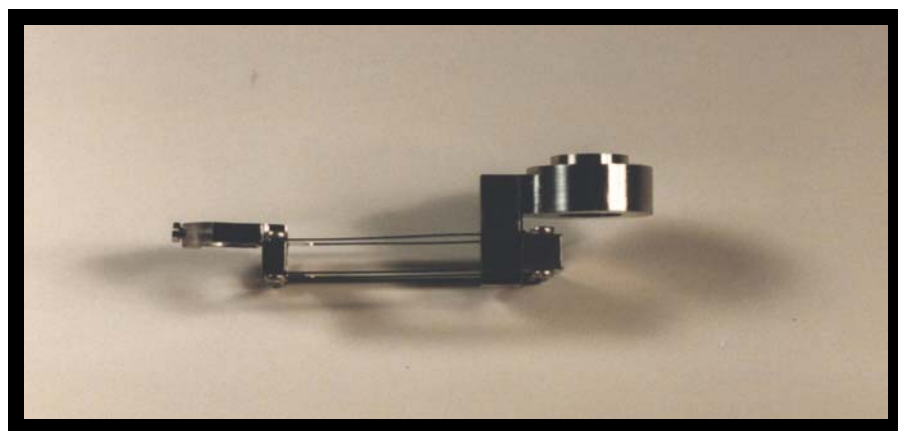
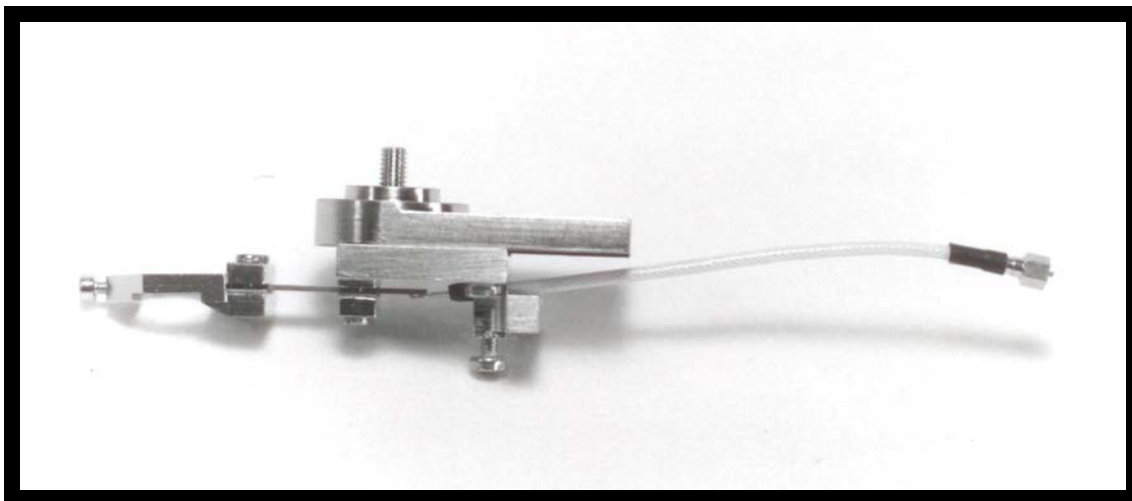
Figures 25. (A) Photograph of SYRINGE INJECTOR (other designs available). (B) Best way to inject droplet of liquid between the surfaces in “droplet experiments”: allow the liquid to flow down into the gap, where it will collect as a bridge at the center and be held there by capillary forces (so long as the contact angle is less than 90° ; otherwise the droplet will be forced out from the center). The syringe needle could be inserted from the right or left sides, depending on the SFA (SFA 3 or SFA 2000), and through which hole it is being inserted (the thermistor hole, the vapor pressure bath hole, etc.).



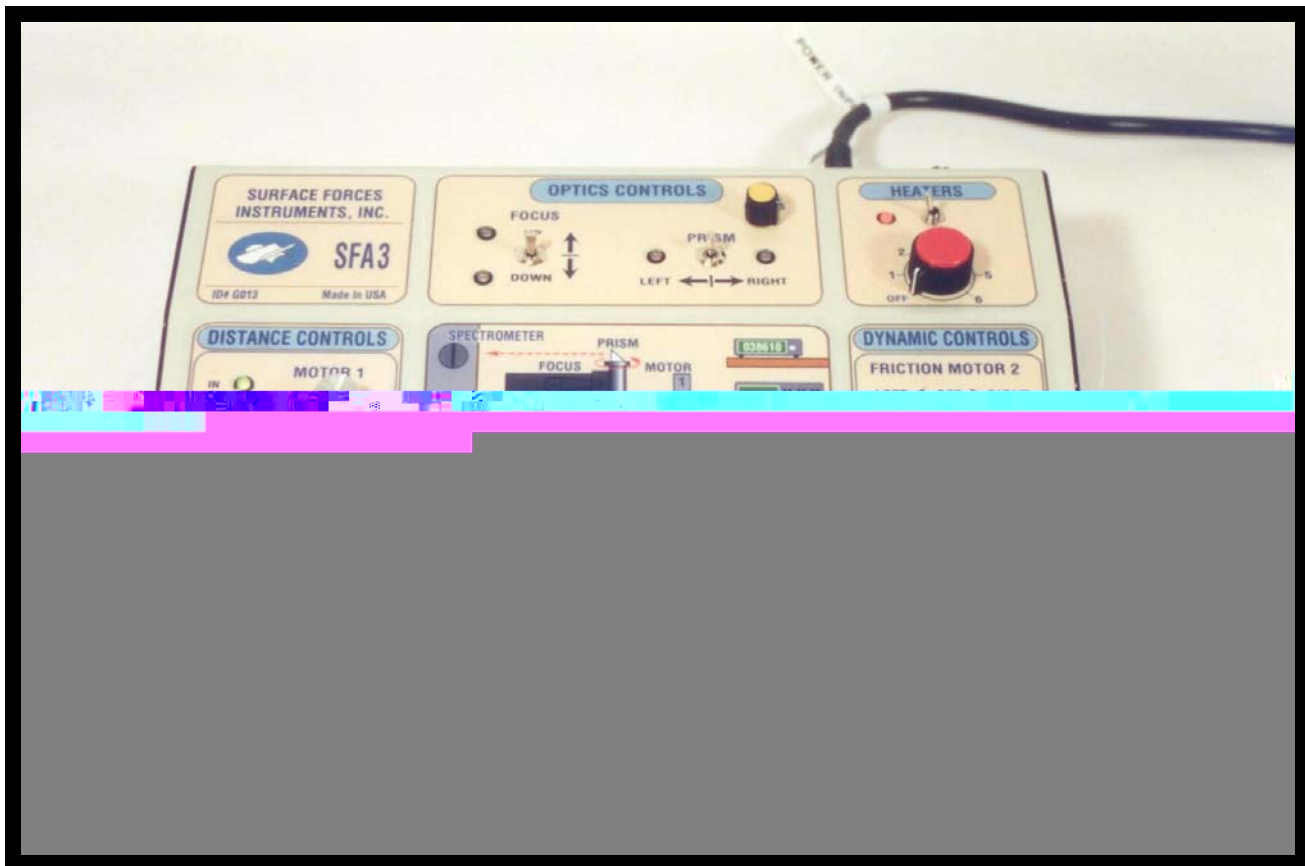
Figures 26. Photograph of FRICTION DEVICE and removable/exchangeable barrel.



Figures 27. Photo of BIMORPH SLIDER (now replaced by extended bimorph slider – see page 223).



Figures 28. Photograph of BIMORPH VIBRATOR and FIXED SPRING MOUNT.



Figures 29. Drawings and photographs of CONTROL BOX (front and back, and inside wiring).

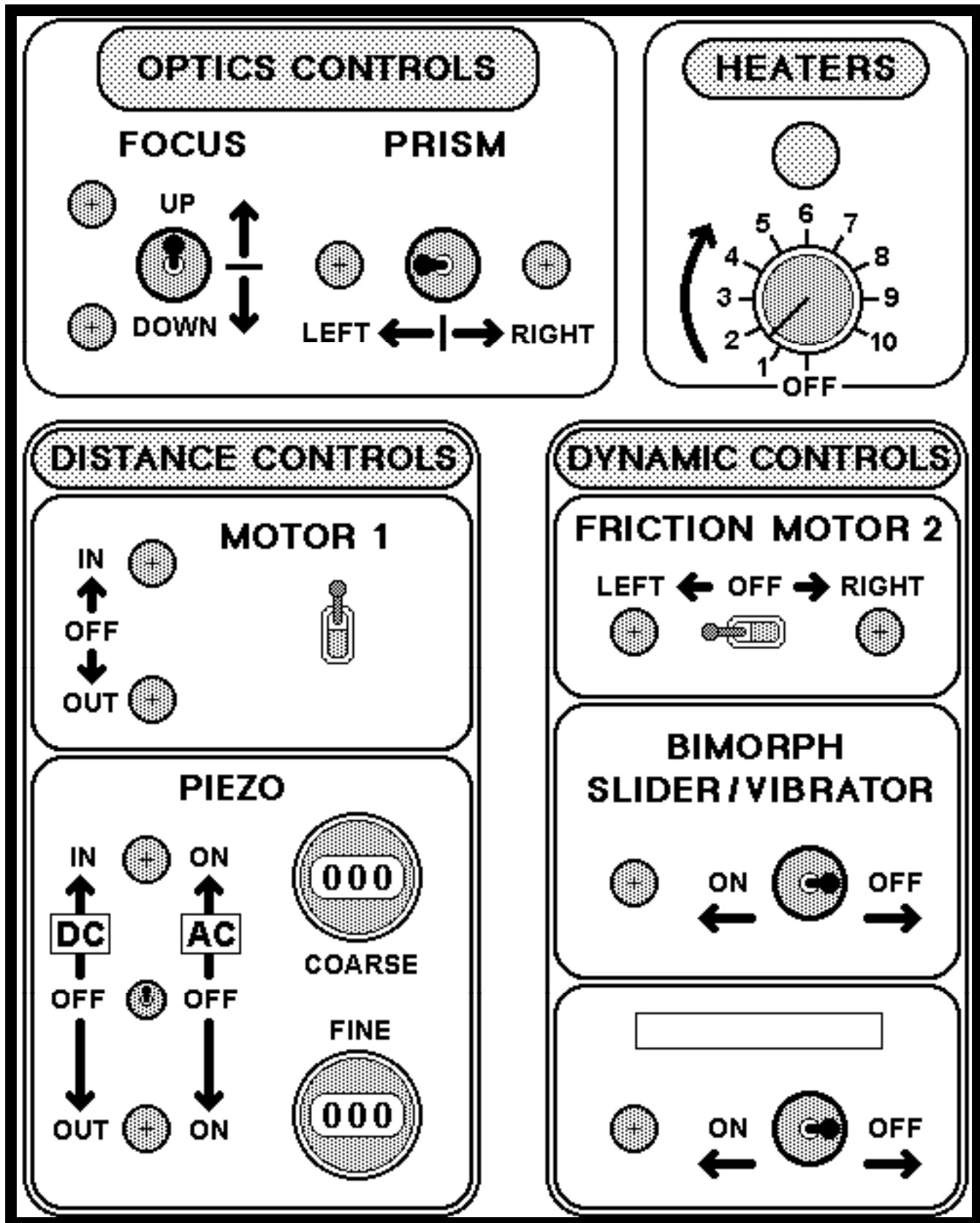


Figure 29a. CONTROL BOX – Front panels.

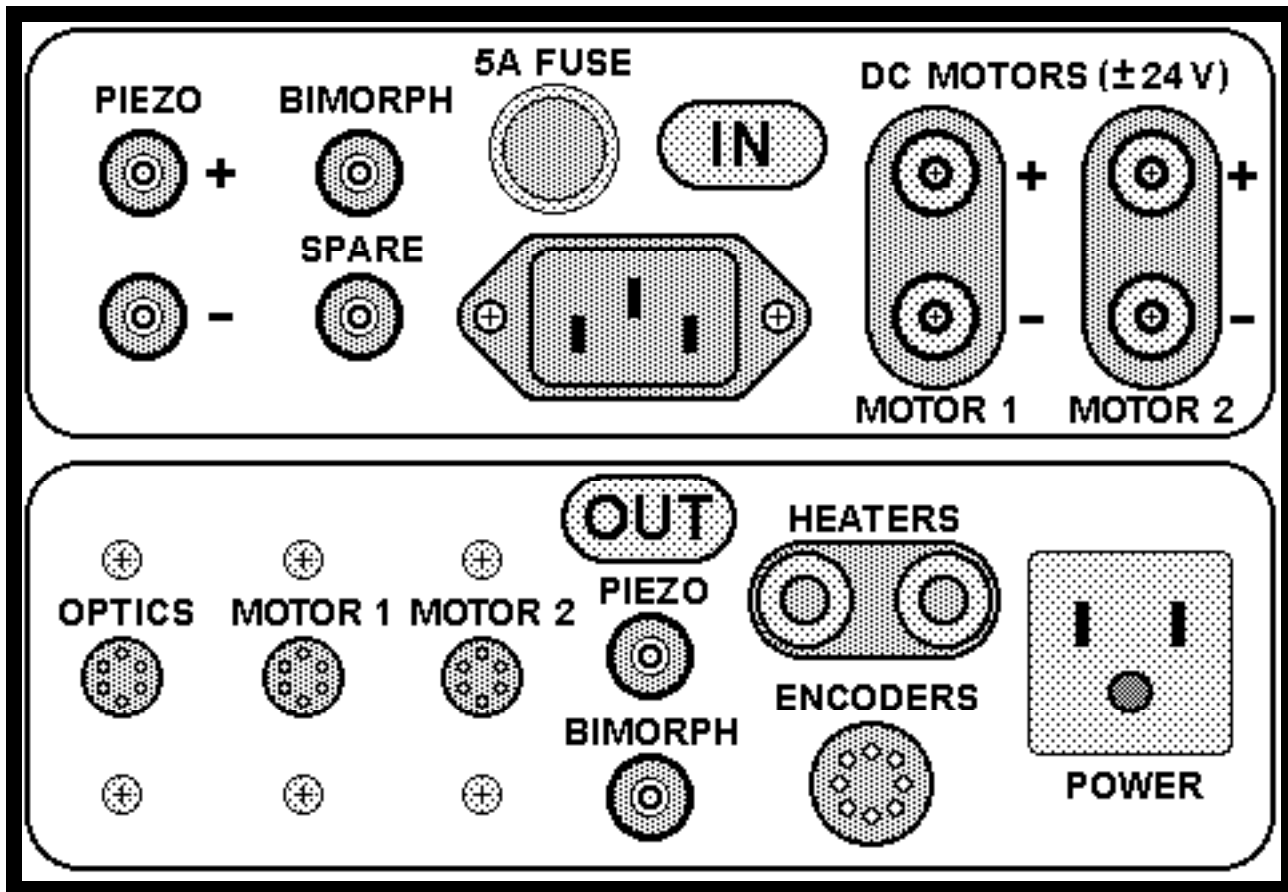
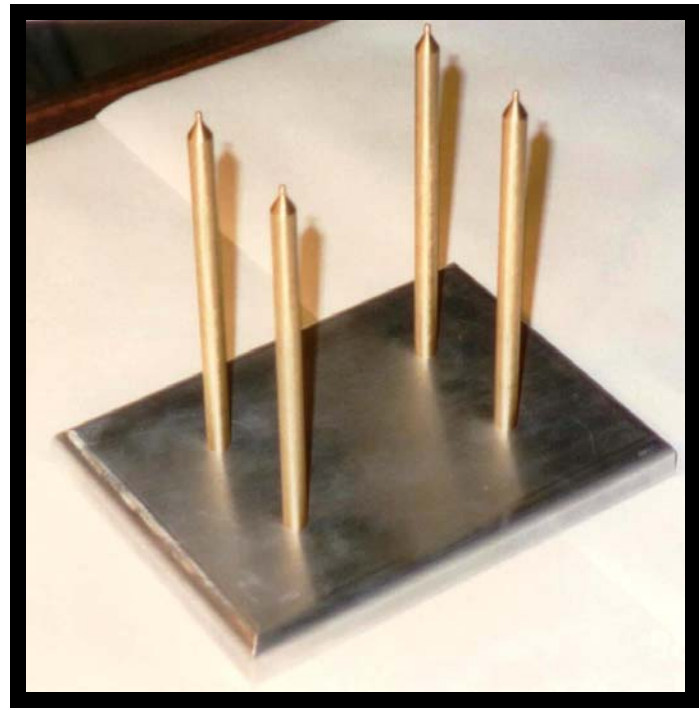


Figure 29b. CONTROL BOX – Back INPUT and OUTPUT panels. Power input and output voltages are 110V @ 60Hz for the US, 220V @ 50Hz for Europe, and 100V @ 50 Hz for Japan. Each control box has been adjusted for the local mains voltage supply.

Earth loops / ground loops

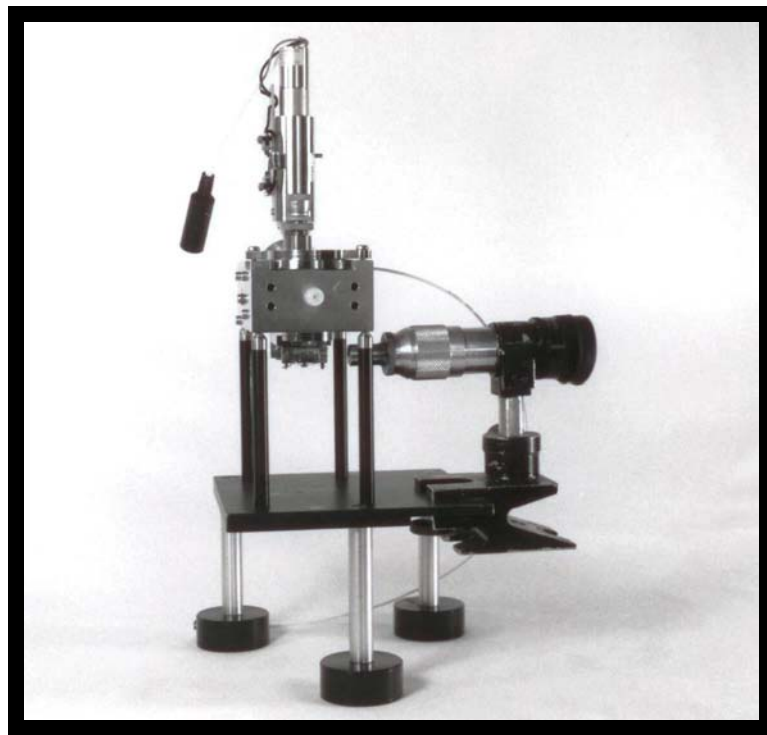
When wiring up the control box and other instruments to the apparatus, one must never earth the apparatus in more than one place or else one is liable to pick up electric noise from "earth loops" or "ground loops" (you may read up on this important phenomenon in any electrical engineering handbook). The earthing contact for the apparatus is a small hole on the front of the base plate, which should be used as the common terminal for connecting the apparatus and all electric units requiring a ground terminal (piezos, bimorphs, motors, etc.). Thus, the outer surfaces of the Piezo Mount is earthed through the electric contact of its housing with the apparatus when it is bolted into place (check that all conducting metal parts of the piezo housing are indeed electrically connected to the outer *earthed* wall of the piezo tube but not the inner *live* wall). Likewise, all bimorphs should have their earthed sides connected to the steel wall of the apparatus and not independently through the outer shield of its coaxial cable.



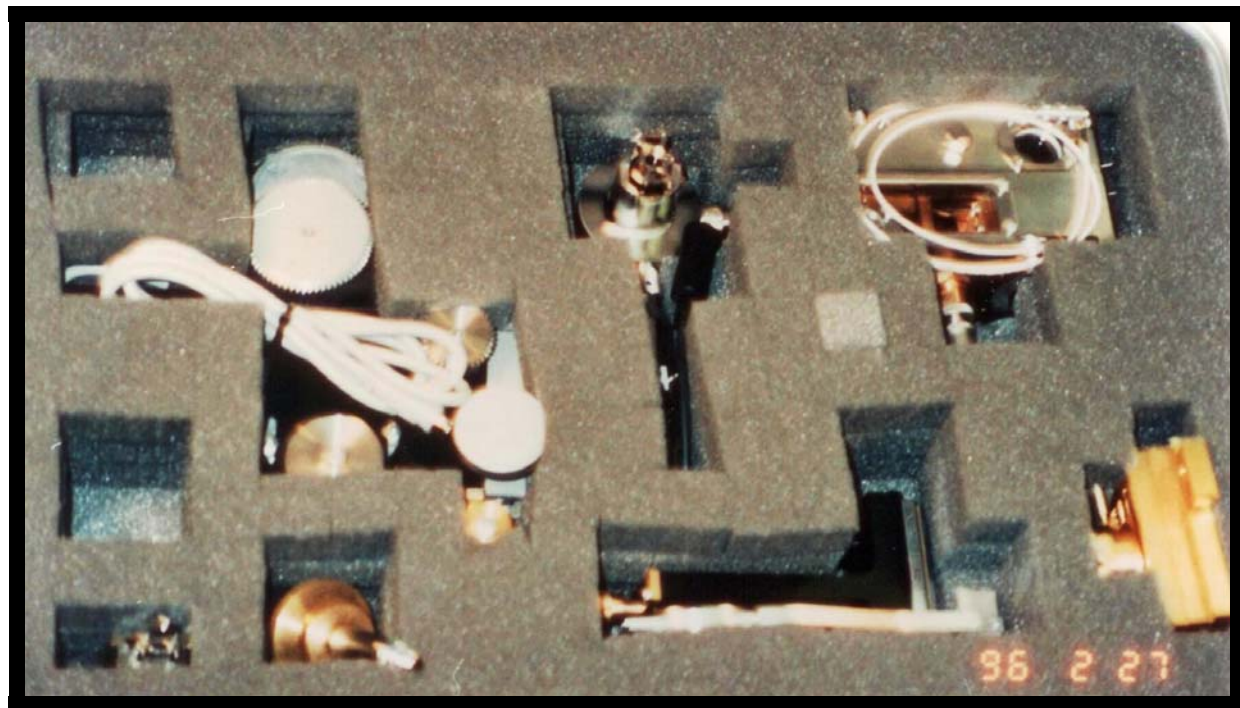
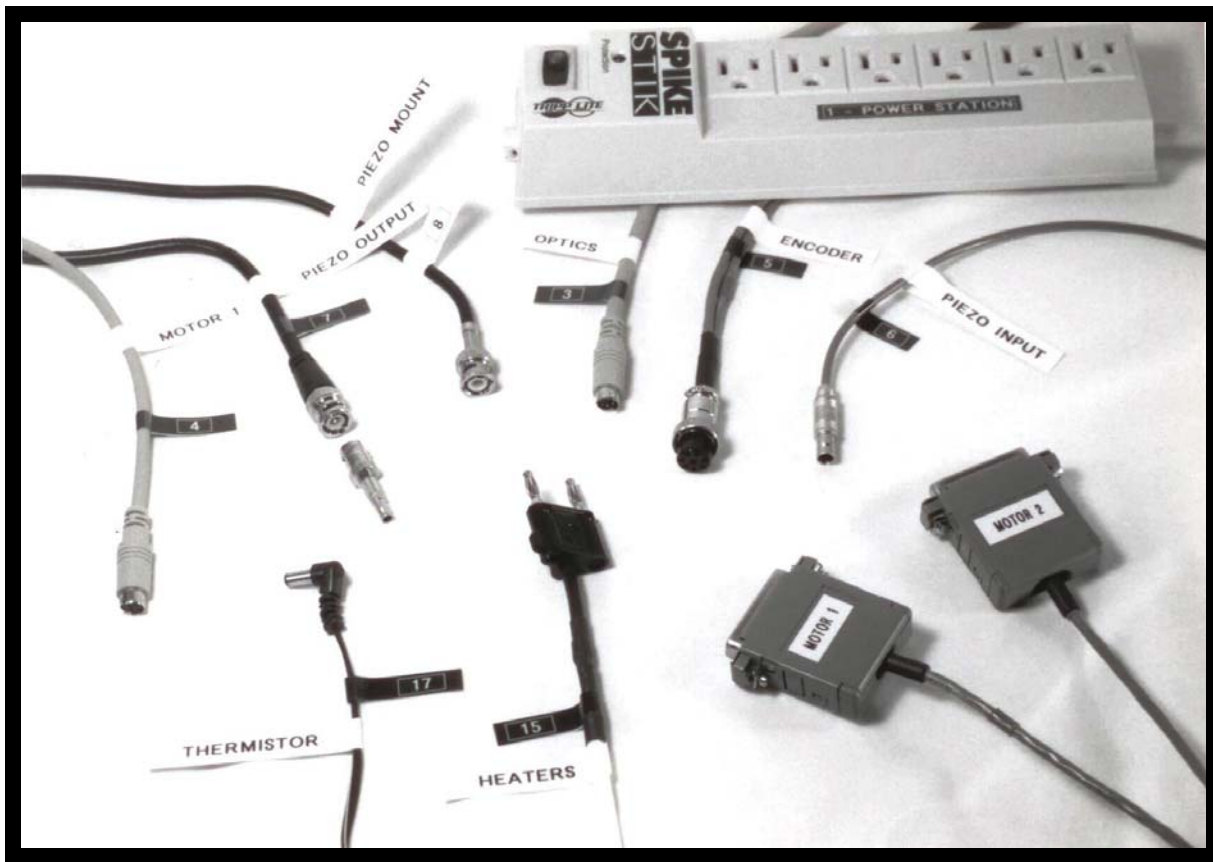
**Figures 30. MISCELLANEOUS PARTS, SUPPLY ITEMS, ELECTRIC CABLES,
ASSEMBLY TOOLS, LUER FITTINGS, etc.**



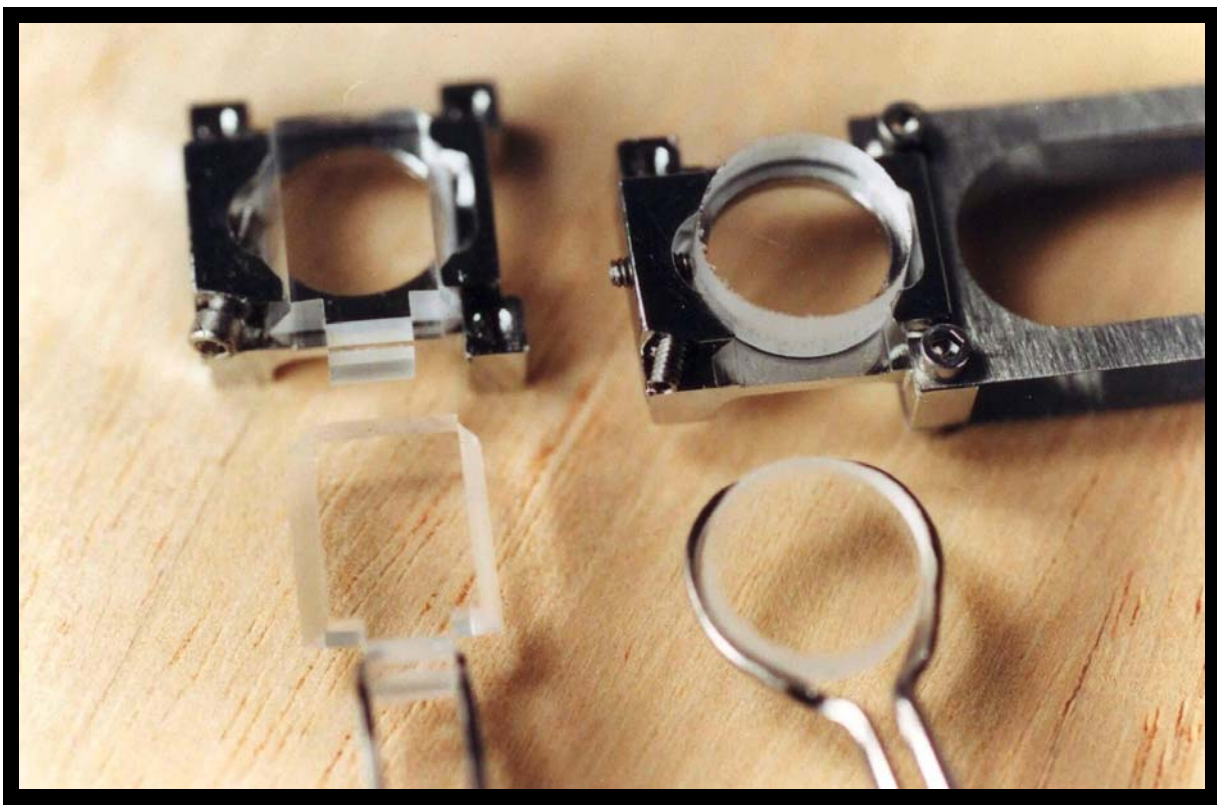
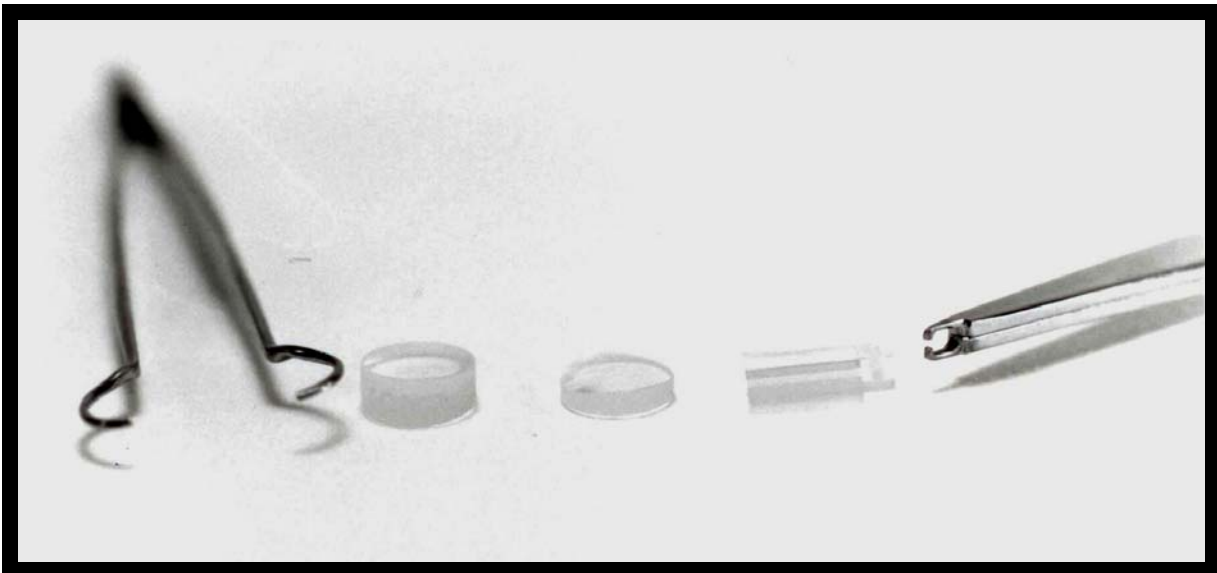
**Figures 30 (continued). MISCELLANEOUS PARTS, SUPPLY ITEMS,
ELECTRIC CABLES, ASSEMBLY TOOLS, LUER FITTINGS, etc.**



Figures 30 (continued). MISCELLANEOUS PARTS, SUPPLY ITEMS, ELECTRIC CABLES,
ASSEMBLY TOOLS, LUER FITTINGS, CALIBRATING TRAVELLING
MICROSCOPE for calibrating spring stiffnesses, etc.



Figures 30 (continued). MISCELLANEOUS PARTS, SUPPLY ITEMS,
ELECTRIC CABLES, ASSEMBLY TOOLS, LUER FITTINGS, etc.



Figures 30 (continued). MISCELLANEOUS PARTS, SUPPLY ITEMS,
ELECTRIC CABLES, ASSEMBLY TOOLS, LUER FITTINGS, etc.

HANDLING THE SFA: CLEANING AND ASSEMBLY (BASIC UNIT ONLY)

Assembly/disassembly between experiments

When not in use, i.e., between experiments, the Basic Unit can be left assembled, or it can be partially disassembled into its different UNITS, or selected UNITS can be fully disassembled into their individual PARTS. All UNITS are already assembled on delivery, and most will not require any special attention, such as disassembly, between experiments. However, it is wise to check that they are functioning properly before each new experiment (these checks are described in Section 2). Only the LOWER CHAMBER and VARIABLE SPRING UNIT need to be regularly disassembled, cleaned (each part at a time), and reassembled before each new experiment, although this may not be necessary if a series of similar experiments are being conducted one after the other, for example, if each experiment involves filling the apparatus with the same liquid or solution. In this case, simply draining the box and flushing it out with clean ethanol a few times should be sufficient. The apparatus can then be left, closed and filled with ethanol, until the next experiment. As a general rule, full disassembly of a UNIT should not be necessary between experiments unless (1) a thorough cleaning is called for, as might occur after an experiment with strongly adsorbing compounds or after an accidental spill, (2) the internal stainless steel surfaces need to be passivated – a type of 'servicing' that is recommended once every 6–12 months depending on the corrosiveness of the aqueous solutions used, or (3) a faulty part needs to be fixed or replaced.

The following small tools and glassware are needed for cleaning and assembly, some of which are shown in Figure 30 on pages 46 and Figure 31 on page 53 (starred items ★ are supplied with each SFA). Before proceeding, make sure that all tools needed for cleaning and/or assembly are clean and ready for use inside the laminar flow cabinet.

- ★ SFA3 supply items, assembly tools kit, and electric cables.
- ★ Luer fittings and stop-cocks for inlets and outlets.
- ★ Syringes and needles.
- ★ Thermistor.
- ★ Micrometers.
- ★ O-rings.
- ★ Screws, nuts and washers.
- ★ Spatulas (both Teflon-coated and stainless-steel).
- ★ Various miniature cleaning brushes (toothbrush-type, pipe-cleaning type).
- ★ Screw driver set, including Philips-head, hex-head and nut-head types.
- ★ Allen keys: metric and English.
- ★ Stainless steel and Teflon-tipped tweezers and forceps – various sizes and types.

★ Spanners and wrenches.

Acetone.

Ethanol (clean liquid in sealed bottle or squirt bottle).

Ethanol gun (pressure rinser).

Air gun: compressed clean dry nitrogen gas gun (compressed gas should come from liquid nitrogen tank, not compressed gas cylinder, and all connecting tubes should be made of clean Teflon tubing or stainless steel).

Beakers: 2 large flat-bottomed (6" or 15 cm diameter).

Beakers: 8 small (100-200 ml).

Petri dishes (can also be used as beaker covers).

Beaker covers for all of the above (petri dishes will do).

Lint-free absorbing tissues.

Small files and de-burring tools.

Passivation of stainless steel (SS 316) parts

All internal steel parts have already been passivated in 30% conc. HNO₃. Repassivation of those steel parts whose surfaces come into contact with the experimental solution is recommended every 12 months or more often if experiments routinely involve strong aqueous salt solutions, especially chlorides, or if the internal surfaces have become scratched. To passivate, immerse the stainless steel parts (but *not* any protruding electrical connections such as the piezo crystal) in 30% HNO₃ at 60°C for 30 minutes (note: Kel-F is inert to conc. HNO₃), then remove all excess acid by thorough washing in clean distilled water.

Degreasing, deburring and sonication

If some parts have become visibly dirty or greasy, for example, if a part has been sent to the machine shop, a degreasing in acetone is recommended. Use small scrubbing brushes if necessary, making sure that the bristles are not dissolved by acetone. This could be followed by sonication, especially if new thread holes have been tapped. All threaded holes and other cavities should have any debris or burr finally removed by air-blasting or squirting ethanol into the holes using an ethanol gun.

Cleaning of fully disassembled parts before assembly

The following describes the recommended cleaning procedure of individual parts. All cleaning and drying should be done in a clean air, dust-free atmosphere, e.g., in a laminar flow cabinet.

First, thoroughly clean all glassware and tools (glass beakers, stainless-steel forceps, etc.) with clean ethanol (absolute alcohol). Carefully place all non-electric, non-piezo parts into ethanol-filled glass beakers. The larger parts may all be placed into the 15 cm diameter flat bottomed beaker. The smaller parts, including small screws and O-rings, should be placed into well-marked smaller beakers. You may wish to identify different beakers for the small parts, otherwise you may confuse different screws and O-rings that look similar. Use Teflon-coated tweezers to pick up the parts and carefully place (not drop)

them into the beakers. When handling the parts, be particularly careful not to scratch any of the smooth polished surfaces, particularly the O-ring grooves and sealing surfaces. Teflon O-rings need particular care when being handled.

While still immersed in ethanol, scrub metal parts with a *soft* chemically inert brush (fine toothbrush type). Use the miniature pipe-cleaning type brushes to clean inside screw holes. Note that vigorous scrubbing should be avoided since this will remove the protection afforded by the passivation layer causing possible contamination by Cr³⁺ leaching. One by one, remove parts from beaker, squirt ethanol from a hand-held ‘ethanol gun’ directly onto all sides and into holes of each part. Direct the ethanol jet outwards, being careful to ensure that the reflected ethanol spray does not land inside the laminar-flow cabinet or on surfaces that need to remain clean. When all sides of a part have been squirted, place the part in a second ethanol-filled beaker. Cover the beakers, then cover everything with a transparent glass globe (Figure 31) and leave to ‘soak’ until ready for assembly.

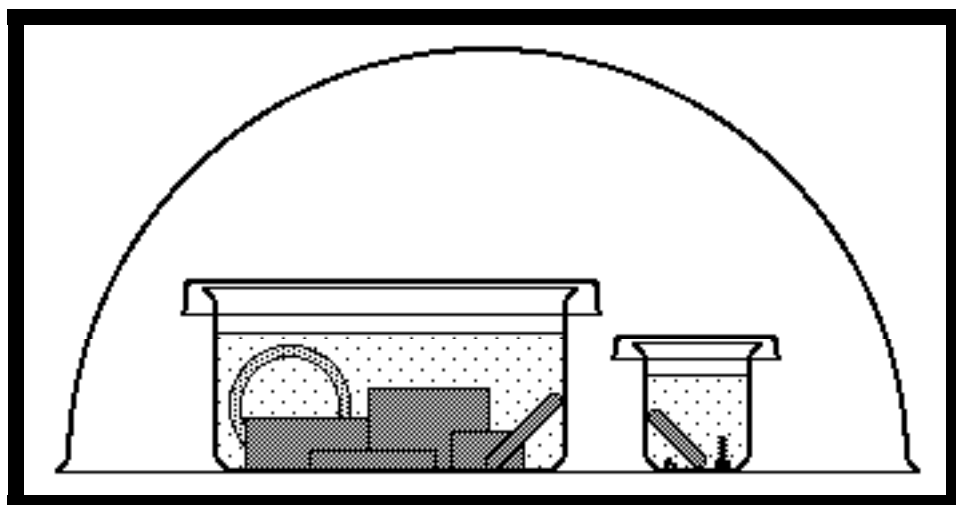


Figure 31. Soaking of metal, glass and Teflon parts in ethanol prior to assembly or between experiments. Round transparent perspex (plexi-glass) domes or flat-faced boxes are readily available from a number of suppliers (see table I).

Prior to assembly, remove each part from the beakers, rapidly blow-drying (especially the small holes and threads) with a nitrogen jet as they are taken out. Direct the nitrogen jet outwards, being careful not to blow away small parts. Note: blow drying is essential; if apparatus parts are simply left to dry by allowing the ethanol to evaporate, only the ethanol is removed leaving behind undesirable contaminants. By blowing the surfaces dry with a pressurized N₂-gun both the ethanol and contaminants are swept away quickly (the pressure rinser by Gelman is recommended; plastic squirt bottles are not since they suck in air contaminants continuously as they are used). Place dry parts on a clean stainless-steel surface or clean Teflon-coated paper sheet inside the laminar flow-cabinet. When all the parts (or units) have been cleaned and dried, proceed with the assembly, as described below.

Routine cleaning between experiments (requiring no disassembly)

The following describes the recommended cleaning procedure between experiments when full disassembly is not required, for example, during a series of experiments using similar liquids. In most cases, it is only necessary to rinse the apparatus a few times with ethanol: each time filling the apparatus then draining, aspirating and blow-drying, following the instructions given in the above paragraphs. For a more thorough cleaning, especially after experiments with polymer and surfactant solutions, a preliminary light scrubbing with soft brushes in ethanol or chloroform (CHCl_3) is recommended followed by soaking in chloroform, depending on the polymer (see above). When all units have been cleaned and dried, proceed with the next experiment. Alternatively, fill the chamber with clean ethanol, close the apparatus and all outlets (using the large glass disk instead of the piezo mount), and leave until required.

Greasing of micrometer threads

The two micrometers on the Upper Chamber and the one on the Friction Device do not come into contact with the internal chamber and so can be greased with any suitable low VP grease. For greasing the micrometers of motors 1 or 2, remove the motor housing by unscrewing it (you may have to loosen the limit switch board first). Note the position of the protruding shaft and then loosen the two set screws on the housing and gently unscrew the threaded micrometer shaft until it comes away from the housing. Clean the thread by rubbing with acetone or alcohol. Rub some grease between your thumb and index finger, then rub your fingers round the thread only. Reinsert shaft and lock back into place in exactly the same position as before. For greasing the Differential Micrometer, first remove the micrometer housing by unbolting nut 01150 (Fig. 7), then turn the top knob all the way until the small part comes out. Grease both threads separately. Don't over grease and don't use force in any of the above operations.

ASSEMBLY OF BASIC UNIT

Make sure that all tools needed for assembly are clean, dry and placed ready for handling inside the laminar flow cabinet (cf. Figures 30). Newly machined parts and screws may sometimes be difficult to fit together or screw into. This may be because a small piece of metal (burr) is still lodged in a hole or thread or screw head. Rather than force the parts together, use a small needle file or deburring tool to remove such pieces of metal until the parts fit together smoothly.

BASE (Figures 13, 21)

Attach the three legs 03030 into the base plate 03010 using the hex nuts and washers provided. Screw on the four base hinges 03020 with the 8 flathead screws provided. Place base on flat table and check that it is level using the spirit level.

You may adjust the level and height of the base plate by turning the legs (parts 03040) and tightening with the leg nuts (parts 03030 B). Later, screw in the three locating disks (kinematic mounts) 03050A, B and C to your experimental table using threaded machine screws or wood screws so that the base will always settle at precisely the same place each time you put it down.

LOWER CHAMBER (Figures 9, 20)

The following operations should be carried out by use of clean forceps, tweezers and screwdrivers, without touching any of the parts by hand and with care so as not to scratch the surfaces (this procedure should always be adopted when handling parts that will come into contact with the chamber fluids and internal surfaces).

Put into place the following:

- **Side window** – part 02040 against the round silica window and O-ring (size -020), using 4 Philips head screws.
- **Thermistor** – part 02070 against thermistor and O-ring (size -006 or -007). Alternatively, the thermistor hole may be sealed (plugged) with part 02080 and the same O-ring.
- **Syringe port plug** – place O-ring (size -012) in hole, then press in and screw on plug 08080 with three

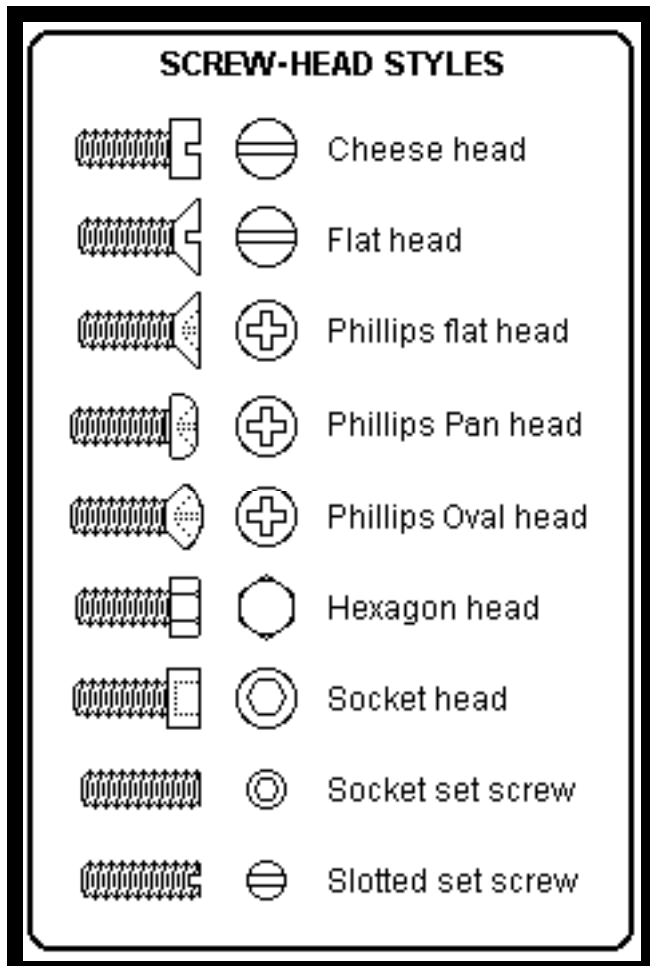


Figure 32. Types of screws used in SFAs.

screws (or using the three threaded studs 08090 and hex nuts 08100). Do not overtighten. If you have a syringe unit, assemble as per Figure 11. If you want to use the syringe port for controlling the vapor pressure inside the chamber, screw on 08110 instead of 08080 with three ordinary nuts or the hex nuts 08100 without tightening, then press in part 08051 and tighten the three nuts gently (a light pressure will ensure a good seal). Close off the end of 08051 with a Luer plug. If you want to use the syringe, after inserting the O-ring, press in syringe housing assembly 08010 with the steel ball 08020 against the O-ring, and tighten with three ordinary nuts or the hex nuts 08100 (tighten gently – enough to ensure a good seal but not too much that turning the syringe holder becomes difficult). Insert a 7.5-9.0 cm long, 0.071" diameter flat-ended needle (supplied), and observe that it just comes out from the other end. Turn part 08010 to tighten the sealing grip around the needle inside the syringe unit (see Figures 11 & 25). To seal (plug up) the needle hole, plug the exposed end with a Luer plug (e.g., male-male connector and end-cap).

- **Inlet hole** – screw in male Luer connector into the inlet hole. To ensure a good seal, you may insert a – 003 O-ring first and/or wrap some Teflon tape around the thread before screwing in the Luer connector. Close end with Luer cap.
- **Hinge** – screw part 02060 with the two oval-head screws provided.
- **Heaters** – insert after the apparatus has been fully assembled and placed on the base.

UPPER CHAMBER (Figures 7, 19)

Place the parts to be assembled also in the laminar flow cabinet as shown in Figure 18. Fit main and top O-rings into Upper Chamber [01010]. Tightly bolt steel part 01050 to the Cu-Be part 01040 using the two flathead screws provided. Tightly bolt 01040 to the Cu-Be spring 01030 using two cheese-head screws (ensure the right orientation and parallelism). Press the helical spring 01310[†] into the recessed holes in the two Cu-Be parts 01210 and 01080 and slide assembly into position in the Upper Chamber. Slide the Cu-Be assembly 01030 into place using the thin metal spatula to part and ease the slippage between the cantilever springs of parts 01030 and 01210 while gently pressing down the sharp edge of 01210 (no force should be required during this operation). Bolt 01030 into the Upper Chamber 01010 using four screws and the special right-angled screw driver provided. Screw in the two guiding pins 01090 through the roof of the Upper Chamber (do not tighten yet), passing them through the two slots of part 01080. Check for smoothness of motion of 01080 by pressing it in and out through the top hole using the flat end of a soft rod (the flat end of a pencil or the soft plastic end of the steel spatula). Tighten guiding pins 01090 while ensuring perfect smoothness of motion when tight.

Centralize part 01210 by hand. Screw part 01120 into part 01040 tightly but carefully (without scratching or bending any of the surfaces): Part 01120 should not be touched by hand. Slip or screw in the Teflon bellows 01290 into place, ensuring that the inner and outer lips are pressed all the way in and are lying

[†] Different helical springs may be used, depending on the range and sensitivity required for the differential spring control (the third distance control) which is currently set at about 1000:1. An alternative spring having a lower stiffness is supplied with each SFA3.

flat against the steel seats. Screw in rings 01100 and 01110 using the two key spanners 01130 and 01140: this operation must be done incrementally by tightening each ring alternately a little at a time so that there is no residual stress on the bellows.

Screw part 01150 into place, then insert and screw in the differential micrometer and locking nut. Turn both the coarse and differential heads to test for smoothness of rotation over their full ranges (6 mm for the coarse, limited by the Cu-Be part 01030 touching the ceiling and floor, respectively, of the inner chamber). The fine control head should not be turned beyond the red ring. Turn the coarse head on the differential micrometer anti clockwise until the rounded end of the micrometer shaft is above the flat ceiling of the internal chamber. Loosely bolt 01060 to 01200 using two screws with washers, then bolt 01200 to the Upper Chamber from the back with 4 screws. Loosen 01060 by loosening the two screws holding it from the back. Raising part 01050 to the ceiling and part 01060 as low as possible, insert helical spring 01300 using the medium sized serrated forceps provided so that each end 'clicks' into place in the recessed holes on 01060 and 01050 (protect yourself during this delicate operation: the spring may suddenly fly out in your face). From the back of the chamber, gently tighten the two screws but allow enough space for them to be moved up and down the two slots. Raise both screw heads with the back edge of the steel forceps and tighten fully* so that part 01060 is level and horizontal and positioned so that the micrometer and the cantilever springs of 01030 can move the whole way from the chamber ceiling to the floor without hindrance (a total distance of 6 mm, or ± 3 mm from the mean position). Set the coarse control so that the cantilever springs of 01030 are horizontal, that is, at the mean position. Set the differential (fine) control at the black ring, which is at the middle of the recommended range of travel (do not go beyond the red ring).

Screw on part 01270 and insert the normal micrometer barrel through it, pressing it in to the end. Tighten the barrel with the two set screws on 01270 (not too tight). Test the micrometer for smoothness of rotation and absence of backlash by hand over the whole range of travel – about 10 mm from top to bottom – but do not force it beyond either end. Limit switches on the driving motor will ensure that you will not be able to exceed the safe travel range during experiments. However, before using for the first time, check that the micrometer and limit switches are working properly and smoothly over the desired range by moving the micrometer electrically or by hand (in case the limit switches are not going to be used).

Assemble the bevel-gear unit and wheel: place small -007 O-ring into the shaft hole and screw in part 01160, gently tightening it against the O-ring. Slip shaft 01230 of the bevel-gear unit into the hole, and close up the top with part 01180 using two screws. Test the up-down movement of the unit and smoothness of wheel rotation. The positive pressure of the O-ring on the shaft should be felt. Screw in the locking screw 01170 almost to the end, but do not lock.

Press dovetail part 04010 of the variable spring unit into the recess hole in 01120 and align perfectly

parallel to the long axis of the upper chamber. Tighten with screw 04130. Neither of these parts should be touched by hand – special gloves should be worn.

Place upper chamber on lower chamber 02010, positioning the two together with the dowel pins. Screw in male Luer connector into air-outlet port on 01010 and close with a Luer cap. Blow clean internal chamber of Upper Chamber to remove dust, then close off with transparent side window 01190 using three screws (making sure that it does not press against the locking screw 01170). You may also close the piezo hole by placing the Piezo Mount into it and clamping it in place with the clamping plate 00080 (at this stage, it doesn't matter if you align the clamp in the NE or NW directions). Remember to screw on the small disk-locking screw 00030 into the disk mount 05020 before inserting the piezo mount. It is also worth checking, every now and again, that the piezo crystal connections are in order, that is, having infinite resistance across the coax cables, and closed circuit between the outer cable, the crystal mount (05010), the outer piezo wall, the upper disk mount (05020), and ground. The base should be grounded by connecting a ground wire to a screw on the front side of the base plate.

Slip in the four chamber tightening screws 02050 upwards at the four corners of the lower chamber and rotate by hand until the lower and upper chambers are sealed together. Place apparatus on base with the lower window on top of the oval hole. Tighten the two pointed locating screws on base hinges 03020A into the two grooved holes in hinge 02060 at the back of the Lower Chamber, and test that SFA can be tilted about the hinge 02060. Lower the SFA back onto the base and tighten the other two locating screws (on base hinges 03020B) into the two grooved holes at the front of the Lower Chamber. The apparatus should be sitting comfortably on the base plate.

FORCE-MEASURING SPRING (Figures 10, 20)

The following operations should be carried out by use of clean forceps, tweezers and screwdrivers, without touching any of the parts by hand and with care so as not to scratch the surfaces (this procedure should always be adopted when handling parts that will come into contact with the chamber fluids and internal surfaces). Attach part 04030 to 04020 using two screws. Screw on the small disk-locking screw 00030 into the disk mount 00020. Screw the holed ends of the two cantilever springs 04120 to the lower disk mount 00020 using the four screws provided, but do not tighten fully. Tighten the two rods 04110 into part 04020 and slip in parts 04040 and 04050 between them. Slip the two cantilever springs 04120 on either side of 04040, and screw in the clamping spring 04100 with the long screw provided. Tighten the clamping screw very slightly, so that the two cantilever springs can still slide easily.

Assemble parts 04060, 04070 and 04080 with two screws, ensuring that all 4 beveled edges point inwards, but do not tighten the double cantilever spring so that it cannot be slid out. The double threaded screw 04090 should already be attached to part 04060 and bevel gear 01220. Thread screw 04090 into part 04020 from the 'correct' end until it protrudes from the other side. Slip the two cantilever spring ends between parts 04060, 04070 and 04080 and very gently tighten the two screws on 04080. Slip the whole

spring assembly, part 04020 first, into the dove tail 04010 (which is already attached to the underside of the Upper Chamber) from right to left, and bolt part 04060 to 04010 tightly with two flathead screws.

Test whether the shaft 01230 engages the level gear 01220 exactly at its centre. If not, do not turn wheel 01260. Remove the whole sliding assembly from the dovetail slide 04010, readjust and reclamp it with screw 04130. Only when it is perfectly centered with the shaft 01230 will it be safe to rotate the wheel to initiate sliding of the double-cantilever force-measuring spring clamp. To test for good fit, lower the shaft via wheel 01260 until it engages the bevel gear. Press the wheel down until positive engagement is felt (do not press too hard – excess force will cause difficult, uneven motion of the bevel gears), then lock the shaft in place with locking screw 01170. Turn the wheel slowly in both directions, checking that the wheel turns easily and evenly as the dove-tail slides smoothly in either direction.

It is important that the double cantilever springs 04120 are also properly clamped with respect to parts 04060, 04070 and 04080. Turn the wheel counterclockwise until the clamping unit on 04020 starts pushing against the lower disk mount 00020. While pressing the disk mount against 04040 with a steel rod, tighten the screw on the clamp shim 04100 about 2 turns beyond the point where the clamp shim just starts to bend/deform. Now turn the wheel 01260 clockwise until the far ends of the cantilever springs 04120 just start to buckle against parts 04060, 04070, 04080. Reverse the wheel to relieve the buckling, then tighten the two screws on 04080. Now loosen the screw on 04100 by 1 turn, that is, to 1 turn beyond the point where the clamp shim starts to bend. The above procedure should ensure that during reclamping, the two cantilever springs 04120 remain parallel (and therefore that the silica disks do not bend) during the sliding of the dovetail 04020 over the whole range of clamping distances (from 0 to 32 mm).

Now test that the wheel 01260 can be turned (slowly) and the clamp unit moved (smoothly) without the cantilever springs 04120 buckling. Buckling will occur if the clamp shim is bent too much by the clamping screw. However, if an experiment at a fixed spring stiffness is being planned, especially a high stiffness (as might be required for experiments at high loads only), it is worth tightening this screw more than for experiments where the stiffness will be varied.

Set the clamp about 1.5 cm from the lower disk mount (requiring about 30 rotations of the wheel) so that it is roughly in the position shown in Figure 5. Unlock the locking screw 01170 and raise the wheel and shaft to the top, then relock the shaft in this position. You may now adjust the height of the spring mount via either micrometer. **IT IS IMPORTANT NEVER TO FORGET TO UNLOCK THE LOCKING SCREW 01170 AND RAISE THE SHAFT BEFORE MOVING THE SURFACES UP OR DOWN. FAILURE TO DO THIS WILL PUT LARGE STRESSES ON THE SPRINGS AND MECHANICAL PARTS.**

Final assembly

Purge SFA chamber with a gentle flow of clean, dry N₂ gas for 1 hour, letting the gas in through a cleaned Teflon filter attached to the Luer inlet in the Lower Chamber and out through the Luer outlet on the Upper

Chamber, or vice versa. Remove gas feed and plug up both holes with Luer caps.

Fit motor housing 00040 with reversible DC motor and encoder to the micrometer head on part 01270 in the upper chamber. Attach limit switches at the appropriate positions. Connect electric cables to Control Box and encoder display panel, and test motorized micrometer for smoothness of motion, absence of backlash, and proper working of encoder display, motor speed control and limit switches.

The apparatus may now be filled with clean ethanol up to about the rim of the lower chamber, but not so high that the liquid will wet the piezo tube, and sealed. Various additional tests and calibrations could be done at this stage: (1) You may calibrate the liquid volume of your assembled chamber by filling/injecting up to a particular level, as seen through the window, and noting the volume injected. (2) When sealing the piezo hole with the round glass cover (supplied) test that the bellows and other seals do not 'leak' by tilting the SFA until it is upright and examine for leaks – but first remove front window on Upper Chamber and be prepared to soak up any leaking fluid immediately, before it has time to spread. Tilt back and continue checking for leaks. Test overnight by noting whether the liquid level – as seen through the window – has dropped; if so, then some ethanol must have evaporated out through a small hole somewhere, in which case you should further tighten all the seals. The apparatus can now be left as it is, preferably covered as in Figure 31, until it is used.

OPTICS STAND AND MIRROR (Figures 14, 23, 24)

These arrive fully assembled. They require no maintenance and their use is fairly self-explanatory. Connect the 6-pin cable from the optics stand to the Control Box OUT panel. Before each experiment, make sure that the dot on the fine focusing stage is positioned between the two horizontal lines on the translation stage. Also make sure that the micrometer is set at the midway point of the scale, i.e., at about 5 mm. Coarse focusing can be done by hand (large round knob). Fine focusing and the prism turntable angle can be controlled from the front panel via two 'momentary' switches. The standard objective fitted at the end of the optics tube is a modified Ealing Electro-Optics X5 objective. If a higher image magnification is required, a X10 objective can be used instead: Ealing Objective (Cat. No. 24-9748) is recommended: the encased X10 objective lens can be readily removed from the housing and screwed directly to the end of the optics tube, part 07290, after removing the X5 objective.

MIRROR (Figures 14, 23)

The two mirror angles and position can be controlled by hand using the three finger screws. Extension cables and replaceable finger screws are provided for remote control.

Adhesion and short-range forces between surfaces.

Part I: New apparatus for surface force measurements

Jacob N. Israelachvili and Patricia M. McGuiggan

Materials Department, and Department of Chemical and Nuclear Engineering, University of California, Santa Barbara, California 93106

(Received 15 March 1990; accepted 27 June 1990)

A new miniature Surface Forces Apparatus (SFA Mark III) is described for measuring the forces between surfaces in vapors and liquids. The apparatus employs similar techniques to those used in current SFAs, but it is easier to operate and is generally more user-friendly. Four stages of increasingly sensitive distance controls replace the three control stages of previous apparatuses. The first three stages allow for rapid manual control of surface separation to within 10 Å, while the fourth piezo-control stage has a sensitivity of better than 1 Å. All four distance controls have been specially designed to produce perfectly linear displacements of the surfaces. In addition, the SFA Mk III is more robust, less susceptible to thermal drifts, easier to clean, and requires smaller quantities of liquid than conventional SFAs. The high performance of this new instrument is illustrated in the succeeding paper (Part II), which describes the subtle effects of surface lattice mismatch on the oscillatory forces in water in the distance regime from 0 to 10 Å.

I. INTRODUCTION

A. Early surface forces apparatuses

We briefly review the current state of direct surface forces measuring techniques, describe their limitations, and discuss why it was felt necessary to develop a new apparatus. In 1969 Tabor and Winterton,¹ and later Israelachvili and Tabor,² developed Surface Forces Apparatuses (SFAs) for directly measuring the van der Waals forces between surfaces in air or vacuum. These were successfully used for measuring van der Waals forces in the distance regime 1.5–130 nm with a distance resolution of 0.1–0.2 nm. In 1976, Israelachvili and Adams³ designed a new apparatus (later known as SFA Mk I) for measuring the forces between surfaces in liquids as well as in vapors, allowing control and measurement of the surface separation to within 0.1 nm. The SFA Mk I enabled the first detailed measurements to be made of the two fundamental forces of colloid science. These are the repulsive electrostatic double-layer forces and the attractive van der Waals forces, which exist between any two charged surfaces immersed in an electrolyte solution. These two forces make up the so-called DLVO Theory, which forms the basis of analyzing the long-range interactions of colloidal and biological structures in solution.⁴

The principles on which Mk I operates are simple³: one of the surfaces (the upper) is rigidly mounted at the end of a piezoelectric crystal tube while the lower surface, which faces the upper, is suspended at the end of a force-measuring spring. The surfaces can be moved toward or away from each other using a three-stage sys-

tem of controls of increasing accuracy. First, a coarse control micrometer drive allows for positioning to within about 500 nm over a range of 1 cm. The second level of control, the medium control, employs a micrometer-driven differential spring having an accuracy of 1 nm over a range of 10 µm. The third or fine control involves applying a voltage to the piezoelectric crystal allowing for final (vibration-free) positioning to an accuracy of 0.1 nm over a linear range of a few thousand angstroms. An optical technique (described more fully below) is used to measure the separation between the surfaces to ±0.1 nm.

The force is measured by moving the two surfaces toward or away from each other using one of the above controls, e.g., by applying a voltage to the piezoelectric crystal, and simultaneously measuring the deflection of the force-measuring spring using the optical technique. This gives the force at any particular surface separation. As mentioned above, the principles used in making direct force measurements are usually very simple; the main challenge has always been in the design of a mechanical device that would successfully apply these principles at the angstrom level.

B. Surface forces apparatus: Mk II

Following the success of Mk I, it was modified and improved, and became known as Mk II.⁵ In particular, various attachments were developed that could be added to Mk II which greatly extended its scope and versatility.⁶ For example, the replacement of the original single-cantilever force-measuring spring by a

variable-stiffness double-cantilever spring greatly extended the range of the forces that could be measured to more than six orders of magnitude. A small bath attachment was constructed that could be inserted into the main chamber to allow for much less liquid to be used than the full capacity of the chamber (about 350 ml), and more recently various attachments have been introduced⁶ for making dynamic, as opposed to static or equilibrium, measurements (e.g., of the viscosity and shear properties of very thin liquid films).

Over the last few years a number of other successful, and often simpler, surface forces apparatuses have also been built based on similar principles as Mk I and II and using the same optical technique for the distance measurements. Thus, Klein⁷ developed a circular glass apparatus and Parker *et al.*⁸ developed a circular steel apparatus (SFA Mk IV), both of which are simpler to assemble and use than Mk II. Other optical^{9,10} and capacitance¹¹ techniques for measuring surface separations have also been recently introduced in surface force measurements. All of these are now being regularly used to measure a whole variety of forces and interfacial phenomena in both vapors and liquids at the molecular level, and their use is expected to continue and expand into new areas.¹²

However, the systems and phenomena being studied are rapidly growing in complexity; these now include multicomponent polymeric and lubricant systems, the deformation and fusion of surfactant or lipid bilayers, dynamic and time-dependent interactions, molecular relaxations in thin films, tribological phenomena, etc.⁶ These studies often require greater accuracy, stability, versatility, and control than can be attained with existing force-measuring apparatuses, even with the new attachments added. Thus a whole generation of new phenomena could be studied if only some of these deficiencies or limitations could be overcome. Our primary aim here was the identification of these limitations, and the design and construction of a new device that did not suffer from these limitations. This will now be described.

C. Limitations of existing surface forces measuring apparatuses

The most serious drawbacks of Mk II are listed below, together with their causes and how they limit the types of measurements that can be made or reduce their accuracy (these also apply to other surface forces apparatuses):

(1) The two surfaces are prone to thermal drifts which can greatly diminish the accuracy of the forces measured below the theoretically attainable limit of at least 10^{-8} N (10^{-6} g). These thermal drifts arise from the long mechanical path between the two surfaces, often passing outside the main body of the apparatus

where it is not thermally insulated by the thermal inertia of the apparatus and chamber. Consequently, even small differential thermal gradients outside the apparatus can lead to slow drifts of the two surfaces relative to each other. These drifts can usually be minimized by thermostating the apparatus or the experimental room to 0.1 °C, but they preclude accurate measurements of forces that take a long time to reach equilibrium, time-dependent adhesion effects, hydrodynamic interactions, etc.

(2) The maximum attainable stiffness is not very high even when the variable-stiffness force-measuring spring is fully clamped.⁵ This, too, is a consequence of the unnecessarily long mechanical path between the two surfaces even at full clamping. This precludes certain types of measurements to be made that require high rigidity, for example, of strongly attractive hydrophobic and capillary forces at small separations.

(3) The coarse control which employs a screw-thread and/or dovetailed slide mechanism is basically incapable of the perfectly linear friction-free motion that is required at the submicroscopic level. This can cause erratic motion, backlash, irreversibility, and undesirable shear motion. Such erratic motion is unavoidable whenever linear motion depends entirely on a screw-thread or dovetail mechanism, regardless of how well the parts are machined. These effects can lead to unreliable control of distance and, at worst, to surface damage on separating two adhering surfaces.

(4) The three distance controls do not adequately cover the required range from about 0.5 cm to 0.1 nm, i.e., a range of more than seven orders of magnitude. A fourth distance control, like a fourth gear in a car, would greatly facilitate measurements.

(5) Most surface forces apparatuses need to be disassembled for the bathing chamber to be properly cleaned, and the chambers are often difficult to clean because of their large volumes and internal surface areas. The whole process is thus cumbersome and time-consuming. In addition, as the chamber or bath is filled with liquid it is difficult to keep the liquid surface clean by aspiration as it approaches, then contacts (i.e., wets), and finally passes across the two solid surfaces. It is thus difficult to prevent a monolayer or submonolayer of some foreign material from being deposited onto the surfaces as the meniscus passes them. This can result in contaminated surfaces even before an experiment is properly underway. Fortunately, such material often dissolves in the immersing liquid, but one cannot always be totally certain of this.

It was decided to design a new and more user-friendly apparatus that did not have any of the drawbacks mentioned above and with some additional features making it suitable for new types of measurements. This new surface forces apparatus (SFA Mk III)

was developed and successfully tested and used during 1985–89 in a series of different experiments, including those described in the following paper. It is shown in Figs. 1 and 3 and will now be described.

II. SURFACE FORCES APPARATUS: Mk III

Figure 1 shows a section through Mk III. Note that Mk III is smaller and more compact than previous models. Forces are measured between the two mica or mica coated surfaces supported on two cylindrical silica disks. The upper disk is attached to the piezoelectric PZT-5A crystal tube which is mounted on a support that can be moved laterally and rotated before it is clamped tightly to the top of the apparatus. The apparatus has two separate parts, an upper (control) chamber, and a lower (bathing) chamber. The control chamber handles the four distance controls, the force-measuring spring adjustment, and the positioning and clamping of the two surfaces. Its workings are totally sealed from the lower chamber via the teflon bellows B. The lower chamber acts as a simple bath that can be bolted underneath the upper chamber and then filled with liquid. It is thus completely sealed both from the outside environment as well as from the mechanical controls of the upper chamber. This design feature of Mk III is similar to that of the surface forces apparatus designed by Klein.⁷ The lower and upper chambers are made of 316 stainless steel. The lower chamber can also be made entirely of teflon (PTFE) or some other inert fluorocarbon material such as Kel-F. It is easy to clean and can be readily replaced by another bathing cham-

ber. At no point during or between experiments does the control chamber have to be opened or dismantled; indeed, once the control chamber has been assembled it requires no further attention.

The four distance controls of the upper chamber will now be described. As shown in Fig. 1, there are three mechanical controls and one piezoelectric control. The three mechanical controls are based on a new spring translation assembly, located roughly at the center of the control chamber (T), whose main design features are shown in Fig. 2. The main part of this assembly is the vertical-motion translation stage (part T₁). This is machined from a single block of Cu–Be alloy and consists of four equal double-cantilever spring systems. This type of design ensures that if the two end parts (A) are fixed, i.e., bolted inside the control chamber (see Fig. 1), then the displacement of the middle part (B) will be perfectly vertical and linear, with no possible movement in any other, e.g., lateral, direction. The eight cantilever springs of this unit also ensure that there is no possibility of any wobble or rotation, or any other type of unwanted movement as occurs with dovetailed slides or screw-thread drives. To ensure further that there is also no buckling of the springs, it can be shown that the vertical force inducing the displacement must be applied through an axis passing through the center of the spring system, i.e., along the direction defined by the vertical arrow drawn through T₁.

The full translation assembly includes another Cu–Be part (Fig. 2, part T₂), which is attached to the translation stage (T₁) by bolting parts C and B together via

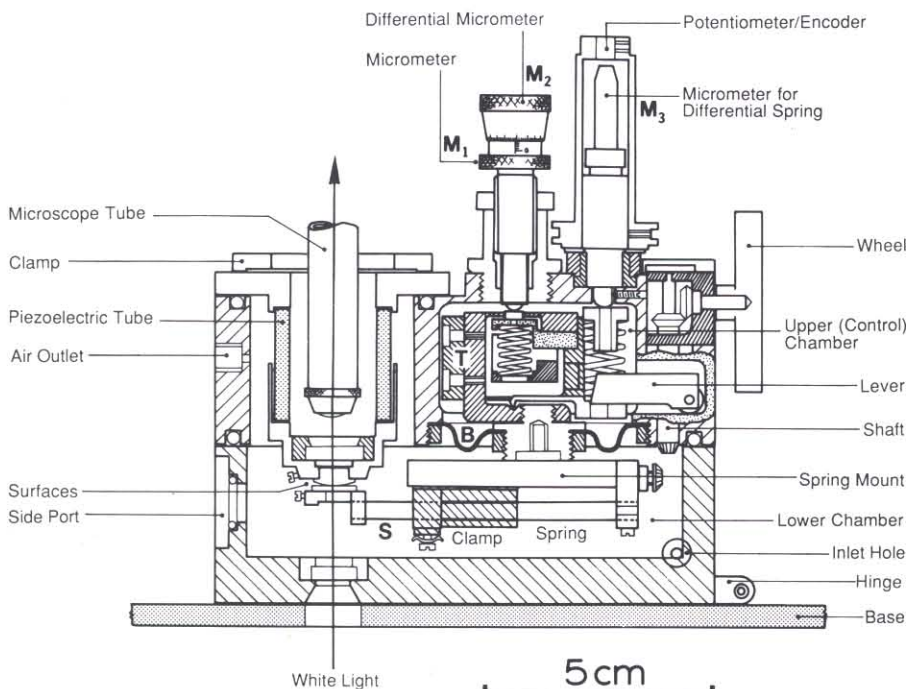


FIG. 1. New Surface Forces Apparatus (SFA Mk III) for measuring the forces between two molecularly smooth surfaces. The figure shows a section through the center of the apparatus. There are four distance controls: normal micrometer (M₁), differential micrometer (M₂), differential spring control (M₃), and piezoelectric tube. The lower surface is mounted at the end of a variable-stiffness double-cantilever force-measuring spring (S) which is connected via the spring mount to the distance controls of the upper (control) chamber via a teflon bellows (B). The wheel and shaft unit are used for laterally moving the spring clamp and thereby changing the stiffness of the force-measuring spring. The lower chamber is bolted to the underside of the upper chamber from which it is completely sealed by the bellows, as well as being sealed with teflon O-rings from the outside. The main translation stage unit (T) is described in Fig. 2 and a photograph of the apparatus is shown in Fig. 3.

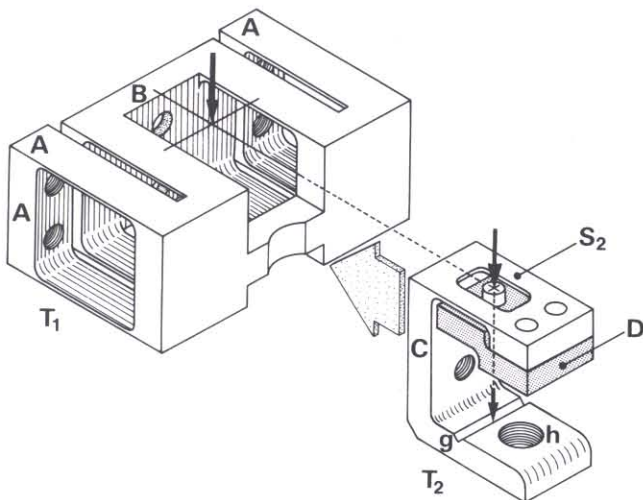


FIG. 2. Basic spring assembly unit (or translation stage) ensuring that the two surfaces move vertically and perfectly linearly relative to each other with no displacement or rotation in any other direction. The main part of the translation stage T_1 is bolted to the inside of the control chamber (Fig. 1). The second part, T_2 , is bolted to T_1 so that the positions of the two arrows coincide. The arrows define the vertical axis passing through the center of the four double-cantilever spring system of T_1 , the single-cantilever spring S_2 , and the groove g on T_2 . The micrometer shaft of M_1 and M_2 presses vertically down on the small steel disk on top of part D , as shown in Fig. 1. The workings of the spring assembly are described in the text. All the spring parts were machined from Cu-Be alloy before they were heat treated (tempered).

two bolts. Once assembled, the two arrows shown on T_1 and T_2 coincide and define the vertical axis through the center of the double-cantilever spring systems of T_1 . The assembled unit of these two parts fits inside the control chamber via four bolts through parts A, as shown in Fig. 1. At the bottom of T_2 there is a threaded hole (h) to which the bellows B and the force-measuring

spring mount are attached (cf. Figs. 1 and 2). The spring mount protrudes into the lower chamber, and the teflon bellows B isolates the two chambers from each other.

A. Characteristics of positioning and force-measuring springs

Table I gives the spring characteristics of the various springs used to perform the following three functions: position the two surfaces (distance control), measure forces, and avoid backlash. In each case the spring type, its stiffness, range of operation, and elastic limit were designed for optimum performance. These are further described in the following sections.

B. Control of surface separation

Coarse controls: There are three mechanical distance controls (two coarse and one medium) and one piezoelectric (fine) control. The coarse controls work as follows. A differential micrometer (M_1 and M_2 : modified from a micrometer obtained from *Microcontrole*, Cat. No. 385034) is bolted to the top of the apparatus. The micrometer axis is along the line of the arrow in Fig. 2. It presses down against the polished flat surface of a small hardened steel disk attached to the stainless steel part (D) on top of the translation stage assembly. Turning the micrometer causes parts T_2 , B, and hence the spring mount in the lower chamber to move along a perfectly vertical axis, and in this way the normal distance between the two surfaces can be moved over a total range of about 6 mm (± 3 mm about the mean position) with control to 500 nm (using the normal micrometer, M_1) and 50 nm (using the differential micrometer M_2). This positioning can be done by hand. A stiff helical spring located inside T_2 (see Fig. 1)

TABLE I. Spring specifications.^a

Function and location	Spring type	Stiffness (N/m)	Operating range (length)	Range of loads
1st and 2nd (coarse) distance control (T_1)	Unit of four double-cantilevers	3.6×10^3	0 ± 3.5 mm	<Elastic limit
Anti-backlash for T_1 (under M_1, M_2)	Helical	4.3×10^3	7–14 mm	1.7–4.7 Kg
3rd (medium) distance control (under M_3)	Helical	1.5×10^3	9–24 mm	0.3–1.8 Kg
3rd distance control (S_2) (in series with above)	Cantilever	1.5×10^6	0 ± 10 μ m	<Elastic limit
Force-measuring (S) (variable stiffness)	Double-cantilever	$30-5 \times 10^5$	Clamping: 0–32 mm Vertical: 0 ± 1 mm	10^{-6} g–100 g

^aThe first four springs are located within the upper (control) chamber and are made of machined Cu-Be alloy that is later hardened by heat-treatment. The force-measuring spring (S) located inside the lower chamber is made of noncorrosive stainless steel since it contacts various solvents. The stiffness of the force-measuring spring is related to its variable clamping length L via Eq. (3). The bellows B has a negligible elastic stiffness compared to the other positioning springs. The 4th (fine) distance control is done via a piezoelectric crystal tube.

presses against the underside of D along the main translation axis defined by the arrows and acts as an antibacklash spring (see Table I).

Medium control: The third (medium) distance control is via a differential spring mechanism. Here a helical spring is compressed by a motor-driven nonrotating micrometer (M_3). The spring presses against a lever which in turn presses down on T_2 at the groove (g) which, as mechanically required, is also located along the vertical axis passing through the center of the spring translation assembly. The force acting on T_2 from the action of this spring deflects a cantilever spring (S_2) located on top of T_2 (this spring is also symmetrically displaced about the main translation axis). The deflection of S_2 therefore causes B and hence the spring mount to be displaced vertically, but by a very small amount: the stiffness of S_2 is about 1000 times greater than that of the helical spring under M_3 (see Table I), and the lever ratio is about 2:1. Thus the movement of the micrometer M_3 over a total range of 15 mm is reduced by a factor of about 2000. (Note that spring S_2 is actually acting in parallel with the springs of T_1 , but the effect of T_1 on the reduction ratio is negligible since, as shown in Table I, S_2 is about 500 stiffer than T_1 . However, T_1 does help ensure that the surface displacement remains along a vertical axis.) This third control therefore enables the micrometer displacement, which covers a range of 15 mm with an accuracy of $\sim 1 \mu\text{m}$, to be reduced to a range of $7.5 \mu\text{m}$ with a positioning accuracy about 0.5–1 nm between the two surfaces.

Fine control: The final, nonmechanical control of surface separation is effected by changing the dc (or ac) voltage across the inner and outer silver-coated walls of the piezoelectric tube that supports the upper surface. The outer wall is grounded (earthed), while the inner wall is the active surface. The tube expands by about 1.0 nm per volt, so that when working from -500 V to $+500 \text{ V}$ the surfaces can be moved over a range of about $1 \mu\text{m}$ with an accuracy of better than 0.1 nm—this accuracy now being limited by factors such as the background vibrations and thermal drift of the two surfaces relative to each other (discussed below) and the performance of the piezoelectric material. Most commercial piezoelectric crystals are rated to withstand many thousands of volts, but we have found that their motion is linear and creep-free only below about 500 V (corresponding here to a total movement of $\pm 500 \text{ nm}$). We have also found that there is no lateral displacement of the piezoelectric tube when it is expanded vertically, so long as it is properly glued into place, i.e., with its axis perfectly vertical.

To summarize, the four distance controls have the following resolution and workable range: normal micrometer (500 nm over a range of 6 mm); differential

micrometer (50 nm over a range of 0.1 mm); differential spring (1 nm over a range of $5 \mu\text{m}$); and piezo control (<0.1 nm over a range of 1 μm).

The three micrometer controls, M_1 , M_2 , and M_3 , are conveniently positioned for manual control, but any one of them can also be controlled by a variable-speed reversible 24 V dc motor and gear-box (Philips 4322 010 75143 and 9912 200 02036) via a gear wheel and belt. The differential spring facility of M_3 is similar to the lower motor control of Mk I and II,^{3,5} and the displacement of the spring can likewise be measured from a resistance potentiometer or encoder attached to the top of M_3 .

C. Control of stiffness of force-measuring spring

The stiffness of the double-cantilever force-measuring spring (S) can be adjusted by sliding the spring-loaded clamp laterally along the spring supporting mount. This clamp is attached to a dovetailed slide and has a screw thread passing throughout its length. The clamp can be moved by rotating this screw at the point where it protrudes from the spring mount at its right end. To accomplish this adjustment the O-ring-sealed shaft and wheel are unlocked and, by holding the wheel, manually lowered until the two bevel gears engage. The wheel is then turned until the desired clamping position is attained. Each turn corresponds to 0.5 mm displacement, and the range of clamping of this spring is from 0 to 32.5 mm (65 turns of the wheel). After the desired clamping position has been reached, the wheel and shaft are raised and locked back into place (the locking mechanism is not shown in Fig. 1 but it is essentially a screw that can be turned by hand so that it presses against the wheel assembly; this screw is seen in Fig. 3 as the circular knob that protrudes from the front of the apparatus just to the left of the wheel). The whole process of changing the spring stiffness takes no more than 1 min. The range of stiffnesses attainable is from below 30 N/m to about $5 \times 10^5 \text{ N/m}$ (see Table I). This is about 4 orders of magnitude. Since at each stiffness one can usually measure 3–4 orders of force, the Mk III can measure a force-law over a range of 6–7 orders of magnitude.

D. Experimental procedure

The mica sheets are first cut, silvered, glued onto the cylindrical silica disks, pretreated with some desired surface coating (if needed), and installed into position in the apparatus so as to face each other as shown in Fig. 1. The lower chamber is then placed underneath the upper chamber and bolted to it.

Optimization of the optics (see below) is carried out more or less as for Mk I and II,^{1–3} except that with Mk III the three micrometers M_1 , M_2 , and M_3 are all

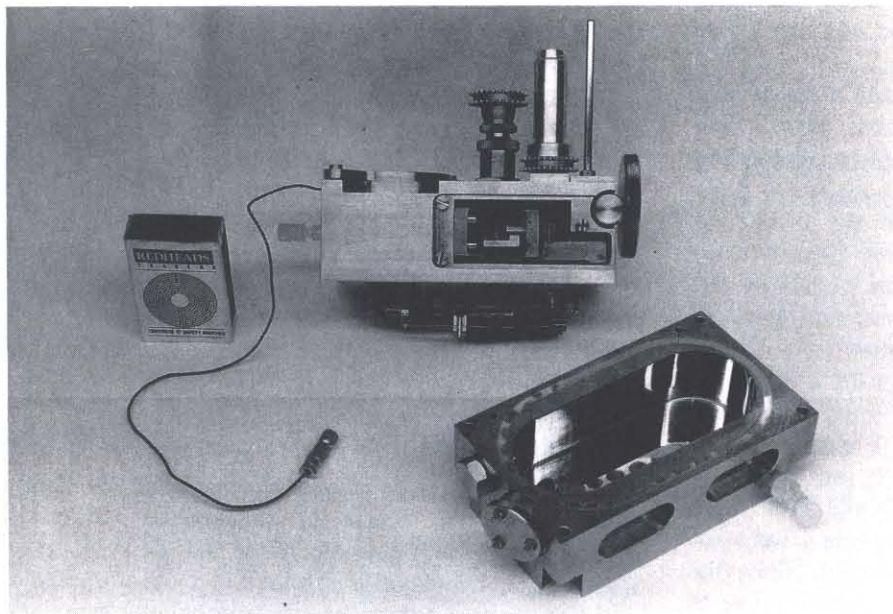


FIG. 3. Photograph of Mk III with the upper and lower chambers disconnected. A matchbox on the left gives an idea of the size of the apparatus.

accessible by hand so that it is possible to make very fine adjustments manually before tightening the belt around the micrometer M_2 or M_3 . The desired spring stiffness can be obtained by moving the spring clamp as described above, and the apparatus (or lower chamber) is now ready for filling with liquid.

By tilting the apparatus clockwise about the hinge (see Fig. 1) until it is almost vertical, one may fill the chamber through the inlet hole. The capacity of the chamber is 50–60 ml, so that it can be filled with a syringe. As the liquid level rises and approaches the two solid surfaces, its surface can be continuously aspirated through the side port on the left wall of the lower chamber, while gently purging the atmosphere with clean N_2 gas through the air outlet port. Once filled, the apparatus is lowered back onto its base and force measurements can proceed as described below.

E. Measuring distances and surface profiles using the FECO technique

Surface separations and profiles can be measured to within about 0.1 nm by monitoring the movement of multiple beam interference fringes known as Fringes of Equal Chromatic Order (FECO).^{13–15} These sharp fringes are produced when a beam of white light is made to pass through the two mica sheets (Fig. 1). The transparent mica sheets are of equal thickness (about 1–3 μm) and are each coated with a 98% reflecting layer of silver (thickness $\sim 550 \text{ \AA}$) before they are glued, silvered sides down, onto the cylindrically curved silica disks. The interference fringes are produced by multiple reflections of light between the two silvered layers, so that only certain wavelengths (which interfere con-

structively) emerge from the other side of the sheets. The emerging beam is focused onto the slit of a normal grating spectrometer which separates out the different colors (interference fringes). Depending on the shapes of the two surfaces, these fringes appear as sharp lines or curves at the exit of the spectrometer^{13–18} and can be viewed by eye through a normal microscope eyepiece or recorded on film or a video camera.

From the positions and shapes of the FECO fringes one can determine not only the surface separation but also their shapes and the refractive index of the medium between them. Equations describing how one translates the measured wavelengths to surface separations and refractive indices have been given by Israelachvili¹⁵ together with photos of FECO fringes and a working example of how these can be used to measure the thickness and refractive index of thin films.

More recently, the FECO technique has been used to measure the capillary condensation of liquids,¹⁷ the elastically deformed shapes of contacting surfaces,¹⁶ and the fusion of surfactant films.¹⁸ These papers may be referred to for pictures of the FECO fringes and further details of the optical technique.

There are two major advantages of using this technique over other techniques (such as a capacitance technique). The first is that the surface separation is actually measured at the point of closest approach of the two surfaces; i.e., the separation is measured where one actually wants to know it. Most other techniques measure the displacement of a spring or balance arm at some point away from the interaction zone, and in this way any elastic deformations of the surfaces occurring around the contact zone become mixed in with the

measured distance displacement. With the FECO method, the distances between the two surfaces and any deformations of the materials are unambiguously distinguishable and independently measurable. The second advantage is that one can measure the surface profile, and in particular the local radius of curvature R of the two apposing surfaces. This is important when one wants to compare the measured forces with theory or when one needs to translate adhesion forces to surface energies [see Eq. (5)].

F. Measuring forces

Given the facility for moving the surfaces toward or away from each other and independently measuring their separation, each with a sensitivity or resolution of about 0.1 nm (1 Å), the force measurements themselves now become straightforward. The force is measured by expanding or contracting the piezoelectric crystal by a known amount and then measuring optically how much the two surfaces have actually moved. Any difference in the two values when multiplied by the stiffness of the force-measuring spring gives the force difference between the initial and final positions. Thus if the surfaces are initially at D_0 where the force between them is $F(D_0)$, and the piezoelectric crystal is expanded by ΔD_p , so that the surface separation changes by ΔD_s to D , the force at D is related to the force at D_0 by

$$F(D) = F(D_0) + (\Delta D_p - \Delta D_s)K \quad (1)$$

where K is the stiffness of the force-measuring spring. Thus, if $\Delta D_p = \Delta D_s$ we have $F(D) = F(D_0)$, so that if the force is zero at D_0 , it is also zero at D . However, if $\Delta D_p > \Delta D_s$ we have $F(D) > F(D_0)$ and the force at D is repulsive, whereas if $\Delta D_p < \Delta D_s$ we have $F(D) < F(D_0)$ and the force at D is attractive. In this way, by starting at some large separation where there is no detectable force and working systematically toward smaller separations both repulsive and attractive forces can be measured with a sensitivity of about 10^{-6} g (see Table I) and a full force-law can be obtained over any distance regime.

As an example, we consider a typical experimental run where there is a monotonically repulsive force between the two surfaces in a liquid at separations below 15.0 nm. The piezoelectric tube is first calibrated at large distances (> 15 nm) where there is no detectable force using the optical technique. This calibration yields, say, 1.0 nm/V. The two surfaces are now brought to a separation of 20.0 nm and the voltage across the piezoelectric tube is changed by 5.0 V, corresponding to $\Delta D_p = 5.0$ nm. This results in an inward displacement of the surfaces, as measured from the shift in the FECO fringes, from 20.0 nm to 15.0 nm, corresponding to $\Delta D_s = 5.0$ nm. Thus, $\Delta D_p = \Delta D_s$, so

that $F(D = 15 \text{ nm}) = F(D = 20 \text{ nm}) = 0$. Next, the surfaces are brought to $D = 15.0$ nm, and the process is repeated. This time, however, the surfaces are found to move to 11.0 nm, so that $\Delta D_s = 4.0$ nm. The net force at $D = 11.0$ nm is therefore repulsive and, using Eq. (1), is equal to $K(5.0 - 4.0) \times 10^{-9}$ N. The spring constant, K , can be calibrated at the end of the experiment by replacing the silica disks with small weights and measuring the deflection using a micrometer eyepiece or traveling microscope.¹⁻³ For example, if the value obtained for K is 100 N/m, then the repulsive force at $D = 11.0$ nm is 10^{-7} N (10^{-2} dynes or 10^{-5} g).

The force-measuring spring can be varied during an experiment by a factor of up to 10 000 (see Table I), so that both very weak and very strong forces may be measured. When strongly attractive forces are measured, instabilities can occur wherein the surfaces suddenly jump from one stable position to another. This is analogous to bringing a magnet suspended from a spring down toward a block of iron where at some point it will jump into contact with the block. Both inward and outward jumps can occur (cf. the outward jump from contact when the spring attached to the magnet is pulled back). Instabilities occur whenever the gradient of the force exceeds the spring stiffness, i.e., when $\partial F/\partial D > K$, and is common whenever complicated force laws are being measured, such as oscillatory forces.^{3,19} Note that Eq. (1) still applies when instabilities occur, though certain distance regimes now become inaccessible to force measurements (these being regions where no stable equilibrium can occur). However, by increasing the spring stiffness these regions can become accessible, though at the cost of reduced sensitivity.

G. Measuring adhesion forces

Measuring outward jumps from contact is a particularly suitable way of measuring adhesion forces. For example, with $K = 100$ N/m, as before, an outward jump of 15 μm implies an adhesion force of 1.5×10^{-3} N (0.15 g). Alternatively, using a higher spring stiffness of $K = 10^4$ N/m, the jump apart corresponding to the same adhesion force would now be only 150 nm. This is just as easy to measure as 15 μm, and it has the advantage that the whole operation can be done much more quickly with the piezoelectric control (no moving mechanical parts), and then repeated many times to test for reproducibility just as quickly.

Using a stiffer spring setting for measuring large forces also has the advantage that the lateral displacement (shearing) of the two surfaces can be reduced as they are being pulled apart. If the active length of the double-cantilever force-measuring spring (S) is L , then it can be shown that a vertical displacement of ΔD at the point of contact of the two surfaces results in a lat-

eral displacement of the surfaces by Δx , where

$$\Delta x = \frac{2\Delta D^2}{3L}. \quad (2)$$

Further, the stiffness (or spring constant), K , of a double-cantilever spring is given by

$$K = 2YbT^3/L^3 \propto 1/L^3 \quad (3)$$

where Y is the Young's modulus, b the spring width, and T the spring thickness. Since the adhesion force is related to the spring constant K and deflection ΔD by $F = K\Delta D$, we obtain for a double-cantilever spring with variable clamping length L :

$$\Delta x \propto \Delta D^2/L \propto (F/K)^2/L \propto (FL^3)^2/L \propto F^2L^5. \quad (4)$$

Equations (2) and (4) are important for determining the shear displacement of two surfaces when forces of magnitude F between them are being measured with a double-cantilever spring of length L and stiffness K . Equation (4) shows that to reduce Δx (at a given F) one must use a shorter spring length L . This can be achieved with the Mk III by reducing the clamping distance of the force-measuring spring during an experiment. It is worth mentioning that it is possible to design a nonshearing force-measuring spring,^{5,6} but it is not easy to design one whose stiffness can also be varied during an experiment.

Returning to the above example where an adhesion force of $F = 1.5 \times 10^{-3}$ N was measured using spring constants of either $K = 10^2$ N/m or $K = 10^4$ N/m, these correspond to spring lengths of $L = 2.1$ cm and 0.45 cm, respectively (see Table I). With the weaker spring setting we have $\Delta D = F/K = 1.5 \times 10^{-5}$ m, so that the lateral displacement is given by Eq. (2) as $\Delta x = 7.1$ nm, which may introduce unwanted frictional forces during pull-off. However, with the stiffer spring setting Eq. (4) shows that the shear displacement falls to $\Delta x = 0.003$ nm (0.03 Å), which is totally acceptable. It is with these stiffer spring settings that the adhesion forces, described in Part II,²⁹ were measured.

There is a well-known expression, known as the Derjaguin approximation,⁴ which relates the force between two curved surfaces to the energies of flat surfaces. In particular, the adhesion energy (otherwise known as the surface or interfacial free energy) E per unit area between two flat surfaces is simply related to F by:

$$E = F/2\pi R. \quad (5)$$

Thus, in the above example where $F = 1.5 \times 10^{-3}$ N, if the radius of the surfaces were $R = 10^{-2}$ m (1 cm), the surface energy would be $E = 25 \times 10^{-3}$ mJ/m² (25 erg/cm²).

H. Performance characteristics of Mk III

Mk III is much more stable against thermal drifts, and is easier to operate and keep clean than previous models. The thermal drift of the two surfaces has been found to depend mainly on the temperature stability of the room (apparatus environment), and is typically less than 0.1 nm/min if the ambient temperature is controlled to within 0.1 °C. The improved thermal stability of the apparatus is due to its compactness and because all the critical moving parts are internalized. In addition, the mechanical path between the two surfaces is very short and does not go outside the apparatus (as in previous models). All these factors reduce the susceptibility of the apparatus to transient temperature gradients.

The replacement of the dovetailed slide and screw threads by the purely spring-loaded translation assembly of Fig. 2 has also helped to ensure linear motion and significantly reduced backlash and other erratic motions of the two surfaces.

The four distance controls now make it easy to quickly bring the surfaces together manually within a few hundred angstroms and then, depending on the strength of the forces, to measure these using either the piezoelectric crystal, the differential spring, or the differential micrometer; i.e., there are three rather than two choices for measuring forces. The short path between the two surfaces also allows for a higher stiffness to be attained with Mk III than with existing apparatuses.

Finally, the ability to have the surfaces immersed in a passivated stainless steel or an all-teflon bath allows for very clean work to be done, and the aspiration capability during filling significantly reduces the chances of having contaminated surfaces.

I. Additional features and attachments

Mk III has been designed to be as versatile as possible, and to easily accept new attachments. As an example of the former, note that the lower chamber may be readily removed (without disturbing the two surfaces) and replaced by a different chamber. This allows for different types of baths to be used for different experiments; for example, one bath for experiments with surfactant-coated surfaces using the Langmuir-Blodgett technique, another bath for experiments in vapors of controlled vapor pressures, and yet another bath whose walls are well thermostated suitable for experiments over a wide range of temperatures.

The new SFA Mk III can also be used with a variety of different attachments, as can its predecessor.⁶ Typically, these attachments would be secured to the bottom of the translation stage T_2 , replacing the spring mount. Two attachments currently in the design stage

are (1) a sliding facility for shearing two surfaces laterally past each other, suitable for friction measurements and for studying various tribological phenomena, and (2) a constant-force electromagnetic balance attachment, for making accurate measurements of truly equilibrium forces across thin liquid films regardless of thermal drifts and the time it takes to reach equilibrium. Finally, for the experiments reported in the following paper a new attachment was developed for measuring the dependence of adhesion and short-range forces in liquids on the twist angle between the two interacting surface lattices.¹³

ACKNOWLEDGMENTS

We thank Allan Reading and Robert Hill for their excellent technical expertise, Dr. Roger Horn for his valuable comments, and the United States Department of Energy for financial support under DOE grant DE-FG03-87ER45331, although this support does not constitute an endorsement by DOE of the views expressed in this article.

REFERENCES

- ¹D. Tabor and R. H. S. Winterton, Proc. R. Soc. London, Ser. A **312**, 435 (1969).
- ²J. N. Israelachvili and D. Tabor, Proc. R. Soc. London A**331**, 19 (1972).
- ³J. N. Israelachvili and G. E. Adams, Nature **262**, 774 (1976); J. Chem. Soc., Faraday Trans. I **74**, 975 (1978).
- ⁴J. N. Israelachvili, *Intermolecular and Surface Forces* (Academic Press, London and New York, 1985).
- ⁵J. N. Israelachvili, Proc. Natl. Acad. Sci. U.S.A. **84**, 4722 (1987).
- ⁶J. N. Israelachvili, Chemtracts—Analytical and Physical Chemistry **1**, 1 (1989).
- ⁷J. Klein, J. Chem. Soc., Faraday Trans. I **79**, 99 (1983).
- ⁸J. L. Parker, H. K. Christenson, and B. W. Ninham, Rev. Sci. Instrum. **60**, 3135–3138 (1989).
- ⁹D. C. Prieve, F. Luo, and F. Lanni, Faraday Discuss. Chem. Soc. **83**, 297 (1987); S. G. Bike and D. C. Prieve, Langmuir (in press).
- ¹⁰R. Erlandsson, G. M. McClelland, C. M. Mate, and S. Chiang, J. Vac. Sci. Technol. A **6**, 266 (1988); Y. Martin, C. C. Williams, and H. K. Wickramasinghe, J. Appl. Phys. **61**, 4723 (1987); S. Alexander, L. Hellemans, O. Marti, J. Schneir, V. Elings, P. K. Hansma, M. Longmire, and J. Gurley, J. Appl. Phys. **65**, 164 (1989); A. L. Weisenhorn, P. K. Hansma, T. R. Albrecht, and C. F. Quate, Appl. Phys. Lett. **54**, 2651 (1989).
- ¹¹A. Tonck, J. M. Georges, and J. L. Loubet, J. Colloid Interface Sci. **126**, 150 (1988).
- ^{12a}“Frontiers in Chemical Engineering,” Chairman: Neal Amundson, National Academy Press, Washington, DC (1988).
- ¹³S. Tolansky, *Multiple Beam Interferometry of Surfaces and Films* (Oxford University Press, 1948).
- ¹⁴S. Tolansky, *An Introduction to Interferometry* (Longmans, Green & Co., London, 1955).
- ¹⁵J. N. Israelachvili, Nature-Phys. Sci. **229**, 85 (1971); J. Colloid Interface Sci. **44**, 259 (1973).
- ¹⁶J. N. Israelachvili, E. Perez, and R. K. Tandon, J. Colloid Interface Sci. **78**, 260 (1980); R. G. Horn, J. N. Israelachvili, and F. Pribac, J. Colloid Interface Sci. **115**, 480 (1987).
- ¹⁷L. R. Fisher and J. N. Israelachvili, J. Colloid Interface Sci. **80**, 528 (1981); Colloids & Surfaces **3**, 303 (1981).
- ¹⁸C. A. Helm, J. N. Israelachvili, and P. M. McGuiggan, Science **246**, 919 (1989).
- ¹⁹R. G. Horn and J. N. Israelachvili, J. Chem. Phys. **75**, 1400 (1981).
- ²⁰P. M. McGuiggan and J. N. Israelachvili, J. Mater. Res. **5**, 2232 (1990).

GENERAL OPERATING PROCEDURES

PREPARATION OF MICA SURFACES FOR FORCE MEASUREMENTS OR INTERFEROMETRIC EXPERIMENTS

Prepare the laminar flow cabinet for cleaving by laying out clean tweezers and mini-forceps (Figure 33), the metal blocks for holding mica sheets during cutting, the hot wire cutter connected to a low voltage DC power supply, platinum wire (0.2 mm or 0.006"-0.008" diameter), large scissors, petri dish (10 cm or 4" diameter), ethanol cleaning liquid, a few large mica sheets, and 5 dangling clips from the ceiling of the cabinet for hanging mica sheets from.



Figure 33. Tweezers and other small tools used in various mica-handling operations such as cutting, gluing and mounting (see also Fig. 30). Tools should be cleaned before each stage.

Select a 15cm X 20cm X 0.5 mm thick sheet of Ruby Muscovite mica, trim its edges with large strong scissors, and remove all excess edge flakes, beat sheet a few times to allow edge flakes to disperse (don't do this near delicate surfaces). From this sheet a semi-thick sheet is cleaved (peeled) *slowly* to expose two smooth surfaces that are largely step-free as ascertained by eye. Step-free surfaces are usually obtained when the bifurcation line moves smoothly, without jerking or 'cracking' during the peeling. Cleavage may be initiated by inserting the tip of a sharp needle into the edge of the thick sheet, opening up the crack by gentle lateral movement of the needle, followed by careful peeling away of the two sheets. The freshly cleaved sheets are examined in the neon light of the laminar flow cabinet for the number/location and direction of the steps. One of the two sheets (the best or thinnest) is chosen as the 'backing sheet' and hung vertically from a clip parallel to the air-flow direction and well away from the cleaving area to

avoid flakes from settling on its freshly cleaved surface. The other is chosen for further cleaving of much thinner and smaller sheets to be used as the substrate surfaces in experiments. When cleaving/peeling, insert the needle as close to the freshly cleaved surface as possible and try to cleave in a direction *parallel* to the step lines. If a sheet is sufficiently thin (2-3 μm thick) interference colors are seen reflected by the surface. These colors change abruptly at cleavage steps, but remain uniform over regions of constant thickness. Thinner sheets (<1-2 μm) have brighter colors that change less with the angle, and these sheets also flap about more in the flowing air stream. When cleaving thin mica sheets from a thick sheet, it is essential to do it in as stress-free way as possible. This is usually best achieved by slowly peeling a thin sheet from the thick sheet, *parallel* to the direction of the steps. The thin sheet should be peeled away very slowly, at a uniform rate of about 5mm/sec, without tearing or sticking occurring.

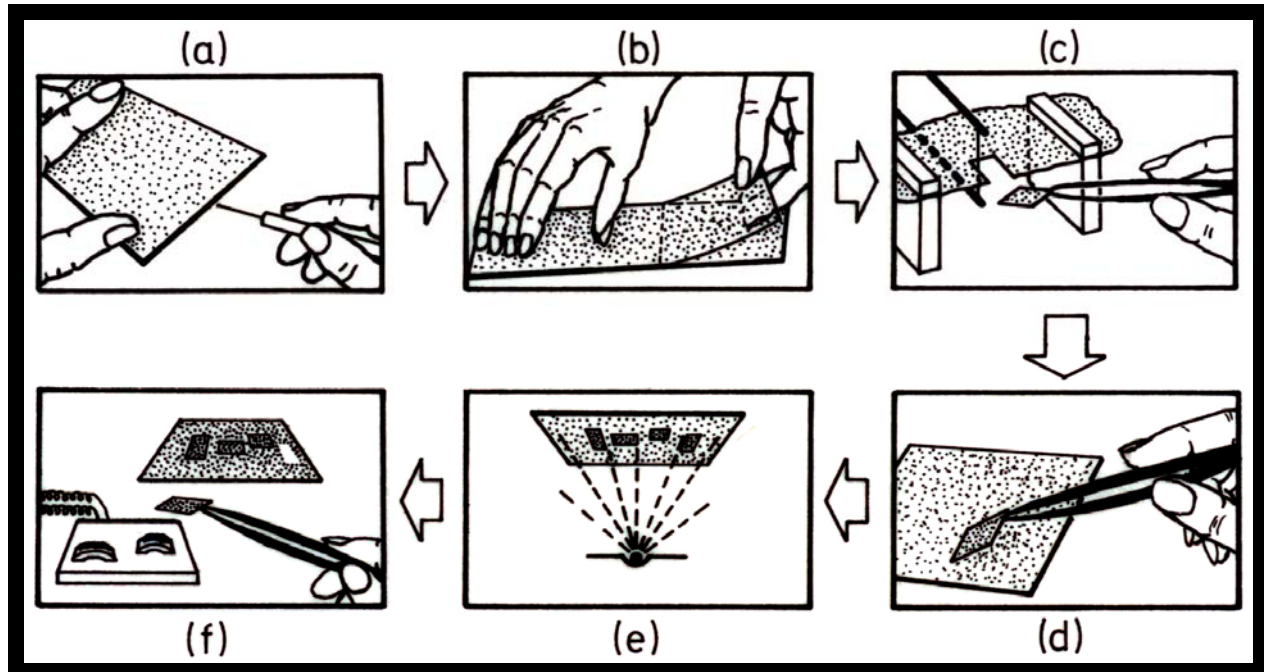


Figure 34 (Continued on next page). Stages in the preparation of mica sheets: (a)-(b) cleaving (sheets should peel away slowly and smoothly, *along* the steps), (c) cutting (fairly rapid movement of the hot wire is recommended), (d) placing cut sheets on backing sheet to which they should immediately adhere, (e) silvering, followed by storage in dessicator or (f) gluing (do not overheat). Stages (a)-(d) and (f) must be carried out in a laminar flow cabinet (horizontal air flow type); stage (e) is carried out in a vacuum coating unit or evaporator.

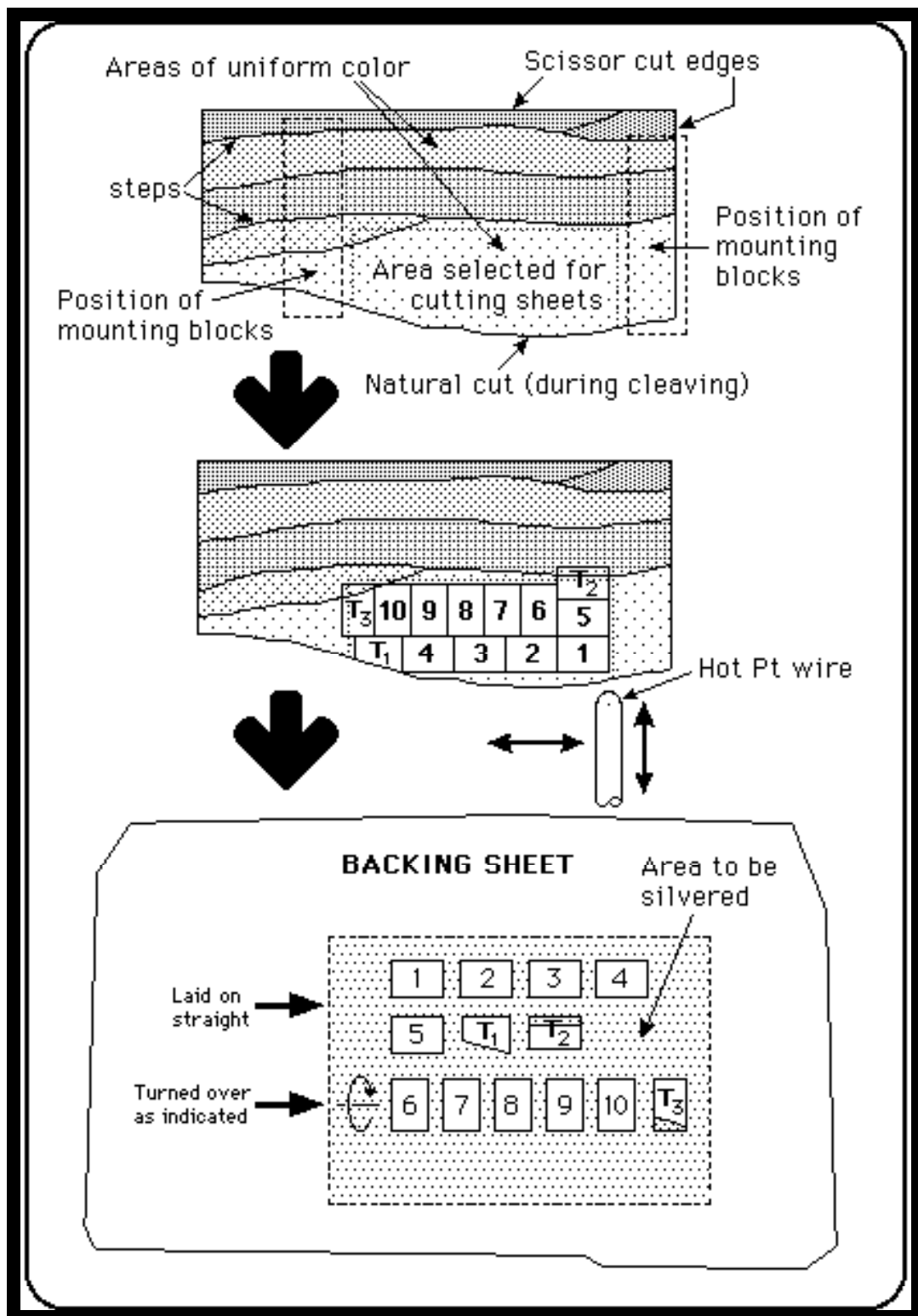


Figure 34 (continued). When pairs of sheets (1 and 6, 2 and 7, etc.) are cut and placed on the backing sheet as shown above, after gluing and mounting into the apparatus, the sheets will be in crystallographic register, displaying maximum birefringence of the FECO fringes (see Figure 35).

With experience it is possible to cleave sufficiently large regions (approx. 1 sq. inch or 10 cm²) that are a few microns thick and free of steps on either side. If a large enough step-free region is found, place it across two clean metal blocks and hold it in place with two smaller block, as shown in Figure 34(c). The platinum wire cutter should have a short ~7 mm long platinum wire of diameter 0.2 mm or 0.006"-0.008" vertically mounted between two parallel rods as shown in Figure 34(c). The rods are attached to an X-Y translation carriage. The wire is heated above the melting point of mica by passing a low voltage current through it.

Adjust the height of the platinum wire so that the centre of the wire, which will be the hottest part, is exactly at the level of the mica sheet, which should be stretched taught between the two blocks so as to be completely flat (this can be done by gentle moving the blocks apart once the mica sheet is held down on each block by the smaller block). Place the large backing sheet, face up, somewhere in the laminar flow cabinet well away from the cutting area, and note where you intend to place the small mica sheets (preferably away from steps). Check that the tips of your sharp tweezers are not bent and that they meet symmetrically. Place the wire cutter well away from the mica. Gradually increase the current through the wire until it becomes yellowish-white. After the wire has 'outgassed' (a few seconds) bring the translation stage up to the mica, position it 'correctly', and start cutting (burning) the sheets. Cut each sheet one side at a time by moving the hot wire at a uniform but fairly rapid rate of about 1-2 seconds per side. As each rectangular sheet is cut free from the main sheet it is immediately picked up with the straight, sharp tweezers and placed on the freshly cleaved surface of the backing sheet (but see Figure 35). At once, molecular contact should take place across the whole rectangular contact area, except at the edges which have been damaged during the melting; but this is to advantage as it allows the sheets to be picked up again later with tweezers. If the cut sheets do not adhere well, try turning them over; if they still adhere poorly, it is wise to reject them.

In this way, six or more small rectangular sheets (about 6 mm x 9 mm) are cut out in pairs, some length-wise, some width-wise, and placed on the same backing sheet, as shown in Figure 34. In this way the surfaces of the rectangular sheets in contact with the large sheet are protected from contamination as long as they remain there. It is advisable to keep track of each sheet, its orientation relative to the other sheets, whether it was turned over before being placed on the backing sheet and about which axis. Figure 35 gives further details on how to cut and place sheets so that their relative crystallographic orientation is preserved or rotated by a known angle during experiments. After making a sketch of the disposition and orientation of all the pieces on the backing sheet, it can be turned over and placed, like a cover, on the clean petri dish for transporting out of the laminar flow cabinet.

It is also wise to cut a few "test" sheets (labelled T in Figure 34) that can be used for measuring the thickness and orientation of the mica sheets prior to using them in an experiment. After silvering the backing sheet (see below), one of the test sheets can be glued onto a glass plate (a microscope cover slip is ideal) and another laid on it as in a normal experiment, ensuring that the silvered surfaces are on the outside in both cases. This test piece can then be stuck directly onto the entrance slit of the spectrometer and the fringes observed by directing a light beam from a small flashlight (torch) onto the surfaces by hand. Alternatively, the fringe positions can be more accurately measured by placing the glass plate below the microscope tube of the Optics Stand, aligning the optics and adjusting the position and angle of the surfaces as in a normal experiment, and measuring the fringes accurately.

All the above operations should be carried out in a laminar flow dust-free laminar flow cabinet (hood) to prevent dust and mica flakes from settling on the freshly cleaved surfaces (the flow of air should be *horizontal* and *outwards* towards the worker). Surgical gloves may be worn to prevent oily secretions from spreading onto the surfaces. The mica should always be handled at its edges only. It should be remembered that inhalation of fine particles is a health hazard, so precautions are advisable for protection of both lungs and eyes when cleaving the mica.

Next, the exposed surfaces are silvered in a vacuum coating unit at a pressure of $\sim 10^{-5}$ torr (allow 1-2 hrs for outgassing) as shown in Figure 34(e). Standard precautions should be taken to ensure that a uniform layer of pure silver (about 550 Å thick and/or of $\sim 98\%$ reflectivity) is deposited at $\sim 1 \text{ \AA/sec}$ at a pressure of $\sim 10^{-6}$ atm. In particular, *the mica backing sheet should be at least 40 cm away from the crucible* (e.g., molybdenum boat) to avoid overheating of the deposited silver layer. An overheated layer will look brownish rather than bluish and have a lower reflection coefficient. After silvering, the large sheet is returned to the dust free cabinet for gluing, as shown in Figure 34(f), or stored in a dessicator for later use. The adhering surfaces will be protected from environmental contaminants so long as the sheets remain on the backing sheet, but it is also important to prevent deterioration of the silver layers by ensuring that the dessicator atmosphere is dry and free of oily vapors (otherwise the silver surface may not adhere well when the sheets are later glued onto the glass surfaces).

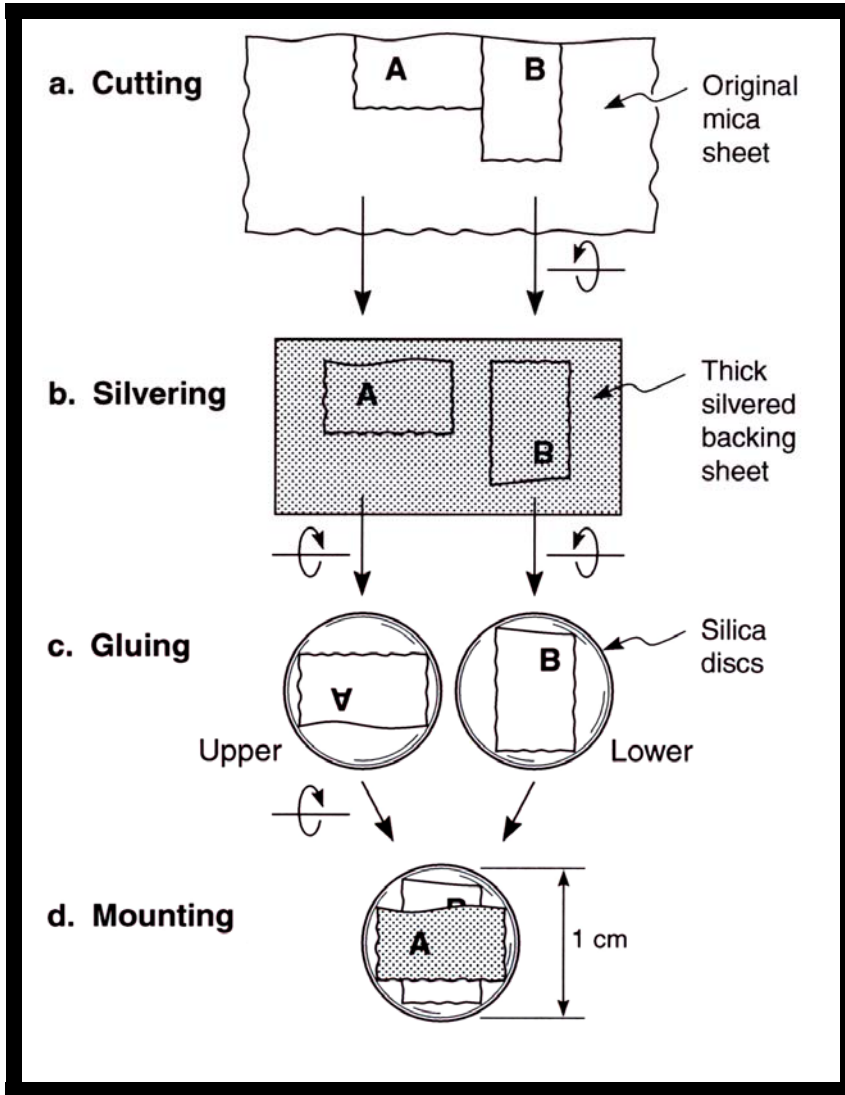


Figure 35. The birefringence of the FECO fringes varies as $\cos\theta$, being maximum for $\theta=0^\circ$ and zero for $\theta=\pm 90^\circ$, as described later. This figure gives the procedure for preparing and mounting mica sheets so as to preserve or control the mutual crystallographic orientation, or twist angle θ , of the two sheets (refer also to Figure 34).

First, a mica sheet is cleaved to produce an area with a uniform thickness of about one micron. Two rectangular pieces, A and B, are carefully cut from this area so that all the edges are either parallel or perpendicular to each other as in (a). One piece, say B, is turned over before it is put on the backing sheet to which it adheres. The other sheet, A, is also placed on the backing sheet but without being rotated (b). After silvering, the mica sheets are peeled off from the backing sheet and glued, silver sides down, onto the cylindrically curved surfaces of two silica disks as

shown in (c). The longer side of each rectangular sheet is positioned parallel to the principle cylindrical axis of each disk. Inside the apparatus chamber, the lower disk, supporting B, is mounted at the end of the force-measuring spring, while the upper is attached to the end of the piezoelectric tube. The aim is to make the two mica surfaces face each other at the same angle as in the uncleaved mica, that is, at $\theta=0$, as shown in (d), although other, non-zero orientations can also be achieved. Final alignment is done by viewing the surfaces via the microscope tube that passes through the piezoelectric tube. Exact crystallographic matching is established visually by rotating the piezo tube mount until the corners and edges of the rectangular sheets are aligned, very much as one would align two pieces of paper. This method generally allows for rough initial alignment to within $\pm 2^\circ$.

A special ring attachment (provided with each Friction Device) can be fitted snuggly around the circular Piezo Mount. This allows the upper mica sheet to be rotated by any desired 'twists' angle around a fixed vertical axis during an experiment. For very precise angular rotations, a rigid horizontal arm can attached to the top of the Piezo Mount, and a micrometer positioned at the end of the arm. This allows the twist angle θ to be controlled to better than 0.01° . Due to the fact that the two surfaces are cylindrical, it may be impractical to rotate them by more than $\pm 30^\circ$ from zero in any one experiment.

A video is available showing all stages of mica preparation: cleaving, silvering, gluing on, and mounting (inserting) into the SFA.

PREPARATION OF APPARATUS FOR FORCE MEASUREMENTS

Having previously cut, silvered and treated the mica sheets as described above, they are now ready for gluing on the silica disks and mounting into the apparatus.[†] The following assembly tools should be clean and ready for use inside the laminar flow cabinet: hot-plate, needle-sharp 'biological grade' tweezers (for lifting up mica sheets), various small forceps and tweezers, screw-drivers, glue, ethanol squirt gun.

[†] For experiments requiring 'treated' surfaces, for example, two different surfaces, or surfaces other than mica, or mica surfaces that are first coated with a layer of surfactant, polymer, metal or biological material, a number of additional stages are required before the surfaces are mounted into the apparatus. One of these is shown in Figure 36.

Switch on sodium lamp in the experimental room. Blow a filtered nitrogen gas jet into all parts of main chamber, piezoelectric mount, silica discs, tools, etc., to finally get rid of dust, concentrating on holes, outlets, inlets, etc. Attach filter to Luer outlet of Upper Chamber, then close off with Luer cap. Close off the Luer inlet on the Lower Chamber with Luer cap (attach filter first, if required). Depending on the type of experiment to be conducted, a Teflon tap (supplied) may be screwed into the Lower Chamber instead of the Luer connector. Place the Piezo Mount on the working area, facing 'up'. Note that there is also an all-steel replacement mount 00010 without the piezo tube – this can be useful for experiments in which the fine sensitivity of the piezoelectric crystal is not required. This part is also less sensitive to temperature drifts than the crystal mount. Unscrew screws 00030 on both the piezo mount 05020 and the lower disk mount 00020 just enough that there is space to slip in the silica disks.

GLUING

Gluing of mica is done by putting two silica discs on a small electrically heated hot-plate and placing some crystals of EPON RESIN, sym-diphenylcarbazide or sugar (total volume ~1 mm³) on the top curved surfaces of the discs. As the crystals melt, the liquid is spread evenly over the surfaces with curved tweezers, and a mica sheet is then peeled off the large backing sheet with straight pointed tweezers and placed on top of the glue, silvered side down. Ensure that the mica lays down out evenly over the glue layer, exposing a smooth, unbuckled surface of uniform (cylindrical) curvature. To do this, you may need to press the edges and sides gently into the glue with Teflon-tipped tweezers. The disc should be removed from the hot-plate as soon as good adhesive contact is established (underheating of the glue can cause bad adhesion, but overheating can cause small bubbles to form or even deterioration of the silver layer). On removing the disk from the hot-plate, inspect the surfaces at grazing incidence to see that no edges or flakes are sticking up. The other mica sheet of the 'matching pair' (cf. Figures 34 and 35) is now glued similarly to the second disc. If anything goes wrong (e.g., a mica sheet tearing on being stripped off) other sheets from the remaining pairs on the large sheet can be used instead.

If a 1 mm cube crystal of glue is used in the gluing, which after melting spreads out over an area of, say, 6 mm × 8 mm (~50 mm²), the final thickness of the glue layer will be 1/50 mm or 20 µm. In some experiments it is important to know this thickness, which can be deduced at the end of an experiment by first estimating the glued area per sheet, then weighing each glass disk with the mica sheets still glued on, and again after the mica and glue have been removed (see below). The density of the glue is also needed (Shell EPON RESIN series glues have a density of about 0.61 g/cm³). Sym-diphenylcarbazide (a white powder of M.P. 176°C) may also be used as a glue; it is

suitable for work in inert non-polar (but not aromatic) solvents, and aqueous solutions (so long as the temperature remains at room temperature). But it is slightly soluble in water, and more so in solutions containing divalent cations, so that after a few days dissolves away or becomes opaque. Most glues are also sensitive to high concentrations of chloride salts. The polymers EPON RESIN 1004 or 1009 (Shell) – also thermosetting glues – are better suited for work in water: they are not affected by water even at higher temperatures (60°C). However, they are more viscous than the carbazole – they have a glass transition, T_g , rather than a true melting point – and are therefore more difficult to handle. For room temperature aqueous experiments, the EPON 1004 ($T_g \approx 90\text{--}100^\circ\text{C}$) is recommended; at elevated temperatures, a higher T_g resin, such as EPON 1009, would be more suitable. Other glues can be used for work in strong organic solvents such as acetone, chloroform and toluene. Sugars are particularly good for this purpose, such as a mixture of dextrose and galactose for toluene. UV-curing glues can also be used such as Norland Optical Adhesive #61 from Edmund Scientific (see also Table I and, for example, S. M. Kilbey, F. S. Bates, M. Tirell, R. Hill, H. Yoshizawa, J. Israelachvili. *Macromolecules* **28** (1995) 5626–5631). Such glues are particularly useful for producing two flat, parallel surfaces (rather than curved surfaces), which may be desirable for some experiments. To achieve this, after gluing the mica sheets, they are brought into flattened contact inside the apparatus and the glue is then cured (set) by UV irradiation (5 Watt Hg pen-ray lamp at a distance of 3-5 cm from the surfaces) for 5-10 minutes inside the SFA chamber while the surfaces are still in contact. After curing, the two surfaces remain flat and parallel on separation. This glue dissolves in chloroform.

To remove glued mica from the discs at the end of an experiment, place in acetone or chloroform for an hour or overnight then peel off sheets.

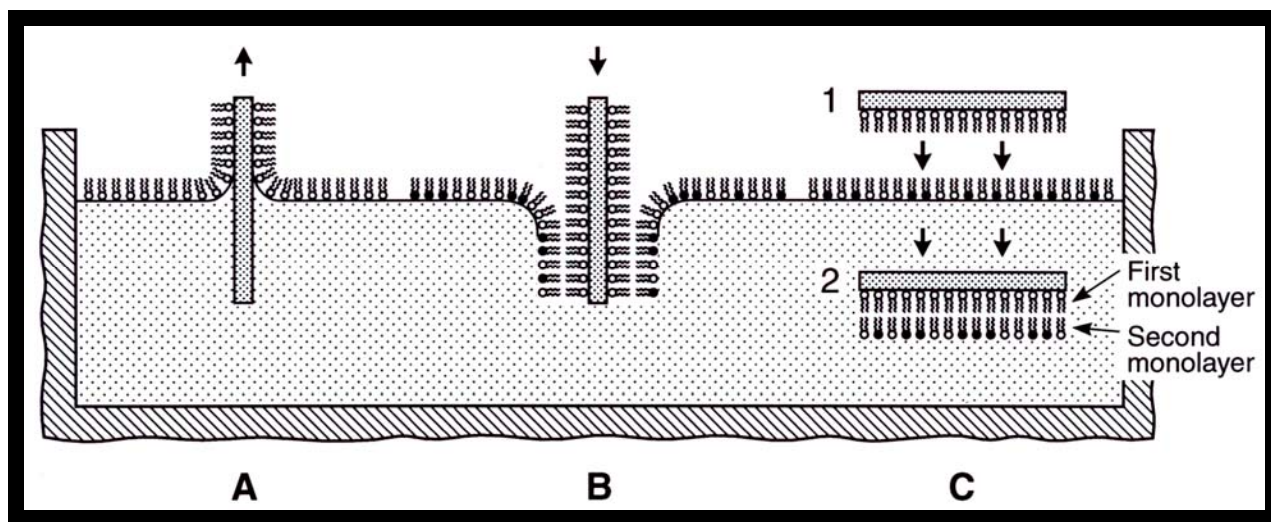
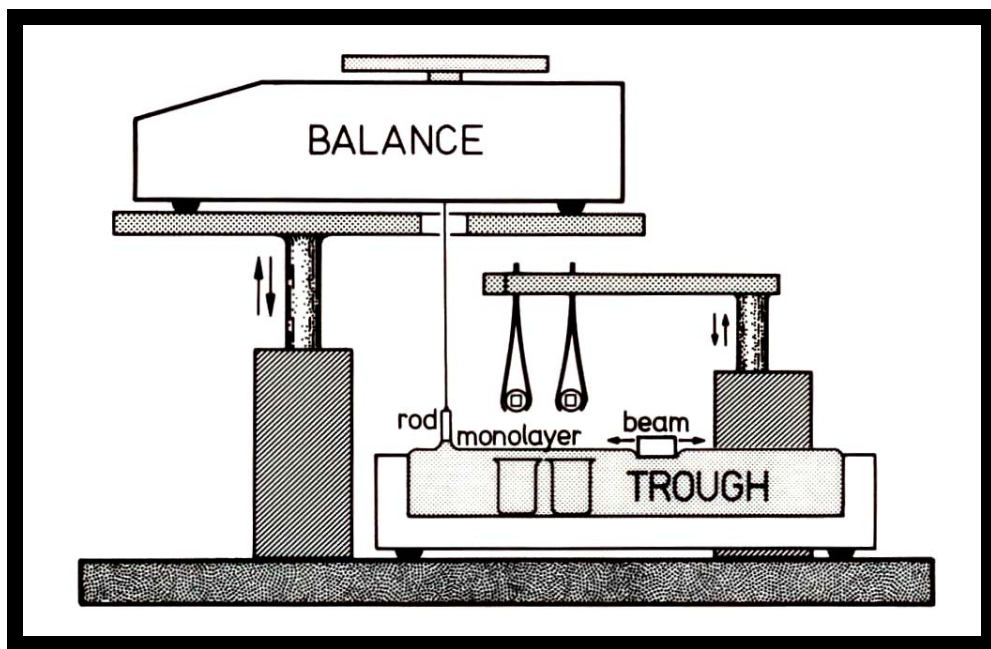


Figure 36. Langmuir-Blodgett deposition trough set-ups suitable for pre-coating mica (and other) surfaces with insoluble surfactant or lipid monolayers or bilayers prior to their installation into the apparatus. The mica sheets are shown glued to the two silica discs ready for depositing a (second) monolayer followed by insertion into the two beakers in which they will be transferred (under water) to the apparatus and mounted into position through the large front window (the apparatus must be placed on its side during this operation). A special Teflon DEPOSITION CELL may also be used for transferring the disks under water to the apparatus for insertion through the side window. Depositions may also be done in the straight contact (Langmuir-Schaeffer) method, as shown. For good, clean depositions, the trough should be fully enclosed.

INSTALLATION OF SURFACES INTO THE SFA 3

Carefully choose the 'right' disks for your experiment. Disk heights vary from 2.5 mm to 5.5 mm and can be used in various combinations (two 4 mm disks are considered 'standard'). The optimum choice depends partly on the vertical setting of the two bolting screws on part 01200 at the back of the apparatus, which in turn depends on the type of experiment being conducted – whether normal force measurement, friction experiment, bimorph sliding experiment, deposition 'under water' experiment, etc.

Glue on mica sheets on two silica discs as described in the previous section. Any additional surface treatment of the mica surfaces could be done now, for example, coating of surfactant layers (cf. Figure 36) or of metal oxide, silica or polymer layers via some other deposition, evaporative or spin-coating method. Some types of surface treatments may have to be done before the gluing.

Establish which disks and at what angles they will be mounted into their respective disk mounts so that the final configuration is the desired one (cf. Figure 37) and that the coaxial cable on the Piezo Mount protrudes at a convenient direction. Using straight but curved-ended tweezers, pick up lower disk and place into hole on the Disk Mount 00020 and tighten into place with a hex head (Alan key) or Philips head screw driver. Check that the disk is really sitting firmly in place by gently trying to lift the disk with a spatula or screw-driver and establishing that the disk does not move. Turn the coarse micrometer control to ensure that the lower surface is sufficiently low that it will not touch the upper surface when it is installed (see * below). A specially constructed STAND for supporting the UPPER CHAMBER during these operations is highly recommended (see photo of STAND in Figure 30).

Place upper silica disk and place into hole on top of the piezo mount and tighten into place. Again, check that the disk is firmly in place by gently trying to lift the disk with a thin spatula or screw-driver and establishing that the disk does not move (this will avoid making this discovery when you turn the piezo mount upside down). Turn the piezo mount over and place into position on top of the Upper Chamber without hitting the lower surface (see * above). Rotate and centralize piezo mount in its hole so that coaxial cable comes out at a convenient direction. Clamp 00080 into place in the 1:30 – 7:30 clock directions using the two Philips head screws provided (do not clamp tightly at this stage).

Position two dowel pins of Upper Chamber on holes of Lower Chamber and lower Upper Chamber gently into place. Bolt the two chambers firmly together with the four screws 02050.

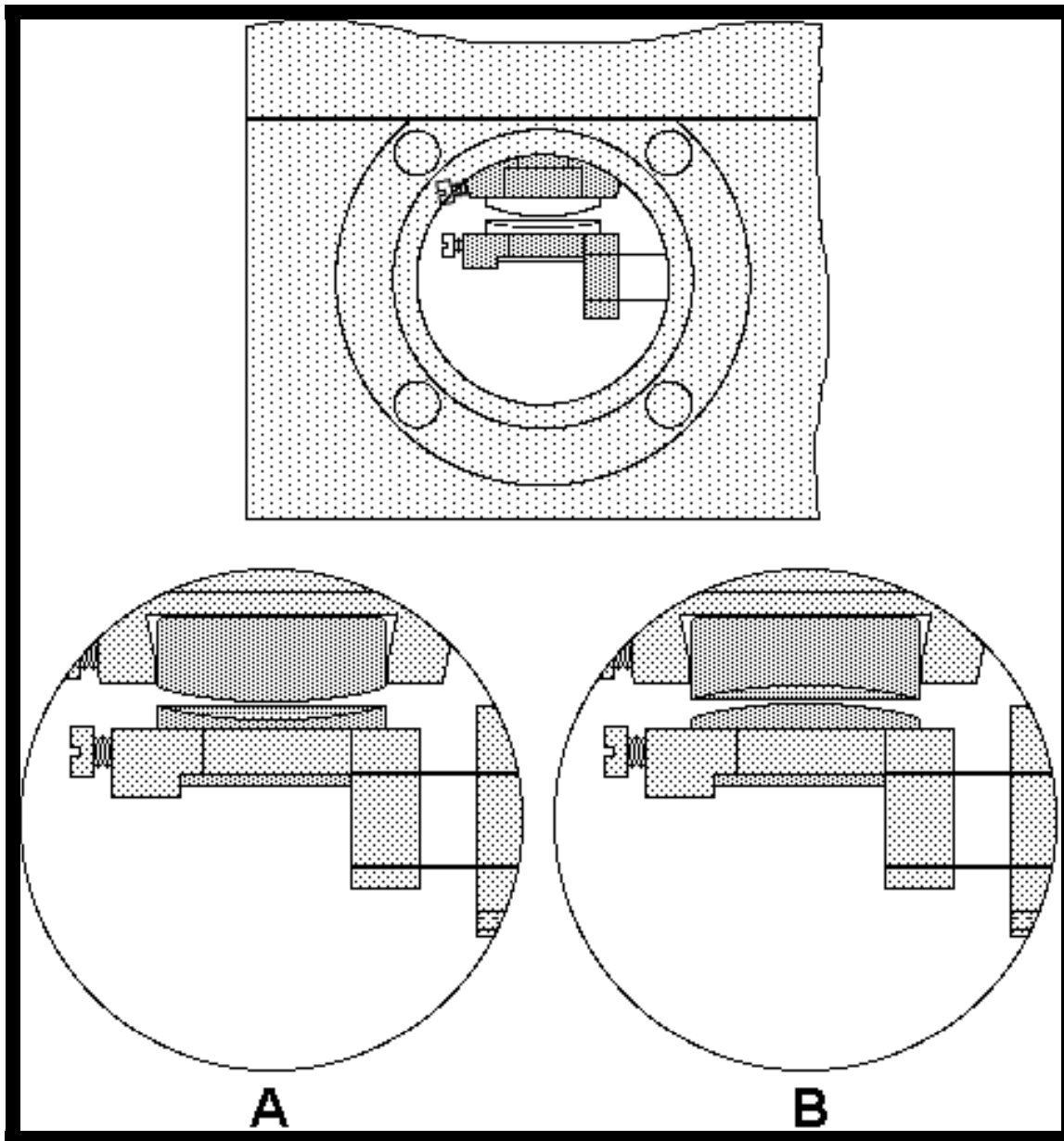


Figure 37. View through window of assembled Basic Unit after installation of the two disks (see also next page). Note that the disks may be positioned in two different ways, as shown above (angles other than 0 or 90° are also possible). In experiments involving frictional sliding this difference is important. For example, in geometry **A** the FECO fringes will remain centered in the field of view during in-out sliding of the upper surface but move during left-right sliding, whereas in geometry **B** they will move away from the centre during in-out sliding but remain fixed during left-right motion. The situation is different again when the lower surface is the one that moves, as occurs with the Bimorph Slider. One should avoid having the contact area that move away from the center of the eyepiece during sliding since this will complicate the accuracy of the optical measurements.

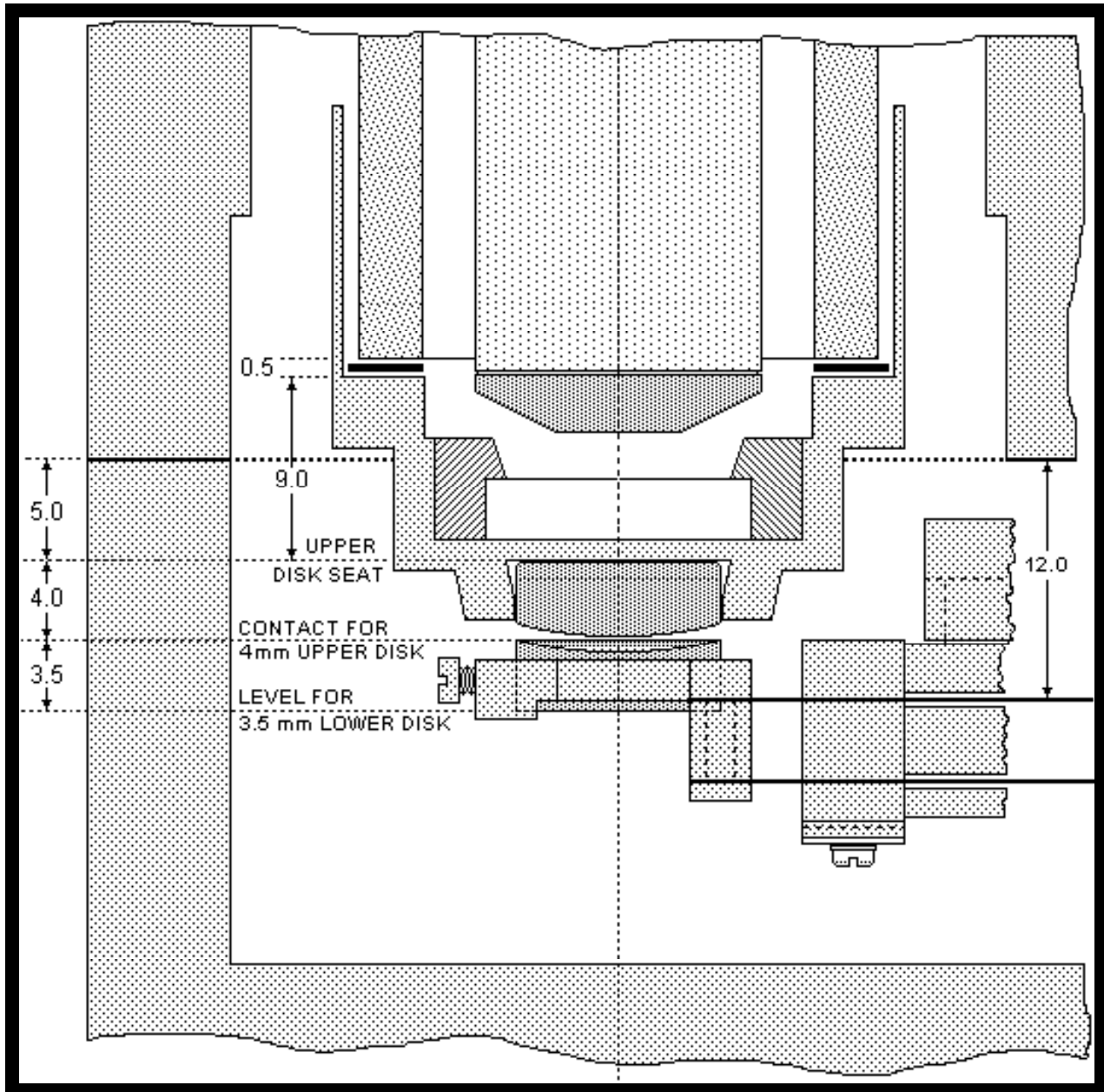


Figure 37C

INITIAL OBSERVATION OF SURFACES WITH NEWTON'S RINGS

Flush out chamber with dry, clean N₂ gas for 10–30 minutes via one of the filtered inlets and outlets as previously described.

Place apparatus on a table (preferably an anti-vibration table) and place sodium lamp under lower window. Place microscope tube with X5 or X10 objective through piezoelectric tube and place eyepiece on top. Bring lower surface close to upper surface (<<1 mm) by rotating the coarse micrometer head by hand while viewing the approaching surfaces through the front plate window (a torch light beamed at the surfaces from one of the windows helps).

After moving the surfaces close together but not into contact, observe the Newton's rings. Loosen the two clamping screws, move and rotate the piezo mount and bring the surfaces closer together manually until the Newton's Rings appear clear and central (or near central) in the field of view, and circular (or near circular). Test for reversibility *with no backlash* of differential micrometer controls, Establish that, on bringing the surfaces *very* gently together, good contact occurs and that on separation an abrupt jump apart is seen. Good contact is seen by the sudden absence of vibrations, sharpened circular rings, and fixed radius of the Newton's rings when the load is further increased (unless the force-measuring spring stiffness is high). Separate the surfaces to about 1 mm (2 turns of the coarse micrometer) and carefully (without jogging the Piezo Mount or clamp 00080) tighten the two clamping screws on 00080 that will lock the piezo mount in place. Recheck contact and note the approximate contact position on the coarse micrometer head as well as by checking the disposition of the cantilever springs on part 01030.

Flush out the apparatus with dry Nitrogen gas for at least one hour (depending on how dry or inert an atmosphere is required) then close the Luer taps and/or plug up inlets and outlets with Luer caps.

Bring surfaces into contact once again and separate to ensure that all is well (still viewing them via the Newton's rings). Separate surfaces about 0.5 mm (one full turn of the coarse micrometer).

Note: One turn of the coarse micrometer head corresponds to 0.5 mm displacement of the surfaces. The differential (fine) micrometer head provides about 0.07 mm (70 µm) per turn.

OBSERVATION OF SURFACES WITH FECO FRINGES and INITIAL MEASUREMENTS AND CALIBRATIONS

Check that the mirror, when placed in position to direct the light beam into the apparatus, reflects the light beam vertically up and brings it into focus roughly where the surfaces will be. This can be tested with a piece of paper.

Place the three legs of the Base on the three kinematic mounts 03050 (A, B, C) previously fixed onto the experimental table (preferably an anti-vibration table) suitably positioned for FECO viewing with a spectrometer, as shown in Figure 2. The entry slit of the latter should be about 50 cm from the microscope tube (or prism) and about 30 cm above the table floor. Place the Optics Stand into position.

CONNECTING THE SFA3 TO THE CONTROL BOX (Figure 29)

The Control Box provides access to the various electrically driven parts of the apparatus: the motors and piezoelectric elements for driving the surfaces together or laterally shearing them, the focusing microscope and prism turntable for optimizing the light beam from the apparatus to the spectrometer, and the heaters of the lower chamber.

All necessary electric cables for the Control Box have been supplied. Plug in the Control Box to a 3-pin power line outlet via the multi-terminal surge protector provided. Connect the optics stand cable to the OPTICS OUTPUT terminal at the back of the control box. Connect motor 1 to the MOTOR 1 OUTPUT terminal via the 2 m (6 ft) cable with the two 6-pin DIN plugs at either end (motor 2 is connected in the same way). Connect two cables from one of the independent outputs of a $\pm 25V$ (or greater) dual or triple output DC power supply to the + and - INPUT terminals for MOTOR 1 (the inputs for motor 2 are connected in the same way to the second output of the power supply). Connect one end of the ENCODER cable to the ENCODER OUTPUT terminal and the other two ends to the two encoders for motors 1 and 2. Connect a $\pm 5V$ or $\pm 10V$ fixed DC power supply outputs (no ground) to the + and - PIEZO INPUT terminals using the two PIEZO cables. Connect the PIEZO OUTPUT terminal to a high voltage $\pm DC$ amplifier (see Table 1) via a BNC-BNC cable and set the gain at $\times 50$ to $\times 100$ so that the piezo will receive a maximum of $\pm 500 V$ DC under normal operations (the piezo can easily take $\pm 1000V$ or more, but this can cause stress-induced drifts afterwards). Connect the amplifier output to the PIEZO MOUNT via the PIEZO cable (BNC-LEMO type). Connect Function Generator output to BIMORPH BNC INPUT using a BNC-BNC cable, and the BIMORPH BNC OUTPUT to the bimorph mini-coax connection on the apparatus via the BIMORPH cable. Connect the HEATER cable to the Control Box through the dual banana plug HEATER

OUTPUT. Connect the thermistor leads to a multimeter and set for resistance readings. Ground (earth) the base via the threaded hole at the front thin edge of the base plate.

Test all the Control Box switches, knobs, indicator lights, motors (Upper Chamber motor 1, Friction motor 2, prism turn-table and focus control sync. motors), bimorph and piezo voltage controls (coarse and fine), reversibility of all switches, etc.

Place mirror under lower window (it may already be there) and direct white light from tungsten-halogen or arc-lamp (see Table 1) vertically upward through the surfaces and focused on the surfaces (an I.R. filter or cold mirror is recommended for reducing heating due to the white light, this may be positioned just before or after the collimating lens). Look under the apparatus to see that the light beam is indeed entering the apparatus through the centre of the window. View surfaces with 10X eyepiece, moving the microscope tube so that the contact region is in the center of the field of view. Play with lamp focus (collimating lens), light angle, and the three mirror controls until light intensity is maximum. Bring surfaces very close together but not touching, as viewed through front window or from the known position of contact on the coarse micrometer head.

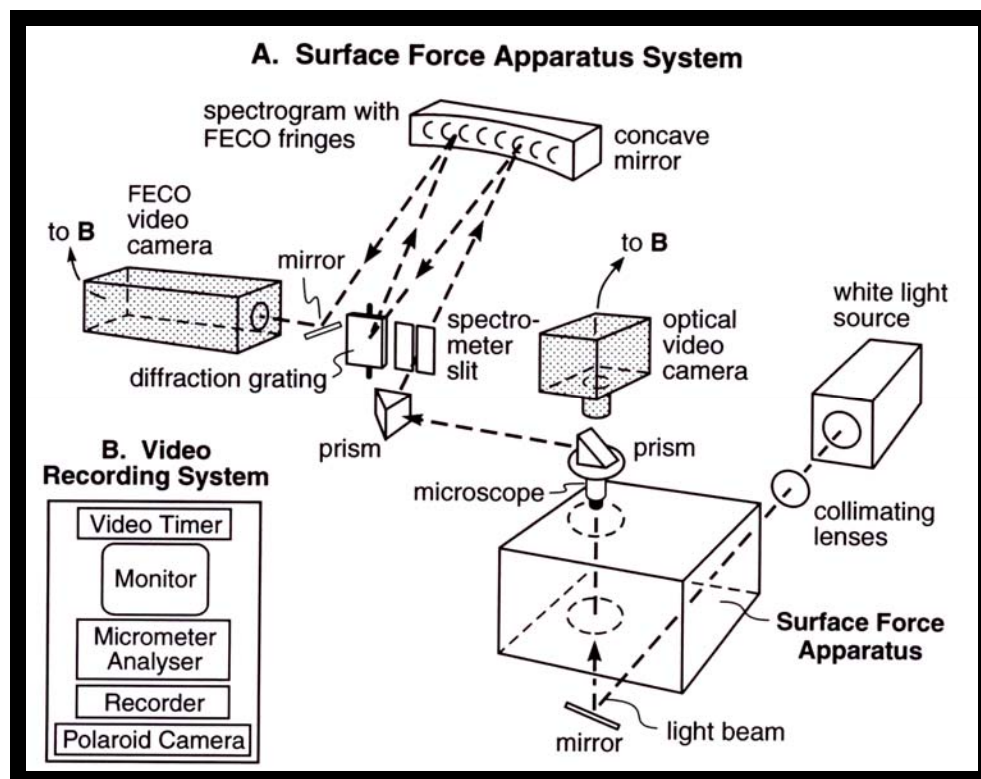


Figure 38. FECO optical system.

Replace eyepiece on turn-table by prism, darken room, focus and direct outgoing light onto spectrometer slit by adjusting the coarse focus, tilting the prism stage and rotating the turn-table. Observe FECO fringes in spectrometer exit eyepiece. When performed in air, vibrations will cause fringes to be very blurred. Mounting the apparatus on an anti-vibration table will greatly reduce this. These vibrations disappear almost totally when the box is filled with liquid, especially at surface separations below 2000 Å, so that an anti-vibration table is not essential for experiments in liquids at small separations. Vibrations also disappear in air once the surfaces come into adhesive contact.

Very gradually bring surfaces into contact. Once in contact finally adjust all the optics – lamp focus, mirror angles, prism turn-table control, prism tilt angle, microscope fine focus, slit width, etc. to make the fringes bright, sharp and as far to the *red-end* of the spectrum as possible (see Figure 43). Ensure that the contact remains flat on ‘scanning’ the surfaces by rotating the prism turn-table. Note whether alternate fringes have similar shapes over a wide spectral range (this establishes equality of the thickness of the two mica sheets).

Pick a suitable odd-shaped fringe (see Figure 39) and wavelength range (normally between the green and yellow mercury calibration lines) for measurements. Measure the fringe contact positions, and mercury calibration lines. Take photos or record fringes on video, if required. Separate surfaces manually, slowly with the coarse and fine differential micrometer and note sudden and clean jump apart. Repeat contact-separation if necessary. Test for proper functioning and reversibility, with no backlash, of micrometer controls, DC motor, encoder readout and piezoelectric controls (although this is easier to do after the apparatus has been filled with liquid). Test that thermistor and heaters are working properly. Check that the apparatus is electrically earthed (grounded).

The OPTICS STAND has been designed especially for use with the surface forces apparatus. It has the following controls, which should also be tested:

- (i) Two focus controls: manual knob and motorized. Start each new experiment with fine control at the center of the total range – the dot should be positioned mid way between the two parallel lines.
- (ii) Two prism turn-table controls: manual for coarse and motorized for fine. Start each new experiment with the micrometer reading at about 5 mm. To manually rotate turn-table, first unscrew or 'ease' slotted screw on side of turn-table.
- (iii) Linear movement (manual screw).
- (iv) Rotation of stand about main pillar (manual).
- (v) Prism tilt angle control (vertical manual screw).

Addition of a second camera

One can employ a second camera at the same time as looking at the FECO fringes by simply splitting the emerging beam by 90° using a normal 50-50 beam-splitter. The vertical (undeflected) beam can then be directed to a "top-view" camera, such as a CCD camera or fluorescence microscope, and the horizontal (deflected) beam is directed to the spectrometer, as in normal operations. For a description, with pictures, of how to combine normal optical microscopy with FECO interferometry see "Direct Visualization of Cavitation and Damage in Ultrathin Liquid Films", T. Kuhl, M. Ruths, Y-L. Chen, J. Israelachvili, *Journal of Heart Valve Disease* 3 (1994) S117–S127.

FILLING THE SFA CHAMBER WITH LIQUID

It is recommended that the chamber be filled from a 75–100 ml gas-tight syringe (the total internal volume is about 75 ml, but this depends on which attachment is installed). Aqueous solutions should be de-aerated well before filling with a suction pump or vacuum for ~1 hour. An inert material such as a piece of Teflon may be placed inside the liquid during de-aeration to aid the nucleation of bubbles. Once the liquid is ready, it should be placed in the experimental room together with the apparatus for some hours to allow both to reach the same temperature; this will reduce thermal drifts of the surfaces after filling. The room itself should be thermostatted at the desired temperature of the experiment ($\pm 0.1^\circ\text{C}$) a few hours before starting. Before filling, the chamber should be flushed out (purged) with a gentle stream of clean, dry N₂ gas through one of the inlets (open other outlet). This is always advisable, especially prior to experiments with nonaqueous liquids where trace amounts of water could prove detrimental. The surfaces should be <0.1 mm apart during the flushing (close enough to keep particles from settling on them) which should continue for about 1 hour. The chamber is now ready for filling with liquid through the right inlet on the lower chamber.

Separate surfaces about 0.25 mm and tilt apparatus on hinge 02060 so that on filling, the liquid will rise vertically past the surfaces (a supporting block may have to be inserted under the apparatus to keep it upright). Open air-outlet tap. Remove inlet Luer cap or open stop-cock and attach syringe or Teflon feed tube from filling flask. Inject liquid slowly, holding syringe and apparatus steady with both hands. The liquid surface may also be aspirated during filling through the syringe port to remove any surface-active matter before the liquid surface passes across the surfaces (this should be done inside the Laminar flow cabinet and preferably by a second person). Close syringe port (if open) and bring apparatus down onto base. Liquid level should be

above upper disk surface, as viewed through window. If all 'looks good', close or plug inlet and outlet ports. Manually bring surfaces closer together but not yet into contact.

Check that there are no leaks by noting that the liquid level does not drop over time (every few hours).

GENERAL OPERATING PROCEDURES

Manually bring surfaces to within a few microns separation using the coarse and fine (differential) micrometer heads. The fine head should be close to the mid-point of its travel range. Observe the FECO fringes in the spectrometer or video monitor, and optimize the optics (focus, mirror angles, mercury calibration lines, prisms, etc.). Fully tighten the coarse micrometer nut making sure that the surfaces are not forced into contact. From now one, only the differential (fine) micrometer, the differential spring micrometer (motor 1) and the piezo crystal controls will be used. Move surfaces closer together and test all three distance controls for smoothness and absence of backlash and drift (thermal drifts may take one hour or more to die down after filling the chamber - longer if the liquid and/or apparatus are initially at a different temperature from the room temperature, which should be thermostatically controlled to $\pm 0.1^\circ\text{C}$.

Measure forces, record fringes, etc., as described below.

The range of operation of the differential micrometer is ± 3 mm (coarse) and ± 1 mm (fine). The fine movement is reduced by a factor of about 8 between the surfaces.

The range of operation of motor 1 is 10.5 mm. This movement reduced by a factor of about 1,000 between the surfaces (i.e., 1 μm movement results in a 10 Å displacement of the spring supporting the lower surface). However, other helical springs with higher or lower spring rates (stiffnesses) can be used instead of the standard one 01310, which will result in a lower or higher 'gearing ratio' of the differential spring control (note: using *stiffer* helical springs is not recommended).

For changing the concentration of electrolyte, surfactant or polymer in the liquid, keep surfaces $\lesssim 1 \mu\text{m}$ apart (not more). Open air-outlet (with filter attached). Remove some liquid through liquid inlet on front-plate and close, always ensuring that the level stays above the mica surfaces. Slowly inject new solution through syringe inlet ensuring that no bubbles are injected. Mix contents by inwards and outwards movements of syringe. Close air-outlet tap. Allow to settle for 10–30 minutes. Rapidly separate surfaces with coarse micrometer to 1–2 mm and bring them

back again, repeating a few times – the final motion being in the 'in' direction. Now allow surfaces to equilibrate with the solution at a separation of a few μm , though for polymer solutions a much larger separation of 1–2 mm may be required.

The above procedure minimizes the probability that any impurity particles coming in with the injected liquid will settle on the surfaces, while ensuring that the solution is properly mixed.

If a particle does come between the surfaces this is readily apparent from the way the surfaces abruptly stop approaching each other at some finite (usually large) separation, and distort, as readily seen on the fringes. On other occasions a large steeply repulsive force may be measured close in which is clearly not the force that is being investigated. When this happens it is best to look for a new position of the two surfaces as follows: separate the surfaces, then loosen the two clamping screws on 00080. Replace the prism with the eyepiece and focus the microscope tube so that you can see the contact region. As you look down onto the surfaces, move the piezoelectric mount 05010 in both z and y directions to ensure that both the upper and lower surfaces have moved to a new 'contact' area. Reclamp and proceed as before. At each contact position, measure the radii of curvature of the surfaces from the FECO fringes in two perpendicular directions, using a rotating DOVE prism.

At the end of an experiment, disconnect leads (motor, piezo, friction or bimorph attachment, ground). Carefully lift off upper part of Optics Stand without moving the base (see * below). Switch off white light and mercury lamps. Remove apparatus and place in laminar flow cabinet. Attach Teflon feed tube to liquid inlet and drain chamber, tilting the box if necessary, with air outlet open and filter removed.

Calibrate the spring 04120 with weights and a traveling microscope or vernier eyepiece. One calibration should be enough – all subsequent values should be the same if the spring is clamped in the same way each time. However, if the spring is exchanged or the unit is disassembled, or if the clamping screw has been adjusted, it should be recalibrated.

Calibrate the lateral magnification of the microscope, as seen in the spectrometer, as follows: First, return the microscope tube to the same vertical position it had in the experiment (see * above). Then, place a graticule where the mica surfaces were. Focus and view the graticule markings (as dark horizontal lines) on the spectrometer entrance slit and view them in the exit eyepiece. Repeat for the perpendicular magnification with the graticule rotated by 90° and the beam rotated by 90° using the DOVE prism. Again, one calibration for the normal and

perpendicular magnifications should suffice if the apparatus and microscope stand are positioned in the same way each time (relative to the spectrometer).

If the chamber is to be used again soon with a similar liquid, there is no need to dismantle the apparatus after an experiment: fill with ethanol and drain; refill with ethanol and leave overnight. You may replace the piezo mount with the special thick round glass disk supplied for this purpose. Drain and aspirate out alcohol and pass dry N₂ gas for a few hours. Never dry the inside walls by 'wicking' with filter paper, aspirate or blow dry only. When leaving the apparatus for a long time, relieve some of the pressure on the O-rings.

Alternatively, dismantle all parts that come into contact with liquid and place in an ethanol bath; cover bath, and keep until needed again. Most O-rings need not be removed, but they should be changed once they have flattened too much after many experiments (this occurs more often with the smaller, thinner O-rings). The inlet and outlet windows are permanently press fitted into place and should never need replacing unless a leak develops.

Loosen or disconnect microscope belts when not in use for a long time.

DISTANCE MEASUREMENTS WITH FECO FRINGES

Unique features of the SFA-FECO force–measurement technique

The SFA technique for measuring forces, when used together with the FECO optical technique for visualizing two surfaces, allows for the unambiguous measurements of the following parameters that cannot be independently measured by any other combination of techniques: (i) simultaneous measurement of the static and dynamic forces, both normal and lateral, between two surfaces, (ii) independent measurement of the separation between the two surfaces at their point of closest approach at any time during the approach, separation or shearing of two surfaces, (iii) quantitative visualization of the local surface geometry and how it changes or evolves with time, for example, due to force-induced elastic deformations or damage during an interaction or during frictional sliding, and (iv) the ability to visualize contamination, trapped particles and cavitation in thin films between the surfaces from the deformed shapes of the FECO fringes in combination with refractive index measurements.

The limits of resolution of FECO fringes using modern optical techniques make it possible to measure film thicknesses to better than 1 Å (using, for example, a 32 Å/mm spectrometer), and this sets the effective limit to which distances (and refractive indices) may be measured by the method.

But to achieve this degree of accuracy, careful attention must be paid to the collimation and alignment of the light – the light must pass normally through the surfaces.

FECO fringe patterns are normally observed using a spectrometer. The microscope focuses the light emerging from the surfaces onto the spectrometer slit (ideally, the light must enter the slit at exactly 90°), and the fringes appear as a series of bright colored fringes in the spectrogram. The *lateral* magnification is, therefore, no better than that of the microscope used and, in practice, rarely exceeds 500. In any case, there is a theoretical limit to the *lateral* resolution that is possible, and is of the order of a wavelength of light.

The experimental conditions needed to obtain optimum results with multiple beam interferometry using "Fringes of Equal Chromatic Order" (FECO), have been described by S. Tolansky in *Multiple Beam Interferometry of Surfaces and Films*, Oxford University Press, 1948, and *An Introduction to Interferometry*, Longmans, Green & Co., London, 1955. The theory and use of FECO interferometry in surface studies has been described by Israelachvili in *J. Colloid & Interface Sci.* **44**, 259 (1973); Horn, Israelachvili & Pribac in *J. Colloid and Interface Sci.* **115**, 480 (1987), and Heuberger, Luengo & Israelachvili, *Langmuir* **13**, 3839 (1997). For a review of deposition techniques, see Hass, Heaney & Hunter in *Physics of Thin Films* **12**, 1 (1982).

Introduction to FECO interferometry

If two back silvered sheets of mica or other transparent material are in contact, and if white light is passed normally through them, the emerging light consists of discrete wavelengths λ_n^0 ($n = 1, 2, 3, \dots$) which can be separated and measured as sharp fringes (FECO) in an ordinary grating spectrometer. If the two sheets have the same thickness, T, and if the surfaces are then separated by a distance D, these fringes shift to longer wavelengths λ_n^D given by

$$\tan(2\pi\mu D/\lambda_n^D) = \frac{2\bar{\mu} \sin \left[\frac{1 - \lambda_n^0 / \lambda_n^D}{1 - \lambda_n^0 / \lambda_{n-1}^0} \pi \right]}{(1 + \bar{\mu}^2) \cos \left[\frac{1 - \lambda_n^0 / \lambda_n^D}{1 - \lambda_n^0 / \lambda_{n-1}^0} \pi \right] \pm (\bar{\mu}^2 - 1)} \quad (1)$$

where + refers to odd order fringes (n odd), and - refers to even order fringes (n even). $\bar{\mu} = \mu_{\text{mica}}/\mu$, where μ_{mica} is the refractive index of mica at λ_n^D , and μ is the refractive index of the medium between the two mica surfaces at λ_n^D . For separations less than 300Å, the above equation simplifies to the following two approximate equations

$$D = \frac{n F_n (\lambda_n^D - \lambda_n^0)}{2\mu_{\text{mica}}} \quad \text{for } n \text{ odd (positive sign in Eq. 1)} \quad (1a)$$

$$D = \frac{n F_n (\lambda_n^D - \lambda_n^0) \mu_{\text{mica}}}{2\mu^2} \quad \text{for } n \text{ even (negative sign in Eq. 1)} \quad (1b)$$

where $F_n = \frac{\lambda_{n-1}^0}{(\lambda_{n-1}^0 - \lambda_n^0)}$ (1c)

from which the refractive index can be calculated from

$$\mu = \left(\frac{(\lambda_{n-1}^D - \lambda_{n-1}^0)(n-1)F_{n-1}}{(\lambda_n^D - \lambda_n^0)nF_n} \right)^{1/2} \mu_{\text{mica}} \quad (1d)$$

which requires a simultaneous measurement of λ_n^D and λ_{n-1}^D .

By use of the above equations both the distance D and the medium refractive index μ can be determined independently by measuring the shifts in wavelengths of an odd and adjacent even fringe. The accuracy is about ± 0.1 nm for measurements of D in the range 0–200 nm, while for μ it is better than 1% at large D but is less accurate as D falls below 10 nm. To use the above equation we only require an accurate prior determination of the refractive index of the mica. The refractive index and dispersion of mica can be measured with an Abbé Refractometer using Hg and Na light.[†] The accuracy is ± 0.0002 – more than adequate for most purposes. Mica is birefringent, so that each fringe appears as a doublet – its exact location in the spectrum being determined by the refractive indices of the two components, known as the γ and β components. Typical values for the refractive indices, which vary from mica to mica, are

$$\left. \begin{aligned} \mu_\gamma &= 1.5846 + 4.76 \times 10^5 / \lambda^2 (\text{\AA}) \\ \mu_\beta &= 1.5794 + 4.76 \times 10^5 / \lambda^2 (\text{\AA}) \end{aligned} \right\} \mu_{\text{mean}} = 1.5820 + 4.76 \times 10^5 / \lambda^2 (\text{\AA}) \quad (2)$$

for red or brownish micas, and

[†] Because mica is birefringent, these measurements can be tricky and require that the rectangular or square mica sheet used in the refractometer have its edges cut parallel to the two optic axes (this can be established with crossed polaroids) and polished flat. Two measurements are made at each wavelength (e.g., Hg and Na), with each axis respectively parallel and perpendicular to the light, which give the γ and β components at that wavelength.

$$\left. \begin{array}{l} \mu_\gamma = 1.5953 + 4.76 \times 10^5 / \lambda^2 (\text{\AA}) \\ \mu_\beta = 1.5907 + 4.76 \times 10^5 / \lambda^2 (\text{\AA}) \end{array} \right\} \mu_{mean} = 1.5930 + 4.76 \times 10^5 / \lambda^2 (\text{\AA}) \quad (2)$$

for greenish micas. These values correspond to a birefringence of $\Delta\mu = \mu_\gamma - \mu_\beta = 1.5846 - 1.5794 = 0.0052$ for brownish micas, and $\Delta\mu = 1.5953 - 1.5907 = 0.0046$ for greenish micas. When two equally thick mica sheets are in contact, the resulting fringes will have an 'effective' birefringence (Figure 39) given by

$$\Delta\mu_0 = \Delta\mu \cos\theta \quad (3)$$

where $\Delta\mu$ is the intrinsic, or maximum, birefringence of the sheet material, obtained for a single sheet or for two perfectly aligned sheets (as given above), and where θ is the 'twist' angle between the crystallographic axes of two misaligned sheets (see example below). When the effective birefringence is less than the maximum, the refractive index of the β and γ components is then given by

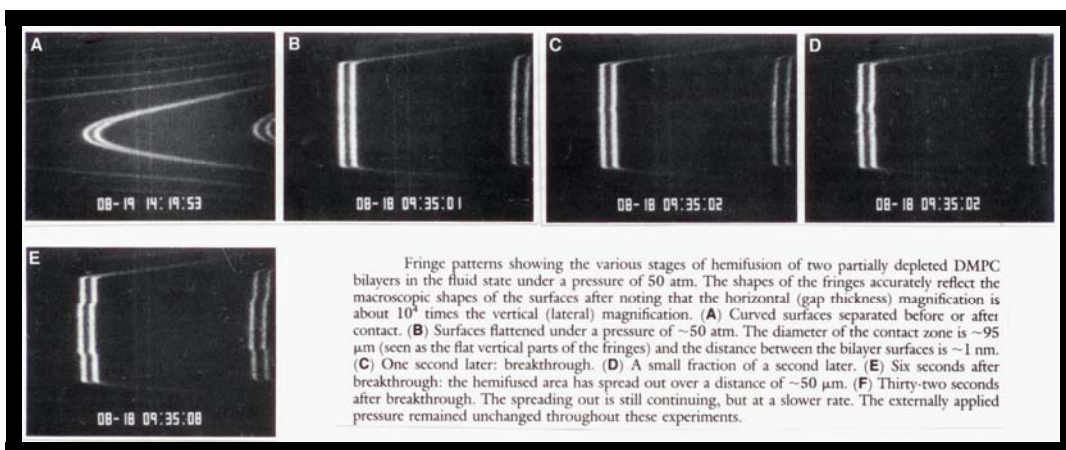
$$\mu_\gamma = \mu_{mean} + \frac{1}{2} \Delta\mu_0 \quad \text{for the } \gamma\text{-components}$$

and

$$\mu_\beta = \mu_{mean} - \frac{1}{2} \Delta\mu_0 \quad \text{for the } \beta\text{-components} \quad (4)$$

which are the values that must be used in Equation 1.

As an example of the use of Equation 1, consider an experiment where the contact wavelengths of the β and γ components of three adjacent fringes, λ_n^0 , λ_{n-1}^0 and λ_{n-2}^0 , are measured and found to be as given in the upper set of boxes in Figure 39. After separating the surfaces, the positions of the curved tips of the n and $(n-1)$ order fringes are measured and the corresponding wavelengths, λ_n^D and λ_{n-1}^D , are given in the lower set of boxes in Figure 39.



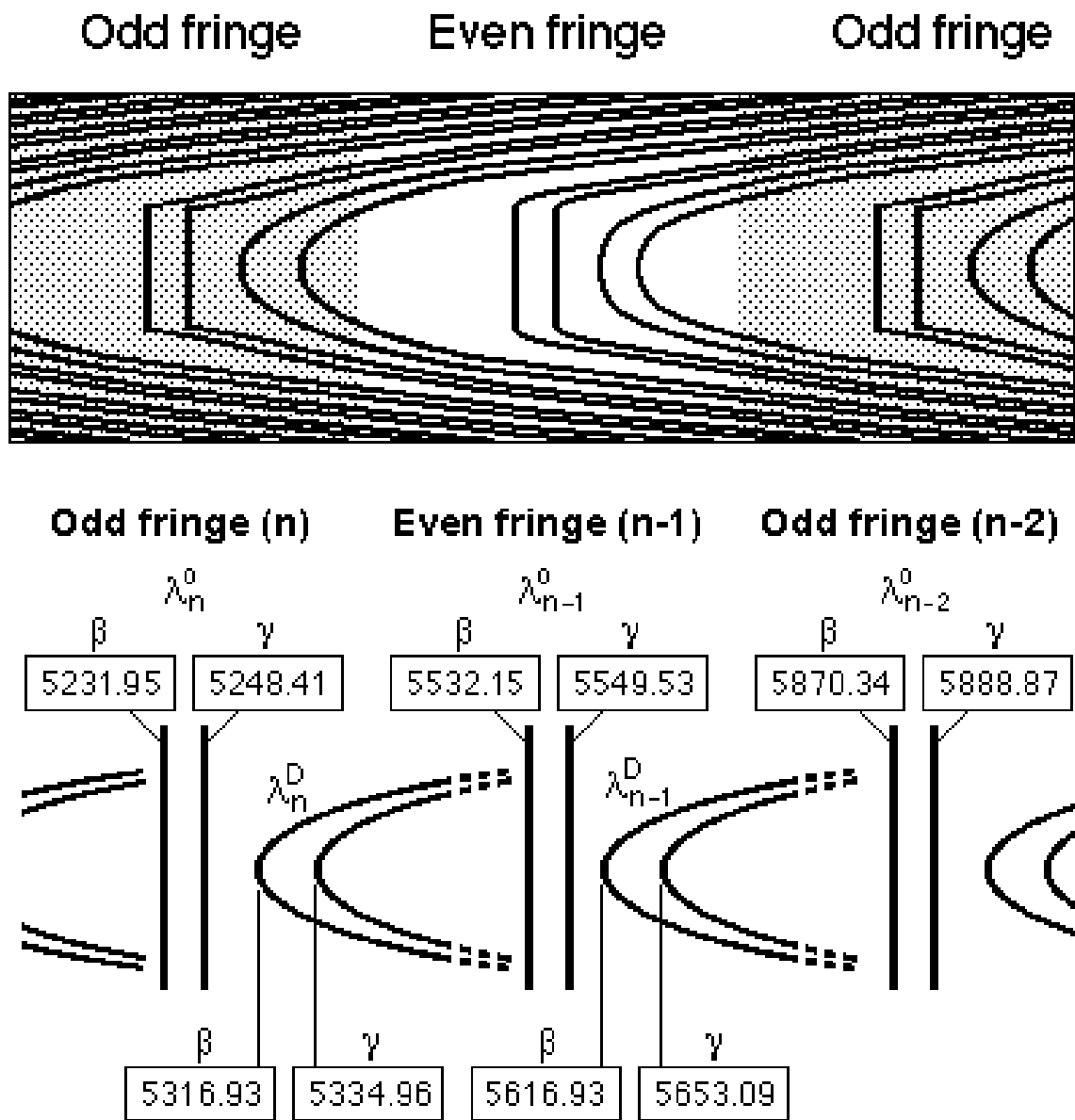
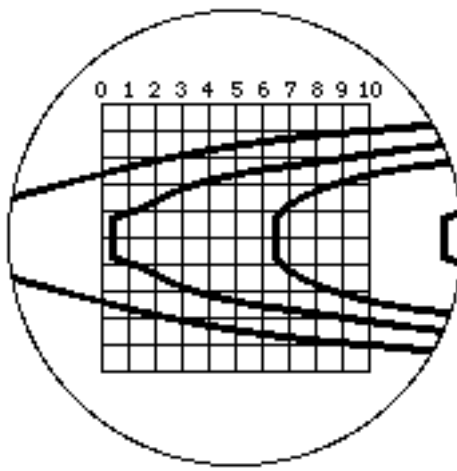


Figure 39. Numerical example of analysis of FECO fringe patterns. To measure the positions of the flat or curved tips of fringes, it is recommended that the movable eyepiece on the spectrometer exit have a graticule placed in the focal plane with a 10×10 grid of vertical and horizontal lines 1 mm apart, as shown below and in Figure 40.



The effective birefringence of two mica sheets in contact can be calculated from the contact wavelengths at λ according to

$$\Delta\mu_0 \approx \frac{(\lambda_\gamma^0 - \lambda_\beta^0)\mu_{\text{mica}}}{\lambda} \quad (5)$$

which for the above values gives $\Delta\mu_0 \approx 1.60 \times (5248.41 - 5231.95)/5240 = 0.0050$. For this brownish mica $\Delta\mu \approx 0.0052$, which implies that $\theta \approx 0$, i.e., that the two sheets are well aligned. From Equations 2–5, the refractive indices of the γ and β components at different wavelengths are therefore: $\mu_\gamma = 1.5845 + 4.76 \times 10^5 / \lambda^2 (\text{\AA})$ and $\mu_\beta = 1.5795 + 4.76 \times 10^5 / \lambda^2 (\text{\AA})$. Using these values, Equation 1 can be solved simultaneously for the pair of adjacent odd (n) and even fringes ($n-1$) – independent solutions being obtained for the γ and β components – to give

for the β -component: $D = 493 \pm 1 \text{ \AA}$, $\mu_{\text{medium}} = 1.540$,

for the γ -component: $D = 493 \pm 1 \text{ \AA}$, $\mu_{\text{medium}} = 1.717$.

The above values were measured in an experiment across a thin film of the birefringent liquid crystal 5CB whose bulk refractive index components are very close to the above two values.

Normally, however, μ_{medium} is known and the intervening liquid is not birefringent, so that Equation (1) can be solved directly for one fringe only (normally the β -component of an odd fringe) without iteration for odd and even fringes or simultaneous measurements of β and γ fringes.

The method for measuring D described above is recommended for distances up to 5,000–10,000 \AA (but can be used at all distances). For larger separations, above about 10,000 \AA , we may note

that on bringing the surfaces into contact, and counting the number of fringes that have to pass the contact wavelength λ_n^0 in the process, one can readily obtain the separation: each time a fringe passes λ_n^0 , the distance moved until the next fringe passes λ_n^0 is exactly $\lambda_n^0/2\mu$ where μ is the refractive index of the medium (liquid, vapor) between the surfaces. Thus if ~ 9.3 fringes are moved until contact, the original separation is therefore $9.3 \lambda_n^0/2\mu$. This method is not exact, but is rapid and accurate to at least 1%.

The following formula gives the exact surface separation for an arbitrary fringe shift and requires only that the contact positions $(\lambda_n^0, \lambda_{n-1}^0)$ of two adjacent (odd and even) fringes be measured: At some large surface separation where two adjacent fringes of unknown order p and $p-1$ having wavelengths λ_p and λ_{p-1} are situated between λ_n^0 and λ_{n-1}^0 (i.e., $\lambda_n^0 < \lambda_p < \lambda_{p-1} < \lambda_{n-1}^0$) the surface separation D is given by

$$\begin{aligned} D &= \frac{\lambda_p \lambda_{p-1}}{2\mu(\lambda_{p-1} - \lambda_p)} + \frac{\lambda_{p-1} T_p}{\lambda_{p-1} - \lambda_p} - \frac{\lambda_p T_{p-1}}{\lambda_{p-1} - \lambda_p} \\ &= \frac{1}{(\lambda_{p-1} - \lambda_p)} \left[\frac{\lambda_p \lambda_{p-1}}{2\mu} + \lambda_{p-1} T_p - \lambda_p T_{p-1} \right] \end{aligned} \quad (6)$$

where T_p and T_{p-1} are the distances calculated assuming that λ_p and λ_{p-1} have shifted from λ_n^0 , i.e., by using λ_p and λ_{p-1} for λ_n in Equation (1). If $\lambda_p = \lambda_n^0$, then $T_p = 0$ and the above equation simplifies to

$$D = \frac{1}{(\lambda_{p-1} - \lambda_p)} \left[\frac{\lambda_p \lambda_{p-1}}{2\mu} - T_{p-1} \lambda_p \right]. \quad (7)$$

For very large separations, above 10 μm and out to hundreds of microns, a third method of distance measurement becomes more practicable whose accuracy is of the order of 1%. At such large separations the FECO fringes are very close together. If the wavelengths of any two adjacent fringes are measured as λ_p and λ_{p-1} then the separation of the surfaces is given by

$$D = \left[\frac{\lambda_p \lambda_{p-1}}{\lambda_{p-1} - \lambda_p} - \frac{\lambda_n^0 \lambda_{n-1}^0}{\lambda_{n-1}^0 - \lambda_n^0} \right] / 2\mu \quad (8)$$

where $\lambda_n^0, \lambda_{n-1}^0$ are the wavelengths of any two adjacent fringes at contact, and μ is the refractive index of the medium, as above. (Values of λ_p and λ_{p-1} may be obtained more accurately by averaging over a number of, say, ten fringes in the field of view.) The derivation of the above formula is straightforward, viz.

$$2 \frac{\lambda_p \lambda_{p-1}}{(\lambda_{p-1} - \lambda_p)} = 2T\mu_{\text{mica}} + D_{\text{medium}} \quad (9)$$

where T is the (single) mica sheet thickness, given by

$$2T\mu_{\text{mica}} = \frac{\lambda_n^0 \lambda_{n-1}^0}{2(\lambda_{n-1}^0 - \lambda_n^0)}. \quad (9a)$$

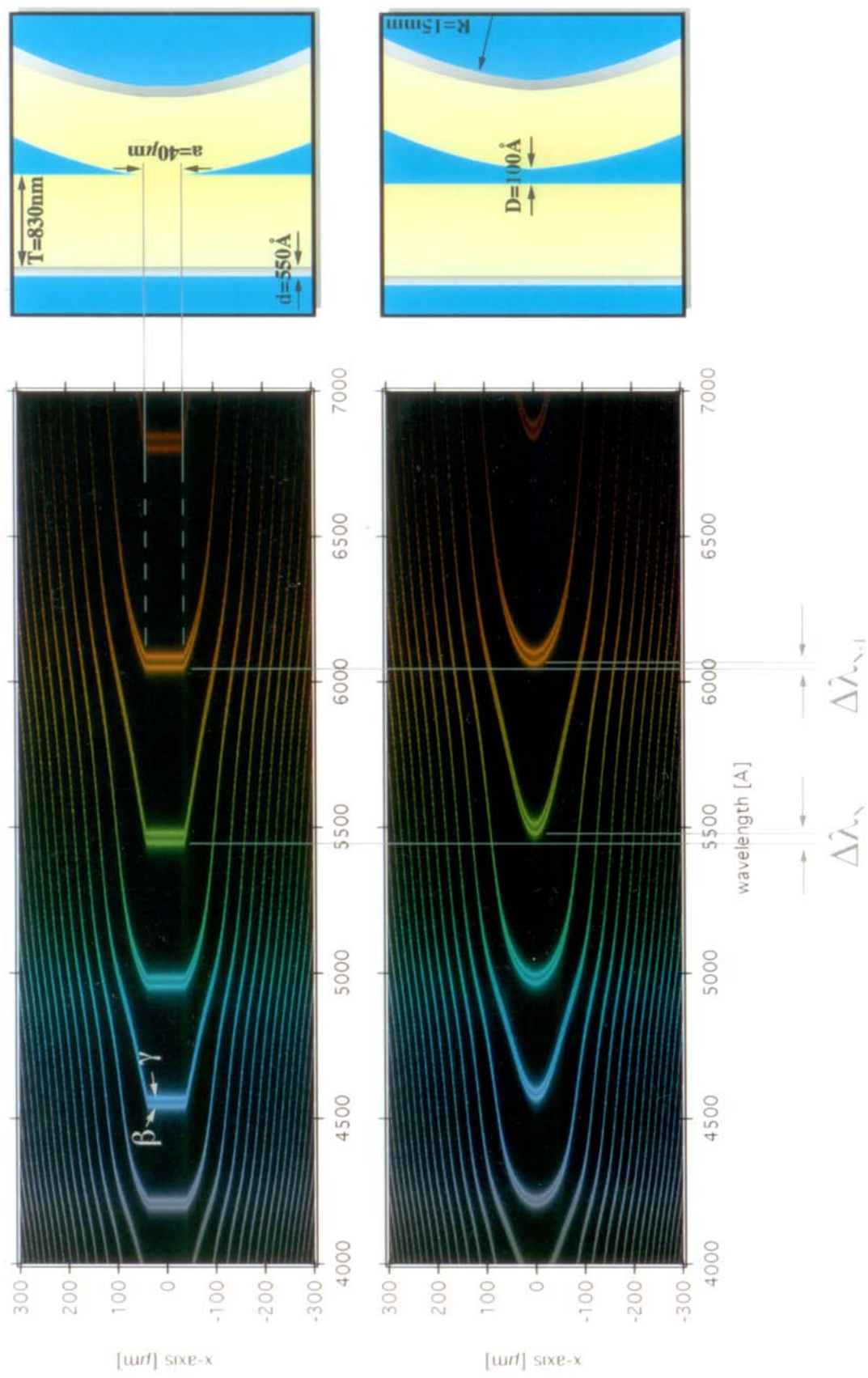
Some useful hints and rules of thumb

- (1) When using a grating with a dispersion of about $32\text{\AA}/\text{mm}$ (the standard value) the thickness of the mica *in microns* may be quickly estimated from the spacing between adjacent contact fringes as measured in the eyepiece *in millimeters* (see Figure 40a): thickness (μm) = $14/\text{spacing}$ (mm). Thus, a spacing of 7 mm between fringes means that the mica is about 2 μm thick.
- (2) When looking into the eyepiece before two surfaces are far from contact, a series of faint vertical bands (\cos^2 fringes) will be seen. When final contact occurs, the odd fringes will be at the centers of the dark regions, and the even fringes will be at the centers of the bright regions.
- (3) When two surfaces are brought towards each other from a large distance, very time a fringe passes a contact wavelength, say λ_n^0 , the surfaces will have been moved by $\lambda_n^0/2\mu_{\text{medium}}$, which for typical values of $\lambda_n^0 \approx 5,500\text{\AA}$ and $\mu \approx 1.33$ (water) means a displacement of about 2,000 \AA .

Additional notes

Note that the optical method for measuring the surface separation actually measures the distance between the two outer silvered layers on the far sides of the mica sheets. For sheets having a typical thickness of $T=2.5 \mu\text{m}$, one can verify that no error greater than $\pm 0.1 \text{ nm}$ in the surface separation is caused by normal temperature variations ($\pm 0.5^\circ\text{C}$) and applied pressures of the experiments (unless these are higher than a few hundred atmospheres, which can be directly measured using the Hertz or JKR theories). For temperature variations above about 1°C , a correction to $2T$ has to be made. The thermal expansion of mica is $(9-12)\times 10^{-6}/^\circ\text{C}$; thus, for example, a 10°C rise in temperature of the liquid will expand the composite mica sheets ($2T$) by $\sim 6 \text{ \AA}$ if $2T = 6 \mu\text{m}$. However, since μ also increases with temperature, the *apparent* increase in T , as measured by an odd fringe, is about twice this value. It is recommended that the effect of temperature on the contact fringe positions be simply calibrated before or after an experiment with two mica sheets in contact. This allows one to establish what correction is required for $D=0$ in a force measurements at different temperatures using the same type of mica.

Multiple Beam Interferometry in the Surface Forces Apparatus



During force measuring experiments it is advisable to periodically check and readjust the position of the Hg (or other) calibration lines in the spectrometer, since temperature drifts in the room can cause the spectrometer to expand and slightly move the Hg line with time. This is particularly important when measurements requiring accuracy at the sub-ångstrom level are being carried out.

OTHER MEASUREMENTS AND OBSERVATIONS WITH FECO FRINGES

FECO interferometry is a powerful technique for measuring not only surface separations but also a host of other surface and thin-film phenomena both at equilibrium (static measurements) and as a function of real time (dynamic measurements). All that is required is a good 1/2 metre grating spectrometer (a 1/4 m can be just as good) with a grating of dispersion 32Å/mm that has been calibrated for both normal and lateral magnification (spare gratings having half and/or twice the nominal dispersion may sometimes be useful for certain types of measurements). A wide-field focusing eyepiece (see Table 1) should be attached at the exit slit, supported on a translation stage that can be moved laterally across the focal plane of the spectrogram over a distance of about 20 mm. An encoder readout on the translation stage allows lateral distance measurements to be later transformed into wavelengths. The eyepiece should have a 10 mm X 10 mm grid in the focal plane (Figure 39 and 40A), although other interchangeable eyepieces with different graticules may sometimes be more useful, such as one with a simple cross-wire or a cross-wire with 0.1 or 0.2 mm graduations on the vertical line (for measuring the length of the flat parts of FECO fringes which give the contact area, as illustrated in Figure 40B). For dynamic measurements, an SIT video camera with monitor, recorder and video analyzer may be attached to the second exit port (camera port) on the spectrometer. This, and other optical accessories that are required or are optional for dynamic optical measurements are listed in Table 1 on page 11.

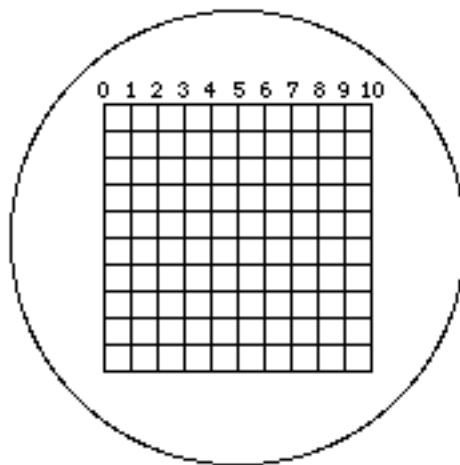


Figure 40A

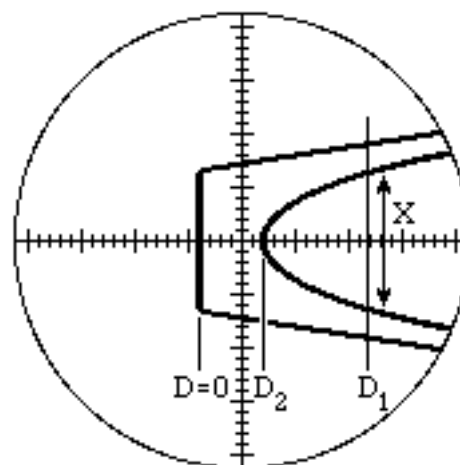


Figure 40B

Measuring surface radii (refer to Figure 40B)

The local radius of curvature in one direction R_{TMTM} may be obtained from the shape of the FECO fringes. Measure the two distances D_1 and D_2 , as well as the lateral distance X on any one fringe. If the spectrometer-microscope magnification factor is f , the radius R_{TMTM} is given by

$$R_{\text{TMTM}} = \frac{(X/f)^2}{8(D_1 - D_2)} \quad (10)$$

The mean radius of curvature is given by $R = \sqrt{R_{\text{TMTM}} R_{\perp}}$, where R_{\perp} is the radius measured perpendicular to R_{TMTM} using a DOVE prism.

Bibliography

The following references provide useful examples of how FECO interferometry can be used to measure surface shapes and deformations, and other surface phenomena (cf. Figure 41).

General papers

- *Thin Film Studies Using Multiple Beam Interferometry.*
J. N. Israelachvili, *J. Colloid Interface Sci.* **44** (1973) 259-272.
- *Multiple-beam interferometry with thin metal films and unsymmetrical systems.*
M. T. Clarkson, *J. Phys. D* **30** (1989) 475–482.
- *Analytic solution for the three-layer multiple beam interferometer.*
Roger Horn and Douglas Smith, *Applied Optics* **30** (1991) 59–65.

Surface shape analysis (topology)

- *Measurement of the Deformation and Adhesion of Solids in Contact*
R. G. Horn, J. Israelachvili, F. Pribac, *J. Colloid & Interface Sci.* **115** (1987) 480-492.

- Topographic information from multiple beam interferometry in the Surface Forces Apparatus.
M. Heuberger, G. Luengo & J. Israelachvili *Langmuir* **13** (1997) 3839–3848.

Surface deformations with time due to viscous forces, bilayer fusion, etc.

- Direct visualization of cavitation and damage in ultrathin liquid films.
Tonya Kuhl, Marina Ruths, You-Lung Chen, Jacob Israelachvili, *Journal of Heart Valve Disease* **3** (1994) S117–S127.
- Role of Hydrophobic Forces in Bilayer Adhesion and Fusion.
C. A. Helm, J. N. Israelachvili, P. M. McGuigan, *Biochemistry* **31** (1992) 1794–1805.

FECO spectroscopy: measuring molecular structure and dynamics in thin films

- Enhanced absorption within a cavity: a study of thin dye layers with the Surface Forces Apparatus. C. Müller, P. Mächtle and C. A. Helm, *J. Phys. Chem.* **98** (1994) 11119–11125.
- A thin absorbing layer at the center of a Fabry-Pérot interferometer.
P. Mächtle, C. Müller and C. A. Helm, *J. Phys. II France* **4** (1994) 481–500.
- Eigenvalue analysis of the surface forces apparatus interferometer.
P. Rabinowitz, *J. Optical Soc. America A* **12** (1995) 1593–1601.

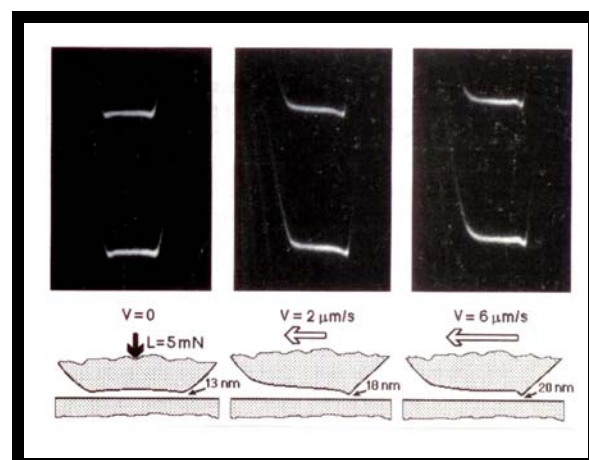
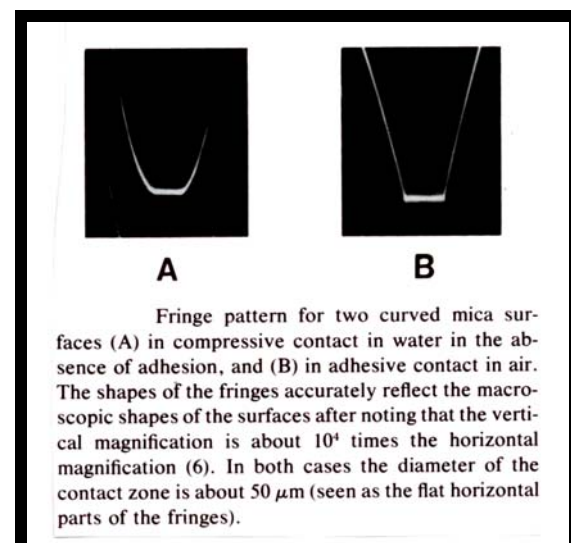
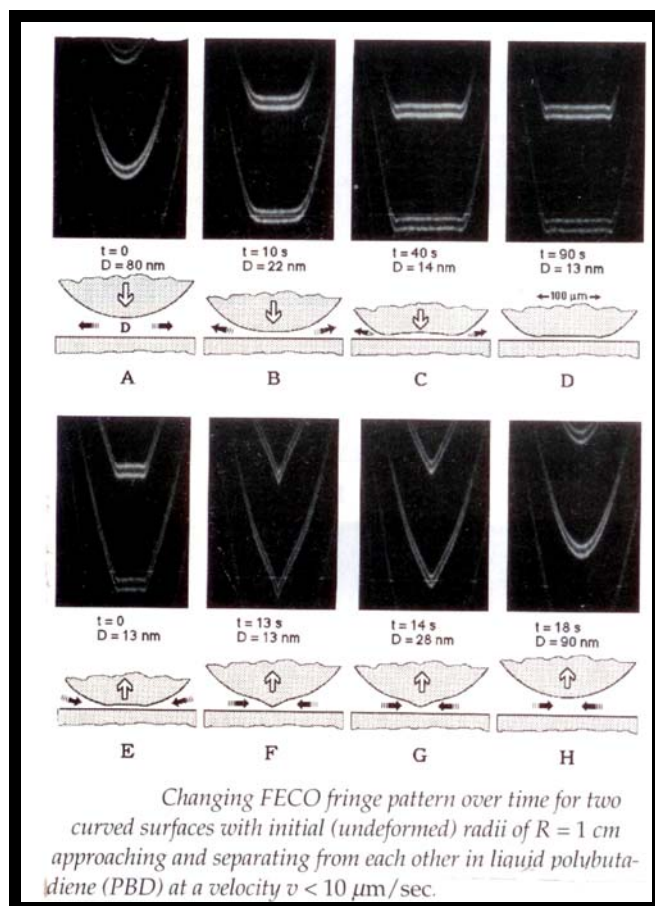


Figure 41. Various types of FECO fringe patterns obtained on different systems.

MEASURING EQUILIBRIUM FORCES

Forces may be measured in a variety of ways depending on their magnitude. For measuring weak forces or for the tail end of a long-ranged force where high sensitivity is required, it is recommended that the piezoelectric crystal be used as follows:

The silica disc supporting the lower mica sheet is suspended at the end of a double cantilever spring of variable stiffness, K , which should be adjusted to some low value, say $K=10^2 \text{ Nm}^{-1}$. The forces are measured by suddenly reversing the voltage of the piezoelectric crystal, which expands or contracts it by a known (previously calibrated) amount. The resulting change in the separation between the two surfaces is then measured optically and any difference in the two values, when multiplied by the stiffness of the spring K , gives the force difference, whether attractive or repulsive, between the initial and final separations. The theoretical basis for this method is as follows: referring to Figure 42, let $x = 0$ define the zero (or laboratory reference) position of the lower surface when the two surfaces are a large distance apart and there is no interaction force between them. As the upper surface is moved downwards to $x=D_0$ the interaction force between the surfaces causes the spring to deflect by $(D-D_0)$ causing the lower surface to move to a new equilibrium position at $x=-(D-D_0)$. For attractive forces the spring deflects upwards towards the upper surface and so $D < D_0$, whereas for repulsive forces the spring deflects downwards and $D > D_0$. At the new equilibrium separation D , the interaction force between the surfaces $F(D)$ is balanced by the restoring force of the spring $K(D-D_0)$, so that at equilibrium we have

$$F(D) = K(D - D_0) \quad (11)$$

where $F(D) > 0$ and $D > D_0$ for repulsion.

Let the piezoelectric crystal expand by a finite amount ΔD_0 , so that $D_0 \neq D_0 - \Delta D_0$, leading to a new equilibrium surface separation at $D - \Delta D$, then from the above equation we have

$$F(D - \Delta D) = K(D - \Delta D - D_0 + \Delta D_0) = K(\Delta D_0 - \Delta D) + F(D) \quad (12)$$

This shows that if an expansion of the crystal by an amount ΔD_0 causes the surface separation to change by ΔD then the difference in the force at the initial position $F(D)$ from that at the final position $F(D-\Delta D)$ equals $K(\Delta D_0 - \Delta D)$. If $\Delta D_0 = \Delta D$ there is no force difference. At large separations, this also implies that there is no force, $F=0$, so that this condition allows for calibration of the piezoelectric crystal, providing its expansion/contraction per volt.

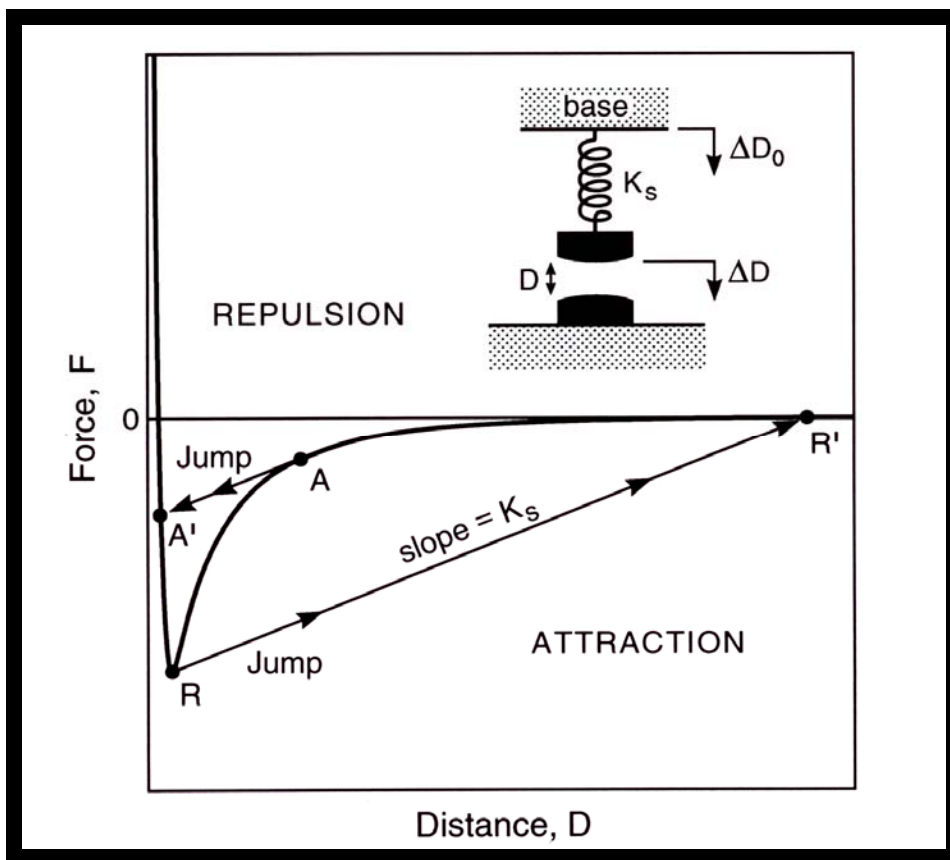


Figure 42. Basic mechanics of the force-measuring spring system.

For example, consider a system as in Figure 41 where the spring stiffness is $K = 10^2 \text{ N/m}$ (10^5 dyne/cm). If the surfaces are initially 100 nm apart, where there is no measurable force, and the crystal is expanded by 10 nm; then if the surfaces come to equilibrium at 90 nm there is, therefore, no force between the surfaces at 90 nm. However, if the two surfaces come to equilibrium at 91 nm there is a repulsive force at 91 nm equivalent to bending the spring by 1 nm, i.e., a force of $K(\Delta D_0 - \Delta D) = 10^2(10 - 9)10^{-9} = 10^{-7} \text{ N}$. For two cylindrical surfaces of radii $R=1-2 \text{ cm}$ the time taken for them to reach equilibrium is about 1 s in water (viscosity $\sim 1 \text{ cP}$). By this method one can start at large separations, where no force is detected, and work one's way down to smaller separations, and thus measure the force over any region of interest down to contact. Thus to measure the force $F(D)$ between the two surfaces using the optical technique we need only to know

- (i) the force-measuring spring stiffness, K . This can be calibrated to within 1% after each experiment by placing small weights at the place where the mica surfaces were contacting and measuring the deflection with a traveling microscope or vernier eyepiece or simply an eyepiece with a graduated graticule inserted.

- (ii) the amount the piezoelectric crystal expands or contracts, ΔD_0 , when the voltage is changed or reversed. This is measured optically at large separations where no forces are detected, before each force run.

The above method is the most accurate, but is time-consuming. Over certain distance regimes (usually below 10 nm) repulsive forces are often very large and rapidly varying with separation. In these regions of rapidly varying forces a second method of force measurement is more suitable: in this method the lower surface is moved *continuously*, either by applying a steadily increasing DC voltage to the piezo crystal or by use of MOTOR 1, stopping every now and again to measure the piezo voltage (or motor encoder reading) and surface separation. In this way much larger displacements ΔD_0 may be attained than possible with the crystal. This method is also much faster. When very strong repulsive forces are measured, the mica sheets will eventually deform (flatten) elastically so that their radius R is no longer constant. Under large compressive forces, one may measure the flattened contact area A and then plot the pressure ($P=F/A$) against distance D, rather than the force F or F/R against D.

It is recommended that forces be measured both on approach (inward run) and separation (outward run). This will establish whether the force is reversible and, if not, the nature of the hysteresis in the force law. Hysteretic forces often arise with polymer systems where the hysteresis is time-dependent, depending both on the rate of approach and separation as well as on the previous history of the surfaces. It is therefore also recommended that force runs be measured at a given (measured) rate of approach and that the time allowed for equilibration between different points on a force curve also be recorded (and varied, if necessary). When measuring forces on separation, the procedure is as on approach but in reverse. In particular, after the surfaces have reached a separation of zero force one must continue to measure the force out to larger distances since these measurements constitute the piezo or motor calibration for the outward force-run.

Before starting a new force run, always check the mercury calibration line and reenter the optics (PRISM control and PRISM turntable) and focus (FOCUS control). Photographing the fringes or measuring the two radii may also be done at this point (with the surfaces outside the force field). A centering check should also be done when the surfaces are closest to each other.

On separating two surfaces from adhesive contact or from a potential minimum they usually jump out to large distance apart, from which the adhesion force may be obtained by multiplying the spring constant K by the distance jumped. Be careful that the 'jump' out is not an apparent one due to viscous forces arising from moving the surfaces apart too rapidly before they jump.

MEASURING VISCOUS FORCES AND OTHER DYNAMIC INTERACTIONS

Various dynamic interactions can be measured, some employing the Basic Unit, others requiring an attachment such the Friction Device, Bimorph Slider or Bimorph Vibrator, which are described in Part III of the manual. The following references provide additional information on different types of dynamic measurements using the SFA technique:

- **The Drainage of Thin Liquid Films Between Solid Surfaces**
Chan, D. Y. C. and Horn, R. G., *J. Chem. Phys.* **83** (1985) 5311-5324.
- **Measurement of the Viscosity of Liquids in Very Thin Films**
J. N. Israelachvili, *J. Colloid and Interface Sci.* **110** (1986) 263-271.
- **Measurements of the Viscosity of Thin Films Between Two Surfaces With and Without Adsorbed Polymers**
J. N. Israelachvili, *Colloid and Polymer Science* **264** (1986) 1060-1065.
- **Measurements of Dynamic Interactions in Thin Fluid Films: the Transition from Simple to Complex (Non-Newtonian) Behavior**
J. N. Israelachvili, S. J. Kott, L. Fetter, *J. Polymer Sci., Part B: Polymer Physics* **27** (1989) 489-502.
- **Measurements of and Relation between the Adhesion and Friction of Two Surfaces Separated by Molecularly Thin Liquid Films**
M. Homola, J. N. Israelachvili, M. L. Gee, P. M. McGuigan, *J. Tribology* **111** (1989) 675-682.
- **Motions and Relaxations of Confined Liquids**
Granick, S., *Science* **253** (1991) 1374-1379.
- **Viscoelastic Dynamics of Confined Polymer Melts**
Hu, H-W., Granick, S., *Science* **258** (1992) 1339-1342.
- **Lubrication forces between surfaces bearing polymer brushes.**
J. Klein, Y. Kamiyama, H. Yoshizawa, J. N. Israelachvili, G. H. Fredrickson, P. Pincus, L. J. Fetter. *Macromolecules* **26** (1993) 5552-5560.

For more on how to measure and interpret both static and dynamic force measurements using the SFA (and other) techniques, see *Intermolecular & Surface Forces*, 3rd Edition, 3rd printing, by J. Israelachvili, especially Chapter 12 and Parts II and III. See also the references listed on the back pages of the brochures to the SFA 3 and SFA 2000.

CALIBRATIONS

A number of calibrations, mostly of a straightforward nature, have to be carried out before, during or after an experiment, or at any convenient time. Some need to be done only once, others need to be done repeatedly with each experiment.

- (1) **Thermistor.** This is straightforward to calibrate anytime and need only be done once. Hang the lower 3/4 of the steel body of the thermistor into cold water in a beaker, and insert a thermometer and magnetic stirring bar. Place on a hot plate and heat while stirring. Calibrate between 5°C and 80°C using a standard multimeter. Fit the data to an exponential function. During experiments, the resistance can be measured anytime, preferably with the same multimeter. For thermistors such as SENSOR SCIENTIFIC, Part No. G198WM103C, that have a nominal resistance of 10,000Ω at 25°C, their resistance at different temperature is approximately as follows:

Temperature °C	Resistance Ω
20	12,500
25	10,000
30	8,050
35	6,550
40	5,300
45	4,350
50	3,600

- (2) **Heaters.** The two identical heaters are rated at 100 Watt each and may be connected in parallel or in series. Voltages of 10–50 VAC across each heater (20–100 VAC across both heaters when connected in series) should raise the temperature of the lower chamber, when filled with liquid, by 10–70°C above ambient, but this is very rough – the heater power controller is non-linear and the voltage-temperature characteristic should be calibrated with liquid in the chamber and the thermistor in place before it is used in an experiment for the first time. There is really no need to calibrate the heaters accurately since the thermistor will measure the temperature in the chamber at any time. Note that once the temperature is stabilized the drifts of the surfaces will die down. It is recommended that when using the heater power controller, the voltage output (the AC voltage across the heaters) is continually monitored with a multimeter. At low voltages, solid state power controllers can sometimes cut-off. This can be adjusted by opening the control box and turning the trimming pot on the heater controller. Variac power controllers do not have this problem.

- (3) **Piezoelectric crystal and MOTOR 1.** These should be calibrated (in distance *vs* volts for the piezo, distance *vs* encoder reading for the motor) using the FECO fringes as part of each force run at large distances where there is no force between the surfaces.
- (4) **Spectrometer dispersion.** Calibrate with the mercury green line and two yellow lines using a mercury pen lamp (see below).
- (5) **Mercury green or yellow lines.** Choose one reference line, say the green line, and check frequently, e.g., every hour or so, during the course of an experiment, resetting the mercury green line to zero on the spectrometer encoder each time (the mercury calibration line can 'drift' due to a temperature change in the room, and also if any part of the optical alignment has been moved or adjusted, for example, if the prism or mirror have been inadvertently jogged). Do not change the mirror angle controls after starting an experiment since this could artificially shift the positions of the fringes, including their contact positions relative to the Hg lines by a small but not insignificant amount. However, if you do make any adjustments to the optics, always reset the Hg line to zero before proceeding further.
- (6) **Force-measuring spring (K variable from 30 to 5×10^5 N/m).** The SFA3 is unique in allowing you to vary the force-measuring spring stiffness by more than 4 orders of magnitude, thanks to the robustness of the dove-tail design (the maximum is set by the stiffness of the beryllium-copper cantilever spring, $K \approx 1.5 \times 10^6$ N/m, on Part 01040 of the Upper Chamber (Fig. 7).

Calibrate once by adding small weights placed at the center of the disk mount (you may remove the disk first) and measuring the deflection using, for example, a vertical traveling microscope or micrometer eyepiece or normal microscope with a scaled graticule installed. Calibrate with force-measuring spring fully clamped (to avoid slip which may occur with the heavier weights or loads than are normally encountered in experiments). The spring constant should not vary from experiment to experiment if it is clamped in the same position each time, except for the stiffest clamping position where $K \approx 5 \times 10^5$ N/m (5×10^8 dyne/cm) and where the contribution from the finite stiffness of the glue supporting the mica sheets (which depends on the type of glue and thickness of the glue layer) may no longer be ignored. This contribution to the effective stiffness of the force-measuring spring system is typically around 10^6 N/m (10^9 dyne/cm), and it reduces the maximum effective stiffness as given by the following equation: $1/K_{\text{eff}} = 1/K_{\text{spring}} + 1/K_{\text{glue}}$. During experiments, one may calibrate the maximum effective stiffness K_{eff} by measuring the jumps apart of the surfaces from adhesive contact under full and weak clamping conditions (where K is known), and

comparing the two values to obtain K_{eff} at full clamping (note that when the jump apart is small, a small correction has to be made for the elastic deformation of the surfaces at contact).

During experiments, one may also calibrate the spring stiffness by measuring the natural frequency of the lower support. This can be readily done by separating the surfaces a large distance (many microns) in air or liquid and vibrating the piezo over a range of frequencies until the blurred fringes become suddenly sharp. This will occur at a particular frequency, v , which is the resonant frequency of the lower support at that spring stiffness, K . Pre- or post-experiment calibrations (with the same disk installed) can be done using this method with Newton's rings to calibrate K as a function of v . The calibration should obey the equation: $\omega = 2\pi v = \sqrt{K/m}$, where m is the mass of the support with disk.

- (7) **Lateral magnification of surfaces as seen in spectrometer eyepiece.** This calibration is needed especially for measuring the radii of the surfaces from the shapes of the FECO fringes. Calibrate with a vernier graticule for 0° and 90° angles of the DOVE PRISM. A one-off calibration should suffice if the apparatus / optics stand / spectrometer positions remain unchanged from one experiment to the next.
- (8) **Liquid volume in chamber.** Note that, on draining chamber, some liquid ($\sim 5\text{-}10$ ml) can remain trapped inside, at edges, holes, cracks, etc. Thus calibrate by filling, not by emptying.
- (9) **Bimorph slider.** For calibrating the bimorph stiffness, K , place upper chamber with bimorph attached on the side and calibrate with as you would the force-measuring spring (item 6) with small weights and a calibrated eyepiece (cf. Figure 40). The lateral movement of the bimorph slider (\AA per volt) may be calibrated by top viewing with a calibrated eyepiece and measuring the lateral deflection due to applying a low voltage (40 Volts max) trying both AC and DC. The deflection should be easily detectable. Alternatively, during experiments, with the surfaces in contact, you may calibrate the movement per volt from the measured displacement of the friction spring as recorded by the Friction Device.
- (10) **Friction device.** For calibrating the friction spring stiffness, K , clamp attachment firmly on the side and calibrate as you would the force-measuring spring (item 6) with small weights and a calibrated microscope.

ANALYZING THE RESULTS

As a general rule, it is wise to analyze the results of your last experiment before proceeding with the next one. Analysis depends to some extent on how the data was recorded – whether by hand, on video tape, on a chart-recorder, fed directly into a computer, or a combination of these. This procedure in turn will depend on the type of experiment being conducted, on the experimental plan, and on the number of people participating. Team work, involving two or three people, is always preferable: it increases the 'brain power' of the planning and observation, reduces the possibility of mistakes, and allows for independent measurements to be made). This section does not deal so much with these aspects of how to conduct experiments, but more with what should be done before, during, and after an experiment. Keep a bound laboratory note book or record book, carefully distinguishing between entries made during an experiment from those made afterwards. For example, use different colors for the planning, actual recording and subsequent analysis or processing of the data (as well as even and odd page numbers for data entry and analysis, respectively).

Before an experiment

Plan each experiment in detail from start to finish. Some experiments may be one-day experiments, others may go on for two weeks. Careful planning of what will be measured and what to look for (and alertness to what is not being looked for) is crucial to a successful experiment.

- ★ Prepare the substrate surfaces (mica sheets or other supporting material): deposit a silver layer of known thickness and note the thickness and orientation of each sheet on the backing sheet. Carefully plan any surface treatment / deposition and how the treated surfaces will be installed into the apparatus.
- ★ Perform any needed pre-calibrations, such as checking the mica thickness (with a 'test-piece'), checking all the motors and piezo crystal, checking the electrical instruments and connections, checking that you have the right grating in the spectrometer, etc. (See CALIBRATIONS).
- ★ Have all tools and liquid solutions ready before starting. Remember easy-to-forget items such as spare light bulbs, photographic films or video tapes, chart-recorder paper, small torch (flash light), alternative grating, etc.

During experiments

Start by perfecting the optical alignment, adjusting the mirror, lamp, base legs and prism turntables, as already described. In particular, try to make sure that the light passes normally (at 90°) through the surfaces (see Figure 42). This will require adjusting the mirror controls but may also require adjusting the heights of the three legs of the Base.

It is important to record everything that may conceivably be relevant, even if it may not seem so at the time. This includes a complete record of the contact fringes (at least three successive order fringes and their birefringence), continuous or periodic measurements of the contact area (for flattened surfaces), measuring the adhesion force of adhering surfaces, checking the mercury calibration lines, reentering and refusing, noting any inward or outward drifts, measuring the temperature, checking for leaks, taking photographs or video recordings, measuring the refractive index at different film thicknesses, measuring forces on the way in as well as on the way out (calibrating the piezo or motor in both directions), recording the rates of approach and separation and the equilibration times between data points, noting the time between force runs and how far the surfaces were kept during the waiting period – and last but not least – repeating measurements at new positions and measuring the birefringence and two surface radii at each new position (Figure 40). When aligning the optics at each position, try to make sure that the light passes normally (at 90°) through the surfaces (see Figure 42).

Being a 'good observer' is essential, as is the habit of following up all unexpected phenomena. Record everything and trust your measurements – by not clearing up loose ends you may miss an important discovery.

Analysis of results after an experiment

Pages 147-158 give an example of a complete experiment where all stages of a real experiment were noted down, including data recorded, subsequent analysis, and plotting of the results.

MISCELLANEOUS HINTS & TROUBLESHOOTING; SERVICING YOUR SFA

Droplet experiments

Distill and dry the fluid to be injected before sucking it up into a small 500 µl syringe. Never expose the liquid to lab air after the distillation (to avoid it picking up dust particles). Once it is in the syringe, it should be injected between the surfaces under conditions of a positive clean-nitrogen gas pressure in the chamber (and then only after a few drops have been placed within or just outside the chamber to ensure that any impurities from the syringe come out first). Separate the surfaces about <0.5 mm and direct the syringe needle to the top surface but well away from the centre. Inject a small quantity of liquid gently onto the top surface and allow the liquid to flow down until it bridges the two surfaces. Immediately bring the surfaces together, but not into contact. Close the syringe port, and fill the small receptacle or boat, part 08051, with a few drops of the liquid to ensure saturated vapor pressure within the chamber. The vapor pressure will actually be below saturation because the surfaces are usually slightly hotter than the liquid in the boat due to the light passing through them; however, if the liquid is placed in a flat-bottomed beaker just above the window so that the incoming light passes through it, this will heat the liquid 'reservoir' enough to significantly reduce the evaporation rate of the droplet between the surfaces. The liquid in the boat (but not the beaker) can be changed at any time from outside the apparatus via the Luer opening on its exposed side. The receptacle can also be used for placing P₂O₅ in it to completely dry the internal chamber and any non-aqueous liquid droplet between the surfaces. For complete drying, allow the system to equilibrate overnight. If there is a leak that lets water vapor come into the chamber (see below) the P₂O₅ will look wet, or have a shiny or glazed appearance.

Liquid condensation on glass surfaces

This problem can arise in droplet experiments where small lenses condense on the surfaces of the glass windows and silica disks causing blurring of the fringes. This problem can be avoided in one of three ways: (1) By injecting bulk liquid into the thin gap between the window and upper disk. (2) By ensuring that the upper window and silica disk are at a slightly higher temperature than the rest of the chamber. This can be done by placing a small flat metal washer, suitably wired at two ends, into the piezo mount so that it sits on the glass window. Gently heat the washer and window by passing a low voltage current through it. (2) A special upper mount exists where there is no gap between the window and upper disk (see Figure 51).

Leaks

It is amazing how a very small leak can allow atmospheric water and organic vapors to enter the internal chamber from outside. In some cases this can have a dramatic effect on the forces between the surfaces. For example, a small leak can totally prevent a non-polar liquid droplet from remaining completely dry; if the surfaces are hydrophilic, water will condense on the surfaces and give rise to strongly attractive capillary forces as well as change the "boundary conditions" for other types of interactions.

A small leak does not mean that liquid will be seen to flow out from the leaking hole. It will usually evaporate on emerging so that there is no obvious sign that a leak is occurring. Leaks often become apparent during experiments, for example, by noting that the liquid level is falling with time, or that P_2O_5 in the receptacle is becoming wet (see above). To check for leaks, fill the box with a volatile liquid such as ethanol or cyclohexane up to a level that can be clearly measured through the window. Close the apparatus in the usual way (with no surfaces installed), and see whether the liquid level falls overnight.

Leaks are most often due to: (1) flattened O-rings, especially small ones, that need replacing, (2) insufficient tightening of the Teflon bellows, (3) forgetting to put an O-ring into one of the small holes, such as the thermistor hole or pinion shaft hole, (4) a hair or scratch on some smooth surface that contacts an O-ring, (5) a crack in the piezoelectric tube or the glue holding the piezoelectric tube to its support (contact SFI, Inc. if the piezo tube feels loose).

Fringe brightness

If the fringes are not bright enough to be observed comfortably, due to oversilvering, one may attach a lens ($f \approx 3.5$ cm) under the light entry port on the lower chamber. This will brighten the fringes but at the expense of some blurring.

Drifts

It is strongly recommended that the experimental room be thermostatted to $\pm 0.1^\circ C$. This will reduce drifts to negligible levels (about $1\text{\AA}/\text{min}$ may be considered). However, the apparatus may need to 'equilibrate' in the room for many hours. It is also wise to have the liquid solution and the apparatus inside the thermostatted room for a few hours before filling.

Allow the surfaces to settle for at least one hour after changing anything, such as filling, injecting liquid, finding a new position, or switching on the light. If a drift persists, check the following: (1) that the coarse nut on the differential micrometer is tight, (2) that a heat-reflecting or absorbing mirror/window, or a 6" water bath, is in the path of the light, (3) that your

thermostatting air-conditioning system has not broken down, (4) insert a filter or two in series to the air outlet (to allow the pressure outside and inside the chamber to equilibrate rapidly – in case the atmospheric air pressure is changing rapidly), (5) reduce the intensity of the lamp by lowering the voltage through the bulb. Also, did you tighten the spring-clamping screw and two small Philips screws on the variable spring mount? Did you check that both silica disks were firmly tightened into place? Did you tighten the piezo mount evenly in place? It is also possible that the piezo crystal tube has become loose; this sometimes happens if the epoxy glue layer that bonds it to the steel support has deteriorated (due to prolonged exposure to humid or certain organic atmospheres). To check that the crystal mount is ‘robust’, hold it firmly with gloved fingers at either end, then gently (without overstressing) twist or bend it to see if the glue layer is loose or ‘gives’.

Is your apparatus enclosed in a (wooden) box inside the thermostatted room? Such an enclosure, with an opening on one side which can be covered with a heavy cloth when the apparatus is in use, can be very useful for preventing drafts and further reducing thermal drifts.

Drifts are more pronounced in droplet experiments (see Fig. 25B). This is because the droplet may be slowly evaporating or because of contact angle hysteresis. Evaporation is a common problem, especially when using volatile liquids such as low MW hydrocarbons, alkanes, organic liquids and even water. Evaporation causes drift because the effective mass of the lower surface is constantly decreasing with time, resulting in a steady inward drift. The second effect (contact angle hysteresis) causes drift after the surfaces are moved towards or way from each other because the meniscus is still relaxing well after the piezo or motor have stopped moving. Such drifts can persist for a long time after a distance adjustment in a direction determined by the previous history of approach and separation of the surfaces. Liquids that wet the surfaces (have zero contact angle) do not exhibit this effect, but can cause drifts due to evaporation. Evaporation can be reduced by saturating the measuring chamber with the liquid’s vapor, either by filling the small bath in the syringe injector port or by simply injecting a few drops of the liquid into the chamber (in this case, however, you will not be able to remove the liquid during the experiment except, perhaps, by a prolonged purge with clean nitrogen gas). The rate of evaporation depends on the temperature of the droplet between the surfaces relative to that of the vapor. When light is passing through the surfaces and droplet, they heat up by ~1 °C above the surrounding which enhances the evaporation rate. This effect can be reduced by following some of the procedures listed above. In addition, one may also completely cover the floor of the lower chamber with a ~1 mm layer of the liquid; this will also ensure that part of the liquid is also

heated by the light coming through the lower window, which raises the vapor pressure. If possible, it is always better to fill the box with liquid than do droplet experiments.

In most cases it is impossible to completely eliminate all drift, the best that can be hoped for is a drift of the order of 1-2 Å/sec. This may be negligible if the time between force measurements (data points taken at different separations) is 15-30 secs, as is usually the case. Additionally, since the drift rate is usually fairly constant over a fairly long time period (many minutes to hours) this constancy can be used to advantage by making force measurements in a time-consistent way. The following two examples illustrate how this can be done depending on the type of force being measured and the system relaxation time: (1) Apply a ramp voltage to the piezo to exactly offset the drift during the more crucial measurements. (2) Measure forces between two points by both increasing and decreasing the voltage on the piezo, i.e., both on going in and going out, and take the average. Use the same times to equilibrate at each position, both on going in and going out. You may also need to calibrate the piezo separately on going in and going out. Similarly for measurements with the DC motor (Motor 1).

Mercury light

Position of Hg lines in spectrogram varies with placement of Hg lamp, so don't move it once you have calibrated the FECO contact fringes during an experiment. At the beginning, make sure it is coming in from the same direction as the FECO beam. This can be done by removing the spectrometer prism and looking back into the microscope prism from the direction of where the center of the spectrometer prism will be located, and noting that both beam spots come from the same point.

Achieving high local pressures

Use small radius disks ($R \sim 1$ mm) with little glue to get high local pressures – up to 0.5 GPa can be achieved in this way. See *The shear properties of Langmuir-Blodgett layers*. B. J. Briscoe and D. C. B. Evans, *Proc. Roy. Soc. (Lond.) A* 380 (1982) 389–407.

Optical alignment

Sharpest fringes are obtained when the white light beam is passing normally through the surfaces at their point of closest approach (which is usually at the center of the interaction zone). If the light is passing at some finite angle θ to the normal, the fringes will become blurred and also shift to SHORTER wavelengths. The reason for the shift to shorter, rather than longer, wavelengths as the mica sheets are tilted relative to the normal is shown in Figure 43.

The path length for each reflection is $2Tn$ for $\theta=0$, and $[2AB.n - AD]$ for $\theta>0$, where n is the refractive index of the sheet of thickness T .

By Snell's Law, $\sin\theta = n \sin\theta'$, so that $AD = AC \sin\theta = 2T \tan\theta' \sin\theta$
 $= 2T \sin\theta' \sin\theta / \cos\theta' = 2Tn \sin^2\theta' / \cos\theta'$, and $2AB.n = 2Tn / \cos\theta'$.

Thus, $2AB.n - AD = 2Tn(1 - \sin^2\theta') / \cos\theta' = 2Tn \cos\theta'$. Since $\cos\theta' < 1$ for $\theta' > 0$, the path length for interference is seen to decrease as θ' (and therefore θ) increase above zero.

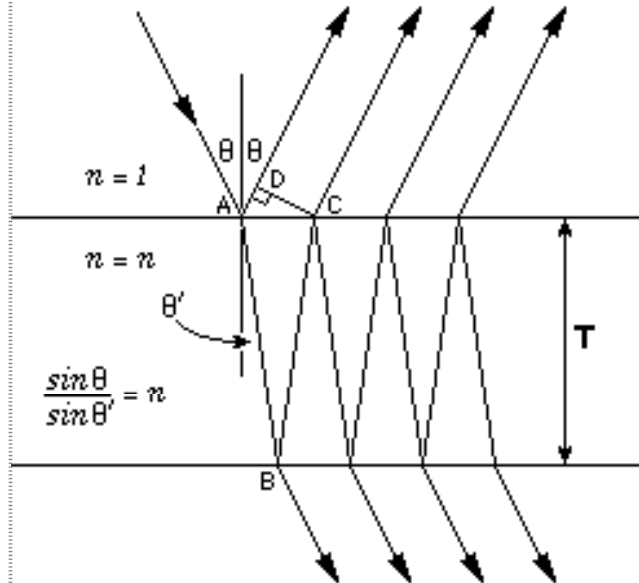


Figure 43

Try to ensure that the light comes through at $\theta=0$ at each new position. This will also ensure that your fringe calibration, and hence your definition of $D=0$, remain valid. If you have rotated the two surfaces during the search for a new position, even though you have kept $\theta=0$, you must compare the *mid-points* of the β and γ doublets since these are the 'conserved' wavelengths at the different positions. The birefringence varies as $\cos\theta$.

Particle contamination

Particulate contamination can be eliminated by better purification of the solutions: ensure that from the final stages of the distillation up to filling, the liquid never becomes exposed to atmospheric air, however momentarily. High speed spinning (centrifuging) a viscous liquid at an elevated temperature helps remove particulates. Reducing the surface radius, R , also reduces the probability of trapping a particle between two surfaces.

Motor speed controls

If movement of the surfaces is too rapid or slow when using motor 1 (differential spring control), replace motor-encoder assembly with another having a different gear ratio. Complete motor-gearhead-encoder units are available from Micro Mo. It is possible to add another motor (Motor 3) to control the differential micrometer. However, this micrometer is usually controlled by hand, although its graduated head can be read to give the displacement of the spring support.

Do-it-yourself modifications

The SFA3 is a versatile modular unit that can have parts interchanged and new attachments added. Some of these are described later in the manual. Others can be designed by the user. An excellent book that provides useful hints on designing small machine components is

Foundations of Ultraprecision Mechanism Design by S. T. Smith and D. G. Chetwynd, Gordon and Breach Science Publishers, Amsterdam (1992, 1994).

SYRINGE INJECTION UNIT

MAIN FEATURES

- ★ Syringe injection facility
- ★ Boat for vapor pressure control

The Syringe Injector (see Figures 11 and 25) is an attachment for injecting small quantities of liquid directly between the surfaces or into the apparatus main chamber during experiments without opening the chamber or exposing its atmosphere to the outside – essential for performing certain types of experiments, such as 'droplet experiments' with very small volumes of liquid. Includes rotating ball-and-socket fixture for directing syringe needle to any desired point near or between the two surfaces. Also provided: small liquid bath (receptacle or boat) that can be interchanged with the syringe fixture – for controlling the vapor pressure of the chamber during experiments – useful to controlling the concentration (activity) of solutes in the liquid. If neither syringe nor small bath are being used, the entry port may be plugged with a Kel-F plug (also provided). Customers should consider ordering this unit with the initial order rather than later since the Lower Chamber has to be shipped back to for modifications before the syringe unit can be used (in some models the syringe port is already machined into the Lower Chamber, at no extra cost). The syringe injector port may also be used for feeding liquids, other attachments and certain probes into the chamber, for example, a pH probe or a UV mercury pen-ray lamp for oxidizing surface organic groups.

COMPONENTS

- Injector port with plug.
- Ball-and-socket syringe fixture.
- Small liquid bath with female Luer port.
- Syringe with 7.5 cm-long needles, Luer connectors and end caps.

In most cases it is not necessary to have a sealed ball-and-socket syringe injector; all one needs to do is open one of the ports close to the surfaces, for example, the thermistor port, and inject a droplet directly between the surfaces using a long needle while viewing through the front window, then close (plug up) the port with a Luer plug or return the thermistor. Make sure that while you do this there is a slight positive pressure in the chamber, which can be done by continually passing nitrogen gas in through the air inlet at a low rate. This will avoid contaminants to enter the chamber during the injection.

FRICTION DEVICE (for the SFA 3)

MAIN FEATURES

- ★ Smooth lateral motion of upper surface
- ★ Large lateral displacement (5 mm total traverse)
- ★ Constant or variable speed in either direction
- ★ Simultaneous measurement of normal and shear or friction forces
- ★ Simultaneous measurement of surface deformations
- ★ Friction force measuring sensitivity: 10^{-5} N.
- ★ Can measure friction coefficients as low as 0.0001

The FRICTION DEVICE for the SFA3, shown in Figures 15 and 26, is a ‘complete unit’ – both producing and measuring shear motion. It is an improved version of the unit originally described by A. M. Homola, J. N. Israelachvili, M. L. Gee and P. M. McGuiggan, in *J. Tribology* **111** (1989) 675-682 for use with the SFA Mk 2. Sliding motion of the upper surface is produced via a digital encoder-controlled motor-driven micrometer, and the shear/friction force is measured from the deflection of a double-cantilever friction-force-measuring spring assembly supporting the upper surface. The spring deflection is measured with a Wheatstone Bridge or strain gauge bridge connected to resistance or semiconductor strain gauges attached to the friction-force-measuring springs (semiconductor gauges are about 100 times more sensitive but more fragile than the resistance gauges). The assembled FRICTION DEVICE includes: spring-loaded anti-backlash translation stage driven by micrometer and reversible DC motor with digital encoder and display counter. Friction force-measuring double-cantilever springs with strain gauges mounted and wired to an output terminal. Clamping ring for attaching to SFA 3 Basic Unit and rotating upper surfaces about a fixed axis.

Operation and description of lateral sliding attachment

Lateral (transverse) movement is achieved by the FRICTION DEVICE attachment (see Figures 15 and 26) which replaced the piezoelectric crystal tube mount supporting the upper silica disk of the basic apparatus. Figures 44 show the basic parts of the Friction Device as mounted into the SFA3. Lateral motion is initiated by a reversible, variable speed, DC motor-driven micrometer shaft which presses against the translation stage which is connected via two horizontal, double-cantilever, Cu-Be springs to the rigid mounting plate. One of these springs acts as a frictional force detector by having four strain gauges attached to it, forming the four arms of a Wheatstone bridge, and is electrically connected to a chart recorder or storage oscilloscope (see Table 1). This spring-loaded arrangement ensures perfect linear motion of the translation stage without backlash. The Friction device is rigidly

clamped on top of the main chamber in the same way as the piezo mount it replaces, and an additional circular clamping ring can be inserted that allows for the moving direction of the upper surface to be rotated about a fixed vertical axis.

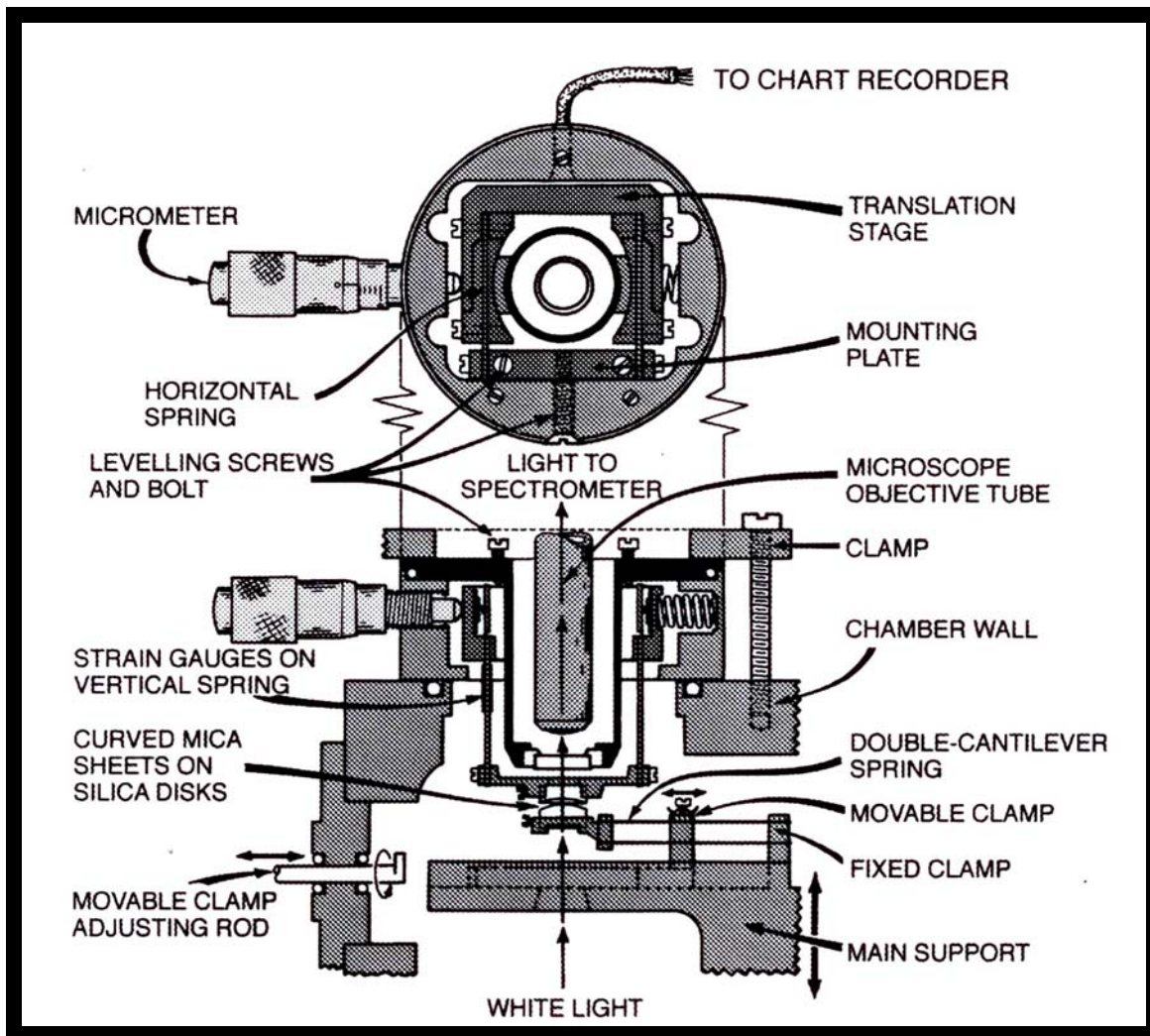


Figure 44. Assembly drawing of the FRICTION DEVICE.

Sliding motion is initiated by driving the micrometer, which deflects the translation stage causing the upper surface to move linearly and horizontally. If the upper mica surface experiences a transverse frictional or viscous shearing force due to its contact with, or proximity to, the lower surface the vertical springs will deflect. This deflection can be measured by the strain gauges attached to the springs. The stiffness of the double-cantilever spring unit can be varied but is typically 3×10^6 dyne/cm (3×10^3 N/m). At this stiffness, a four-arm resistance strain gauge system has a sensitivity in measuring transverse forces of about 10 dynes (10^{-4} N) which corresponds to a displacement of the upper surface of about

300 Å. Semi-conductor gauges are more than an order of magnitude more sensitive, the practical limit of detection being determined by electrical noise in the instrumentation. Good results can be obtained using strain-gauge amplifier Model 2311 from MEASUREMENTS GROUP, chart recorder Model 1242 from SOLTEC and/or storage scope recorder Model 2232 from TEKTRONIX (see Table 1).

By suitably mounting the two cylindrical surfaces so that they are oriented as shown in Figure 37, the contact zone can be made to remain in the same place (at the center of the eyepiece) during the sliding of the upper surface. Note, too, that the Friction Device can be attached in either one of two perpendicular directions (Figure 45), thereby allowing for the upper surface to be moved in either the in-out or left-right directions. This, in turn, will determine the way the two silica disks are mounted.

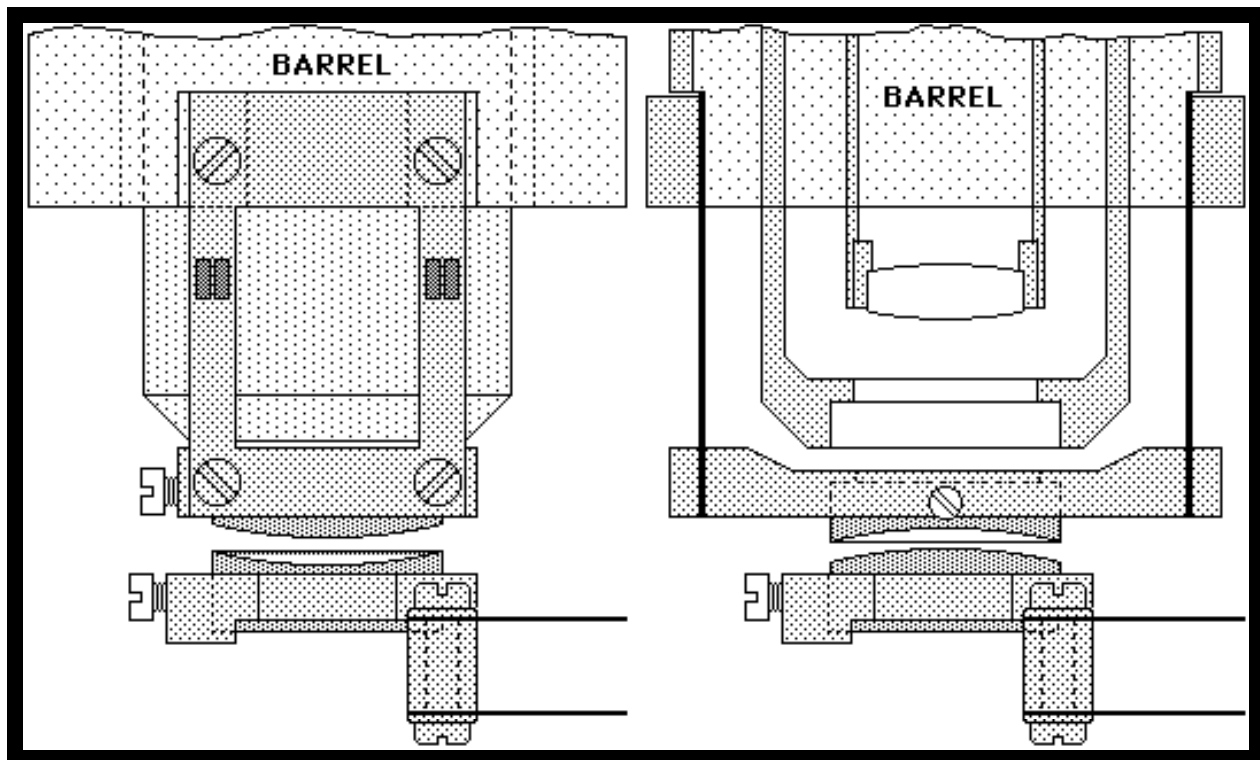


Figure 45. Different mounting configurations of the Friction Device as viewed from the front window. Note: Before using the Friction Device, check that the friction barrel, part 11110, is truly vertical. If it is not, you can adjust its angle by applying a medium force with your fingers to bring it back into vertical alignment.

The Friction Device attachment allows for the two surfaces to be sheared past each other at sliding speeds which can be varied continuously from $0.01\text{-}100 \mu\text{m s}^{-1}$ while simultaneously measuring the transverse (shear) force F between them. At the same time the normal force or load L can be controlled and varied by moving the lower surface vertically, as in normal Basic Unit operations. The load L is given by multiplying this displacement by the (adjustable) spring constant of the horizontal double-cantilever force-measuring spring supporting the lower surface. The range of positive or negative loads that can be applied varies from 0 to ± 100 gm. Finally, the distance between the surfaces D , their true molecular contact area A , their elastic (or viscoelastic or elastohydrodynamic) deformation, and their lateral motion can all be simultaneously monitored by recording the moving FECO fringe pattern using a video camera (SIT type) and recording this on tape for later analysis with a video micrometer analyzer and single freeze-frame camera (Polaroid Freezeframe Video Image Recorder).

Note: Before using the Friction Device, check that the barrel, part 11110, is truly vertical. If it is not, you can adjust its angle by applying a medium force with your fingers to bring it back into vertical alignment.

For a review on shear studies using the Friction Device see the Chapter entitled

Surface Forces and Microrheology of Molecularly Thin Liquid Films

by J. N. Israelachvili, in *CRC Handbook of Micro & Nanotribology*, Ch. 8, 1995.

See also references listed at the end of the brochures for the SFA 3 and SFA 2000.

BIMORPH SLIDER

MAIN FEATURES

- ★ Provides smooth lateral motion of lower surface.
- ★ Total traverse: 1 mm (± 0.5 mm).
- ★ Constant, sinusoidal or programmable motion in either direction.
- ★ Large dynamic range of frequencies, sliding speeds, shear rates.
- ★ Simultaneous measurement of normal forces and surface deformations.
- ★ Should be used simultaneously with the FRICTION DEVICE.

The BIMORPH SLIDER (see Figures 16 and 27) produces only lateral (or shear) motion of the lower surface via two parallel sectored bimorphs in a ‘double-cantilever’ geometry. Sinusoidal, saw-tooth, step-function and other types of displacement-time functions can be generated over a frequency range from micro-Hertz to 100 Hz, corresponding to sliding speeds from 10 cm/s to 10 Å/s. This dynamic range is much greater than can be attained with the motor-driven Friction Device. The assembled unit includes bimorphs and coaxial wiring to an external supply (function generator – see Table 1), a fixed-stiffness normal force-measuring double-cantilever spring with disk mount, and a means for mounting the unit to a SFA3. The BIMORPH SLIDER attachment allows for simultaneous lateral and normal forces to be measured. In addition, the surfaces may be imaged using the FECO optical interference technique which gives the surface separation and a direct visualization of the local surface geometry at all times during sliding. The BIMORPH SLIDER can be used simultaneously with the FRICTION DEVICE, which *must* be used if shear/friction forces are also to be measured.

For more information on the Bimorph Slider, see the following article:

Thin film rheology and tribology of confined polymer melts: contrasts with bulk properties. Gustavo Luengo, Franz-Josef Schmitt, Robert Hill, Jacob Israelachvili, *Macromolecules* **30** (1997) 2482–2494.

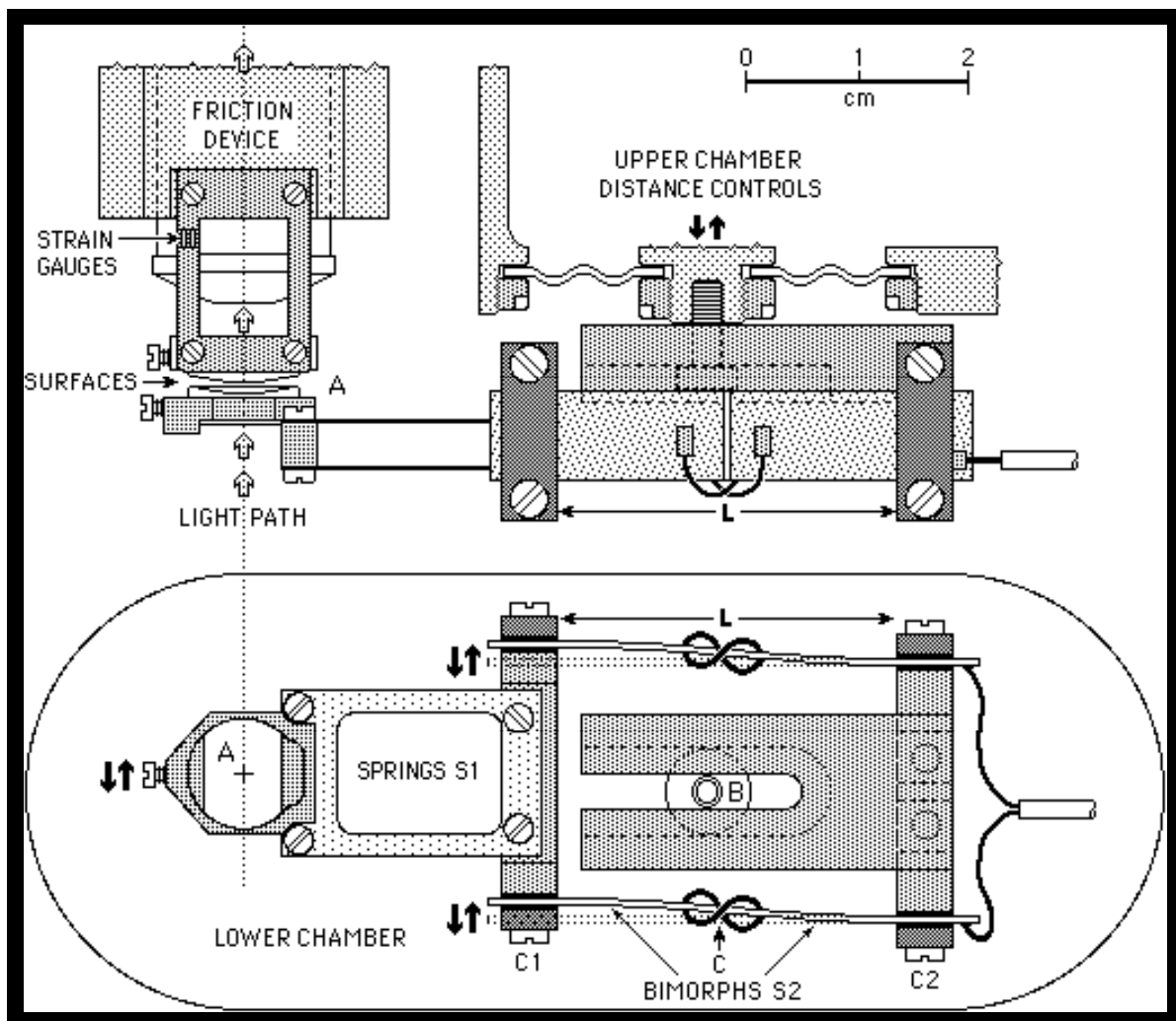


Figure 46. The Bimorph Slider attachment has been designed for making friction and shear measurements over a large range of sliding velocities or driving frequencies. Longer “extended” bimorphs, allowing for larger displacements, are now available for both the SFA 3 and SFA 2000 (see pages 220 and 223).

Operation and description of the Bimorph Slider

The lower surface is supported at the end of a double-cantilever spring (Figure 46 – S1) used for measuring the normal forces between the surfaces. Lateral movement is accomplished with two (or – for increased driver stiffness – four) parallel piezoelectric bimorph strips S2. Bimorphs are ‘piezoelectric couples’ made of two thin sheets of piezoelectric ceramic bonded together by a thin layer of hard conducting material. The two outer faces of each bimorph are coated with thin conducting layers of metal (usually of silver or nickel), which provide protection and serve as suitable electrode surfaces for electrical connections, such as the soldering of connecting wires. Before two piezoelectric sheets are bonded to form a

bimorph, their polarity is reversed relative to each other, so that when a DC voltage is applied across the bimorph, one sheet expands lengthways as the other contracts, resulting in a net bending of the bimorph. For low applied voltages (<100V) the bending, or lateral displacement of each end, is proportional to the applied voltage V. Bimorphs are capable of producing much larger displacements than piezoelectric crystals for the same applied voltage. Bimorphs also work in reverse, as force sensors. Thus, when a force is applied to one end, a large voltage develops across the two outer electrode faces, which can be easily measured. (Bimorphs have long been used in SFA force measurements, both as displacement transducers and as force sensors.) The bimorphs used in the Bimorph Slider are typically PZT 4, 0.023 inches thick, 6 cm long, silver coated, from Morgan Matroc Corp.

To convert the pure bending motion of a bimorph into a linear displacement, one may create a ‘sectored’ bimorph by scraping away a thin strip of the conducting metal coat from the center of each face **C** and then electrically connecting the two pairs of diagonally opposite faces as shown in Figure 46. This splits the direction of the applied voltage across the two halves (sectors) of the bimorph, making each half bend in the opposite direction. If the two halves are of equal length, the resulting effect is a pure linear displacement of the two ends relative to each other, just as occurs with a double-cantilever spring, with no net rotation or bending component. By using two or more parallel bimorphs in this way, a highly robust linear displacement transducer is produced, and this mechanism is used to drive the lower surface, as shown in Figures 46–48. In addition, normal vertical motion of the whole slider assembly and lower surface **A** is produced by a three-stage mechanical translation mechanism composed of micrometers and springs located in the Upper Chamber.

The active length, **L**, of the sectored bimorph can be adjusted by moving the two clamps, **C1** and **C2**, closer or farther apart. This changes the stiffness of the bimorphs (in proportion to $1/L^3$). The increased stiffness or decreased L also results in a decreased range of travel for a given applied voltage (proportional to L^2), and to an increased natural frequency of the lower surface ‘drive’ (proportional to $1/L^{3/2}$). Since the two clamps, **C1** and **C2**, have to be spaced symmetrically about the strip **C**, changing the clamping positions also changes the horizontal position of the lower surface, **A**. To keep the horizontal distance **A–B** constant, the whole bimorph mount may be relocated by shifting it to the left or right and then relocking it to the Upper Chamber with screw **B**.

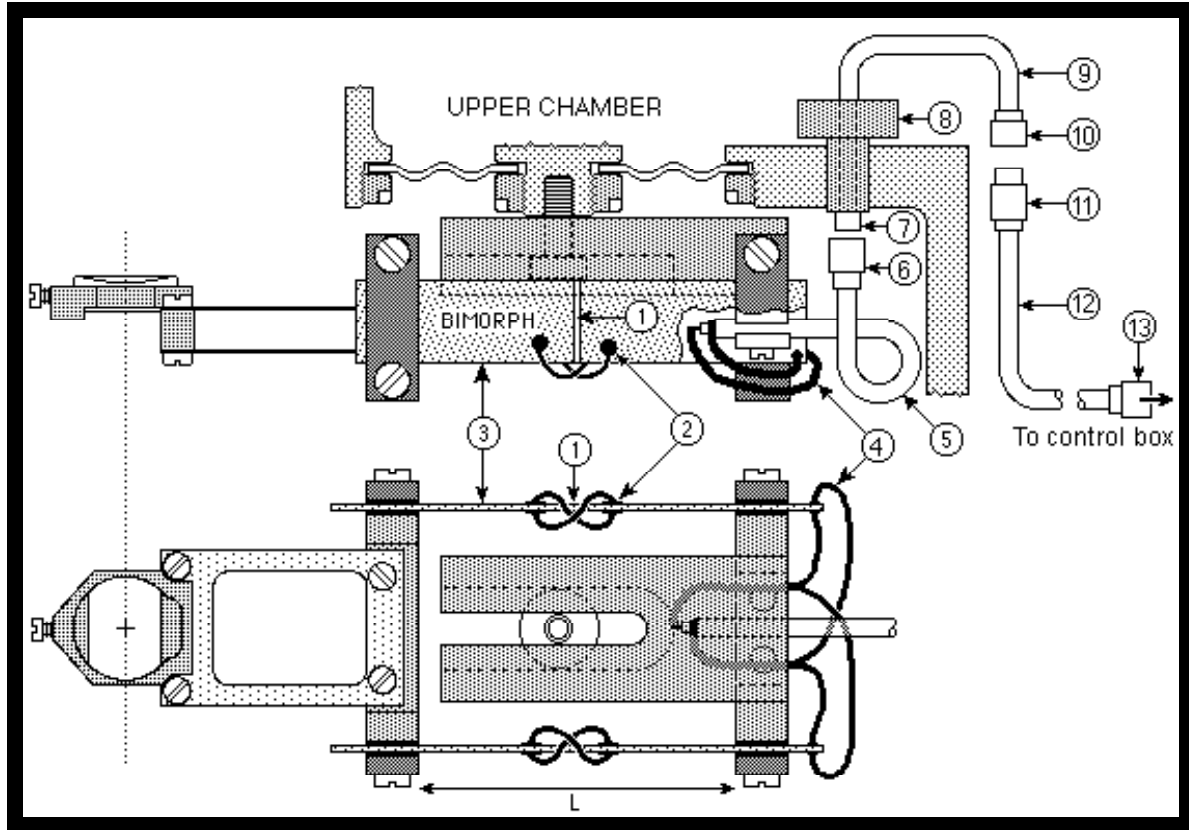


Figure 47. Electrical wiring and connections of Bimorph Slider.

Lateral motion of the lower surface A is produced by applying a DC or AC voltage to the bimorphs through a coaxial cable connected to the outside of the Lower Chamber via a Teflon-sealed Lemo-type connector. In most cases, it is desirable to have a ‘drive’ that (i) can travel over a large distance, (ii) is very rigid (stiff), and (iii) has a high natural frequency (see Theoretical Section below). For a typical PZT bimorph of active length $L = 30$ mm, the range of travel (at ± 100 V DC across the bimorph) is about $\pm 50\mu\text{m}$, and the stiffness of a double-bimorph slider is $K_x \approx 10^4$ N/m (Figure 47). The effective mass of the lower surface support or ‘drive’ is $m_x \approx 8$ g, which determines the upper limit for dynamic measurements (corresponding to the resonant frequency of the drive) at approximately $\nu_x \approx (1/2\pi)(K_x/m_x)^{1/2} \approx 200$ Hz. Higher travel distances, up to 1 mm p-p, can be attained by increasing the active bimorph length, L, using clamps C1 and C2, but at the cost of a decreasing stiffness. Alternatively, higher stiffnesses K_x and resonant frequencies ν_x can be attained by reducing the active bimorph length, but this also lowers the travel distance for a given (maximum safe or linear) voltage. Thus, some compromise is always required. The ability to readily change the active bimorph length provides sufficient flexibility for optimizing the system parameters for most types of experiments.

In sliding experiments, it is often desirable to have surfaces moving (shearing) at some *constant* speed or shear rate rather than sinusoidally. This can be achieved with the bimorph slider by applying a triangular voltage signal. This produces constant velocity motion in one direction until the turning point, and then in the reverse direction, repeatedly. In this way, very low or very high constant velocities can be achieved. For example, using the above operating parameters ($L=30$ mm), the range of practical speeds attainable using a function generator that provides a 1–100V peak-to-peak triangular signal (corresponding to 0.7–70 μm total travel per cycle) is from 0.1 nm/s at a driving frequency of $v=10^{-6}$ Hz to 10 mm/s at $v=10^2$ Hz. For a film thickness of 10 nm, these speeds correspond to shear rates that can be varied from $\dot{\gamma} = 10^{-4}$ to 10^6 s^{-1} – a range of ten orders of magnitude.

Finally, since bimorphs can both induce and detect motion, the bimorph slider may also be used as a friction force-measuring spring.

Using the Bimorph Slider and Friction device together

When used together with the Bimorph Slider, the Friction Device can be used as the 'receiver' (Figure 48). One can change the mass and spring dimensions of the Friction Device to optimize it for use with the Bimorph Slider. For example, the mass m_y of the upper surface or 'stage', and the dimensions of the friction force-measuring springs (length, width and thickness), can be optimized to provide (i) high force sensitivity (bridge output voltage vs. friction force), or (ii) high displacement sensitivity (bridge output voltage vs. lateral displacement), and (iii) high natural frequency ν_y of the 'stage'. The latter property is desirable for obtaining a high dynamic range and the ability to measure rapid transient effects such as stick-slip friction. Typical middle of the range operating values are: $K_y \approx 10^3$ N/m, $m_y \approx 2.2$ g, $\nu_y \approx 120$ Hz. When used with a strain-gauge amplifier (MEASUREMENTS GROUP, Model 2311) and chart recorder (SOLTEC, Model 1242) or storage scope recorder (TEKTRONIX, Model 2232), the DC friction force sensitivity should be better than $\sim 50 \mu\text{N}$ (~ 5 mg), corresponding to lateral displacements of the friction spring of 50 Å. Enhanced sensitivities can be obtained when measurements are made in AC mode with a lock-in amplifier (Stanford Research Systems digital two-phase lock-in amplifier Model SR830) which also allows independent measurements of the in-phase and out-of-phase components of the output signal.

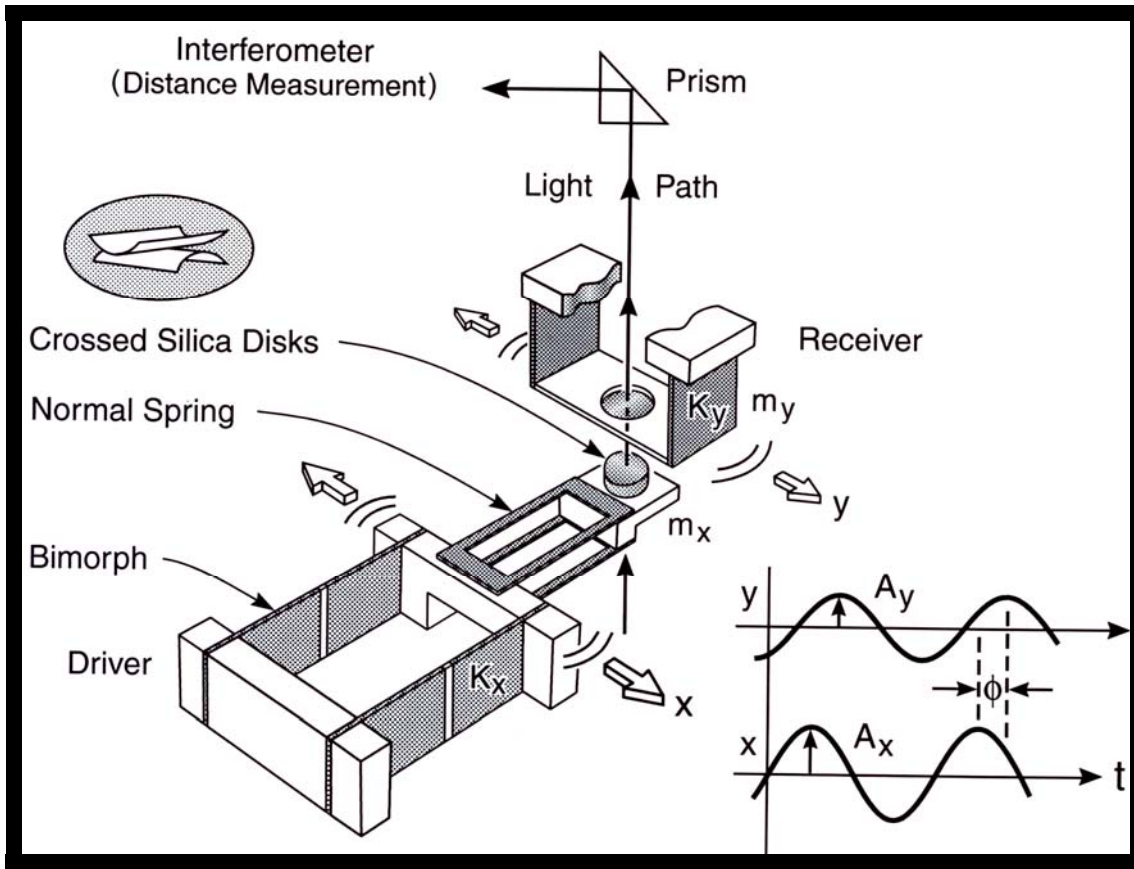


Figure 48. Shear elements of the Bimorph Slider attachment.

In principle, it should also be possible to measure the motion of the friction spring using a capacitance or optical technique, for example, laser light interferometry, instead of strain-gauges. Strain gauge measurements of spring deflections do not have the sensitivity of capacitance or optical techniques but they do have the advantage of fast response times and simplicity of construction and use. Capacitance measurements introduce unwanted forces between the plates, and optical interferometric techniques can be unreliable when used over large distances ($D \gg \lambda$).

The Friction Device also has the capability of driving the upper surface (the stage) at a constant speed using a mechanical drive that is powered by a variable speed DC motor with an encoder readout. The total distance of travel is much larger than can be attained with bimorphs: ~5 mm instead of 0.1–1 mm. However, the range of sliding speeds attainable is much more limited, and sinusoidal motions are not feasible as they are with the Bimorph Slider. Nevertheless, when used in this way, the upper friction attachment serves as a complete, self-contained unit, capable of both generating movement and measuring the resulting friction forces. The lower (bimorph) attachment is only capable of generating

movement, and so must be used in combination with the Friction Device whenever friction forces need to be measured as well.

It is also possible to use the Bimorph Slider as a displacement sensor, recording the output voltage produced by the bimorphs when they are disturbed. When used in this way, the motor on the Friction Device is used to move the upper surface (which now becomes the drive), and the lower surface now becomes the stage. This set-up is not as practical as the first one described above because the motor cannot provide AC motion and piezoelectric bimorphs, because they are lossy, are unreliable as DC sensors at low frequencies or driving speeds.

Equations of motion for Bimorph Slider in AC mode (refer to Figs 48 and 49)

When undergoing forced oscillations, the mechanical system may be described in terms of two coupled, damped, forced harmonic oscillators (Figure 49, top):

$$\begin{aligned} m_x \ddot{x} + K_x x + \kappa_x \dot{x} + \kappa(\dot{x} - \dot{y}) &= F_0 e^{i\omega t} \\ m_y \ddot{y} + K_y y + \kappa_y \dot{y} - \kappa(\dot{x} - \dot{y}) &= 0 \end{aligned} \quad (13)$$

where $(x - y)$ is the relative lateral displacement of the lower and upper surfaces. The subscripts x and y refer to the **drive** (bimorph slider) and **receiver** (stage and strain gauges), F_0 is the driving force, and $\kappa(\dot{x} - \dot{y}) \equiv \kappa v = F$ is the real friction force between the two surfaces defined in terms of κ , the damping of the lubricating fluid between the two surfaces. The coefficient κ contains all the information on the friction force between the surfaces, and thus depends on the geometry of the surfaces, on the relative velocity v , and for non-Newtonian lubrication it will also depend on other factors such as time and previous history. At periodic driving frequencies $\omega = 2\pi\nu$ much lower than the resonance frequencies ω_0 of the drive and receiver the inertial terms $m_x \ddot{x}$ and $m_y \ddot{y}$ can be neglected. Likewise, we may neglect the two independent damping terms of the drive and stage, κ_x and κ_y , which are both much less than κ , and mainly affect the amplitude of the oscillations close to resonance ($\omega \approx \omega_0$). The glue layers supporting the substrate surfaces are generally much more rigid than the other compliant parts of the system and their contributions are automatically incorporated into K_x and K_y . If required, this contribution can be independently calibrated with the two surfaces rigidly clamped together with a metal rod. If the stiffness of the bimorph drive K_x is greater than that of the friction force-measuring spring K_y ($K_x > K_y$) the above equations simplify to

$$\begin{aligned} x &= (F_0 / K_x) e^{i\omega t} = A_0 e^{i\omega t} \\ K_y y - \kappa v &= 0 \end{aligned} \quad (14)$$

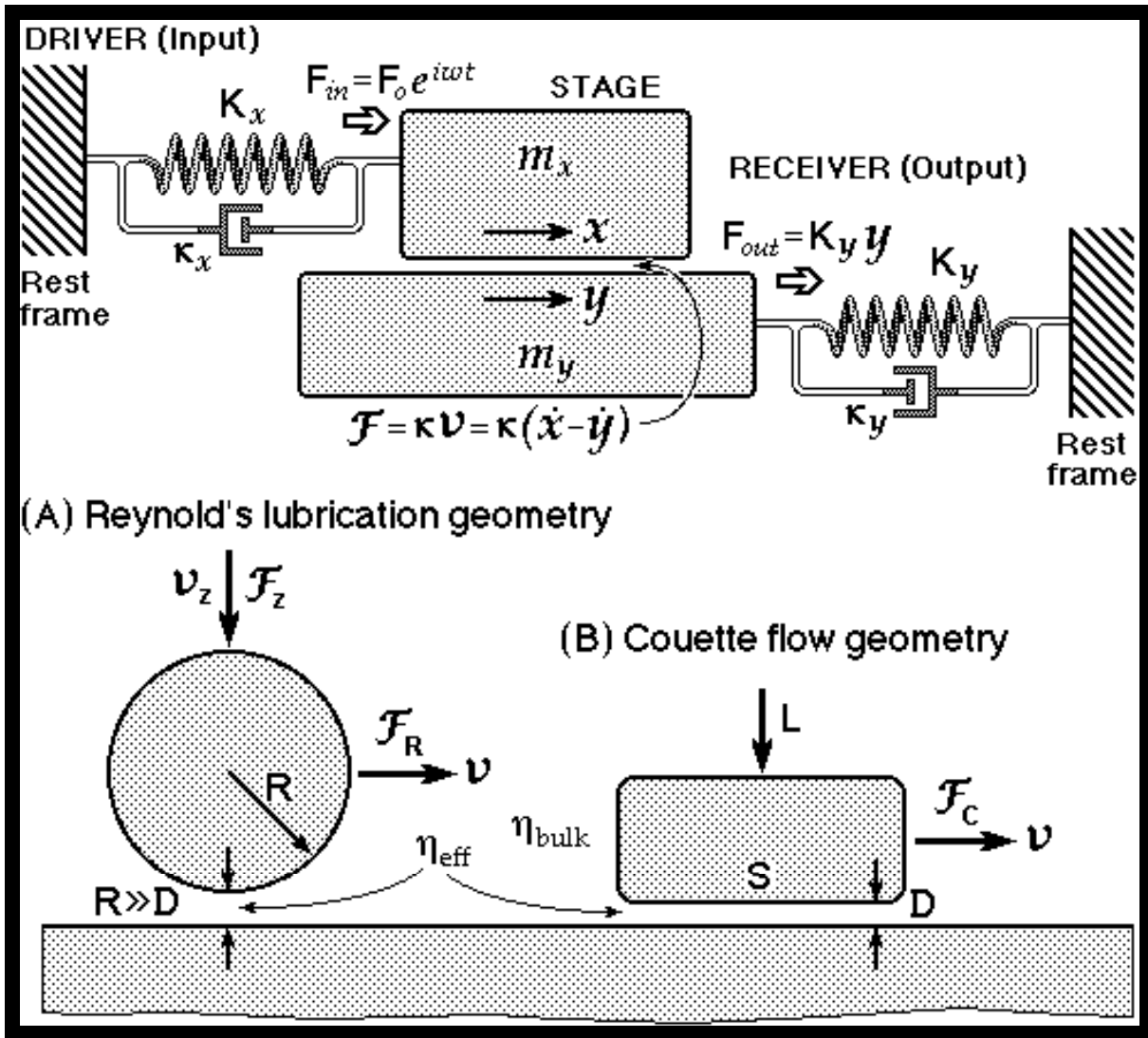


Figure 49. Equivalent mechanical circuit of the Bimorph Slider and Friction Device (top). The geometry and direction of motion of the surfaces determines the hydrodynamics of the problem, for example, whether sphere on flat (A) or flat on flat (B), as described in the text.

The forced movement of the lower surface x is thus transmitted via the friction force to the upper surface where it is measured by the strain gauges as a displacement, y (Figure 48). The oscillatory response is of the form

$$y = A_y \exp[i(\omega t + \phi)] \quad (15)$$

where the amplitude and phase of the upper surface are given by

$$A_y = \frac{A_0}{[1 + K_y^2 / (\omega^2 \kappa^2)]^{1/2}}$$

$$\tan \phi = -\frac{K_y}{\omega \kappa} \quad (16)$$

From the above, the damping coefficient is given by

$$\kappa = \frac{K_y}{\omega[(A_0 / A_y)^2 - 1]^{1/2}} = \frac{K_y}{\omega \tan \phi} \quad (17)$$

We may note that all the parameters on the RHS of the above equations are known or directly measurable. The above solution is similar to one which applies to two surfaces undergoing normal vibrations along the z-direction [Israelachvili, J. N., Kott, S. J. and Fetter, L. J., *J. Polym. Sci., Polym. Phys. Ed.* **1989**, 27, 489]. The main difference between normal and shearing motion is in the damping coefficient, κ , which depends on different surface geometry parameters (grouped in Ω) and the viscosity. For example, for a sphere moving towards or away from a flat surface in a simple Newtonian liquid with shear viscosity η (Figure 49A), we have

$$F = \kappa v \equiv \Omega \eta v = 6\pi R^2 \eta v / D \quad (18)$$

whereas for a (non-rotating) sphere moving parallel to a flat surface surface[†]

$$F = \kappa v \equiv \Omega \eta v = 6\pi R \eta v \left[\frac{8}{15} \log\left(\frac{2R}{D}\right) + \dots \right] \quad (19a)$$

$$\approx \frac{16}{5} \pi R \eta v \log\left(\frac{2R}{D}\right) \quad \text{for } R \gg D \quad (19b)$$

where R is the radius of the sphere and D is the closest distance of separation in both cases. For two crossed cylinders, the geometry adopted here, the effective hydrodynamic radius R is related to the cylinder radii R_1 and R_2 by (Chan, D. Y. C. and Horn, R. G., *J. Chem. Phys.* **1985**, 83, 5311)

$$R^2 = 2(R_1 R_2)^{3/2} / (R_1 + R_2) \quad (20)$$

when $R_1 = R_2$, we may put $R = R_1 = R_2$ and the geometry is equivalent to a sphere of radius R near a flat surface.

[†] O'Neill, M. E. *Mathematica* **1964**, 11, 67.

O'Neill, M. E.; Stewartson, K. *J. Fluid. Mech.* **1967**, 27, 705.

Goldman, A. J.; Cox, R. G.; Brenner, H. *Chem. Eng. Sci.* **1967**, 22, 637.

Another important geometry that was also studied is that of two flat parallel surfaces (Figs 1 and 49B). If one surface of area S is moving laterally past the other at a fixed surface separation D , the situation corresponds to Couette flow and the viscous force is given by

$$F = \kappa v + \Omega \eta v = \frac{\text{Area} \times \text{viscosity} \times \text{velocity}}{\text{Film thickness}} = \frac{S \eta v}{D}. \quad (21)$$

We should emphasize again that the above relations hold only for Newtonian fluids. In some cases, when film thicknesses approach molecular dimensions and fluids cease to be Newtonian, we shall use the above equation to compute an effective viscosity, η_{eff} , defined by

$$\eta_{\text{eff}} = FD/Sv \quad (22)$$

where all the parameters on the RHS are measured values.

If we deal with a viscoelastic liquid, the viscosity η may be represented by a complex function $\eta = \eta' - i\eta''$ where η' is the viscosity component that is in phase with the rate of strain, and η'' is the component that is 90 degrees out of phase. Solving Eq. 14 for the case of linear viscoelasticity, we obtain

$$\begin{aligned} \eta' &= \frac{K_y f \sin \phi}{\omega \Omega [f^2 - (2f \cos \phi - 1)]} \\ \eta'' &= \frac{K_y (f \cos \phi - 1)}{\omega \Omega [f^2 - (2f \cos \phi - 1)]} \end{aligned} \quad (23)$$

where $f = (A_0/A_y)$. The magnitude of the viscosity is given by

$$\eta = \sqrt{\eta'^2 + \eta''^2} = \frac{K_y}{\omega \Omega [f^2 - (2f \cos \phi - 1)]^{1/2}} \quad (24)$$

and the 'storage' and 'loss' shear moduli are, respectively

$$G' = \omega \eta'', \quad G'' = \omega \eta' \quad (25)$$

which together define the complex 'shear' modulus $G = G' + iG''$. We should note that η'' and G'' are proportional to the energy stored elastically in the system, whereas η' or G' are proportional to the energy lost per cycle through irreversible viscous (thermal) dissipation. When the viscosity is different from the bulk value, as occurs in thin films, the 'effective

viscosity', η_{eff} , as measured by use of the hydrodynamic equations 18–22 and defined by Eq. 24 is used instead of η in all of the above equations.

It is also useful to know the shear rates, the shear strains and the shear stresses. When using sinusoidal signals the shear rate can be calculated from

$$\dot{\gamma} = \mathcal{V} / D = \frac{i\omega[A_0 - A_y \exp(i\phi)]\exp(i\omega t)}{D} \quad (26)$$

In general, we will refer to the maximum shear rate, given by

$$\dot{\gamma} = \frac{\omega \sqrt{(A_y \sin \phi)^2 + (A_0 - A_y \cos \phi)^2}}{D} \quad (27)$$

Using Eq. 24, this can be transformed into

$$\dot{\gamma} = \frac{K_y A_y}{\eta \Omega D} \quad (28)$$

The maximum shear strain, γ , is consequently

$$\gamma = \dot{\gamma} / \omega \quad (29)$$

It is now straightforward to calculate the maximum shear stress, σ , imposed on the sample using the general viscoelastic relations:

$$\sigma \equiv F_0 / S_{eff} = \eta_{eff} \dot{\gamma} \quad (31)$$

Equation 22 allows us to calculate an effective area of shear, S_{eff} , in any geometry.

All the above equations assume that the response y is directly proportional to x , which is the case in the absence of yield points as occurs in the tribological regime. They also assume that the viscosities η' and η'' , and shear moduli G' and G'' depend only on the frequency and not on the amplitude of the stress or strain, which has indeed been verified in experiments with thicker films [Luengo et al., *Macromolecules* **30** (1997) 2482–2494].

BIMORPH VIBRATOR

MAIN FEATURES

- ★ Detects vertical displacements of the lower surface, especially oscillatory.
- ★ Can be used to measure thin film viscosity and rheological properties.
- ★ Versatile mount that can receive other types of attachments, including a fixed-stiffness force-measuring spring.

DESCRIPTION

The BIMORPH VIBRATOR (see Figures 17 and 28) is an attachment for vibrating one surface (vertically) while measuring – for example, with a lock-in amplifier – the amplitude and phase of the vibrations induced in the other surface. This attachment is useful for measuring rheological and visco-elastic properties of fluids and thin fluid films near surfaces or between two surfaces. For experiments with the bimorph totally immersed in a liquid such as water (Figure 50), it is possible to chemically and electrically seal the bimorph surfaces and its attached wires by dipping slowly into HUMISEAL Protective Coating type 1A20, then withdrawing at 1 cm/min, then allowing to dry overnight. In this way a semi-hard, chemically inert 15-20 μm thick polyurethane film protects the surfaces, while exhibiting sufficient flexibility (elasticity) so that the mechanical characteristics of the bimorph are not impaired.

The equations of motion of the bimorph vibrator are similar to those of the Bimorph Slider, detailed above, except that the oscillatory motion is normal rather than lateral (cf. Figure 49). This means that the liquid film experiences squeeze flow rather than shear flow, so that the response is much more sensitive than in the case of the Slider. The Bimorph Vibrator has provided some important results on the viscosity of thin fluid films and the location of the slipping plane that cannot be obtained with other techniques. See, for example:

1. **Measurements of Dynamic Interactions in Thin Fluid Films: the Transition from Simple to Complex (Non-Newtonian) Behavior.**
J. N. Israelachvili, S. J. Kott, L. Fetter, *J. Polymer Sci., Part B: Polymer Physics* **27** (1989) 489-502.
2. **Measurements and Relation Between the Dynamic and Static Interactions Between Surfaces Separated by Thin Liquid and Polymer Films.**
J. N. Israelachvili, *Pure & Appl. Chem.* **60** (1988) 1473-1478.
3. **Shear Properties and Structure of Simple Liquids in Molecularly Thin Films: the Transition from Bulk (Continuum) to Molecular Behavior with Decreasing Film Thickness.**
J. N. Israelachvili, S. J. Kott, *J. Colloid Interface Sci.* **129** (1989) 461-467.

The Bimorph Vibrator also comes with a number of additional attachments, including one for mounting a fixed stiffness spring (which takes up very little volume and so can be used with very small quantities of liquid), and a general-purpose mounting connector suitable for fitting new attachments that one may wish to design and incorporate in the future.

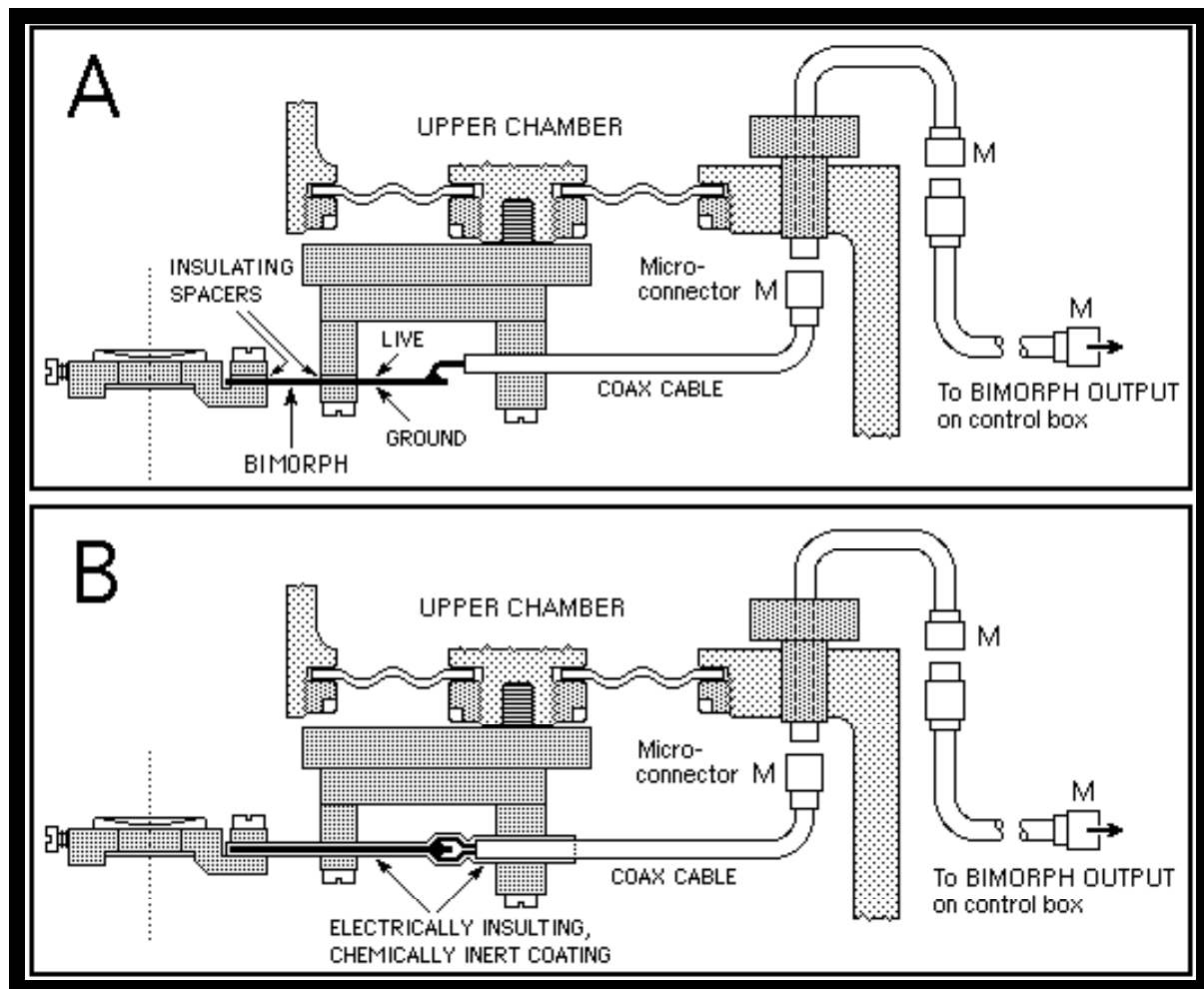


Figure 50. Schematic drawing of BIMORPH VIBRATOR assembly. (A) Unsealed bimorph for 'droplet' experiments in vapors. (B) Sealed bimorph for experiments in liquids. Note: when handling the micro-connectors (M), do not push or pull the coaxial cable – always connect and disconnect by turning and pushing or pulling the brass hex head.

OTHER FEATURES, INCLUDING OPTIONAL ATTACHMENTS AND CUSTOMIZED MODIFICATIONS

Various additional attachments and modifications are available for use with the SFA3 (and SFA 2000 – described further in the following sections). Custom-built and specialized attachments can always be made for, or constructed by, the user since the SFA3 is a modular apparatus, designed to have its parts interchanged and added to (an excellent book that provides useful hints on designing small machine components is *Foundations of Ultraprecision Mechanism Design* by S. T. Smith and D. G. Chetwynd, Gordon and Breach Science Publishers, Amsterdam, 1992, 1994). Examples of the types of additional attachments or modifications that are available for the SFA 3 (and SFA 2000) are as follows:

★ Customized modifications

Purchasers can specify certain customized ‘modifications’ for their SFA, for example, the dimensions of the certain parts, the mass of the moving surfaces in friction experiments, the stiffness of the friction-force-measuring-spring, etc. One or other of these options and modifications could be very important for optimizing certain types of experiments.

★ Experiments with small volumes of liquid

The capacity of the SFA3 chamber is about 75 ml, depending on which attachment is being used. A special lower chamber for doing experiments with small quantities of liquids (about 25 ml) is available (see Figure 51). This chamber also has an adjustable-height window for the incoming light beam to allow for nearly opaque liquids to be studied.

★ Variable friction force-measuring spring

An attachment is available that allows the stiffness (inertia) of the 'stage' in friction measurements to be adjusted from outside the apparatus during experiments, without the need to open the apparatus. Stiffnesses can be varied over a range of two orders of magnitude, which can be very useful in certain types of shear experiments.

★ Installing surfaces 'under water', especially useful for biological experiments

The retractable side window in the Lower Chamber of the SFA3 has been so designed to allow for its easy removal so that pre-prepared surfaces can be installed into the chamber 'under water' without removing them from solution. This is important when surfaces that have been pre-coated with delicate biological molecules in a Langmuir-Trough, for example, must be transferred into the apparatus without removing them from water.

Installation is achieved as follows: place the filled apparatus on its side, remove the window, fit the 'deposition cell' to the window (this Teflon cell or bath, which has to be specially made, is filled with liquid that immerses two small beakers containing the ready-to-be-installed surfaces), remove the 'plug' of the cell and insert the two disks. Special dove-tailed disks are available that can be inserted into the apparatus straight through the side window. These must be used with special dove-tailed disk mounts on the Piezo Mount and force-measuring spring, as shown in Figure 52.

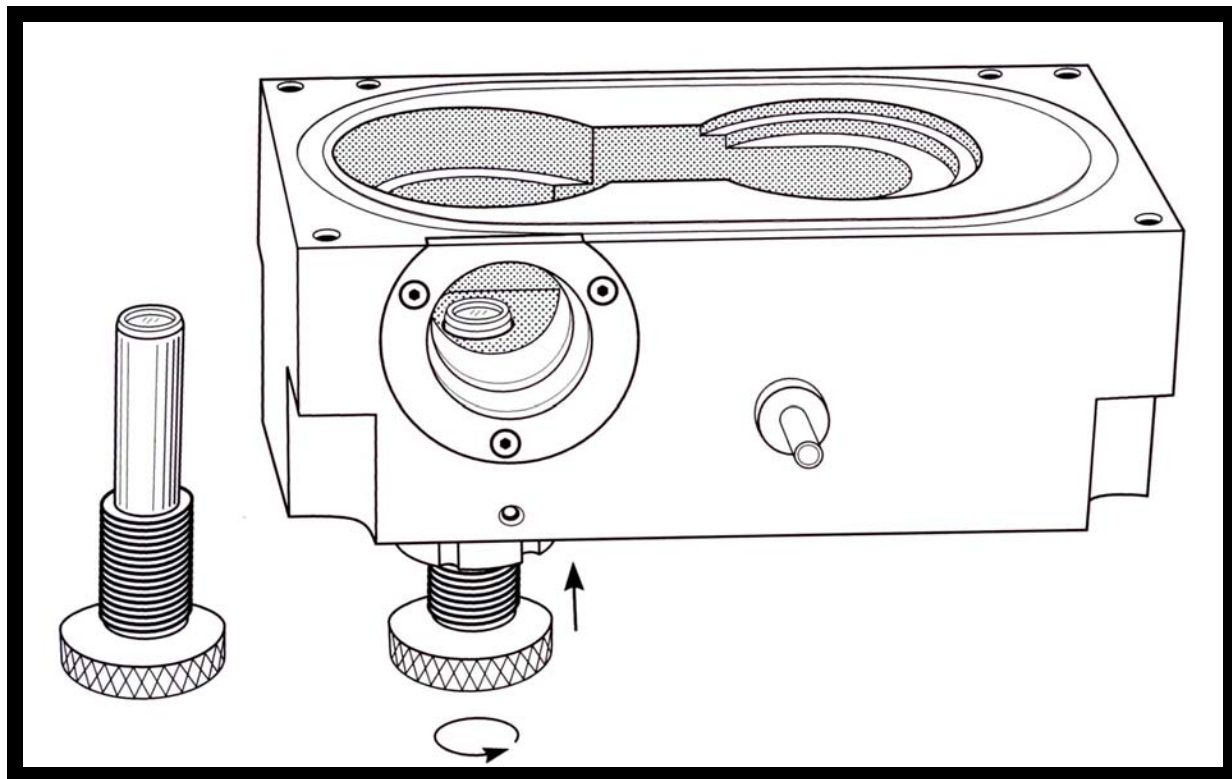


Figure 51. Small volume bath for the SFA 3 with a height-adjustable lower window (the SFA 2000 has a different small volume chamber).

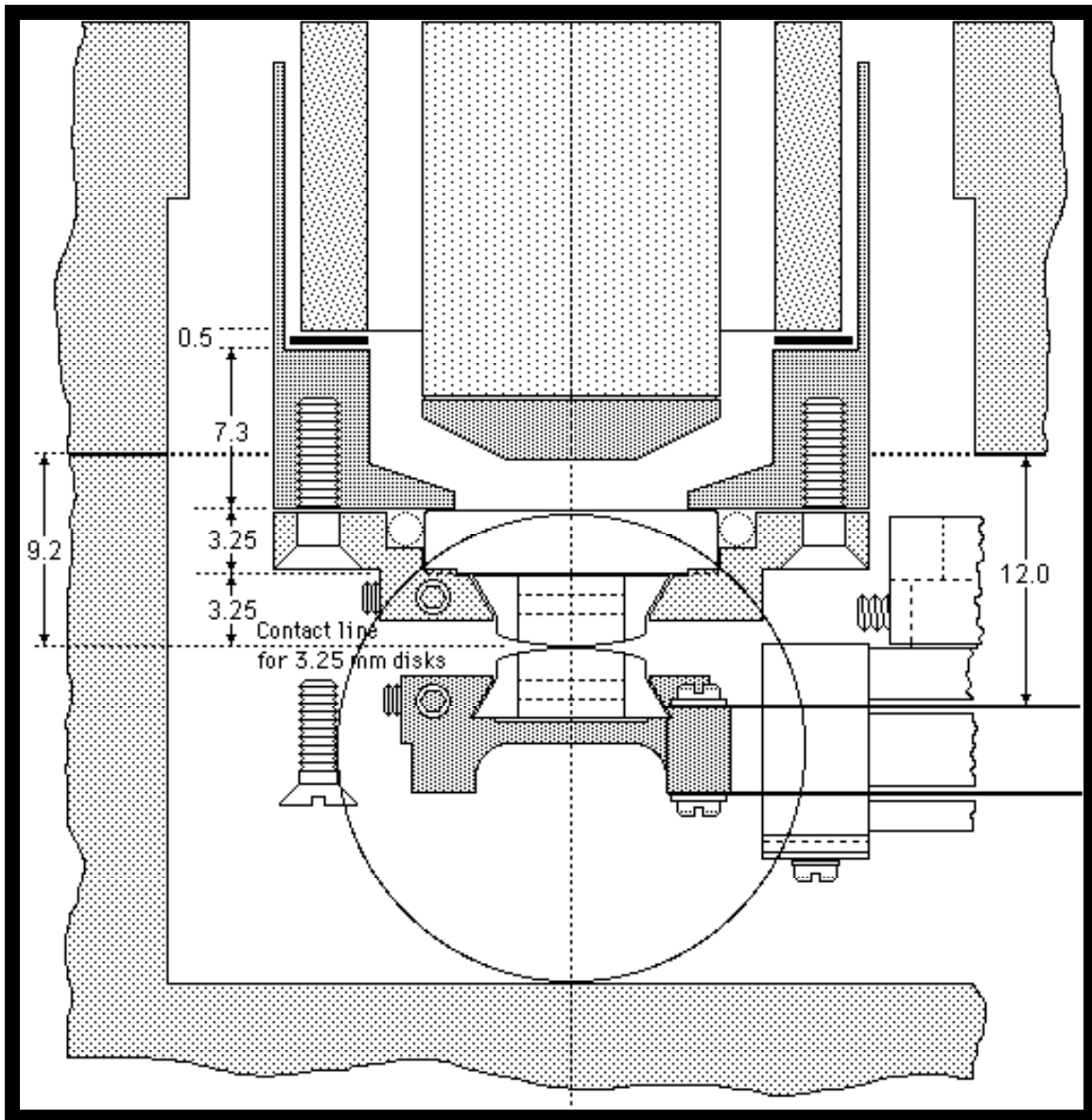


Figure 52. Dove-tailed disks and disk mounts, and view through side window.

PERFORMANCE SPECIFICATIONS OF SFA 3 AND ATTACHMENTS

The following values are approximate, and should be calibrated for each instrument and attachment before use as described in the User's Manual. It is also advisable to check these calibrations periodically or before critical experiments. This is because some properties, for example, of piezoelectric crystals and bimorphs, can age with time and anyway depend on the temperature and humidity.

Power requirements

100 to 240 V and 50 or 60 Hz (specify when ordering).

SFA 3 Basic Unit¹

Sensitivity of measuring normal and adhesion forces: 10 nN (1 millidyne).

Distance resolution: 0.1 nm (1 Å)²

Lateral distance resolution: 1 μm.³

Range of force-measuring spring stiffnesses attainable: $50 - 5 \times 10^5$ N/m (4 decades).

Maximum compressive pressure attainable (using curved surfaces of radii

0.5–1 mm and a thin layer of hard glue): 0.5 MPa (5,000 atm).

Thermal drift: <0.1 Å/sec (after 1 hr equilibration in a room or enclosure
that is temperature stabilized to ±0.1°C).

Friction Device (semi-conductor type)

Sensitivity of measuring lateral, shear and frictional forces: $1 - 10 \mu\text{N} = 0.1 - 1$ dyne.⁴

Friction spring stiffness: 10^{10} N/m = 10^7 dyn/cm (other stiffnesses available).

Lateral distance sensitivity: approx. 10 Å.⁴

Resolution of measuring Friction Coefficients: 0.0001.⁴

Range of lateral sliding speeds: 0.05 to 5 μm/s using a *single* motor, but range can be increased
almost indefinitely up or down by exchanging motors with different gearheads.

Bimorph Slider

Maximum recommended applied voltage (peak to peak): ±50 V (100 V p-p).

Maximum lateral displacement (at maximum voltage): ≈ 1 mm.

Stiffness of bimorphs: 10^7 mN/m.⁵

Range of lateral sliding speeds attainable: 10^{-8} to 1 cm/s.

Resonant frequency of bimorphs and support: ≈ 250 Hz.⁵

Recommended range of driving frequencies: 10^{-6} to 200 Hz (or up to resonance).

Maximum shear rates attainable: 10^5 s⁻¹ in squeeze mode (much higher rates are attainable
in shear/sliding mode depending on the test fluid).

¹ All stainless steel parts of internal surfaces are 316 or 316L chemically non-corrosive, non-magnetic steel. Other internal parts are either silica, PTFE (Teflon) or Kel-F.

² Assumes a medium sized spectrometer (1/4 to 1/2 meter type). There is no theoretical limit to the distance resolution. Using special image analysis techniques, Vanderlick and Davis [19??], and Hueberger [20??], have shown that surface separations can be measured reproducibly to ±0.15 Å.

³ Much smaller particles trapped between two surfaces can be “detected” due to the much larger elastic deformations they produce on the surrounding surfaces.

⁴ Depends on the sensitivity and quality of the strain gauge amplifier/bridge, and on the type of strain gauge being used. Values quoted are for semi-conductor gauges. Resistance strain gauges are about 100 times less sensitive.

⁵ Depends on number of bimorphs used (double or quadruple). Stiffness and hence resonant frequency can be varied up or down by changing the bimorphs' active clamping length, which is adjustable.

TABLE II: COMPLETE LIST OF PARTS & SUPPLY ITEMS

The following Table is a complete inventory of all the PARTS in each UNIT and their accompanying SUPPLY items. Numbers in brackets refer to the number of parts and supply items, including spares, provided per unit (if more than 1).

PART No.	NAME (No. PER UNIT)	ACCOMPANYING SUPPLY ITEMS
01000		UPPER CHAMBER
01010	UPPER CHAMBER	Main O-ring (3), top O-ring (3), shaft O-ring (3), male Luer connector (2), female Luer connector (2), female Luer cap (2),
01030	CANTILEVER SPRING	Long screws (4), short screws (2), assembly spatula, screw driver.
01040	TRANSFER SPRING	Flathead screws (2).
01050	SPRING HANGER	
01060	SPRING CARRIER	Screws (2), washers (2).
01070	HANGER BUTTON	
01080	SPRING GUIDE	
01090	GUIDE PINS (2)	
01100	OUTER RING	
01110	INNER RING	
01120	DOVETAIL SCREW	
01130	WIDE KEY	
01140	NARROW KEY	
01150	MICROMETER NUT	Differential micrometer – attached.
01160	SEALING NUT	
01170	LOCKING SCREW	
01180	GEARS STOP	Screws (2).
01190	FRONT PLATE	Screws (3).
01200	BACK PLATE	Screws (4).
01210	TRANSFER LEVER	Roller bearings w. washers (2) – attached.
01220	BEVEL GEAR	Set screws (2).
01230	PINION SHAFT	
01240	GEARS MOUNT	Mitre & bevel gears, matching pair – attached.
01250	GEAR SHAFT	
01260	GEAR WHEEL	Set screw.
01270	COUPLING CONNECTOR	Set screw (2).
01280	---	
01290	TEFLON BELLOWS (2)	
01300	ANTIBACKLASH SPRING	Medium-sized serrated forceps.
01310	COMPRESSION SPRING	
00040	MOTOR HOUSING	Micrometer head, O-ring, flexible coupling, DC motor with gearbox and encoder, 6-pin electric cable, low voltage DC motor power supply, encoder display counter, limit switches (2) screwed on board with scale, small screw with washer.
00050	MOTOR BUSHING	Dowel pins (2) – attached, flathead screws (2).

02000		
LOWER CHAMBER		
02010	LOWER CHAMBER	Silica window – attached, side window O-ring (2), inlet O-ring (3), thermistor O-ring (4), syringe port O-ring (3), heaters (2) with electric cable, male Luer connector (2), female Luer connector (2), m-m Luer coupling (1), m-f Luer coupling (2), f-f Luer coupling (2), female Luer cap (2), PTFE valve, Teflon tubing (2), 50 ml syringe.
02030	ENTRANCE FRAME	Silica window – attached.
02040	VIEWING FRAME	Silica window, flathead screws (4).
02050	CHAMBER SCREWS (4)	
02060	HINGE	Ovalhead screws (2).
02070	THERMISTOR HOLDER	Thermistor (2).
02080	THERMISTOR PLUG	
03000		
BASE		
03010	BASE PLATE	Grounding screw, circular spirit level.
03020 A	BASE HINGES A (2)	Flathead screws (8).
03020 B	BASE HINGES B (2)	
03020 C	HINGE PINS C (4)	
03030 A	LEG EXTENSION (3)	Hex nut (3), washer (3).
03030 B	LEG NUT (3)	
03030 C	BASE LEG (3)	
03040	RUBBER PADS (3)	neoprene rubber – attached, steel balls (3) – attached.
03050 A	LOCATING DISK A	Wood screws (6).
03050 B	LOCATING DISK B	
03050 C	LOCATING DISK C	
04000		
VARIABLE SPRING		
04010	DOVETAIL SLIDE	
04020	SLIDER MOUNT	Screw.
04030	SLIDER NUT	Flathead screws (2).
04040	UPPER SLIDE	
04050	LOWER SLIDE	
04060	SADDLE	Flathead screws (2).
04070	UPPER RETAINER	
04080	LOWER RETAINER	Screws (2).
04090	LEAD SCREW	Bevel gear with pin & washer.
04100	CLAMP SHIM	
04110	CLAMP PIN (2)	
04120	FORCE SPRING (2 + 2 SPARE)	
04130	DOVETAIL SCREW	
00020	DISC MOUNT	Screws (4 + 2 spare), silica discs (2).
00030 A	DISK SCREW (1+ 2 spare	
00030 B	SCREW TIP (1+ 2 spare)	
05000		
PIEZOMOUNT		
05010	CRYSTAL MOUNT	Piezocrystal tube – attached, wire inserts – attached, cable with Lemo connector.
05020	DISC MOUNT	
05050	EXIT FRAME	Silica window – attached.
05060 A	PIEZOMOUNT INSULATOR A	
05060 B	PIEZOMOUNT INSULATOR B	
00030 A	DISK SCREW (1+ 2 spare	
00030 B	SCREW TIP (1+ 2 spare)	
00080	CLAMPING RING	Long screws (2).

06000	MIRROR	
06010	UPPER BASE	This UNIT usually comes fully assembled. Remote control cables (3).
06020	MIRROR BASE	Flathead screws (4), helical spring with screw.
06030	MIRROR SLIDER	Ball bearings (36) – attached, remote control cable.
06040	MIRROR SWIVEL	Screws (2), flathead main screw, remote control cable.
06050	SLIDER GUIDE (2)	
06060	SCREW HEAD	Roller bearing.
06070	MIRROR MOUNT	Rectangular mirror – attached, ball bearings (2), spring with screw,
06080	MIRROR TURNTABLE	Flathead screw.
06090	PIVOT PINS (2)	
06100	PIN	
07000	OPTICS STAND	
07010	OPTICS BASE	
07020	SWIVEL RING	Large screw.
07030	SWIVEL ROD	
07040	LOCKING KNOB (2)	
07050	LOCKING SCREW (2)	
07060	MICROSCOPE PLATE	Flathead screws (3), motor screws (2), reversible motor with cable, belt, large gear wheel, small gear wheel.
07070	MOTOR MOUNT	Top screw, bolting screws (2), reversible motor w. cable, belt, gear wheel.
07080	MICROMETER MOUNT	Set screw, bolting screws (4), micrometer head.
07090	MICROMETER NUT	Set screw.
07100	ARM ROD	Glass plate – attached, flathead screws (2).
07110	ARM PLATE	Thumb screw.
07120	PLATFORM	
07130	PRISM DOVETAIL	
07140	DOVETAIL PIN	Helical spring.
07150	MICROSCOPE DOVETAIL	Flathead bolting screws (4), microscope stage.
07160	END PLATE	Bolting screws (2).
07170	CONTROL SCREW	
07180	CONTROL KNOB	
07190	PRISM SUPPORT	Screw, nut & washer (2), small screw, nut & washer (2).
07200	MICROSCOPE TUBE	Thrust bearing (1) with washers (2).
07210	TURNTABLE	
07220	ARM HOLDER	Set screw (2), clamping screw.
07230	SOCKET SCREW	
07240	PRISM TABLE	Prism.
07250	PRISM SCREW	
07260	SPRING ARM	Helical spring.
07270	WHEEL AXLE	
07280	---	
07290	MICROSCOPE TUBE	Objective lens.
08000	SYRINGE INJECTOR	
08010	SYRINGE SUPPORT	Small syringe, syringe needles (2).
08020	SYRINGE BALL	
08030	CHECK NUT	
08040	SYRINGE SLEEVE	
08050	RECEPTACLE	Luer connectors.
08060	BALL HOLDER	
08070	BALL RETAINER	

08080	PORT PLUG	
08090	PORT STUDS (3)	
08100	HEX NUTS (3)	
08110	RECEPTACLE HOLDER	Bolting screws (3).

11000

FRICTION DEVICE

11010	RING HOLDER	Bolting screw.
11020	SPRING HOUSING	Teflon sealing plugs (2) – attached, O-ring.
11030	COUPLING	Bolting screws (2).
11040	MICROMETER CONNECTOR	Set screws (2), O-ring.
11050	TRANSLATION STAGE	4-pin connector, wired – attached.
11060	FLAT DISK	
11070	COMPRESSION SPRING	
11080	TRANSLATION SPRING (2)	Bolting screws (8).
11090	SPRING CLAMP A (2)	
11100	SPRING CLAMP B (2)	
11110	FRICTION TUBE	Bolting screws (4), 4-pin connector, wired – attached.
11120	FRICTION SPRING (2 + 2 spare)	Bolting screws (4), semi-conductor or resistance strain gauges, temperature compensated, mounted & wired.
11130	TUBE CLAMPS (2)	
11140	DISK SUPPORT	Bolting screws (4), silica disk (2), disk screw (2).
11150	SUPPORT CLAMPS (2)	
11160	FRICTION COVER	Silica window – attached, O-ring (2), extra long clamping screws (2).
11171	ELECTRIC CONNECTOR	O-ring, 4-pin Lemo receptacle.
11180	MICROSCOPE TUBE	Objective lens.
00040	MOTOR HOUSING	Micrometer head, O-ring, flexible coupling, DC motor with gearbox and encoder, 6-pin electric cable, low voltage DC motor power supply, encoder display counter, limit switches (2) screwed on board with scale, small screw with washer.
00050	MOTOR BUSHING	Dowel pins (2) – attached, flathead screws (2).

12000

BIMORPH SLIDER

12010	SLIDER MOUNT	Bimorphs, wired w. connector (2 + 2 spare).
12020	CABLE CLAMP	Screws (2).
12030	LOCKING SCREW	
12040	SPRING MOUNT	
12050	BIMORPH CLAMP (4)	Screws (8).
12060	MICA SPACERS (8)	
12070	SLIDER SPRING A (2)	Bolting screws (4).
	SLIDER SPRING B (2)	
00090	SEALING CONNECTOR	Coax cable with miniature end-connector.
00020	DISC MOUNT	Screws (4 + 2 spare), silica discs (2).
00030 A	DISK SCREW (1+ 2 spare)	
00030 B	SCREW TIP (1+ 2 spare)	

13000

BIMORPH VIBRATOR

13010	BIMORPH MOUNT	Bolting screws (4)
13020	BIMORPH SUPPORT	Bimorph strip, wired with connector (1 + 1 spare).
13030	CLAMP A	Screws (2)
13040	CLAMP B	Screws (2)
13050	LENS HOLDER	Screws (4)
13060	FIXED MOUNT	

13070	BIMORPH SPRING (4)	Screws (4)
13080	LOCKING SCREW	
00020	DISC MOUNT	Silica discs (2).
00090	SEALING CONNECTOR	Coax cable (no need if already provided with SLIDER)
00030 A	DISK SCREW (1+ 2 spare)	
00030 B	SCREW TIP (1+ 2 spare)	

15000

ACCESSORIES

15010	CONTROL BOX	Connecting cables.
15020	PACKING CASE	
15030	TOOL KIT (assembly)	Screw driver set, Allen keys, tweezers, forceps, spatula.
15040	MISC. SUPPLIES	Glue (Epon Resin 1004, 1007, 1009), spirit level
15050	MANUAL	
15060	VIDEOS	

REFERENCES TO SFA TECHNOLOGY AND LITERATURE ON FORCE MEASUREMENTS

Review on surface force measurements

- Chapter 12 in *Intermolecular and Surface Forces*, 3rd Edition, 3rd printing, Elsevier (2011). J. Israelachvili.

Description of SFA2000

- Recent advances in the surface forces apparatus (SFA) technique. J Israelachvili, Y Min, M Akbulut, A Alig, G Carver, W Greene, K Kristiansen, E Meyer, N Pesika, K Rosenberg and H Zeng, *Reports on Progress in Physics* **73** (2010) 1-16.

Description of SFA3

- "Adhesion and Short-Range Forces Between Surfaces – New Apparatus for Surface Force Measurements", J. N. Israelachvili, P. M. McGuiggan, *J. Mater. Res.* **5** (1990) 2223-2231.

Description of SFA Mk 2

- "Measurement of Forces Between Two Mica Surfaces in Aqueous Electrolyte Solutions in the Range 0-100 nm", J. N. Israelachvili, G. E. Adams, *J. Chem. Soc., Faraday Trans. I* **74** (1978) 975-1001.

Description of the optical interference (FECO) technique

- Tolansky, S., "Multiple Beam Interferometry of Surfaces and Films", Oxford University Press, 1948; "An Introduction to Interferometry", Longmans, Green & Co., London, 1955.
- **Review of modern deposition techniques:** Hass, G., Heaney, J. B. and Hunter, W. R., *Physics of Thin Films*, **12**, 1 (1982).
- "Thin Film Studies Using Multiple Beam Interferometry", J. Israelachvili, *J. Colloid Interface Sci.* **44** (1973) 259-272.
- **Papers showing photos of FECO fringes:** See above paper, as well as "Role of Hydrophobic Forces in Bilayer Adhesion and Fusion", C. A. Helm, J. N. Israelachvili, P. M. McGuiggan, *Biochemistry* **31** (1992) 1794–1805. One can employ a second camera at the same time as looking at the FECO fringes by simply splitting the emerging beam by 90° using a normal 50-50 beam-splitter. The vertical (undeflected) beam can then be directed to a "top-view" camera, such as a CCD camera or fluorescence microscope, and the horizontal (deflected) beam is directed to the spectrometer, as in normal operations. For a description, with pictures, of how to combine normal optical microscopy with FECO interferometry see "Direct Visualization of Cavitation and Damage in Ultrathin Liquid Films", T. Kuhl, M. Ruths, Y-L. Chen, J. Israelachvili, *Journal of Heart Valve Disease* **3** (1994) S117–S127.
- **FECO spectroscopy (extension to non-uniform and absorbing media):** "Enhanced absorption within a cavity: a study of thin dye layers with the Surface Forces Apparatus", C. Müller, P. Mächtle and C. A. Helm, *J. Phys. Chem.* **98** (1994) 11119–11125. "A thin absorbing layer at the center of a Fabry-Pérot interferometer", P. Mächtle, C. Müller and C. A. Helm, *J. Phys. II France* **4** (1994) 481–500.

Using surfaces other than mica in SFA studies

- **Sapphire:** Horn, R.G., Clarke, D.R., and Clarkson, M.T., "Direct Measurements of Surface Force Between Sapphire Crystals in Aqueous Solutions", *J. Mater. Res.* **3** (1988) 413-416.
- **Zirconia:** "Effect of substrate on shearing properties of ultrathin polymer films", S. J. Hirz, A. M. Homola, G. Hadzioannou & C. W. Frank, *Langmuir* **8** (1992) 328–333.
- **Alumina:** "Van der Waals Epitaxial Growth of α -Alumina Nanocrystals on Mica", S. Steinberg, W. Ducker, G. Vigil, C. Hyukjin, C. Frank, M. Tseng, D. Clarke, J. Israelachvili, *Science* **260** (1993) 656–659.
- **Silica:** "Surface Forces and Viscosity of Water Measured Between Silica Sheets", R. G. Horn *et al.*, *Chem. Phys. Lett.* **162** (1989) 404–408.
- **Silica:** "Interactions of Silica Surfaces", G. Vigil, Z. Xu, S. Steinberg, J. Israelachvili, *J. Colloid Interface Sci.* **165** (1994) 367–385.
- **Biological surfaces:** "The surface forces apparatus – a tool for probing molecular protein interactions", D. Leckband, *Nature* **376** (1995) 617–618.

Measurements of viscosity and rheology of thin liquid films

- "Surface Forces and Viscosity of Water Measured Between Silica Sheets", R. G. Horn *et al.*, *Chem. Phys. Lett.* **162** (1989) 404–408.
- "Measurement of the Viscosity of Liquids in Very Thin Films", J. N. Israelachvili, *J. Colloid and Interface Sci.* **110** (1986) 263-271.
- Peachey, J.; Van Alsten, J.; Granick, S. *Rev. Sci. Instrum.* **1991**, 62, 463.

Tribological measurements using the SFA

- "Measurements of and Relation between the Adhesion and Friction of Two Surfaces Separated by Molecularly Thin Liquid Films", A. M. Homola, J. N. Israelachvili, M. L. Gee, P. M. McGuigan, *J. Tribology* **111** (1989) 675-682.
- Granick, S., "Motions and Relaxations of Confined Liquids", *Science*, **253** (1991) 1374-1379. Hu, H-W. and Granick, S., "Viscoelastic Dynamics of Confined Polymer Melts", *Science* **258** (1992) 1339-1342.

SFA coupled to other techniques

- **Simultaneous X-ray synchrotron and SFA measurements:** "The X-Ray Surface Forces Apparatus: Structure of a Smectic Liquid Crystal under Confinement and Flow", S.H.J. Idziak, C.R. Safinya, R. Hill, K.E. Kraiser, M. Ruths, H. Warriner, S. Steinberg, K.S. Liang, J. Israelachvili, *Science* **264** (1994) 1915–1918.
- **Coupling surfaces forces with charge-transfer interactions:** "Contact Electrification and Adhesion between Dissimilar Materials", R. G. Horn, D. T. Smith, *Science* **256** (1992) 362–363.

- FECO spectroscopy: "Enhanced absorption within a cavity: a study of thin dye layers with the Surface Forces Apparatus", C. Müller, P. Mächtle and C. A. Helm, *J. Phys. Chem.* **98** (1994) 11119–11125.

Reviews and miscellaneous applications

- **Ceramics:** "Surface Forces and their Action in Ceramic Materials", R. G. Horn, *J. Am. Ceram. Soc.* **73** (1990) 1117-1135.
- **Polymers:** "Surface Forces with Adsorbed Polymers", J. Klein, *Macromol. Chem. Macromol. Symp.* **1** (1986) 125-137.
- **Polymers:** "Measurement of Forces Between Surfaces in Polymer Fluids", S. S. Patel and M. Tirrell, *Annu. Rev. Phys. Chem.* **40** (1989) 597-635.
- **Attaining high local pressures (0.5 GPa):** Briscoe, B. J. and Evans, D. C., "The Shear Properties of Langmuir Blodgett Layers", *Proc. Roy. Soc. London, A* **380** (1982) 389-407.

For further references see the SurForce LLC website and the brochures for the SFA 3 and SFA 2000.

ADDITIONAL INFORMATION MATERIAL

- **Instructional films:** A number of videos are available on procedures for doing SFA experiments – preparation of surfaces, installation into the apparatus, etc. – and the optical technique. In this video one can see moving fringes as they appear in different types of systems and interactions, which can be invaluable for getting a feel for the full potential of the optical technique. Five videos, of about one hour each, are available.

Example of a real SFA experiment to measure the forces between two surfactant monolayer-coated surfaces in a hydrocarbon liquid

1

MASTER II



CALCIUM SULPHONATE ACROSS WHITE OIL

This is a record and analysis of a real experiment, the first using Ca-sulphonate surfactant.
Aim: To measure forces between calcium-benzene-sulphonate surfactant monolayer adsorbed on mica in white oil (Blandol), and to test effect of water on the forces.

Materials: Calcium-benzene-sulphonate was from Exxon (SA 119) commonly used to stabilize colloids in lubricating oils (lube oils). The oil was Blandol, a mixture of mainly branched hydrocarbons with carbon numbers between 12 and 36. The oil had been previously dried, centrifuged and kept with 4A molecular sieves. The surfactant had been purified by recrystallization following the method of John Marsh and Isabelle McDonald.

18 JULY 1988

3pm. Mica sheets from JMI 7/5/88 A3 and A4 were glued onto two 5mm discs with 1004 glue. Small beakers of pure water ready. Water surface touched with surfactant then aspirated. One disc dipped into beaker, then after a few minutes slowly withdrawn (all this time surfactant was in contact with water surface). Surface came out dry. Disc dried. Repeated with second disc. Discs placed in apparatus, Mk II, then purged with N₂ for 30 minutes.

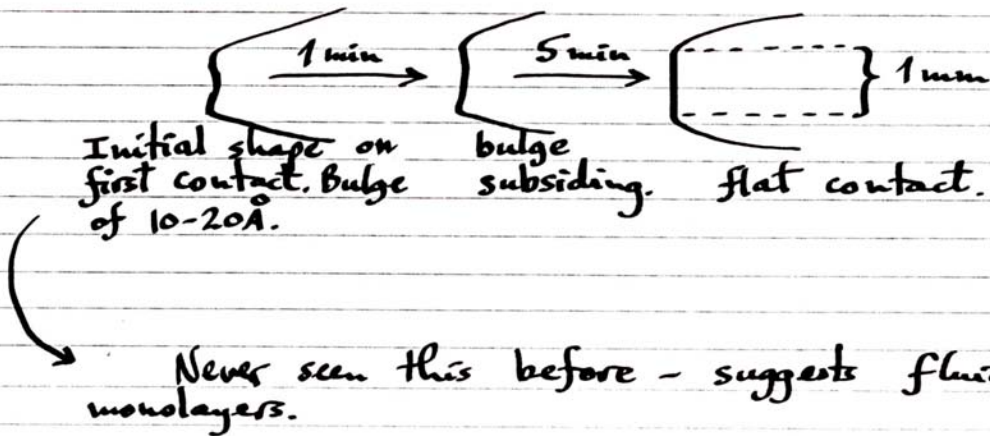
left overnight in dark room for temperature drifts to equilibrate. All controls checked and found to be working (motors, prism, focus, multimeters, flash light, dove prism, video system, tape ready, temperature setting, etc.)



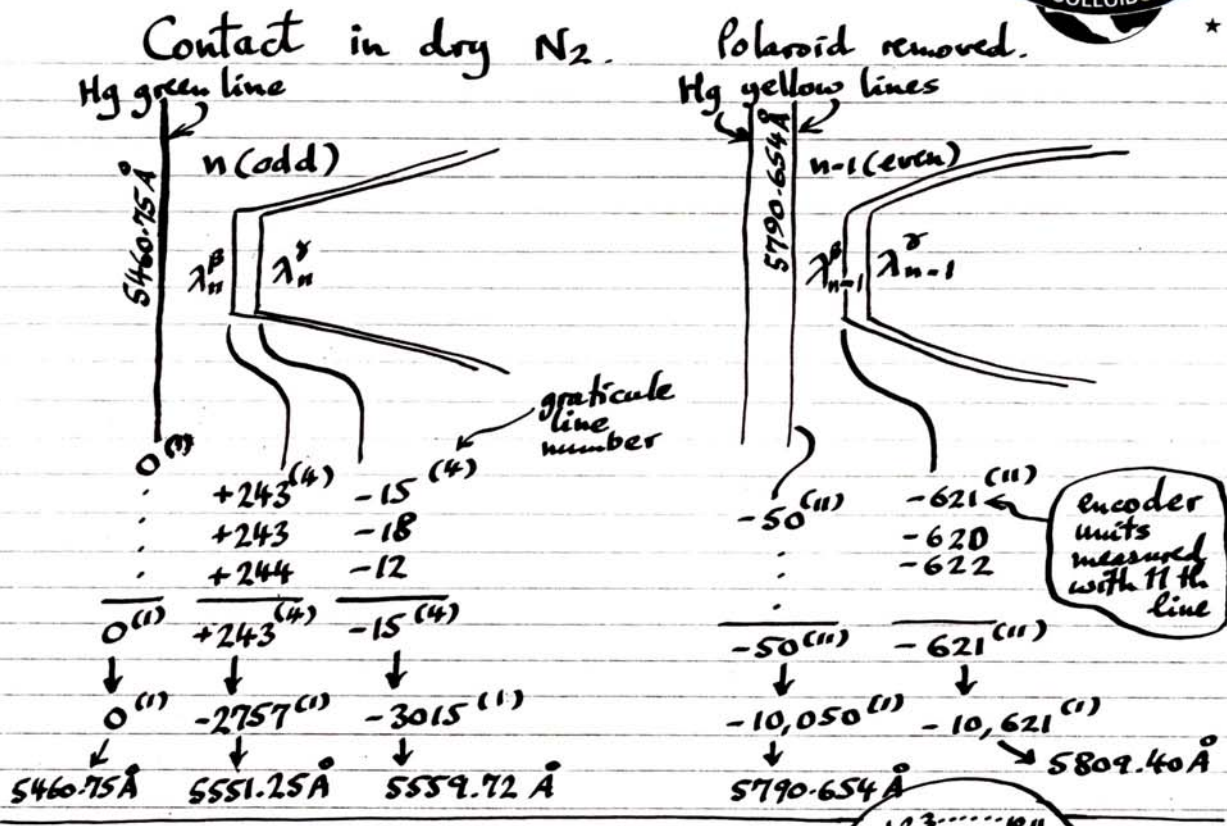
19 JULY 1988

- 9 AM Purged with N₂ for 30'. Newton's rings circular, contact and separation fine.
- 10 AM P₂O₅ put into small receptacle. N₂ purge stopped.
- 2 PM FECO contact excellent. Almost zero birefringence, polaroid used. Symmetry of odd and even fringes checked. Flat contact on scanning checked. Surfaces separated: nice jump apart until adjacent fringes 3.6 mm apart.

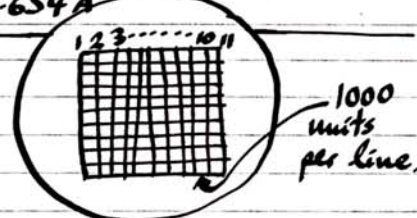
2:15 Surfaces brought into contact again, pressed together until contact diameter $\phi \approx 1$ mm. Noticed that:



Optics optimized: mirror controls, focus, centering, prism table controls, slit, dove prism, Hg line, polaroid, etc.



$$\therefore \text{DISPERSION: } \frac{5790.654 - 5460.75}{10,050 - 0} = 0.03282627 \text{ Å/unit.}$$



$$\therefore \begin{cases} \lambda_n^\beta = 5551.25\text{Å} \\ \lambda_n^\delta = 5559.72\text{Å} \\ \lambda_{n-1}^\delta = 5809.40\text{Å} \end{cases} \} n^{\text{th}} \text{ fringe}$$

$$\Delta \mu = \mu \Delta \lambda / \lambda = 1.60 (\lambda_n^\beta - \lambda_n^\delta) / \left(\frac{\lambda_n^\beta + \lambda_n^\delta}{2} \right)$$

$$= 1.60 \times 8.47 / 5555.5 = 0.0024$$

$$\therefore \mu_n^\beta (\lambda = \infty) = 1.5835 - 0.0012 = 1.5823$$

$$\text{and } \mu_n^\delta (\lambda = \infty) = 1.5835 + 0.0012 = 1.5847$$

$$\frac{1}{n F_n} = \frac{5809.40 - 5551.25}{5809.40} = 0.04444, \therefore n F_n = 22.50$$

$$\text{try } n (\text{odd}) = 21, \therefore F_n \approx 1.024 + \frac{1}{21} = 1.0716$$

$$\therefore n \approx 22.50 / 1.0716 = 20.998 \rightarrow 21.0 \text{ good!}$$



$$D \propto n F_n \delta \lambda_n / 2 \mu_{\text{medium}}$$

$$\approx 22.50 \times 0.0328 / 2 \times 1.60 = 0.231 \text{ \AA/unit.}$$

Now put following values into HP 15C storage registers:

register	store
0	5460.75 ← Hg reference line $\lambda(\text{\AA})$
1	0 ← encoder reading of above
2	0.03282627 ← dispersion ($\text{\AA}/\text{unit}$)
3	5551.25 ← λ_n^B
4	5809.40 ← λ_{n-1}^B
5	1.467 ← ref. index of medium (oil)
6	1.5823 ← $\mu_n^B (\lambda=\infty)$

Check the program by pressing \downarrow (243-3000) to get $D \approx 0$, and $+2857$ to get 23.1 \AA .

Also check by pressing $+10,621$ to get $\frac{\lambda_{n-1}^B}{2\mu_{\text{medium}}} = \frac{5809.4}{2 \times 1.467} = 1,980 \text{ \AA}$

Surfaces separated. Jumpered apart to where adjacent fringes 3.6 mm apart, as before.

\hookrightarrow 3600 units
Put $\mu_{\text{medium}} = 1.00$ into register 5

Enter -3600

Press D

→ gives $D_{\text{jump}} = 8.93 \mu\text{m}$

Now $R = 0.45 \text{ cm}$ (see later)

$K = 1.52 \times 10^5 \text{ dyne/cm}$ (calibrated at end)

$$\therefore F = 8.93 \times 10^{-4} \times 1.52 \times 10^5 = 4\pi R \delta$$

$$\therefore \delta = 24.0 \text{ erg/cm}^2 \text{ (or } 32 \text{ erg/cm}^2 \text{ if use } F = 3\pi R \delta\text{).}$$



20 JULY 1989

Insert 1.467 into 5.

11⁴⁵ AM droplet of white oil with surfaces apart.
 Purged with N₂ during injection. Surfaces did not come into contact during injection. Brought surfaces together with upper motor. Came to flattened "contact" at +233° → 2.5 Å
 Hg green line checked.
 Separated with lower motor.
 Jumped apart from +178° → 15 Å
 to -5050° → 537 Å } F/R = -1.76 dyne/cm

$$K/R = 3.38 \times 10^5$$

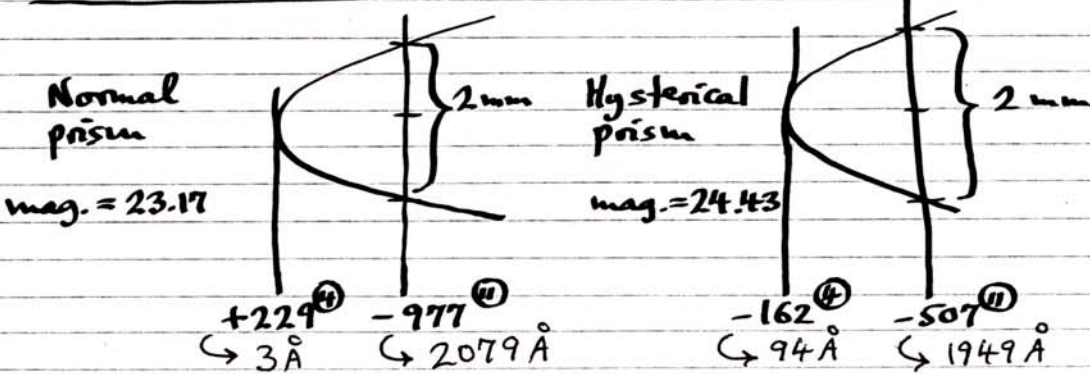
Repeat jump apart more gently with piezo (PZT).

Jumped from 181° → 14 Å

by 1 nm → 250 Å

$$\text{after a short time in contact. } F/R \approx -0.80 \quad \frac{\text{dyn}}{\text{cm}} = \frac{\text{mN}}{\text{m}}$$

RADIUS CALIBRATION



$$R_N = \frac{(0.1 / 23.17)^2}{2 \times 2079 \times 10^{-8}}$$

$$= 0.45 \text{ cm}$$

$$R_H = \frac{(0.1 / 24.43)^2}{2 \times 1949 \times 10^{-8}}$$

$$= 0.45 \text{ cm}$$

$$\therefore \bar{R} = \sqrt{R_N R_H} = 0.45 \text{ cm}$$

$$K = 1.52 \times 10^5 \text{ dyn/cm.}$$

$$\boxed{\therefore K/R = 3.38 \times 10^5 \text{ dyne/cm}^2.}$$



Surfaces brought into flattened contact at $+233^\circ$ $\rightarrow 2.5\text{\AA}$
Hg line checked.

12^{PM} Lower motor reversed until contact rounded, then measured forces with lower motor on way out.

<u>kΩ</u>	<u>D(units)</u>	<u>D(Å)</u>	<u>F/R(dyn/cm)</u>
18.675	+233 ⁽⁴⁾	2.3	
12.589	+220	5.3	
10.030	208	8.1	
5.715	200	9.9	
0.740	192	11.8	
14.982	176-180	15.0	-1.10
↓ Jump (with motor)			
	-1172 ⁽⁴⁾	329	0

Measure outward jumps with piezo (carefully)

Jumped from $+180^\circ$ $\xrightarrow{(1 \text{ min contact})} -1258^\circ$ $\rightarrow F/R = -1.20$
 $\xrightarrow{14.6\text{\AA}}$ $\xrightarrow{4258^\circ}$ $\xrightarrow{349\text{\AA}}$ (1 min)

Jumped from $+178^\circ$ $\xrightarrow{(1 \text{ min})} -1184^\circ$ $\rightarrow F/R = -1.12$
 $\xrightarrow{1510\text{\AA}}$ $\xrightarrow{332\text{\AA}}$ (1 min)

12¹⁵ PM Brought gently with piezo to $+210^\circ$ $\rightarrow 7.6\text{\AA}$
and left there for 20 min. then
jump out from $+195^\circ$ $\xrightarrow{11\text{\AA}}$ -1774° $\rightarrow F/R = -1.55$
 $\xrightarrow{471\text{\AA}}$ (20 min)

Brought together again with piezo then separated
within ~1 minute. Jumped from $+185^\circ$ $\rightarrow -1260^\circ$
 $\xrightarrow{13.4\text{\AA}}$ $F/R = -1.20$
 $\xrightarrow{15.5\text{\AA}}$ (1 min)

30 sec contact: $+176 \rightarrow -789 \rightarrow F/R = -0.81 (30s)$
1½ min contact: $+176 \rightarrow -1340 \rightarrow F/R = -1.25 (1\frac{1}{2} \text{ min})$
 $\xrightarrow{15.5\text{\AA}}$



Definitely looks like the adhesion increases with the time the surfaces remain close to contact (in the potential minimum), but not so much on how close or compressed they are.

$$\begin{array}{ll} \text{25 sec contact: } & 168 \longrightarrow -904 \rightarrow F/R = 0.90 \text{ (25 s)} \\ \text{1 min contact: } & 190 \longrightarrow -1144 \rightarrow F/R = -1.10 \text{ (1 min)} \\ & \downarrow 12.2 \text{\AA} \end{array}$$

Could be that under high compression it actually takes longer for the molecules to relax.
Hg line checked.

FORCE RUN WITH PIEZO $K/R = 3.38$ Piezo: 5.648 \AA/V used
(see next page)

VOLTS	D (units)	D(\AA)	F/R*
-195	-6001 ^④ → 9001 ^②	1,540	0 { 5.68 \AA/V
-98	-3893 ^④ → 6893 ^②	989	0 { 5.63 \AA/V
+10	-1393 ^④	381	0
+115	+180 → 4312 ^②	14.6	+0.77 not equilibrated?
277	+216	6.2	+3.8
499	228	3.5	+8.0
736	230	3.0	+12.5
1013	233	2.3	+17.8
1013			+17.0

Reverse

736	228	3.5	+11.7
499	226	3.9	+7.19
277	212	7.2	+2.97
215	207	8.3	+1.79
151	197	10.6	+0.58
78	187	13.0	-0.77
48	+180	14.6	-1.34

↓ jump

48	-1526 ^④	412	0 { 5.66 \AA/V
-50	-3805 ^④	967	0

945?

Immediate return to 20 sec contact. Jump out from $\longrightarrow -948^{\circ}$ $\rightarrow F/R = -0.93$ (20 sec)



PIEZO CALIBRATION

Fringe passing $+243^{\text{th}}$, viz. $\Delta D = 1892 \text{ \AA}$.
 $\hookrightarrow 5551.25 / 2 \times 1.467 \rightarrow$

14 volts $\xrightarrow{\text{forward}}$ 348 volts (+1 fringe)

12 volts $\xleftarrow{\text{return}}$

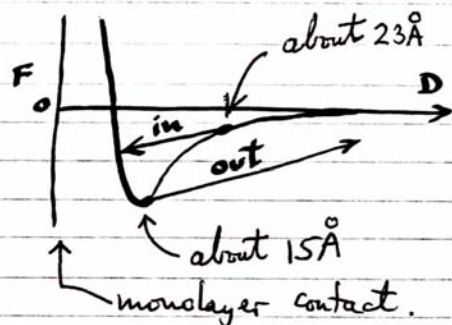
$$\therefore 1 \text{ V} = 5.648 \text{ \AA} \quad (\text{good})$$

Measuring jumps into "contact".

Difficult to measure
since very sluggish and
jump distance obviously small.

Estimate: from $\sim +143^{\text{th}}$ (min. D)

$$\therefore D \approx 23 \text{ \AA}$$



If we assume that the jump is due to van der Waals forces between the mica surfaces across the surfactant and oil (which both have the same refractive index) we obtain for the Hamaker constant

$$\frac{dF}{dD} = K = \frac{AR}{3D^3} \rightarrow A = \frac{3KD^3}{R}$$

$$A = 3 \times 1.52 \times 10^5 \times (30 + 23)^3 \times 10^{-24} / 0.45 \\ = 8.1 \times 10^{-14} \text{ erg}$$

\uparrow 2 × monolayer thickness, see later.

Is this reasonable?



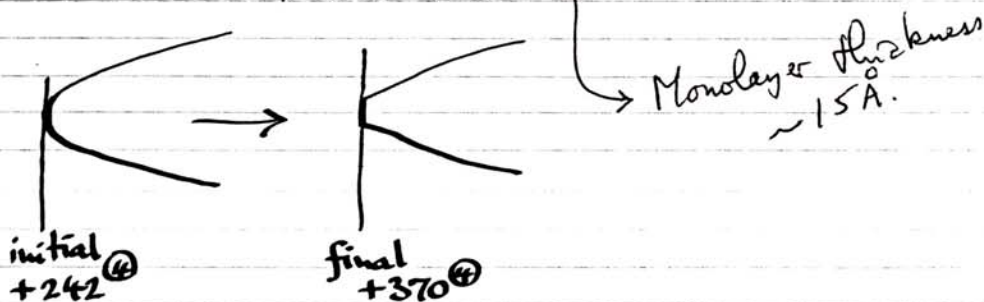
It was noticed that after a high adhesion the subsequent adhesion was also high if measured soon after the separation, but was lower if the surfaces were kept apart for > 10 min. For example, for 1 minute contacts or less, jumps out were ~ 1 mm ($FIR < 1.0$) if the surfaces kept apart for a long time between separations. But if surfaces brought together again within 1-2 minutes, the adhesion rose and remained high as long as adhesions measured repetitively (all after 1 min contact times).

4^{40} pm P_2O_5 replaced by pure WATER.
left overnight.

21 JULY 1988

Brought in gently with upper motor.
Came to $\sim +242^\circ$ then after ~ 1 min slowly moved in to $\sim 370^\circ$ adhesive flat contact at $360 - 370$.

$$\rightarrow D \approx -29\text{ \AA}.$$



Jump apart on separation until fringes 3.3 mm apart,* viz. $D_j = 58,840 \text{ \AA}$
 $\therefore \gamma = 16 \text{ erg/cm}^2$.

* Means separated by 3.3 mm as seen in the eyepiece graticule.

Repeated above: first surface stopped at 242 then moved in to 370 then large jump out as above.



Damage.

New position found.

Brought in with motor, gently to hard wall at
+232°
→ 2.5 Å

Separate: jump out from +214° by 300 V of piezo.
Repeat: " " " " by 380 V
+203 " " 320 V
+196 " " 350 V
+200 " " 345 V
+209 " " 340 V

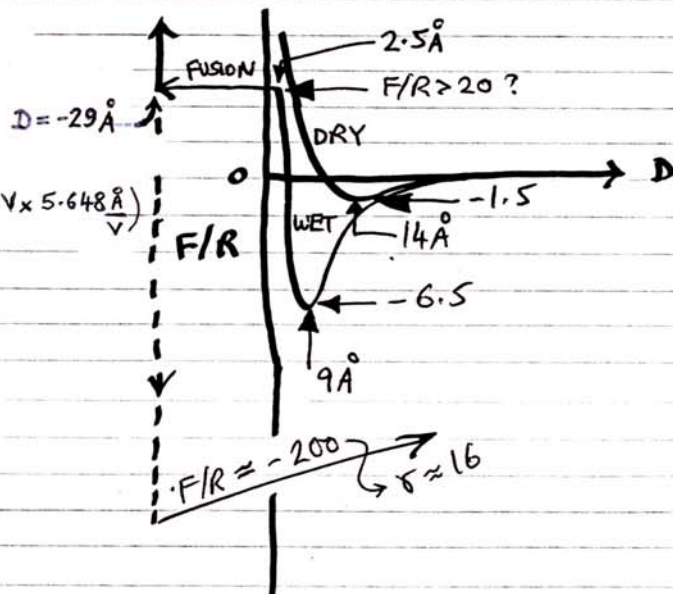
mean: 204 340 V
D = 9 ± 2 Å F/R = -6.5 *

*

$$\frac{\Delta F}{R} = K \frac{\Delta D}{R}$$

$$= 3.38 \times 10^5 \frac{\text{dyn}}{\text{cm}^2} \times (9^\circ - 340 \text{ V} \times 5.648 \text{ Å}) \text{ V}$$

$$= -6.46 \text{ dyn/cm}.$$



Pressed in with upper motor: Ease of breakthrough suggests fluid monolayer. → ← → ← ← breakthrough separate
Jump apart to where surfaces 3.5 mm apart.

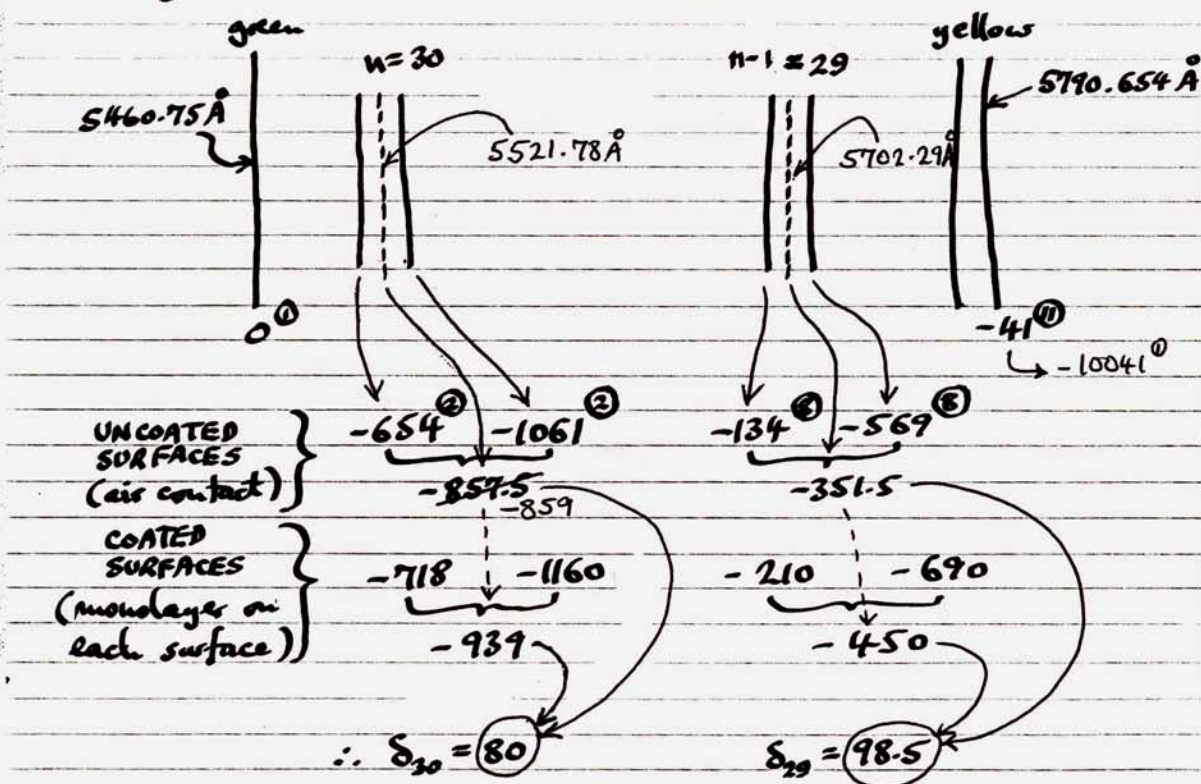
Calibration of K: $1.52 \times 10^5 \text{ dyne/cm.}$

END



THICKNESS & REF. INDEX OF Ca-Sulphonate*

Two identical silvered mica sheets used. On one, Ca-Sulphonate SA 119 deposited by retraction from distilled water. Two test pieces were prepared, one with the surfactant deposited and one without. Test pieces mounted onto test piece "jig" and FECO fringes optimized until fringes are maximum to the right (red end of the spectrum).



$$\text{DISPERSION: } 329.904 / 10041 = 0.0328557 \text{ \AA/unit.}$$

$$\frac{1}{nF_n} = \frac{\lambda_{n-1} - \lambda_n}{\lambda_{n-1}} = \frac{5702.29 - 5521.78}{5702.29} = \frac{1}{31.59}$$

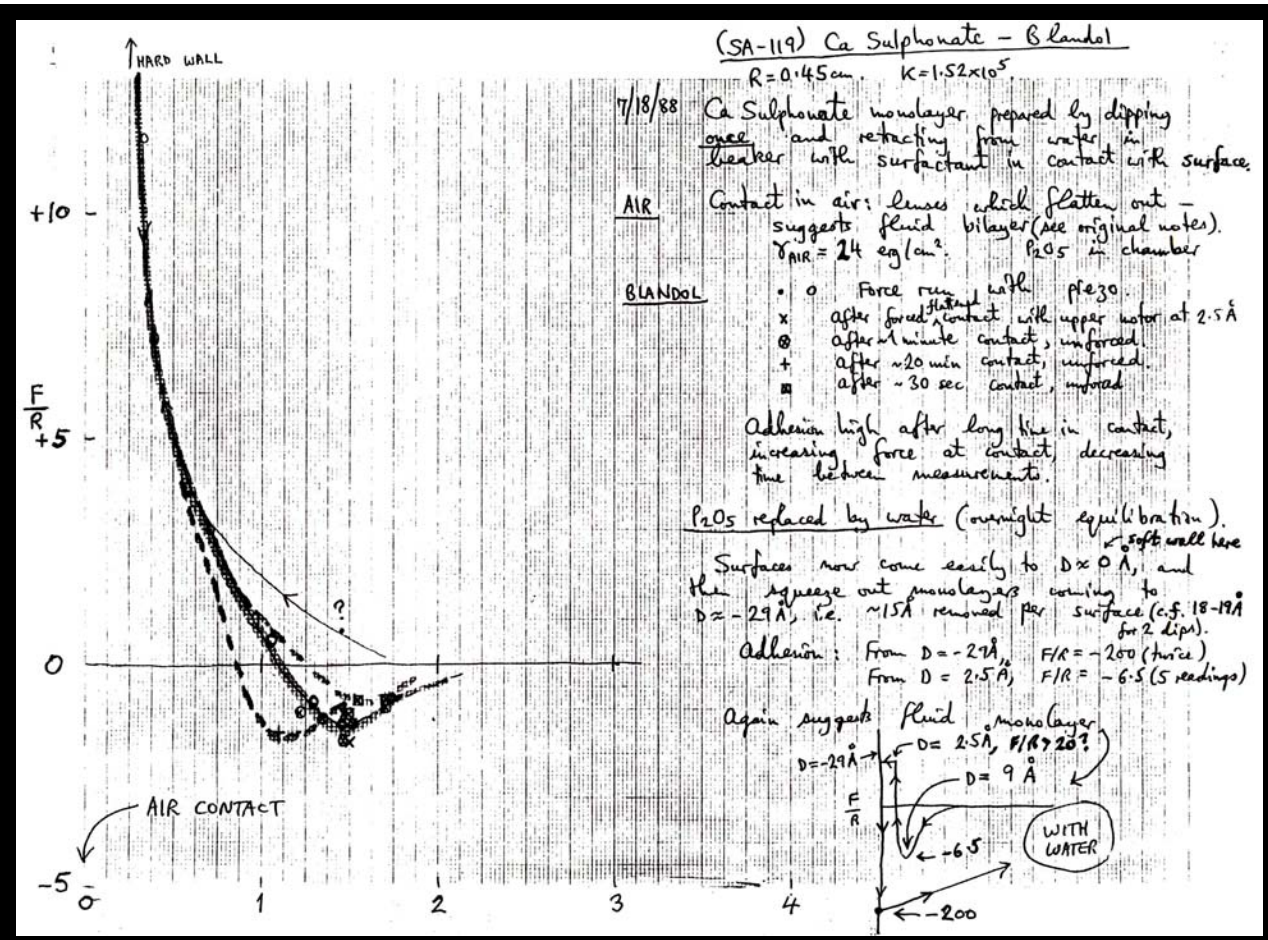
$$\text{Try } n=30^*, 1.024 + 1/30 = 1.0573, 31.59 / 1.0573 = 29.9 \quad \checkmark$$

$$\text{For } n=29, nF_n = 29(1.024 + 1/29) = 30.70$$

* Note change to even fringe for n . $\therefore \text{Monolayer thickness} = 15.5 \text{ \AA}$.

$$\text{Refractive index of monolayer: } \sqrt{\frac{nF_n \delta_n}{n-1 F_{n-1} \delta_{n-1}}} (1.60) = 1.46$$

Note: can also use program C on calculator.



Force-measuring capabilities of the SFA and AFM compared

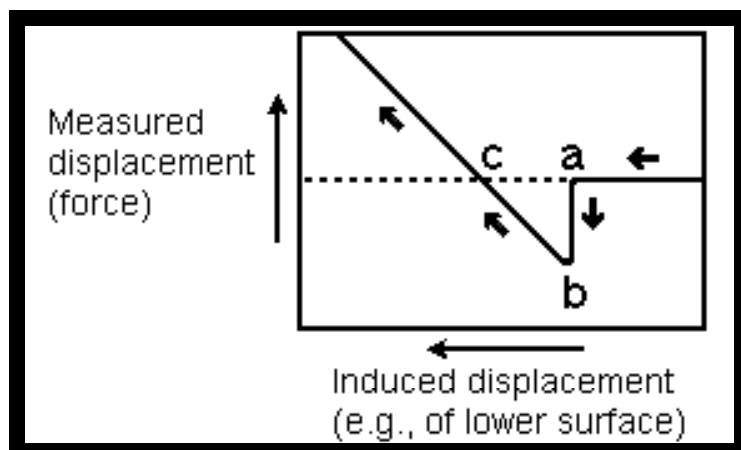
The AFM and SFA are quite different when it comes to force measurements. The AFM cannot measure true force-distance profiles. This may sound surprising because AFM data is often presented in exactly this way – as a plot of force *versus* distance. However, the “distance” in an AFM measurement is not what is normally meant by the “distance” in a force-distance plot: the former refers to the displacement of a spring far from the interaction zone and its deflection relative to a photo-sensing diode or strain gauge on the spring rather than to the opposing surface; the latter refers to the actual separation between two surfaces in the interaction zone. The SFA technique allows one to measure the force and, independently and unambiguously, the geometry and separation between two surfaces. The AFM technique uses the measured force to infer all three. This is elaborated in more detail below.

The AFM was originally designed as a microscope rather than a force-measuring instrument: it uses the force between a tip and a surface to obtain an image of the surface. However, it can also be used in reverse – to accurately measure an adhesive force, say, the force needed to detach a tip from a surface, but so long as the distance-dependence of the interaction is not required. To quantitatively measure a *force-law* or interaction potential (i.e., the force as a function of the surface separation), one has to be able to measure not only the force but also the geometry of the interacting surfaces and their absolute distance of separation. While the AFM can measure a force, it cannot independently measure the geometry nor the surface separation, that is, it cannot measure a true force-distance or energy-distance curve without making assumptions about the nature of the force and compliance of the surfaces. The AFM technique becomes more reliable at large separations, where the forces are weak, but again the surface separation is only known to within an unknown correction factor.

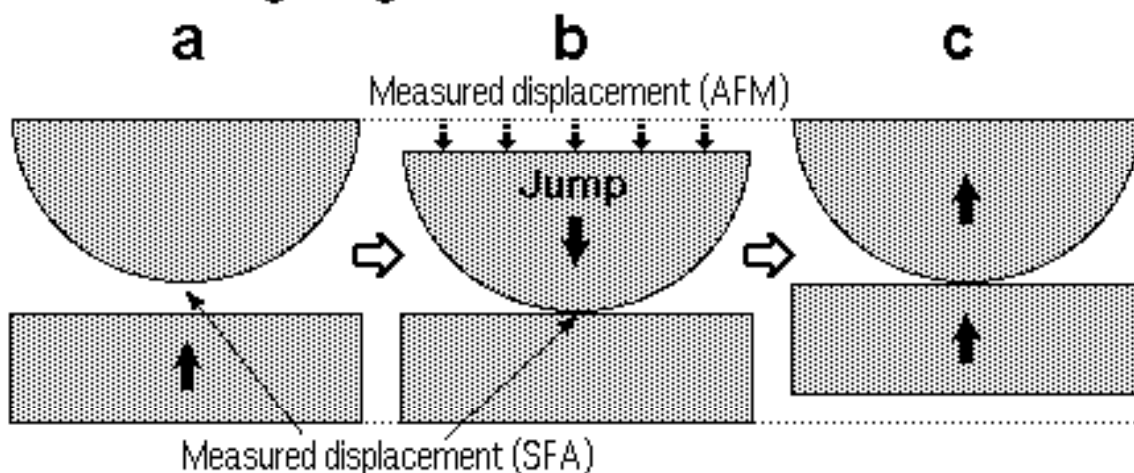
In contrast, the SFA (Surface Forces Apparatus) was designed right from the start to measure not only forces, but also the local surface geometry of the interacting surfaces and the exact separation between them. The SFA can do all this because the FECO optical interference technique used in the SFA measures the surface separation and surface shape profiles precisely at the point where the interaction occurs. The AFM, on the other hand, does not measure the absolute distance between the two interacting surfaces (the tip and a flat surface). Instead, it measures the displacement of a cantilever spring at some point away from the interaction zone, and there is no way of unambiguously telling whether a 10 Å deflection measured corresponds to a 10 Å displacement between the surfaces. It could be that the surfaces are already in contact but are elastically flattening under the influence of an attractive short-range adhesion force, in which case the measured 10 Å deflection corresponds to *zero* change in the surface separation, as illustrated in Figures 53A and B. Similar problems arise with capacitance measurements of surface separations. Furthermore, the local tip geometry in the interaction zone is never known in an AFM experiment, and since all elastic surfaces (especially soft organic, polymer and biological surfaces) generally deform during an interaction, this further complicates interpretation of the results.

Figure 53A.

Typical “spring deflection-displacement” curve measured by AFM when one surface is made to approach the other, which is interpreted as a “force-distance” curve. Figure 53B illustrates the ambiguity of this interpretation.



Case 1: Long-range attraction between two surfaces.



Case 2: Elastic deformations of two adhering surfaces.

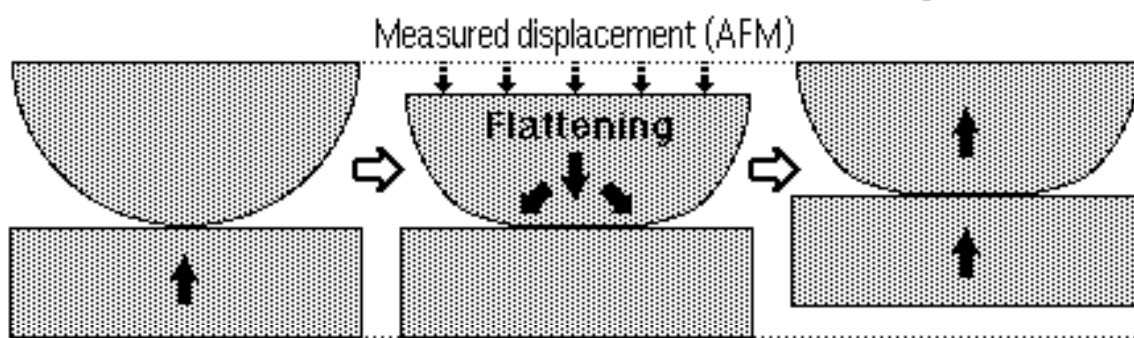


Figure 53B. Two very different interactions that nevertheless give the same “force-distance” curve (Fig. 53A) when measured by the AFM. In Case 1, a real long-range force causes the two surfaces to jump into contact ($a \rightarrow b$). In Case 2, the surfaces are already in contact when an apparent jump occurs. In Case 1, the distance between the two surfaces has changed during the jump, but in Case 2 it has not, yet the AFM method of measuring displacements will record indistinguishable force-distance curves for these two very different situations. On the other hand, the FECO optical technique will record the true change in surface separation during the jump (finite change in Case 1, no change in Case 2) and also give the exact change in shape and contact area of the two surfaces in Case 2.

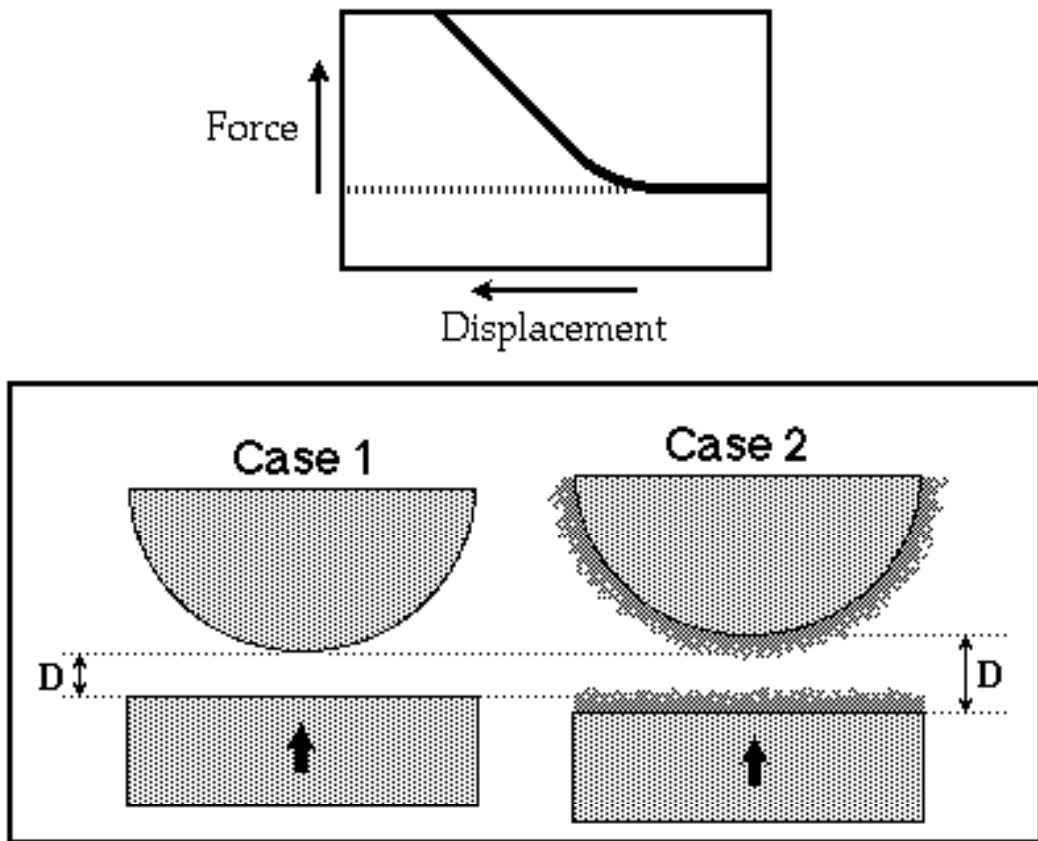


Figure 53C. This shows a different scenario where again the AFM will produce erroneous results. In this case, the recorded force vs distance between two surfaces (or a tip and a surface) in aqueous electrolyte solution may look like the one shown in the top of Figure 53C. Such a curve could be generated by an exponential electrostatic (double-layer) repulsion between two charged surfaces, but the same curve could arise from an adsorbed layer of polyelectrolyte polymer where the tail-end of the force is the same as the double-layer force, but where closer-in there is a sharp steric “hard-wall” repulsion. The AFM will not be able to distinguish between these two very different forces and will not show that there is a polymer layer of finite thickness on the surfaces (which could be a contaminant layer).

One more example illustrating the power of the FECO optical technique in SFA experiments concerns forces measured in sliding (or AFM scanning) experiments. Consider one surface moving laterally across a perfectly smooth surface that is chemically heterogeneous: for example, a surface with hydrophobic and hydrophilic groups at different positions. The AFM will not be able to distinguish a change in surface topography from a variation in the local intermolecular interactions. The resulting “image” could be interpreted either way, with no way of knowing which is correct. Again, SFA measurements of lateral forces can distinguish changes in surface separation from changes in both normal and lateral (friction or lubrication) forces.

Last, but by no means least, the SFA lets you know when you have a contaminant layer or unwanted particle between your two surfaces – the range and magnitude of the forces, together with the irregular surface deformations occurring on approach, clearly indicate when “something is wrong”.

A sophisticated research instrument for directly measuring static and dynamic forces between surfaces (inorganic, organic, metal, oxide, polymer, glasses, biological, etc.) and for studying interfacial and thin film phenomena at the molecular level. Modular design allows for expansion with numerous attachments and customized upgrades (see page 3).



The SFA 2000 Basic Unit with optics stand -
designed by Jacob Israelachvili

APPLICATIONS

Research areas and types of interactions that can be directly measured *

- Dispersion science – “colloidal” forces between surfaces in liquids and controlled vapors
- Adhesion science – long-range colloidal forces and short-range adhesion forces
- Surface chemistry – surface and electrochemical interactions between dissimilar materials
- Detergency, food research – forces between surfactant and lipid monolayers and bilayers
- Biomaterials and biosurfaces – forces between protein and polymer-coated surfaces
- Biomedical interactions – ligand-receptor, protein and model biomembrane interactions
- Tribology – friction, lubrication and wear of smooth or rough surfaces, thin film rheology
- Powder technology – capillary effects and surface deformations during interactions
- Materials research – mechanical and failure properties of metal and oxide surfaces and films

* This list is not exhaustive; contact us for your specific needs (see back Page).

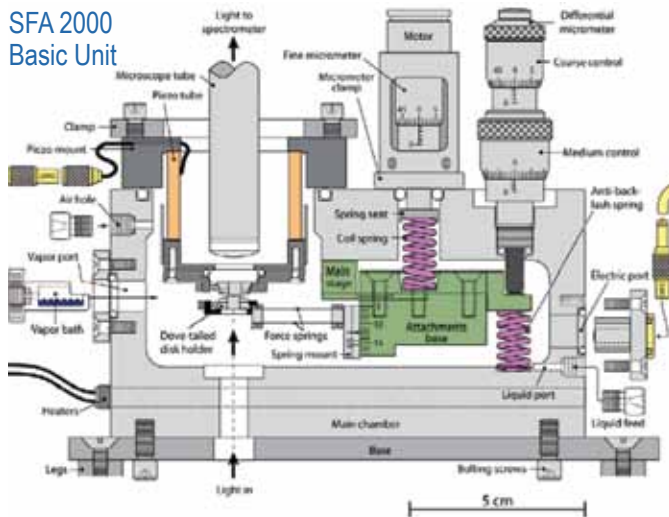
GENERAL DESCRIPTION

The SFA measures forces between two smooth surfaces in vapors or liquids with a sensitivity of a few nN and a distance resolution of 1Å (0.1 nm). It can also measure the refractive index of the medium between the surfaces, adsorption isotherms, capillary condensation, surface deformations arising from surface forces, dynamic interactions such as viscoelastic and frictional forces, thin film rheology, and other time-dependent phenomena in real time at the molecular (nano-) scale. The molecularly smooth surfaces of hard materials such as mica, silica, sapphire, polymers, serve as suitable substrate surfaces in most measurements; these can also be coated with thick or thin layers of surfactants, lipids, polymers, metals, metal oxides, proteins and other biomolecules.

HOW IT WORKS

The figure below is a schematic drawing of the SFA 2000 ready for use. The shapes of the interacting surfaces, the absolute separation between them, and the thickness of any adsorbed layer on the surfaces, are measured (to within 0.1 nm) by analyzing the optical interference fringes (known as FECO fringes) produced when white light passes through the two surfaces. The distance between the surfaces is controlled by a four-stage mechanism of increasing sensitivity from millimeters to ångstroms. The stiffness of the force-measuring springs can be adjusted during experiments to enable forces of greatly differing magnitudes to be measured. Dynamic measurements are conducted with surfaces in motion (vertically, horizontally, or in any direction in 3D space) using one of the attachments described in the following pages.

SFA 2000
Basic Unit



SFA Control Box



USES

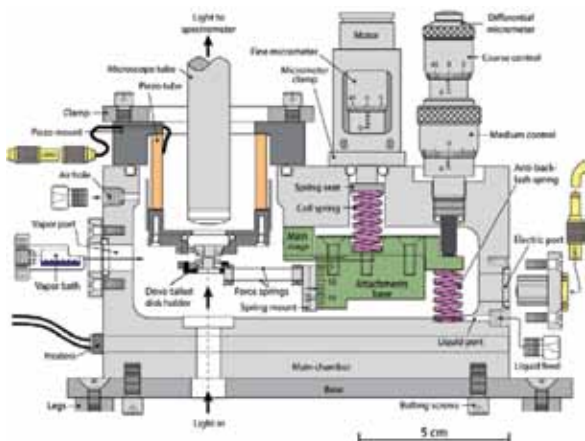
The SFA technique is routinely used to characterize and quantify various types of interactions between surfaces in liquids and vapors (see references on page 4). Static interactions include van der Waals and electrostatic forces, forces due to solvent structure (solvation and hydration forces), capillary forces, hydrophobic interactions, polymer-mediated steric and depletion forces, surfactant monolayers and lipid bilayers, adhesion and bio-specific “lock-and-key” type binding interactions. Dynamic and time-dependent interactions include the viscosity of liquids in ultra-thin films (nano-rheology), slow relaxations of liquids, and polymers in confined geometries, and surface deformations during the approach, separation and lateral sliding of two surfaces. More recent applications have included food technology, the friction of clutches, how geckos run on walls and ceilings, the bioadhesion of mussels, and the biolubrication of joints.

MAIN FEATURES AND ATTACHMENTS

For anyone who wants to accurately measure the forces or any type of “interaction” between two material surfaces at any given separation in air, vapor or liquid, including their local geometry (shape) and deformations, the SFA 2000 stands unrivalled as to directness of measurement and visualization, unambiguous (sub-ångstrom) accuracy, and stability to thermal drift. Unlike some surface force-measuring instruments, such as scanning probe microscopes and pin-on-disk tribometers, the SFA 2000, especially when used with FECO optics, measures forces between surfaces at precisely known surface separations, providing the local surface geometry (shape), directly at the point of interaction. A number of facilities that appeared as accessories in earlier models (such as the SFA 3) are now part of the SFA 2000, and new attachments allow for various dynamic measurements to be made, for example, of friction, lubrication and viscoelastic forces over a large range of speeds or shear rates. Four of these new facilities are illustrated below:

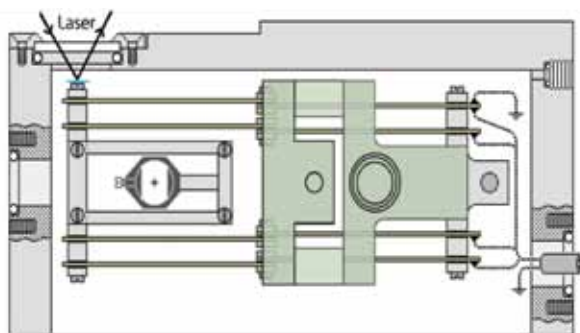
FRICTION DEVICE ASSEMBLY

For friction and lubrication studies



PIEZOELECTRIC BIMORPH SLIDER

For high-speed shearing of thin films



BIMORPH VIBRATOR

For measuring thin-film viscosity



UNDER-WATER MOUNTS

For biological (e.g., protein) surfaces



OTHER CUSTOMIZED ATTACHMENTS INCLUDE:

- (1) Variable stiffness force-measuring spring.
- (2) Constant force-measuring balance (patented).
- (3) Attachments for moving and detecting forces in 3D (patented).
- (4) High-speed friction attachment (pin-on-disk type).
- (5) Attachments for applying electric or magnetic fields.
- (6) In situ fluorescence & FRAP measurements (FL-SFA).
- (7) Attachment for electrochemical studies (the EC-SFA).

THE SFA AND FECO OPTICAL TECHNIQUE

Recent advances in the surface forces apparatus (SFA) technique. J Israelachvili, Y Min, M Akbulut, A Alig, G Carver, W Greene, K Kristiansen, E Meyer, N Pesika, K Rosenberg and H Zeng, *Reports on Progress in Physics* (2010) 73 1-16.

Adhesion and Short-Range Forces Between Surfaces: New Apparatus for Surface Force Measurements [the SFA 3]. J. N. Israelachvili and P. M. McGuiggan, *J. Mater. Res.* (1990) 5 2223.

The extended surface forces apparatus. Part III. High-speed interferometric distance measurement. Zäch, M., J. Vanicek, and M. Heuberger, *Review of Scientific Instruments* (2003) 74 (1) 260-266.

Extending the surface force apparatus capabilities by using white light interferometry in reflection. Connor, J. N. and R.G. Horn, *Review of Scientific Instruments* (2003) 74 (11) 4601-4606.

Topographic information from multiple beam interferometry in the Surface Forces Apparatus. M. Heuberger, G. Luengo, J. Israelachvili, *Langmuir* (1997) 13 3839-3848.

High Speed Friction Measurements Using a Modified Surface Forces Apparatus. D. D. Lowrey, K. Tasaka, J. H. Kindt, X. Banquy, N. Belman, Y. Min, N. S. Pesida, G. Mordukhovich, J. N. Israelachvili. *Tribology Letters* (2011) 42 117-127.

COLLOIDAL, POLYMER AND ADHESION INTERACTIONS

Intermolecular and Surface Forces (3rd Ed). J. Israelachvili, *Elsevier & Academic Press*, 2010.

Direct measurement of depletion attraction and thin-film viscosity between lipid bilayers in aqueous polyethylene oxide solutions. T. L. Kuhl, A. D. Berman, S. W. Hui, J. N. Israelachvili, *Macromolecules* (1998) 31 8250-8257.

Debye length and double-layer forces in polyelectrolyte solutions. Rafi Tadmor, Ernesto Hernandez-Zapata, Nianhuan Chen, Phil Pincus, Jacob Israelachvili. *Macromolecules* (2002) 35 (6) 2380-2388.

Evaporation and instabilities of microscopic capillary bridges. N. Maeda et al. *PNAS* (2003) 100 (3) 803-808.

Transient Interfacial Patterns and Instabilities Associated with Liquid Film Adhesion and Spreading. Hongbo Zeng, Yu Tian, Matthew Tirrell, Jacob Israelachvili. *Langmuir* (2007) 23 6126-6135.

Role of electrochemical reactions in Pressure Solution. George W. Greene, Kai Kristiansen, Emily E. Meyer, James R. Boles and Jacob N. Israelachvili, *Geochimica et Cosmochimica Acta* (2009) 73 2862-2874.

BIOLOGICAL AND BIOMEDICAL INTERACTIONS

Design Rules for Biomolecular Adhesion: Lessons from Force Measurements. Deborah Leckband, *Annu. Rev. Chem. Biomol. Eng.* (2010) 1, 365-389.

Intermolecular forces in biology. Deborah Leckband, Jacob Israelachvili. *Quart. Revs. Biophys.* (2001) 34 (2) 105-267.

Direct Measurement of a Tethered Ligand-Receptor Interaction Potential. J.Y. Wong et al., *Science* (1997) 275 820-822.

Direct measurements of multiple adhesive alignments and unbinding trajectories between cadherin extracellular domains. Sivasankar, S., B. Gumbiner, and D. Leckband, *Biophysical Journal* (2001) 80(4) 1758-1768.

Thin film morphology and tribology of food emulsions: a study of three mayonnaise samples. S. Giasson, J. Israelachvili, H. Yoshizawa, *J. Food Science* (1997) 62 640-652.

Thin film rheology and tribology of chocolate. G. Luengo et al., *J. Food Science* (1997) 62 767-812.

Impact of polymer tether length on multiple ligand-receptor bond formation. Claus Jeppesen, Joyce Y. Wong, Tonya L. Kuhl, Jacob N. Israelachvili, Nasreen Mullah, Samuel Zalipsky, Carlos M. Marques. *Science* (2001) 293 465-468.

Adsorption, Lubrication, and Wear of Lubricin on Model Surfaces: Polymer Brush-Like Behavior of a Glycoprotein. B. Zappone, M. Ruths, G. W. Greene, G. D. Jay, J. Israelachvili. *Biophysical Journal* (2007) 92 1693-1707.

Interaction forces and adhesion of supported myelin lipid bilayers modulated by myelin basic protein. Younjin Min, Kai Kristiansen, Joan M. Boggs, Cynthia Husted, Joseph A. Zasadzinski, Jacob Israelachvili. *PNAS* (2009) 106 3154-3159.

Force Amplification Response of Actin Filaments under Compression. George W. Greene, Travers H. Anderson, Hongbo Zeng, Bruno Zappone, Jacob N. Israelachvili. *PNAS* (2009) 106 (2) 445-449.

Adaptive mechanically controlled lubrication mechanism in articular joints. W. Greene et al., *PNAS* (2011) 108 5255.

DYNAMIC, RHEOLOGICAL AND TRIBOLOGICAL INTERACTIONS

Surface Forces and Nanorheology of Molecularly Thin Films. Marina Ruths and Jacob N. Israelachvili, in *Handbook of Nanotechnology*, 3rd edition, Chapter 29, B. Bhushan, Ed., *Springer-Verlag*. (2010) 857-922.

Surface Forces and Viscosity of Water Measured Between Silica Sheets. R.G Horn et al., *Chem Phys Lett* (1989) 162 404.

Thin film rheology and tribology of confined polymer melts: contrasts with bulk properties. G. Luengo, et al., *Macromolecules* (1997) 30 2482-2494.

Triboelectrification between smooth metal surfaces coated with self-assembled monolayers (SAMs). Akbulut, M., A.R.G. Alig, and J. Israelachvili, *Journal of Physical Chemistry B* (2006) 110(44) 22271-22278.

Friction and tribochemical reactions occurring at shearing interfaces of nanothin silver films on various substrates. Akbulut, Limit cycles in dynamic adhesion and friction processes: a discussion. H. Zeng et al., *J. Adhesion* (2006) 82 933-943.

DIFFERENT SURFACES (MATERIALS) AND INTERFACING WITH OTHER TECHNIQUES

The x-ray surface forces apparatus for simultaneous x-ray diffraction and direct normal and lateral force measurements. Y. Golan et al., *Rev. Sci. Instr.* (2002) 73 (6) 2486-2488.

Interactions of Silica Surfaces. G. Vigil et al., *J. Colloid Interface Sci.* (1994) 165 367.

Contact Electrification and Adhesion between Dissimilar Materials. R.G. Horn and D.T. Smith, *Science* (1992) 256 362.

3D Force and Displacement Sensor for SFA and AFM measurements. Kai Kristiansen, Patricia McGuiggan, Greg Carver, Carl Meinhart, Jacob Israelachvili, *Langmuir* (2008); 24(4); 1541-1549.

Recent advances in the surface forces apparatus (SFA) technique

J Israelachvili¹, Y Min¹, M Akbulut², A Alig¹, G Carver¹, W Greene¹, K Kristiansen¹, E Meyer¹, N Pesika³, K Rosenberg⁴ and H Zeng^{1,5}

¹ Department of Chemical Engineering, University of California Santa Barbara, Santa Barbara, CA 93106, USA

² Artie McFerrin Department of Chemical Engineering, Texas A&M University, 3122 TAMU College Station, TX 77843, USA

³ Department of Chemical and Biomolecular Engineering, Tulane University, New Orleans LA 70118, USA

⁴ Department of Materials, ETH Zurich, Switzerland

⁵ Department of Chemical and Materials Engineering, University of Alberta, Edmonton, Alberta, Canada

E-mail: Jacob@engineering.ucsb.edu and ymin@engineering.ucsb.edu

Received 5 August 2009, in final form 6 November 2009

Published 27 January 2010

Online at stacks.iop.org/RoPP/73/036601

Abstract

The surface forces apparatus (SFA) has been used for many years to measure the physical forces between surfaces, such as van der Waals (including Casimir) and electrostatic forces in vapors and liquids, adhesion and capillary forces, forces due to surface and liquid structure (e.g. solvation and hydration forces), polymer, steric and hydrophobic interactions, bio-specific interactions as well as friction and lubrication forces. Here we describe recent developments in the SFA technique, specifically the SFA 2000, its simplicity of operation and its extension into new areas of measurement of both static and dynamic forces as well as both normal and lateral (shear and friction) forces. The main reason for the greater simplicity of the SFA 2000 is that it operates on one central simple-cantilever spring to generate both coarse and fine motions over a total range of seven orders of magnitude (from millimeters to ångstroms). In addition, the SFA 2000 is more spacious and modulated so that new attachments and extra parts can easily be fitted for performing more extended types of experiments (e.g. extended strain friction experiments and higher rate dynamic experiments) as well as traditionally non-SFA type experiments (e.g. scanning probe microscopy and atomic force microscopy) and for studying different types of systems.

(Some figures in this article are in colour only in the electronic version)

Contents

1. Introduction	2	<i>2.4. High-speed attachment</i>	9
1.1. Before the surface forces apparatus (SFA)	2	<i>2.5. 3D displacement and force sensing probe attachment</i>	10
1.2. Early versions of the SFA	2	<i>2.6. Bimorph vibrator attachment</i>	10
1.3. Some limitations of the existing SFAs	3	<i>2.7. Variable normal force-measuring springs</i>	12
2. SFA 2000	3	<i>2.8. Constant-force (balance) attachment</i>	13
2.1. The basic unit for normal and adhesion force measurements	3	3. Concluding remarks	14
2.2. Measuring shear (friction and lubrication) forces	6	Acknowledgments	14
2.3. Measuring forces in three orthogonal directions (3D or XYZ attachments)	8	Appendix A. Multiple beam interferometry	14
		References	15

1. Introduction

1.1. Before the surface forces apparatus (SFA)

In 1952, Overbeek and Spaarnay were able to measure long-range attractive forces between highly polished glass and quartz plates, but measurements at small distances ($<20\text{ nm}$) were difficult due to dust particles or surface roughness [1]. Distances between the surfaces were determined using Newton interference colors and the forces were determined by measuring the bending of a stiff spring that one surface was mounted on. In 1964, Derjaguin and co-workers used two crossed polarized metal wires (Pt pairs or Au pairs) to measure the potential barrier between the wires in electrolyte solutions [2]. They found that a repulsive force of non-electrostatic origin existed between the surfaces at high electrolyte concentrations and they were able to calculate the Hamaker's constant for the molecular attraction of metallic filaments in water.

1.2. Early versions of the SFA

In 1969, Tabor and Winterton described the first apparatus where forces between surfaces could be measured for separations as low as 5–30 nm with a 3 Å distance resolution [3]. In this apparatus they used the method of multiple beam interferometry (MBI) for the first time to measure jump distances between molecularly smooth surfaces of mica in air to determine normal and retarded van der Waals forces. In this ‘jump method’, one surface is held by a spring, while the movement of the other surface can be controlled by using a piezoelectric transducer. Israelachvili and Tabor then extended this method by using the ‘jump method’ to measure forces in the range from 1.5 to 20 nm, and also used what they called the ‘resonance method’ in the range from 10 to 130 nm [4]. In the resonance method, the surfaces were held in a low pressure vapor environment. One surface was vibrated at a known frequency while the oscillations due to the van der Waals forces on the opposite surface were measured with a piezoelectric bimorph strain gauge. At this time they also showed the usefulness of the method for measuring forces in air between monolayers deposited on mica surfaces.

1.2.1. SFA Mk I. A new apparatus, later dubbed the Mark I, was described by Israelachvili and Adams as a way to measure the forces between surfaces immersed in liquids [5]. In this apparatus the mica surfaces were moved toward and apart from each other using a motor-driven micrometer and a piezoelectric crystal resulting in a range of control from the micrometer to the ångstrom level. As with the earlier versions, the distance between the surfaces was determined using MBI and the forces between the surfaces were measured by mounting the lower surface on a cantilever spring with a known spring constant.

1.2.2. SFA Mk II. The Mark II was developed as an improved version of the Mk I with extra attachments to enable more interfacial phenomena to be studied [6, 7]. Some of the improvements to the Mk II over the Mk I included a double-cantilever spring for increased strength which also prevented

the surfaces from rotating as normal forces were applied. A significant attachment that was added to the Mk II was the ‘friction device’ which allowed the upper surface to be moved in the lateral direction using a motor-driven micrometer while the frictional forces were measured with strain gauges located on springs attached to the upper surface.

1.2.3. SFA Mk III. As the SFA continued to be used for increasingly complex systems, it was found that the Mk II needed to be improved. It needed to be more stable to thermal drifts, have a stiffer spring or a variable stiffness spring, have a more linear and larger range of motion and it needed to be easier to clean. The Mk III was developed and tested during the period 1985–1989 and then described by Israelachvili and McGuigan [8]. In this new version the apparatus was made more compact than previous versions, which was better in systems where the surfaces needed to be completely immersed in liquids. In the Mk III, the control mechanism of the surfaces was confined to an upper chamber which was sealed by Teflon bellows from the lower chamber in which the surfaces and bathing solutions were kept. Thus, the ‘distance control chamber’ was less likely to degrade due to materials used in various experiments. The control chamber held a complex translation assembly that was very stable and linear. Also, the range of the distance control was extended to cover the ångstrom to the millimeter range using four levels of control (see table 1). As with all SFAs, the distance between the surfaces was measured using MBI.

As the SFA became increasingly used for measuring friction, a new attachment was developed for the Mk III which was called the bimorph slider [9]. This attachment will be described in more detail below in reference to the SFA 2000.

1.2.4. Other versions of the SFA. The SFA technique was also extended by other research groups. A significant advance was the introduction of the ‘SFA Mark PI’ for measuring very weak, long-ranged interactions (F/R down to $\mu\text{N m}^{-1}$) between charged surfaces employing a magnetic drive mechanism [13]. In this apparatus, one of the surfaces is driven by two nanomover microstepping motors linked by a differential spring mechanism and the other surface is suspended by a weak cantilever spring connected to a permanent magnet which is driven by passing a current through an external coil.

Parker *et al* [10] developed an apparatus based on the Mk I with a cylindrically shaped chamber and a single seal on top which was later called the Mk IV. The goal of this device was to perform as well as the Mk I but at the same time be simpler to produce, clean and use. The main changes compared with the Mk I are the use of a flexure hinge device as the differential spring instead of a leaf spring and the use of a diaphragm to seal off the mechanical mechanism instead of O-rings. Klein [11, 12] developed a version that was somewhat simpler than the Mk II at the expense of control of the surfaces. Klein was more concerned about the difficulties in removing adsorbed materials from the surfaces of the liquid-containing chamber and tried to focus on minimizing the number of components that would come into contact with the experimental bathing

Table 1. SFA 2000 distance controls and their specifications.

Level of control	Type of control	Surface moved	Positional accuracy (\AA)	Total range of movement (μm)
Coarse	Differential micrometer	Lower	2000	2000 (2 mm)
Medium	Differential micrometer	Lower	500	200
Fine	Differential spring mechanism	Lower	2	10
Extra fine	Piezoelectric tube	Upper	<1	1

solutions. His solution chamber was made of glass which could easily be cleaned overnight in sulphachromic acid.

Tonck and co-workers [14] developed an apparatus where they are able to simultaneously measure the forces and rheological properties of liquid films between opaque surfaces. They used one capacitance displacement transducer, C_1 , to measure the displacement between a flat surface and the base of the force-measuring cantilever spring and one, C_2 , to measure the displacement between the flat surface and the spherical surface at the end of the cantilever spring. Below separations of about 5 nm the roughness of their alumina surfaces began to affect the measured forces between the surfaces.

Sonntag and co-workers [15] developed an apparatus similar to Derjaguin's [2] where they measured the forces between two crossed quartz filaments. In their apparatus, one filament was attached to a micrometer screw and a piezoelectric column with movement control of about 1 nm. The other filament was attached to a transducer that was used to measure the forces between the two filaments.

Heuberger and co-workers [16, 17] have developed what they call the 'extended surface forces apparatus' (eSFA) which takes advantage of fast spectral correlation interferometry for a fast and precise analysis of the interference spectra that give the distance between and shapes of the surfaces, as well as the refractive index of the material between them (or deposited on them). Their method also includes remote control of the SFA.

1.3. Some limitations of the existing SFAs

While the Mk III is an extremely stable and functional apparatus, there are a few drawbacks which are addressed in the design of the SFA 2000. These drawbacks and their causes are listed below.

- (1) The two parts which make up the main translation stage are very difficult to machine and have very little tolerance. The stringent tolerance is important for maintaining the perfectly vertical and linear motion of the lower surface.
- (2) There are many parts in the Mk III due to the design of the sealed translation stage. This makes it more difficult to fully assemble the apparatus to perform experiments.
- (3) The Mk III has very little room for adding new attachments. While the small volume of the chamber is handy for experiments where the apparatus must be filled with a liquid, it does not allow for the easy addition of extra parts.

The SFA 2000 was designed to address these drawbacks and will be described below.

2. SFA 2000

The concepts behind the operation of the SFA 2000 are similar to the Mk II and III, but the 2000 apparatus is designed to have fewer parts and to be easier to produce, assemble, clean and operate, as well as to be able to accept numerous attachments while still performing as well as the previous versions. Although the SFA 2000 is described here for the first time, it has already been utilized for studying various types of tribological (including both dry and lubricated) and rheological systems [18] and materials such as nanoparticles [19–21], polymers [22], hydrocarbons [23, 24], polysaccharides [25], biological materials [26, 27], self-assembled monolayers [28], dye molecules [29, 30] and metal thin films [31].

2.1. The basic unit for normal and adhesion force measurements

The main improvement of the SFA 2000 is the use of one central single-cantilever spring which is used for generating both coarse and fine motions over a total range of seven orders of magnitude (from millimeters to ångstroms). A schematic of the basic SFA 2000 is shown in figure 1. The main components are the micrometers, the main stage containing the central single-cantilever spring, the lower disk holder and the upper disk holder.

There are four main controls for the distance between the surfaces. The controls and their specifications are listed in table 1. Three move the lower surface and one moves the upper surface. The coarse and medium controls are manipulated by hand using the differential micrometer. The fine control is manipulated by using a motor which drives a fine micrometer which then acts against a helical 'coil' spring. The extra-fine control is manipulated by changing the voltage across the inner and outer walls of a piezoelectric tube that supports the upper surface. More specific details of the ways the surfaces move in response to the distance controls is covered in the following text.

The stainless steel main stage, shown in figures 1 and 3, contains a single-cantilever spring that allows for two kinds of pivoting motions about the point P (figure 3). When a normal force acts on the end of the spring (pivot point B) using the coarse and medium control differential micrometer, the spring deflects in the 'bending mode': the spring bends at point P (pivot point A) and the lower surface moves by approximately the same distance upward that the micrometer shaft moves downward. More specifically it will move by ($L \tan \theta \approx L\theta$), where $L \approx 4 \text{ cm}$ is the horizontal distance between pivot points A and B, which is the same as the distance between pivot point A and the surfaces.

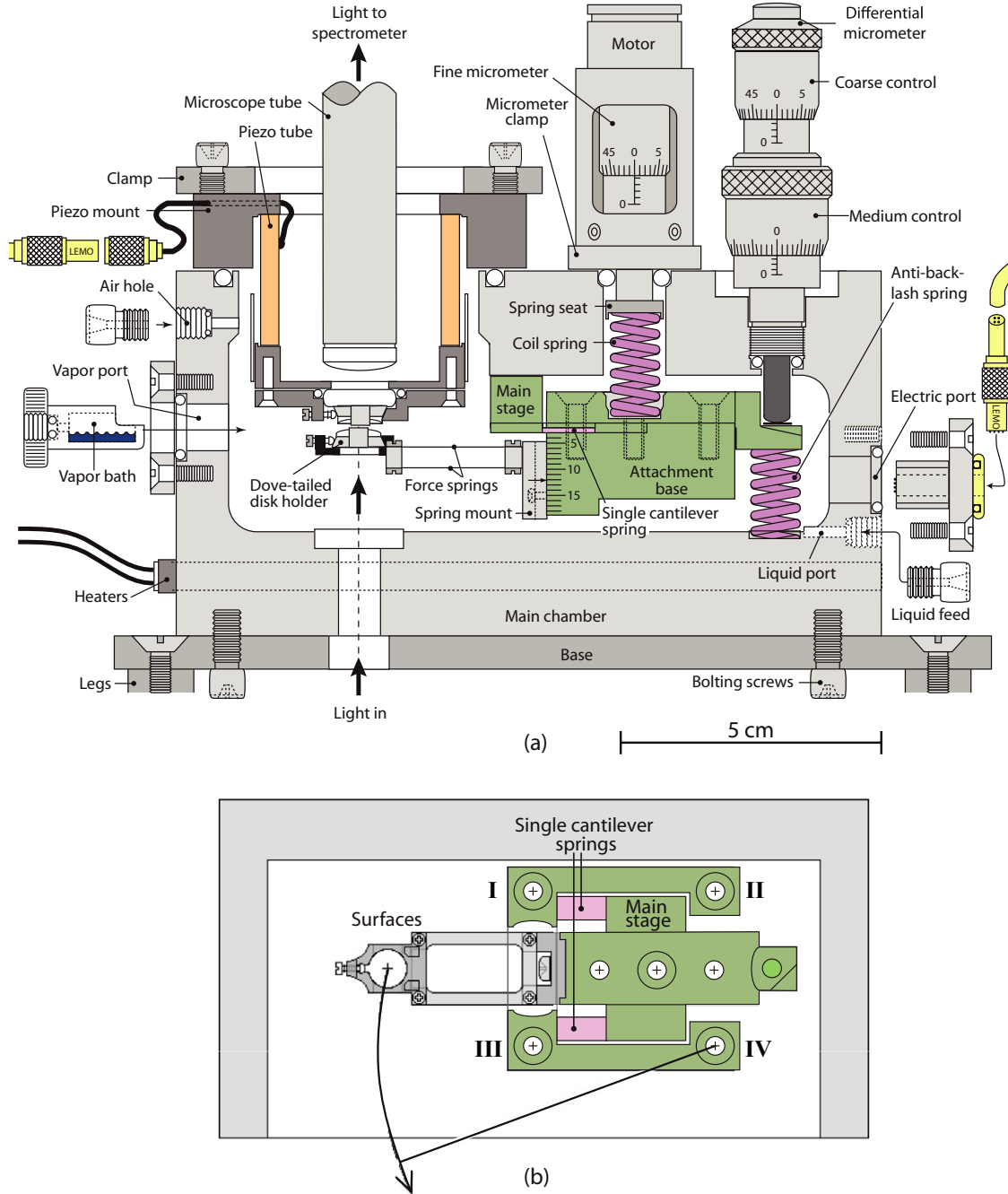


Figure 1. (a) The SFA 2000 for measuring forces between two molecularly smooth surfaces. The figure shows a section through the center of the apparatus. Four different distance control mechanisms are shown and listed in table 1: coarse micrometer, medium micrometer, fine micrometer and extra-fine (piezoelectric tube) control. A new ‘universal disk mount’ has been designed for use with both the upper and lower disks. These new disk supports can accommodate both cylindrical disks and a new type of rectangular dove-tailed disk, shown here. The dove-tail disks can be mounted in the SFA 2000 with the main chamber filled with solution, making them ideal for the transfer of bilayer- or protein-coated surfaces into the apparatus without exposure to air. Teflon O-rings outside the main chamber are used to seal both the upper clamp and the front plate (not shown) when the screws for these components are tightened into place. The pivoting mechanism of the single-cantilever spring colored in light green is described in figure 3. (b) Top view of the main stage and lower disk holder. Removal of the motor, fine micrometer, coil spring and anti-backlash spring and screws I, II and III (which bolt the main stage to the upper chamber wall) allows for the main stage and attachment base (green) to be rotated anti clockwise about screw IV for easy access to the lower surface (dove-tailed disk holder). A photograph of the apparatus is shown in figure 2.

In contrast, the motor-controlled ‘fine control’ micrometer compresses a helical spring which presses against the top of the main stage. The far right part of the main stage remains in contact with the ‘coarse control’ micrometer while the cantilever spring buckles by a very small amount, ΔD ,

as shown in the figure. The tips of the fine micrometer and differential micrometer are precisely positioned in the horizontal center line that also passes through the single cantilever (the pivot point) and the surfaces, so that while the attachment does rotate, its motion at the surfaces is (almost)

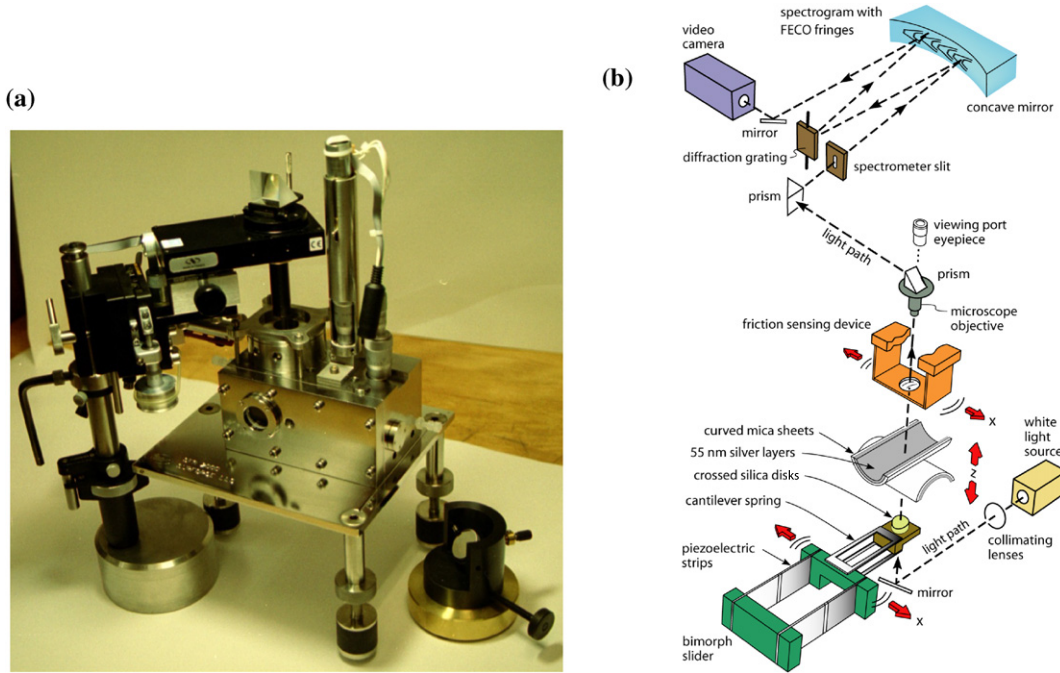


Figure 2. (a) Photograph of SFA 2000 with optics stand, closed and ready for experiments. The mirror, shown in the lower right, is normally placed below the entrance window for the light, as shown in (b). (b) Schematic of SFA setup showing the light path in a typical experiment (here shown with the bimorph slider attachment—section 2.2). The optical (FECO) fringes used to visualize the surfaces during experiments are described in appendix A.

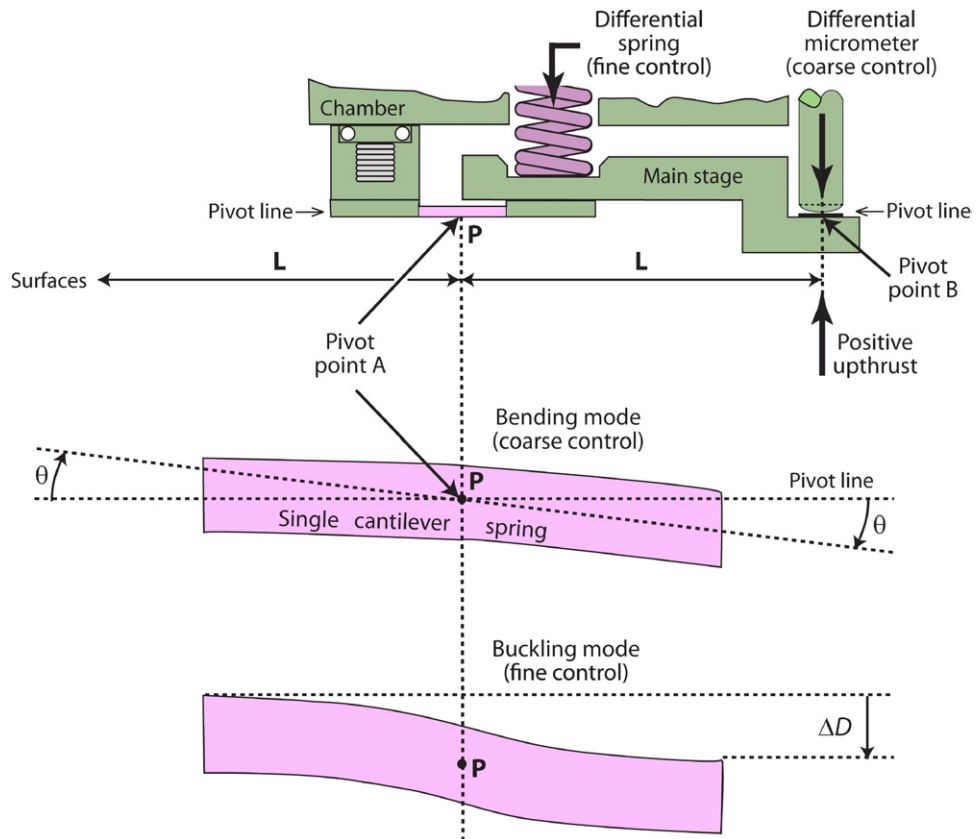


Figure 3. Schematic showing the main stage and the single-cantilever spring. When a force is applied by the coarse control micrometer the pivot point (**P**) is at the center of the cantilever which is in the bending mode. The surface moves by $L\theta$ where L is the distance between A and the surfaces. When the force is applied by the fine control, the pivot point is at point B and the cantilever is in the buckling mode. The surfaces move by $\sim 2\Delta D$ which is typically much smaller than $L\theta$.

perfectly vertical, thereby ensuring that the surfaces move normally to each other. Before each experiment the height of the spring mount is adjusted so that the lower disk is parallel to the upper disk at contact. The displacement, ΔD , is determined by the ratio of the stiffness of the helical spring to the spring constant of the cantilever spring and results in a displacement of the surfaces equal to $\sim 2\Delta D$. This ratio of spring stiffness is chosen so that the fine control is 1000 times more sensitive than the coarse control. The combination of the bending and buckling modes allows for a controlled range of motion from ångströms to millimeters. Strictly speaking the lower surface actually tilts a little when moving up in the bending mode, but this tilt can be minimized by positioning the surfaces to be parallel at contact.

The lower surface is connected to the attachments base under the main stage via a double-cantilever ‘force spring’. A double-cantilever spring is used to prevent the surface from twisting when a force is applied. The choice of the spring constant depends on the system being measured and the type of measurements desired. The larger the forces are expected to be, the stiffer the spring should be. For example, in a system where there are strong repulsive forces present, it would take a high force to bring the surfaces together. Since $F = k\Delta D$, the higher the spring constant, the smaller the ΔD needed to apply the necessary force.

Normal forces between the surfaces are measured by moving the surfaces at the base of the double-cantilever ‘force springs’ by a distance $\Delta D_{\text{applied}}$ using the differential micrometer, motor-driven fine micrometer and/or piezo tube. The actual distance that the surfaces move relative to each other, ΔD_{meas} , is measured by MBI. The changed force ΔF between the surfaces, when they come to rest at a separation D , is therefore

$$\Delta F(D) = k(\Delta D_{\text{applied}} - \Delta D_{\text{meas}}), \quad (1)$$

where k is the spring constant.

When $\partial F(D)/\partial D > k$, there is a mechanical instability and the lower surface will jump either toward or away from the upper surface to the next stable region during approach or separation, respectively. Thus, one can see that, while a weaker spring is more sensitive, it may also result in more inaccessible regions of a complex force profile because of the increased range between instabilities. However, the spring stiffness can be changed during experiments (see section 2.7) to build the full force profile.

Adhesion forces are measured from the force that it takes to separate surfaces from adhesive contact by measuring the distance that they jump apart from contact, ΔD_{jump} (figure 4), then using the following equation:

$$F_{\text{adhesion}} = k \times \Delta D_{\text{jump}}. \quad (2)$$

The spring constant, k , is measured (calibrated) before or after the experiment by placing small weights of mass, m , on the lower disk holder and measuring the displacement, Δd , of the spring using a graduated traveling microscope. The graduated traveling microscope is not part of the apparatus, but a separate microscope that is located outside the apparatus,

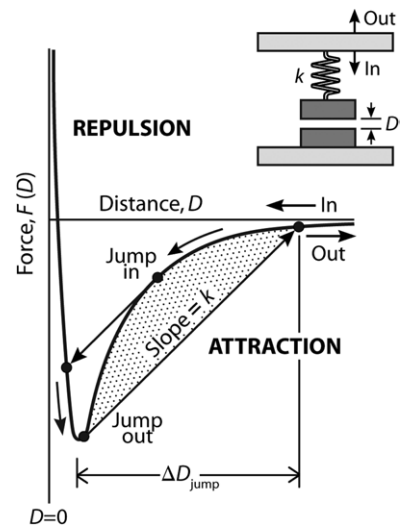


Figure 4. Typical force-law or force-distance profile $F(D)$ showing the instabilities that can occur at the positions shown, manifested by an inward jump on the way in (on approach) and an outward jump on the way out (on separation). Jump instabilities occur only if the effective spring constant k is lower than the maximum slope of the $F(D)$ curve. Thus, if the system is infinitely stiff ($k = \infty$) there will be no instabilities on approach or separation. No equilibrium is possible at surface separations between the jump in and jump out points.

for example, just outside the front window (figure 2). The spring constant is then given by $k = mg/d$ (N m^{-1}), where ‘ g ’ is the acceleration of gravity. The spring constant of the force-measuring spring, k , typically varies from 30 to $5 \times 10^5 \text{ N m}^{-1}$. The maximum stiffness that can be attained, by fully clamping the spring or using a rigid support, is approximately $1.5 \times 10^6 \text{ N m}^{-1}$.

The measured force between the curved cylindrically curved surfaces, normalized by their radius, $F_{\text{curved}}(D)/R$, is directly related to the interaction energy per unit area between two flat surfaces, W_{flat} , by the Derjaguin approximation [32].

$$W_{\text{flat}}(D) = \frac{F_{\text{curved}}(D)}{2\pi\sqrt{R_1 R_2}} = \frac{F_{\text{curved}}(D)}{2\pi R}, \quad (3)$$

when $R_1 = R_2 = R$.

2.2. Measuring shear (friction and lubrication) forces

The surfaces can be sheared past each other by using a motor-driven micrometer to move the upper surface in the lateral direction, or by using a piezoelectric bimorph slider, as shown in figure 5. The motorized friction device has a reversible dc motor, **M**, that can be switched on or off or driven in reverse at different constant or variable speeds using a dc power supply or function generator. At point **M** in figure 5(a) the motor presses against two parallel cantilever springs (double-cantilever spring configuration) which drives the friction device including the upper disk smoothly into or out of the paper with respect to the lower disk. When using a function generator, a square wave voltage function must be used to shear the upper surfaces back and forth at a constant velocity, $\pm V$. When using the piezoelectric bimorph slider,

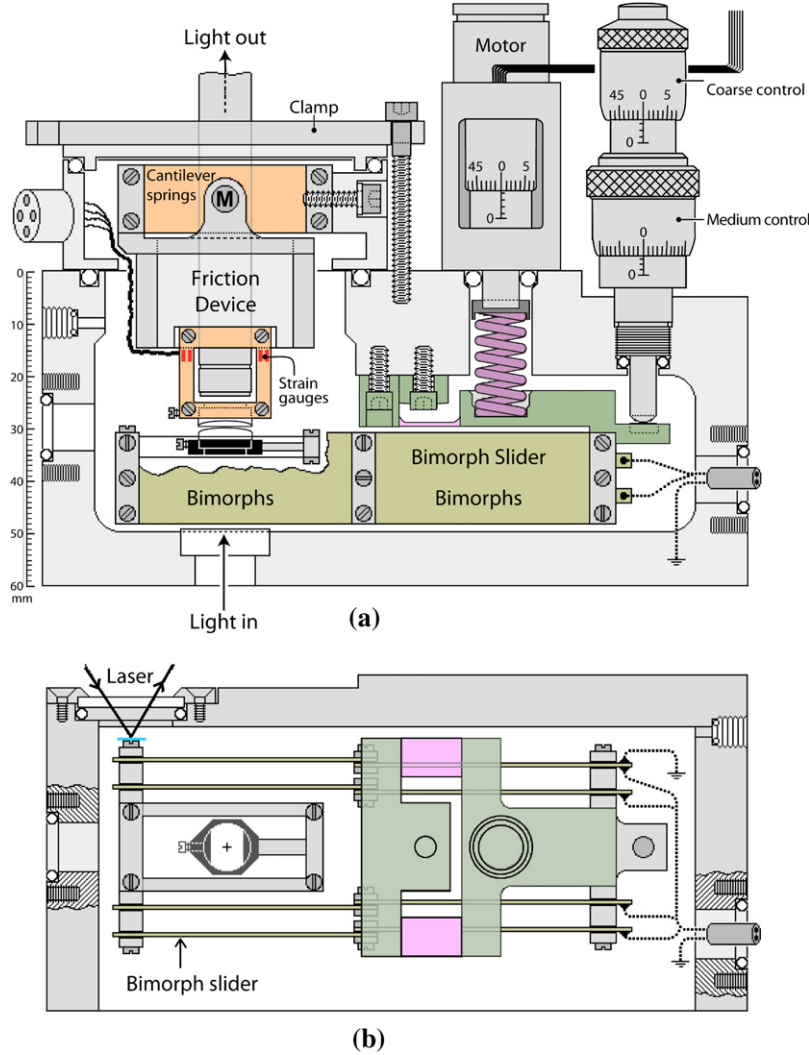


Figure 5. (a) Schematic showing the side view of the SFA 2000 with piezoelectric bimorph slider (bottom surface) and friction device attachment (top surface) and (b) showing the top view of the extended bimorph slider. Top left: optical laser displacement sensor (Keyence, LC-2420) for direct measurement of the lateral displacement of the bimorph slider or upper surface (used for calibrating displacements against the voltages applied to the bimorphs or motor **M**, respectively).

the bimorph plates bend in proportion to the voltage applied to them. Any thermal drift of the piezo-material of the bimorph is minimized in the same way as for the semi-conductive strain gauges by utilizing temperature-controlled experimental rooms and by the thermally well-sealed thick steel chamber walls all around the SFA 2000 (see below). Thus as a constantly increasing voltage is applied, the bimorph bends at a constant rate. To shear the surfaces back and forth at a constant velocity, a triangular wave function must be applied. The bimorphs are designed with a flexure point in the middle which causes the surfaces to displace linearly as voltages are applied.

When using the friction device or bimorph slider, two vertical double-cantilever springs with four semiconductor or resistance strain gauges are attached symmetrically to oppositely bending arms of the springs thus forming the four arms of a Wheatstone bridge strain gauge system. The resistance (foil) strain gauges were from Vishay Micro-Measurements (typically 350Ω gauges such as N2A-13-T028K-350); the semiconductor gauges were custom made temperature-compensated gauges from Micron Instruments,

Simi Valley, California (typically $350\text{--}500\Omega$ gauges, temperature compensation: $10\text{--}60^\circ\text{C}$). All semiconductor gauges have temperature-compensated resistors built into the circuit and adjusted/tested before being shipped. The experimental rooms are also temperature-controlled to $\pm 0.1\text{--}0.2^\circ\text{C}$ in addition to the SFA 2000 being thermally well-sealed by 12.5 mm thick steel walls all around. When a lateral force is applied to the upper surface the strain gauges are used to measure the deflection with a signal conditioning amplifier (Vishay Measurements, 2300), which outputs the signal to either a computer data acquisition system or a chart recorder.

The friction device springs can be calibrated at the end of the experiment by hanging small weights from both sides of the device. The voltage signal is then recorded and calibrated against the weight. The motions of the upper surface need to be calibrated against the voltage applied to the motor or the bimorphs as described in figure 5. When used *in situ* during experiments, the laser beam of the Keyence position detector is reflected off a small reflective silicon wafer piece attached to the end of the bimorph slider. When a triangular function

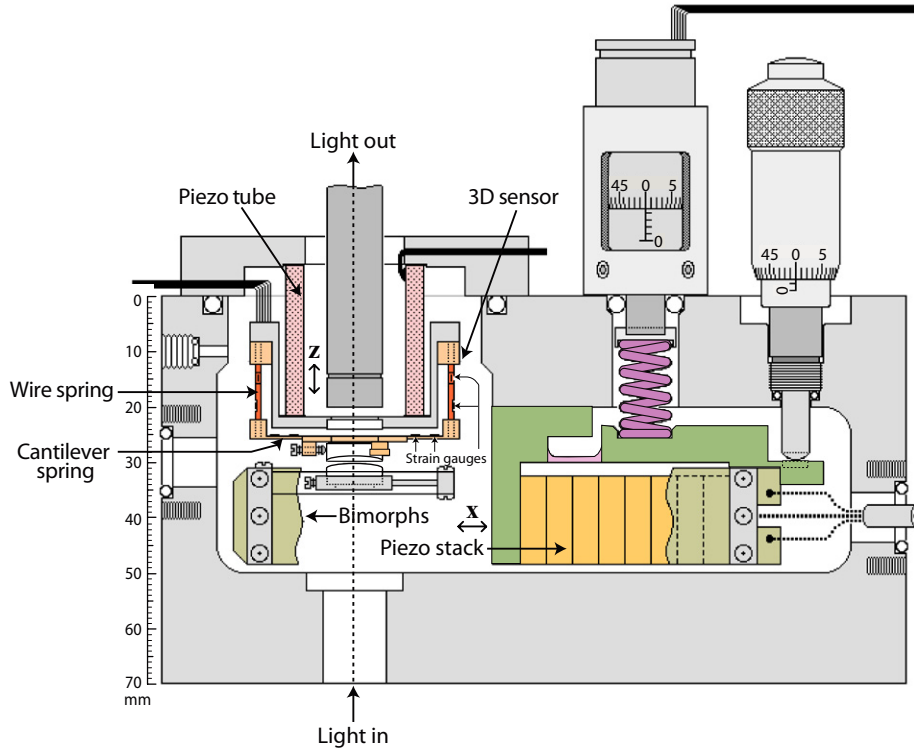


Figure 6. 3D/XYZ translation stages and sensors. A bimorph slider with an additional piezoelectric stack links parts for simultaneous X and Y translations of the lower surface in the horizontal plane. Translation in the vertical, Z-direction, is generated by the piezoelectric tube supporting the upper surface. The upper surface is suspended from four vertical wire springs and four horizontal cantilever springs, each mounted in a square/cross configuration, each with one or two strain gauges on them, allowing for deflections and hence the forces experienced by the upper surface to be measured in the X, Y and Z directions.

is applied to the bimorph slider, the displacement is measured. To calibrate the displacement of the upper motor, the friction device is held vertically *ex situ*, and a disk with a reflective piece attached to it is suspended from the upper disk mount spring. The displacement is then measured with the Keyence position detector as a function of the voltage applied to the motor.

The bimorph slider (figure 5(b)) operates in a similar fashion to previous bimorph sliders as described in [9], but has a longer range compared with previous ones due to the greater space of the SFA 2000, allowing for much longer bimorphs. Thus, for active bimorph of 50–75 mm, the lateral movement of the surfaces can be varied from about 5 to $10 \mu\text{m V}^{-1}$. However, since bimorphs become increasingly non-linear at voltages exceeding 40 V (when deviations from linearity begin to exceed 1%), the calibration of the bimorphs is recommended if the applied displacements are large and need to be known to high accuracy. Bimorphs can be also used in liquids or ‘under water’ after suitably coating their surfaces and all the wiring connections with a suitable HumisealTM or Polydimethylsiloxane (PDMS) coating. This usually increases their stiffness by 10–15% and reduces their sensitivity to movement by a similar amount. The coating (PDMS, SYLGARD[®] 184 Silicone elastomer curing agent) acts as an electrical insulator as well as a protective layer preventing exposure of the bimorph slider to potential harmful chemicals. Since PDMS is resistant to a wide range of liquids, including electrolytes, oils and certain solvents, the coated

friction slider extends the capabilities of SFA 2000 to measure friction forces under liquids. In addition, since PDMS has relatively low modulus, the maximum range of movement of the bimorph is not compromised.

2.3. Measuring forces in three orthogonal directions (3D or XYZ attachments)

A variety of XYZ translation stages (scanners) and detectors (scanners) shown in figures 6 and 7 allow for generating relative movement of surfaces, and independently measuring the resulting forces, in three orthogonal directions: X, Y and Z. Measurement of adhesion, friction and molecular ordering in three directions is made possible by moving one of the surfaces in some arbitrary direction in the X-Y plane and/or the upper surface in the $\pm Z$ -direction. Thus, circular or some other type of non-linear motion, i.e. other than back-and-forth motion, can be induced. Likewise, a force response on the upper surface along any spatial direction (not necessarily in the direction of the applied motion) can be simultaneously measured.

In figure 6, motion in the Z-direction of the upper surface is controlled by applying voltages across the inner and outer walls of the piezoelectric tube, with a linear range of $\sim 1 \mu\text{m}$. The lower surface is supported by a double-cantilever spring used for measuring the normal forces between the surfaces, and the spring is connected to an X-Y translation stage composed of a bimorph slider and a piezo stack. The expansion and contraction of the piezo stack under a certain voltage make the

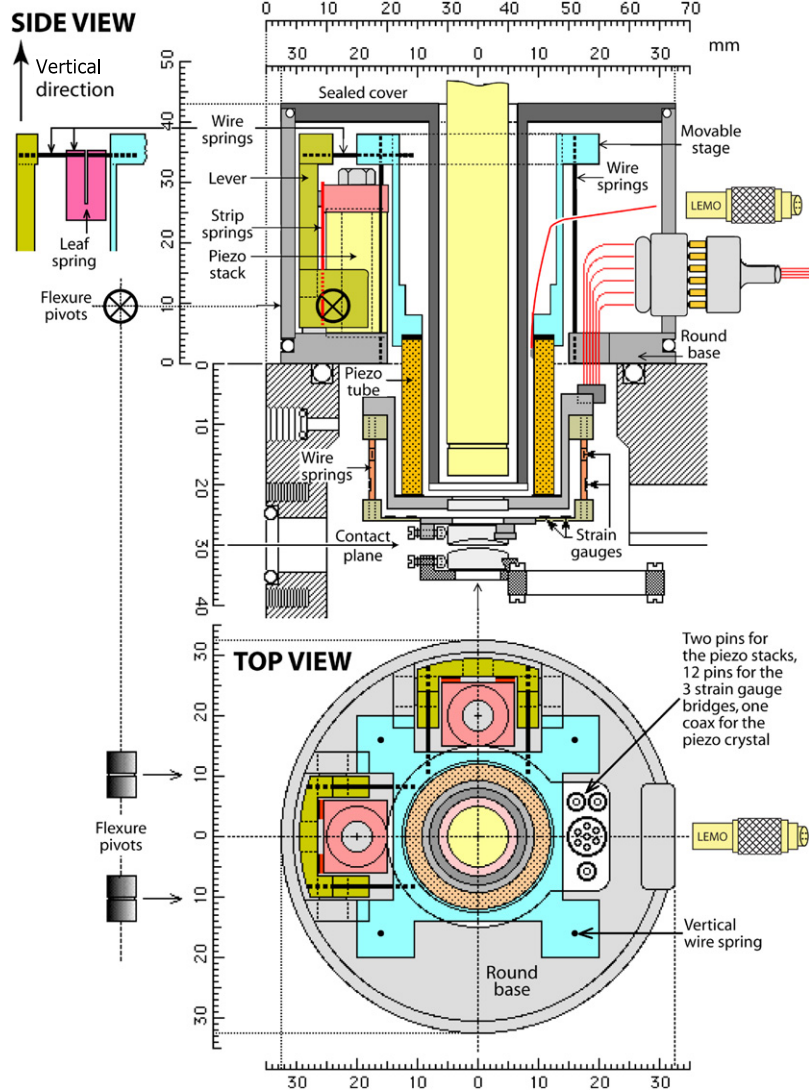


Figure 7. Single unit allowing for 3D translation and sensing. The upper surface is moved in the horizontal (X–Y) plane by two piezo stacks whose motion is amplified mechanically 10-fold by the vertical levers and frictionless cross-spring flexure pivots. Motion in the Z-directions and force sensing is as in figure 6. Mechanical amplification of the piezo-stack motion allows for large displacements using low voltages (50–100 V), where similar displacements of unamplified stacks require 500–1000 V which are invariably accompanied by large hysteresis. There are two places where four vertical wire springs (black and orange) act as the four legs of a square table, allowing for motion in any direction in the horizontal (X–Y) plane. The top springs (two shown in black) move the blue movable stage relative to the gray round base. The movable stage is further connected to two green driving levers (one in the X-direction and one in Y-direction) via horizontal wire springs (also in black). The pink leaf springs (see top left inset) attached to the horizontal wire springs are designed to minimize elastic restoring forces and cross-talk when the blue and green parts are displaced relative to each other, for example, into or out of the paper in the top left inset. The four vertical lower springs (orange) are similarly configured, as described in figure 6.

lower surface travel in the X-direction which is orthogonal to the bending direction of the bimorph slider in the Y-direction, with a maximum linear travel of at least 100 μm (0.1 mm). Non-linear motion in some arbitrary direction in the X–Y plane, e.g. circular or elliptical, can thus be accomplished by simultaneously applying signals at different voltages and phases to the bimorph slider and the piezo stack.

A 3D force sensor, supporting the upper surface in figure 6, can measure the force in any spatial direction. This 3D force sensor has been used successfully in various studies of thin film adhesion, friction and lubrication [33, 34].

Figure 7 describes a single, compact 3D force-measuring unit that is particularly suitable for measurements in liquids,

especially aqueous salt solutions, where contact of bimorphs or piezoelectric elements with such solutions is undesirable. However, it is possible to coat bimorph strips with a soft, chemically inert film of HumisealTM or PDMS that prevents chemical degradation and loss of electrical insulation for at least 24 h in 1 M NaCl solution (see section 2.2).

The XYZ translation stage of figure 7 can also be used as an atomic force microscopy (AFM) scanner, which is described in section 2.5 and figure 9.

2.4. High-speed attachment

The rotating high-speed disk attachment (figure 8) provides a much longer range and higher sliding speeds than previous

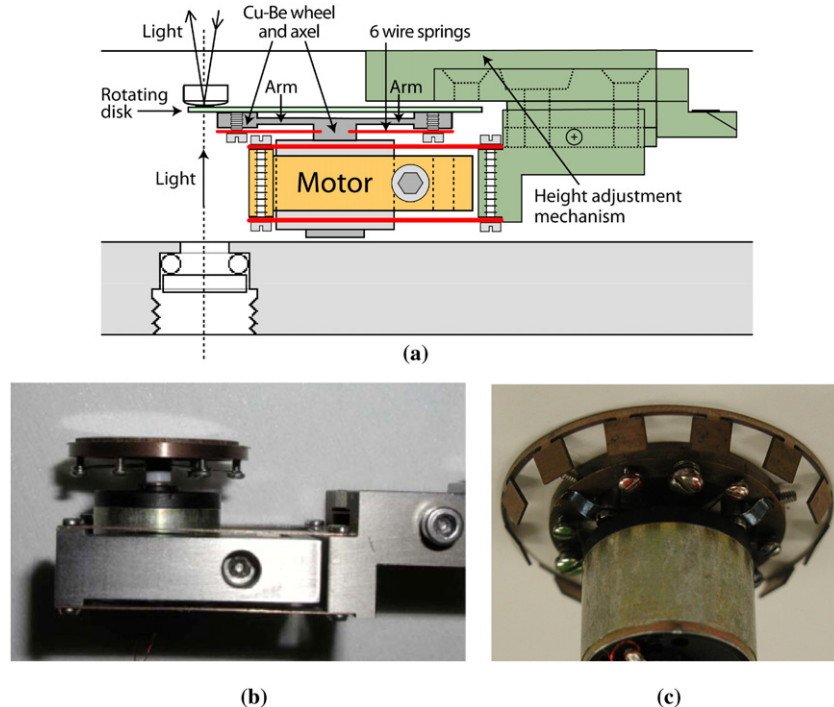


Figure 8. Different views of the rotating high-speed disk attachment to the SFA 2000 for making high-speed shearing measurements using a spherical top surface on a rotating flat mini-CD disk. (a) and (b): to adjust the level, the disk is mounted on a copper–beryllium (Cu–Be) ring or wheel that is held to the central shaft by highly stiff arms at 60° to each other. Below these are six wire springs, three of medium stiffness and three of low stiffness. By adjusting the six screws, one can adjust the angle of the disk, first coarsely then finely, to give a surface that rotates with only a few nanometers of wobble per rotation. (c) View of motor and rotating disk from below, showing the 12 mirrors used for measuring the rpm and nine screw heads: six for adjusting the tilt angles of the disk—three coarse and three fine and three for locating the disk on top of the copper–beryllium wheel. Three additional horizontal set screws protrude from the outer rim of the wheel for ensuring that the center of mass coincides with the axis of the motor shaft.

friction devices. When using this attachment, the lower flat surface is a transparent or opaque disk connected to a miniature dc motor (A2520, Maxon precision motors, inc., MA), allowing for sliding velocities up to around 15 m s^{-1} , i.e. about 6 orders of magnitude faster than current piezoelectric bimorph sliders. This attachment requires a sophisticated position and adjustment system for the rotating disk consisting of numerous adjustable springs and weights, shown in figure 8(b). When using an opaque surface as the bottom surface, a modification of the optical arrangement is required for observing the fringes of equal chromatic order (FECO) in reflected light rather than in transmitted light [35]. Using this method, reflection FECO appears as dark bands on a bright background as the result of destructive interference. The multi-matrix method (MMM) enables conversion of these wavelengths to separation distances [36].

2.5. 3D displacement and force sensing probe attachment

A miniature 3D displacement and force sensing attachment (figure 9) has been designed to measure forces in any spatial direction [33] suitable for both SFA and AFM measurements in the same experiment. Both the scanner and force sensor have been designed so as to minimize unwanted non-linear contributions of rotation, tilting and shear when a probe (tip) is pressed or scanned across the opposing surface, and the sensor springs deflect. This attachment therefore offers the ability to

scan and measure the forces on a probe tip in three orthogonal directions, linearly and simultaneously [33]. The sensitivity of the cantilever foil springs (strain gauges) can be readily varied by *in situ* adjustment of the tensions on the foils. Our mesoscale prototype has been optimized for equal sensitivities in all three directions, and can measure distance deflections as low as 5 nm. The spring constant of this prototype usually is between 100 and 1000 N m^{-1} . A finite element modeling and linear beam theory show that a micro-scale device should function with similar characteristics to current AFM probes [33]. In principle, it should be feasible to scale the device from a macroscale tribometer/indenter to a (mesoscale) SFA to a nanoscale AFM.

The choice of using a resistive method for sensing/detecting force and/or displacement makes this device less sensitive than the beam-bouncing method, but it does make it possible to measure forces and displacement in 3D and also to build compact arrays of independent sensors, thus giving no limit to the number of sensors that can be used simultaneously, something that cannot be currently achieved with the beam-bouncing method.

2.6. Bimorph vibrator attachment

Figure 10 shows the bimorph vibrator attachment. It allows for the top surface to be vibrated vertically using the piezo tube while measuring—for example, with a lock-in amplifier—the

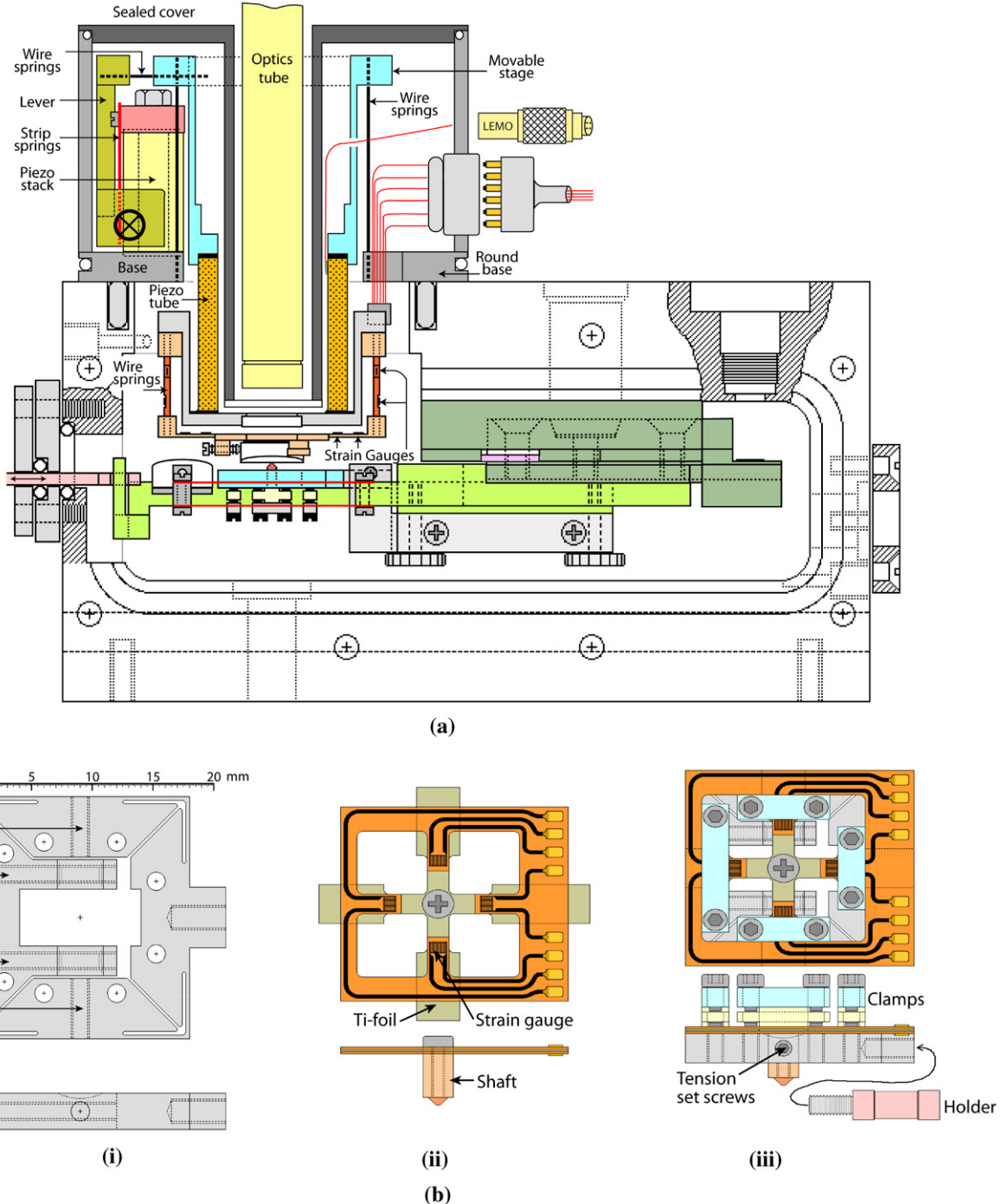


Figure 9. Schematic views of the SFA-AFM 3D displacement and force sensor installed into the SFA (a). (b) The probe is held in the middle of four cantilever foil springs (made of a single $25\ \mu\text{m}$ thick titanium foil). Deflections of the probe in the X, Y and Z directions are detected by the eight strain gauges on both sides of each cantilever (ii). This sensor is placed on a tension adjustable base (i) by clamping the cantilevers down (iii) just outside the strain gauges. The 3D displacement and force sensor is interchangeable with an SFA disk supported at the end of the (red) double-cantilever spring by a laterally sliding platform (light green). This means that during the same experiment one can measure in ‘SFA mode’ using a disk as in a regular SFA experiment, and in ‘AFM mode’ using the probe. The four vertical wire springs with ‘strain gauges’ on the top part (the same as in figure 7) can be removed for purely AFM-mode measurements.

amplitude and phase of the vibrations induced in the lower surface. This attachment is useful for measuring rheological and visco-elastic properties of fluids and thin fluid films near or between two surfaces. The motions of the bimorph vibrator are similar to those of the bimorph slider (figure 5) but its oscillatory motions are normal rather than lateral. This means

that the liquid film experiences squeeze flow rather than shear flow, so that the viscous forces are much larger and the response much more sensitive than in the case of the slider, i.e. the viscosities of thick, including effectively bulk, liquid films can be measured, which are not easily accessible in lateral sliding. For experiments with the bimorph totally immersed in a liquid

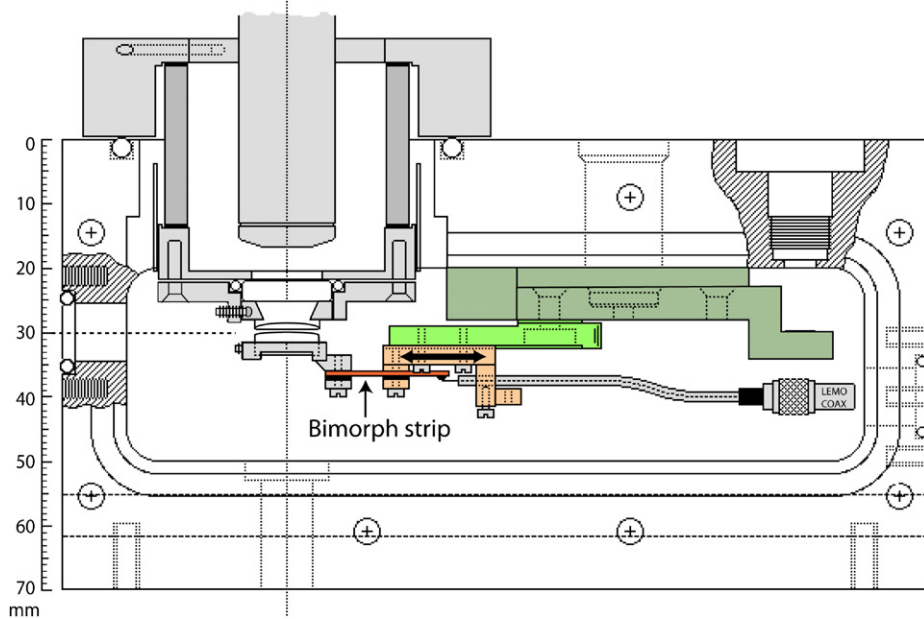


Figure 10. Schematic drawing of bimorph vibrator assembly.

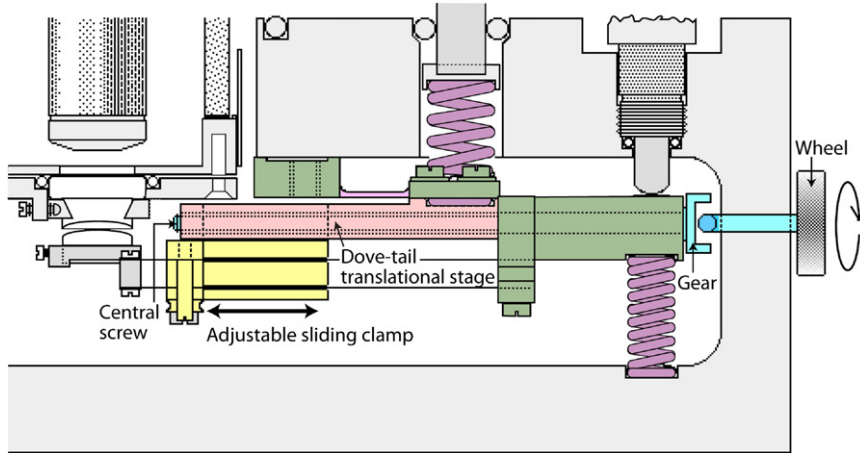


Figure 11. Schematic drawing of variable normal force-measuring springs, allowing for the stiffness of the force-measuring spring k to be adjusted over ~ 3 orders of magnitude.

such as water, it is possible to chemically and electrically seal the bimorph surfaces and its attached wires with a suitable coating (see section 2.2). The bimorph vibrator has provided some important results on the viscosity of thin fluid films and the location of slipping planes [37–39].

2.7. Variable normal force-measuring springs

Often when measuring forces in the SFA, the stiffness of the force-measuring cantilever spring used in the experiment has to be chosen carefully to suit the specific system being investigated. Springs having a high spring constant are typically best suited for measuring large and long-range forces while a low spring constant is often necessary to resolve weaker and more subtle forces. Because many systems investigated with the SFA involve a combination of strong and weak forces [20, 40, 41], it is often difficult to fully characterize all the forces in a system using a single, fixed stiffness spring. Traditionally, changing the spring stiffness was an involved

process that entailed stopping the experiment, disassembling the apparatus, reassembling the apparatus with a new set of cantilever springs and repeating the experiment from the beginning. For this reason, a variable stiffness spring, shown schematically in figure 11, was developed which allows the experimenter to controllably alter the stiffness of the force-measuring spring *in situ* without halting the experiment.

The variable stiffness spring attachment works on the simple principle that the stiffness k of an end-clamped cantilever varies with its active length L as $k \propto L^{-3}$. Consequently, decreasing the L by a factor of 10 will lead to an 1000-fold increase in the stiffness, allowing the experimenter to drastically alter the spring stiffness by simply adjusting the active spring length using a variable clamping mechanism.

In the variable stiffness spring attachment, the lower surface is held at the end of a double-cantilever spring which in turn is held between a spring-loaded ‘adjustable sliding clamp’. The adjustable sliding clamp is supported by a dove-

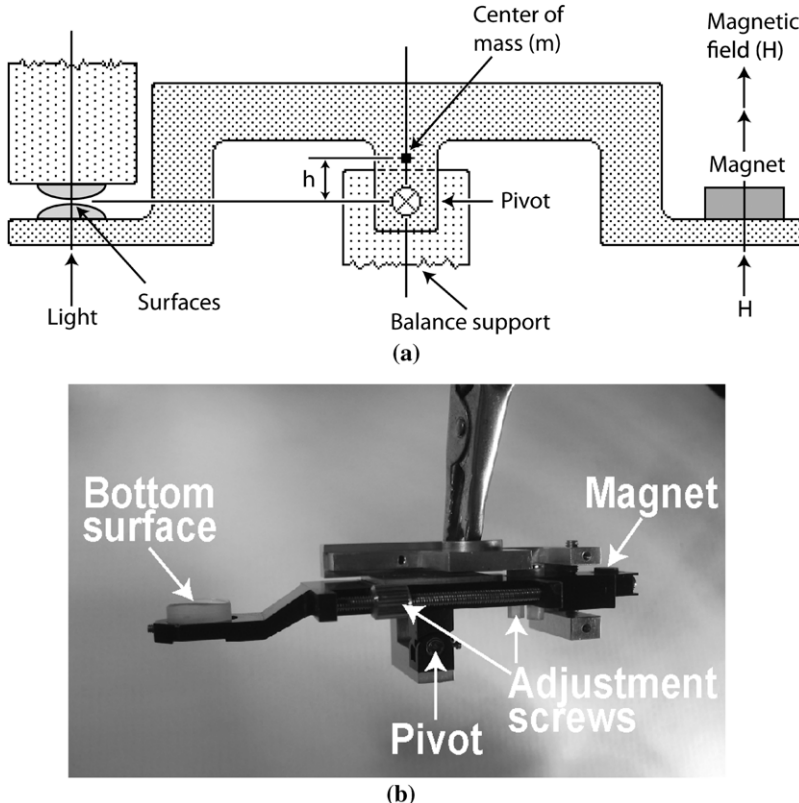


Figure 12. (a) Schematic drawing of the *balance attachment* for illustrating the mechanical principles of a ‘constant-force balance’ where a magnetic field H acting on a magnet (right) produces a constant force between the two surfaces (left). As described in the text, such a balance can have a zero restoring force (for small deflections) and zero friction. (b) Photo of prototype balance.

tail translational stage which moves along a central screw that is connected to an external wheel via a gear mechanism. Turning the external wheel allows the sliding clamp to be moved forward or backward, decreasing or increasing the cantilever spring length and stiffness. Once the desired cantilever spring length is achieved, the wheel is retracted which disengages the gear mechanism allowing forces to be measured.

2.8. Constant-force (balance) attachment

The new balance attachment (figure 12) can be used to measure very weak forces which may take a long time to reach equilibrium, as well as drive surfaces together at constant force.

The idea behind this attachment grew out of the realization that, since it is practically impossible to totally prevent thermal drifts, one must devise a method that can still reliably measure surface forces even in the presence of drifts. It was also appreciated that the applied force could not be produced via the displacement or deflection of a spring element. Figure 12 shows a schematic drawing of a ‘constant-force balance’ that in principle meets all the operational requirements of a constant-force transducer, near zero stiffness, frictionless motion in one direction only with robustness in all other directions, no vibrations, insensitivity to thermal drift and very high force sensitivity. The principle of this balance is as follows. First, imagine that the balance arm is pivoted by a frictionless knife-edge pivot. The center of mass of the whole balance in liquid is then adjusted with small screws so that it is located at the pivot point. The balance therefore has little or no restoring

force when displaced by a small amount (i.e. $K = 0$), and in principle it should remain at whatever angle it is left at. If the left arm supports one of the two surfaces and the right arm has a magnet attached to it, then by applying a magnetic field on the magnet a force will be felt on the other side, trying to displace the surface up or down. If, over the distance ΔD the magnetic field gradient remains uniform (which is easily achieved over the micrometer to millimeter distances of interest in surface force studies), then it is clear that any thermal drifts of the pivoting point relative to the upper or lower surfaces will have no effect on the applied force on the lower surface.

In practice, it is not possible to construct a frictionless knife-edge pivot. The closest one can approach a totally frictionless pivot is to use a combination of metal leaf springs that provide frictionless rotation about some axis. The ‘cross-spring flexure pivot’ is one such design. This type of miniature pivot was successfully used in an early friction attachment to the SFA [42] and has been used again in the 3D scanner of figure 9. But this type of pivot produces a small restoring force when it rotates, that is it has a small but finite elastic stiffness or torque. However, by designing the balance so that the center of mass is located *above* the pivot point (cf figure 12) this introduces a new (opposing) torque into the rotation due to gravitational or buoyancy forces. This opposing torque can be made to offset exactly the torque of the flexure pivot.

Put in mathematical terms, referring to figure 12, if m is the (displaced) weight of the balance whose center of mass is at a distance h above the pivot point, then when the balance rotates through an angle θ there will be a ‘gravitational’

torque of magnitude $mgh \sin \theta \approx mgh\theta$ acting to rotate the balance further. On the other hand, the flexure pivot itself will have developed a restoring torque of magnitude $\tau\theta$ acting in opposition to the gravitational torque. Thus, if $mgh = \tau$ the two effects cancel out, and the balance will behave as a frictionless zero-stiffness balance. This condition can be expressed as $h = \tau/mg$.

The prototype balance (figure 12(b)) is made of aluminum (anodized) and weighs about $m \approx 20$ gm. The pivot is a commercial flexure pivot (Bendix Corp., part number 5006-600) of torque constant $\tau = 10^{-4}$ N m⁻¹, and is mounted at a height $h = \tau/mg \approx 5$ mm below the center of mass of the balance. Small horizontal and vertical adjusting screws, which can be manipulated from outside the SFA chamber, are used to obtain an overall restoring torque of zero. Our preliminary tests indicate that, when suspended in liquid, this system is highly robust and vibration free, and can be adjusted to have an effective stiffness as low as $K = 10^{-3}$ N m⁻¹. This is 4 orders of magnitude lower than the current lowest spring stiffness of ~ 10 N m⁻¹, allowing for forces to be measured in the sub-pico-newton regime over short time periods, and in the 0.1 nN regime over longer times even in the presence of large thermal drifts.

3. Concluding remarks

In this paper we have reviewed the history behind the SFA including the changes involved in each generation of the apparatus and related apparatuses, and the reasons for these developments. The SFA technique can now be used to measure both normal and lateral forces between surfaces in liquids with a distance resolution of less than 1 Å. Recently introduced attachments, many of which were described here, allow for dynamic (non-equilibrium) measurements to be made *in situ*, and for extending the range and scope of surface force measurements to new surfaces and systems, including electrochemical and biological systems. In addition, incorporation of other techniques, such as x-ray scattering [43], IR spectroscopy, fluorescence microscopy [44] and AFM [33], allows for different measurements to be made on a sample at the same time.

Acknowledgments

Research supported by the US Department of Energy, Office of Basic Energy Sciences, Division of Materials Sciences and Engineering under Award #DE-FG02-87ER45331.

Appendix A. Multiple beam interferometry

MBI is used in the SFA to determine the distance between the surfaces as well as the shape of the surface [42, 45]. For a typical SFA experiment a pair of transparent surfaces (e.g. freshly cleaved mica) is used as the surface substrate, which are coated on the back with a highly reflective layer (e.g. silver) for providing a good interfering pattern between the reflecting surfaces. The surfaces are glued onto a cylindrical shaped glass disk and mounted in a cross-cylindrical configuration,

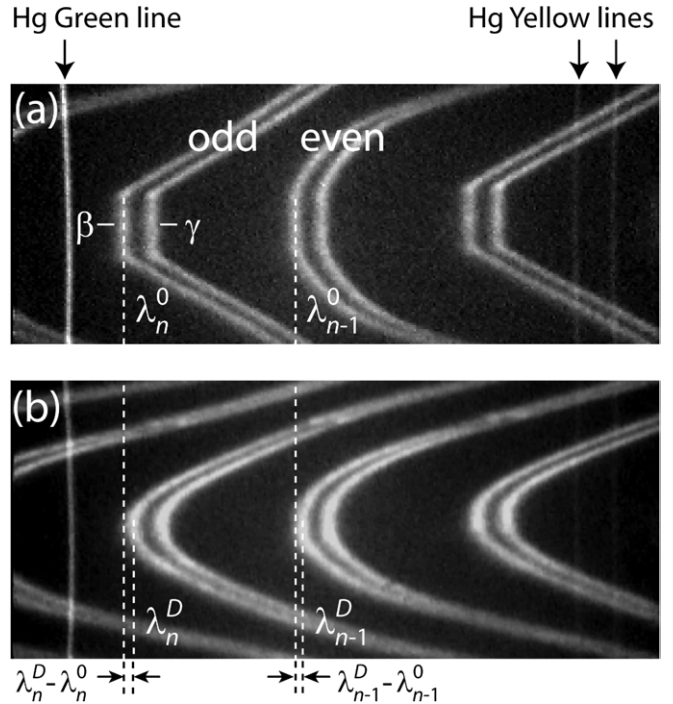


Figure 13. FEKO of mica surfaces in air (a) in adhesive contact ($D = 0$) and (b) separated by $D \approx 9.9$ nm. Note that the odd order fringes appear narrower than the even order fringes. In (a), the contacting parts of the surfaces flatten due to elastic deformations of the mica and supporting glue. Each fringe appears as a doublet with a β - and a γ -component due to the birefringence of mica. The vertical lines at the edges of the pictures are the green and yellow Hg calibration lines.

which simulates a sphere-on-flat geometry. When white light is directed normal to the surfaces the light is reflected back and forth between the silver layers and the transmitted light near the closest contact point between the surfaces creates Newton's rings, as can be seen through a microscope objective. The transmitted light corresponds to a particular set of discrete wavelengths that is made visible by a spectrometer and are the so-called fringes of equal chromatic order (FECO). An example of the FECO between mica surfaces in air is shown in figure 13. In this appendix we will only consider this setup with three-layer (e.g. mica-medium-mica) interferometry, which is the most commonly used setup for SFA experiments. Derivation of the distance measurements for other cases can be found in [42].

When the surfaces are in contact with no medium between them, the interference fringes depend on the mica thickness. Assuming that the mica thickness, T , is the same for both surfaces, T can be determined by the wavelength of the n th order fringe, λ_n^0 , by the relation $T = n\lambda_n^0/4\mu_{\text{mica}}$, where μ_{mica} is the refractive index of mica at λ_n^0 . The fringe order, n , is determined by

$$n = \frac{\lambda_{n-1}^0}{\lambda_{n-1}^0 - \lambda_n^0}, \quad (\text{A.1})$$

where λ_{n-1}^0 is the next fringe at higher wavelength. It can be shown that when the surfaces are separated by a distance D , the amount that the n th fringe shifts by depends on the refractive index of the medium in the gap between the surfaces, and the

original contact positions (because these are related to n and the interferometer thickness) [42, 46].

$$\tan(2\pi\mu D/\lambda_n^D) = \frac{2\bar{\mu} \sin[\pi(1 - \lambda_n^0/\lambda_n^D)/(1 - \lambda_n^0/\lambda_{n-1}^0)]}{(1 + \bar{\mu}^2) \cos[\pi(1 - \lambda_n^0/\lambda_n^D)/(1 - \lambda_n^0/\lambda_{n-1}^0)] \pm (\bar{\mu}^2 - 1)}. \quad (\text{A.2})$$

The + sign is taken when n is odd (standing wave with node in the center) and – is taken when n is even (standing wave with anti-node in the center). At the separation distance D , the n th fringe changes wavelength from λ_n^0 to λ_n^D . The effective refractive index is denoted as $\bar{\mu} = \mu_{\text{mica}}/\mu$ where μ_{mica} is the refractive index of mica at λ_n^D and μ is the refractive index of the medium between the two surfaces at λ_n^D . If the positions of three consecutive fringes are known, then an iterative process can be used to determine the thickness and refractive index of the film between the surfaces. When the surfaces are separated by a distance which results in a fringe shift equal to $\lambda_{n-1}^0 - \lambda_n^0$, it is easy to show that the film thickness is calculated by $D = \lambda_{n-1}^0/2\mu$.

When the distance between the surfaces is small (D below ~ 30 nm), we can use Taylor series expansions to find approximate expressions for the trigonometric functions in equation (A.2):

$$D = \begin{cases} nF_n(\lambda_n^D - \lambda_n^0)/2\mu_{\text{mica}}, & \text{for odd } n, \\ nF_n(\lambda_n^D - \lambda_n^0)\mu_{\text{mica}}/2\mu^2, & \text{for even } n, \end{cases} \quad (\text{A.3})$$

where F_n is a correction factor which takes into account the refractive index dispersion and phase change of the reflection at the silvered interfaces. For light with wavelength $\lambda \sim 500$ nm, the correction factor is $F_n \approx 1.024 + 1/n$. Note that the film thickness determined from the even order fringes depends on μ , the refractive index of the medium between the mica surfaces, but that the film thickness determined from the odd order fringes does not. Therefore, if we know the wavelength shift of two consecutive fringes we can determine an approximate value for the refractive index of the medium:

$$\mu = \mu_{\text{mica}} \sqrt{\frac{(n-1)F_{n-1}}{nF_n} \cdot \frac{\lambda_{n-1}^D - \lambda_{n-1}^0}{\lambda_n^D - \lambda_n^0}}, \quad \text{for } n \text{ odd.} \quad (\text{A.4})$$

Equation (A.3) can also be used to explain why odd fringes look different than even fringes for small D as shown in figure 13. For the odd fringes the shift in the wavelength is proportional to $2\mu_{\text{mica}}D/nF_n$ while the shift in wavelength for the even fringes is proportional to $2\mu^2/nF_n\mu_{\text{mica}}$. Thus if $\mu < \mu_{\text{mica}}$, the shift in the wavelength of the odd fringe will be greater than the shift in the even fringe. This case is most pronounced for mica surfaces in contact in air ($\mu = 1$). Comparing the difference in wavelength $\Delta\lambda$ between light interfering in the contact region and light interfering at a spot just outside the contact region, we see that $\Delta\lambda_{\text{odd}} > \Delta\lambda_{\text{even}}$. Therefore, the edges of the odd fringes appear sharp while the edges of the even fringes appear rounded as seen in figure 13(a). If $\mu = \mu_{\text{mica}}$, the even and odd fringes will have the same shape. Finally, if $\mu > \mu_{\text{mica}}$, the shift in the

wavelength of the even fringe will be greater than that of the odd.

As shown in figure 13, the FECO appear as doublets when the surfaces are mica. Mica is a birefringent material which means that it has two indices of refraction in the plane perpendicular to the incident light (mica also has a third optical axis, α -component, which is parallel to the incident light and thus not observed in SFA experiments). The optical path with the lower refractive index results in the lower wavelength fringe, the β -component, and the higher refractive index results in the higher wavelength γ -component. Typical values for the refractive index of reddish or brownish mica are

$$\mu_\beta = 1.5794 + 4.76 \times 10^5 / \lambda^2 (\text{\AA}^2), \quad (\text{A.5})$$

$$\mu_\gamma = 1.5846 + 4.76 \times 10^5 / \lambda^2 (\text{\AA}^2).$$

When the optical axes of the two mica surfaces are perfectly aligned, the shift between the β - and γ -components of the fringe will be maximized. Conversely, when the optical axes are at right angles to each other, there will be no shift between the β - and γ -components of the fringes. The mica acts as a polarizer for the light going through the surfaces, and if great care is taken to align the surfaces in a known orientation, it is possible to gain insight into the molecular alignment between the surfaces.

References

- [1] Overbeek J T G and Spaarnay M J 1952 Experiments on long-range attractive forces between macroscopic objects *J. Colloid Sci.* **7** 343–5
- [2] Derjaguin B V *et al* 1964 Surface forces and the stability of colloids and disperse systems *J. Colloid Sci.* **19** 113–35
- [3] Tabor D and R H S Winterton 1969 The direct measurement of normal and retarded van der Waals forces *Proc. R. Soc. Lond. Ser. A (Math. Phys. Sci.)* **312** 435–50
- [4] Israelachvili J N and Tabor D 1972 The measurement of van der Waals dispersion forces in the range 1.5 to 130 nm *Proc. R. Soc. Lond. Ser. A (Math. Phys. Sci.)* **331** 19–38
- [5] Israelachvili J N and Adams G E 1976 Direct measurement of long range forces between two mica surfaces in aqueous KNO₃ solutions *Nature* **262** 774–6
- [6] Israelachvili J N 1989 Techniques for direct measurements of forces between surfaces in liquids at the atomic scale *Chemtracts: Anal. Phys. Chem.* **1** 1–12
- [7] Israelachvili J 1987 Direct measurements of forces between surfaces in liquids at the molecular level *Proc. Natl Acad. Sci. USA* **84** 4722–4
- [8] Israelachvili J N and McGuigan P M 1990 Adhesion and short-range forces between surfaces: I. New apparatus for surface force measurements *J. Mater. Res.* **5** 2223–31
- [9] Luengo G *et al* 1997 Thin film rheology and tribology of confined polymer melts: contrasts with bulk properties *Macromolecules* **30** 2482–94
- [10] Parker J L, Christenson H K and Ninham B W 1989 Device for measuring the force and separation between two surfaces down to molecular separations *Rev. Sci. Instrum.* **60** 3135–8
- [11] Klein J 1983 Forces between mica surfaces bearing adsorbed macromolecules in liquid media *J. Chem. Soc. Faraday Trans. I* **79** 99–118
- [12] Klein J 1980 Forces between mica surfaces bearing layers of adsorbed polystyrene in cyclohexane *Nature* **288** 248–50

- [13] Briscoe W H and Horn R G 2002 Direct measurement of surface forces due to charging of solids immersed in a nonpolar liquid *Langmuir* **18** 3945–56
- [14] Tonck A, Georges J M and Loubet J L 1988 Measurements of intermolecular forces and the rheology of dodecane between alumina surfaces *J. Colloid Interface Sci.* **126** 150–63
- [15] Knapschinsky L *et al* 1982 Interaction forces between crossed quartz filaments in presence of adsorbed poly (vinyl alcohol): I. Measuring device *Colloid Polym. Sci.* **260** 1153–6
- [16] Heuberger M 2001 The extended surface forces apparatus: I. Fast spectral correlation interferometry *Rev. Sci. Instrum.* **72** 1700–7
- [17] Zäch M, Vanicek J and Heuberger M 2003 The extended surface forces apparatus: III. High-speed interferometric distance measurement *Rev. Sci. Instrum.* **74** 260–6
- [18] Israelachvili J *et al* 2005 Effects of sub-fingstrom (pico-scale) structure of surfaces on adhesion, friction, and bulk mechanical properties *J. Mater. Res.* **20** 1952–72
- [19] Akbulut M *et al* 2007 Forces between surfaces across nanoparticle solutions: role of size, shape, and concentration *Langmuir* **23** 3961–9
- [20] Min Y J *et al* 2008 Normal and shear forces generated during the ordering (directed assembly) of confined straight and curved nanowires *Nano Lett.* **8** 246–52
- [21] Min Y J *et al* 2008 Frictional properties of surfactant-coated rod-shaped nanoparticles in dry and humid dodecane *J. Phys. Chem. B* **112** 14395–401
- [22] Chen N H *et al* 2005 Adhesion and friction of polymer surfaces: the effect of chain ends *Macromolecules* **38** 3491–503
- [23] Gourdon D and Israelachvili J N 2003 Transitions between smooth and complex stick-slip sliding of surfaces *Phys. Rev. E* **68** 021602
- [24] Israelachvili J, Maeda N and Akbulut M 2006 Comment on reassessment of solidification in fluids confined between mica sheets *Langmuir* **22** 2397–8
- [25] Gourdon D *et al* 2008 Adhesion and stable low friction provided by a subnanometer-thick monolayer of a natural polysaccharide *Langmuir* **24** 1534–40
- [26] Min Y *et al* 2009 Interaction forces and adhesion of supported myelin lipid bilayers modulated by myelin basic protein *Proc. Natl Acad. Sci. USA* **106** 3154–9
- [27] Zhao B X *et al* 2008 Adhesion and friction force coupling of gecko setal arrays: implications for structured adhesive surfaces *Langmuir* **24** 1517–24
- [28] Akbulut M, Alig A R G and Israelachvili J 2006 Triboelectrification between smooth metal surfaces coated with self-assembled monolayers (SAMs) *J. Phys. Chem. B* **110** 22271–8
- [29] Akbulut M *et al* 2005 Crystallization in thin liquid films induced by shear *J. Phys. Chem. B* **109** 12509–14
- [30] Alig A R G, Gourdon D and Israelachvili J 2007 Properties of confined and sheared rhodamine B films studied by SFA-FECO spectroscopy *J. Phys. Chem. B* **111** 95–106
- [31] Akbulut M, Alig A R G and Israelachvili J 2006 Friction and tribocatalytic reactions occurring at shearing interfaces of nanothin silver films on various substrates *J. Chem. Phys.* **124** 174703
- [32] Israelachvili J 1992 *Intermolecular and Surface Forces* 2nd edn (San Diego: Academic)
- [33] Kristiansen K *et al* 2008 3D force and displacement sensor for SFA and AFM measurements *Langmuir* **24** 1541–9
- [34] Kristiansen K *et al* Measurements of off-axis friction forces (in preparation)
- [35] Connor J N and Horn R G 2003 Extending the surface force apparatus capabilities by using white light interferometry in reflection *Rev. Sci. Instrum.* **74** 4601–6
- [36] Heuberger M, Luengo G and Israelachvili J 1997 Topographic information from multiple beam interferometry in the surface forces apparatus *Langmuir* **13** 3839–48
- [37] Israelachvili J N, Kott S J and Fetter L J 1989 Measurements of dynamic interactions in thin films of polymer melts: transition from simple to complex behavior *J. Polym. Sci. Part B—Polym. Phys.* **27** 489–502
- [38] Israelachvili J N 1988 Measurements and relation between the dynamic and static interactions between surfaces separated by thin liquid and polymer melts *Pure Appl. Chem.* **60** 1473–8
- [39] Israelachvili J N and Kott S J 1989 Shear properties and structure of simple liquids in molecularly thin films: the transition from bulk (continuum) to molecular behavior with decreasing film thickness *J. Colloid Interface Sci.* **129** 461–7
- [40] Sivasankar S, Gumbiner B and Leckband D 2001 Direct measurements of multiple adhesive alignments and unbinding trajectories between cadherin extracellular domains *Biophys. J.* **80** 1758–68
- [41] Min Y J *et al* 2008 The role of interparticle and external forces in nanoparticle assembly *Nature Mater.* **7** 527–38
- [42] Israelachvili J N 1973 Thin film studies using multiple-beam interferometry *J. Colloid Interface Sci.* **44** 259–72
- [43] Idziak S H J *et al* 1994 The x-ray surface forces apparatus—structure of a thin smectic liquid crystal film under confinement *Science* **264** 1915–8
- [44] Mukhopadhyay A *et al* 2003 An integrated platform for surface forces measurements and fluorescence correlation spectroscopy *Rev. Sci. Instrum.* **74** 3067–72
- [45] Tolansky S 1948 *Multiple-Beam Interferometry of Surfaces and Films* (Oxford: Oxford University Press) p 187
- [46] Horn R G and Smith D T 1991 Analytic solution for the three-layer multiple beam interferometer *Appl. Opt.* **30** 59–65

SETTING UP AND EQUIPPING A SURFACE FORCES MEASUREMENT LABORATORY (SFA LAB)

See also pages 5-7

Location of SFA lab

Ideally, your laboratory should be located in a basement or ground floor – well away from vibration-producing machinery such as large pumps or air-conditioning units. However, if this is not possible, a simple anti-vibration table is usually sufficient to reduce most vibrations to insignificant levels. The walls, furniture and floor should never be coated or cleaned with oil-based polishes that give off surface active contaminants into the atmosphere (these can usually be smelled if present). All laboratory surfaces, including floors and work benches, should be cleaned with warm water only. The dark room(s) should be thermostatically controllable, to $\pm 0.1^\circ\text{C}$ if possible. The thermostating air-conditioning or air-ducting system should not be connected to other laboratories so as not to introduce air-borne contamination into the lab atmosphere. Ideally, the air pressure of the laboratory should be slightly higher than that of the adjoining rooms, ensuring a steady flow of (clean and thermostatted) air from that room outwards.

Recommended laboratory hardware and fittings for basic SFA measurements

Your **SFA** package should arrive in a condition ready for immediate use in experiments – all necessary apparatus parts, basic supplies, assembly tools, electrical items and cables being provided with your unit. However, a number of additional laboratory hardware items (not provided in the package) are needed for carrying out basic experiments. These are listed in the following Table.

Some labs will already have some of the equipment listed, for example, a vacuum chamber. Other equipment and electronic devices such as video cameras, function generators, strain-gauge bridges, chart recorders, storage O-scopes, Langmuir-Blodgett deposition cell, etc., may be required for specialized tribological or biological experiments (see SFA brochures for a complete list of possible items).

It is assumed that the laboratory is well-equipped with standard lab furniture and disposable items, such as work benches (fume hood), sinks, essential materials (mica) and laboratory supplies such as glassware, chemicals, liquids (distillation unit), filters, etc. A source of pure (and dry) high pressure nitrogen gas is also desirable, either from boil-off (liquid nitrogen source) or from a pressurized cylinder.

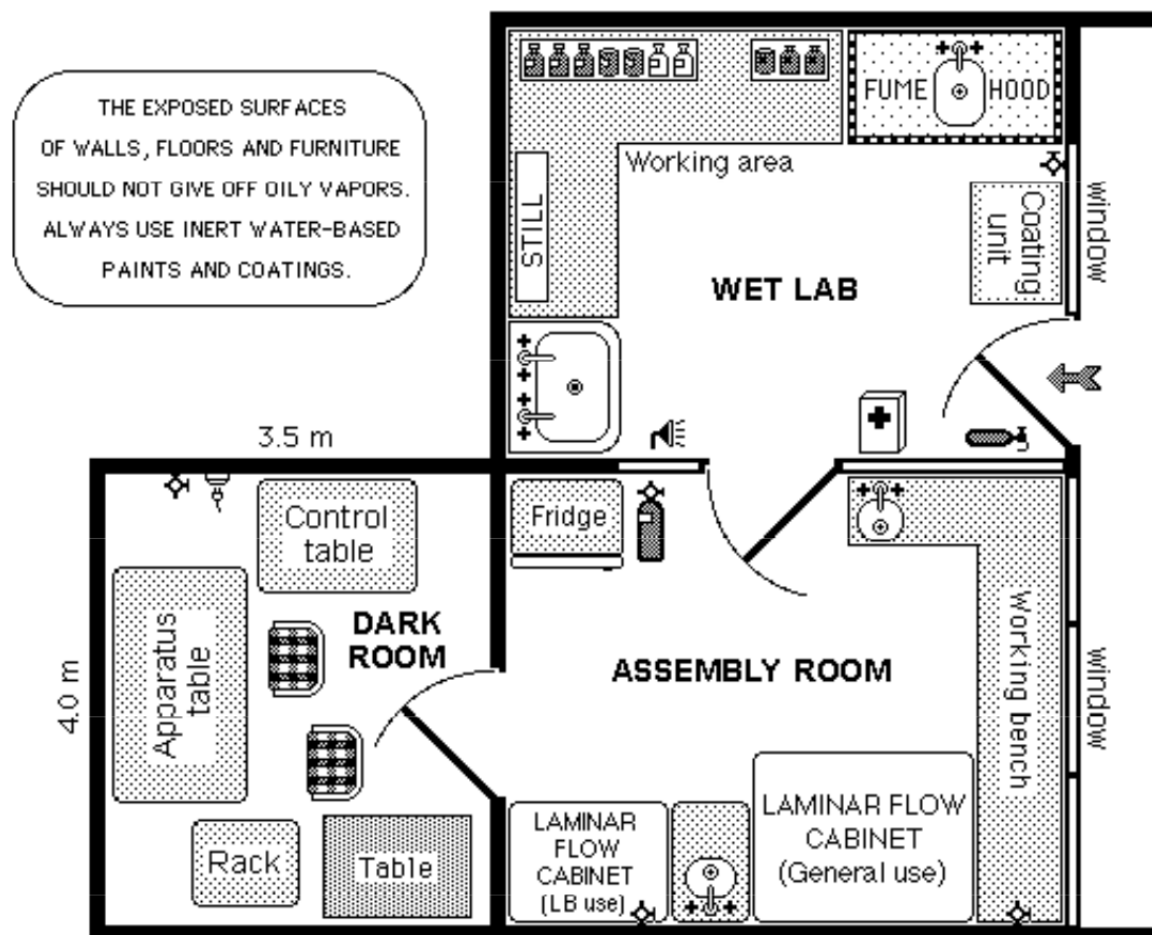


Figure 54

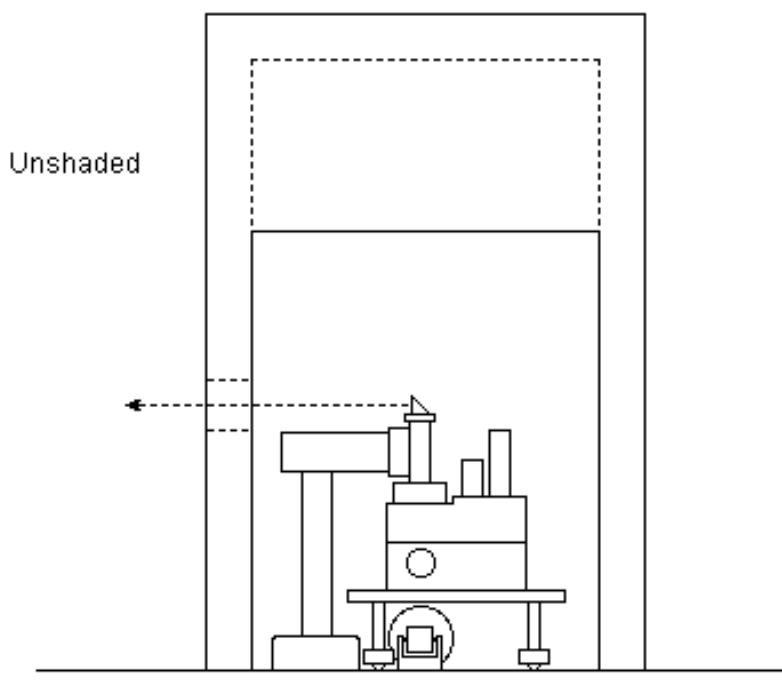
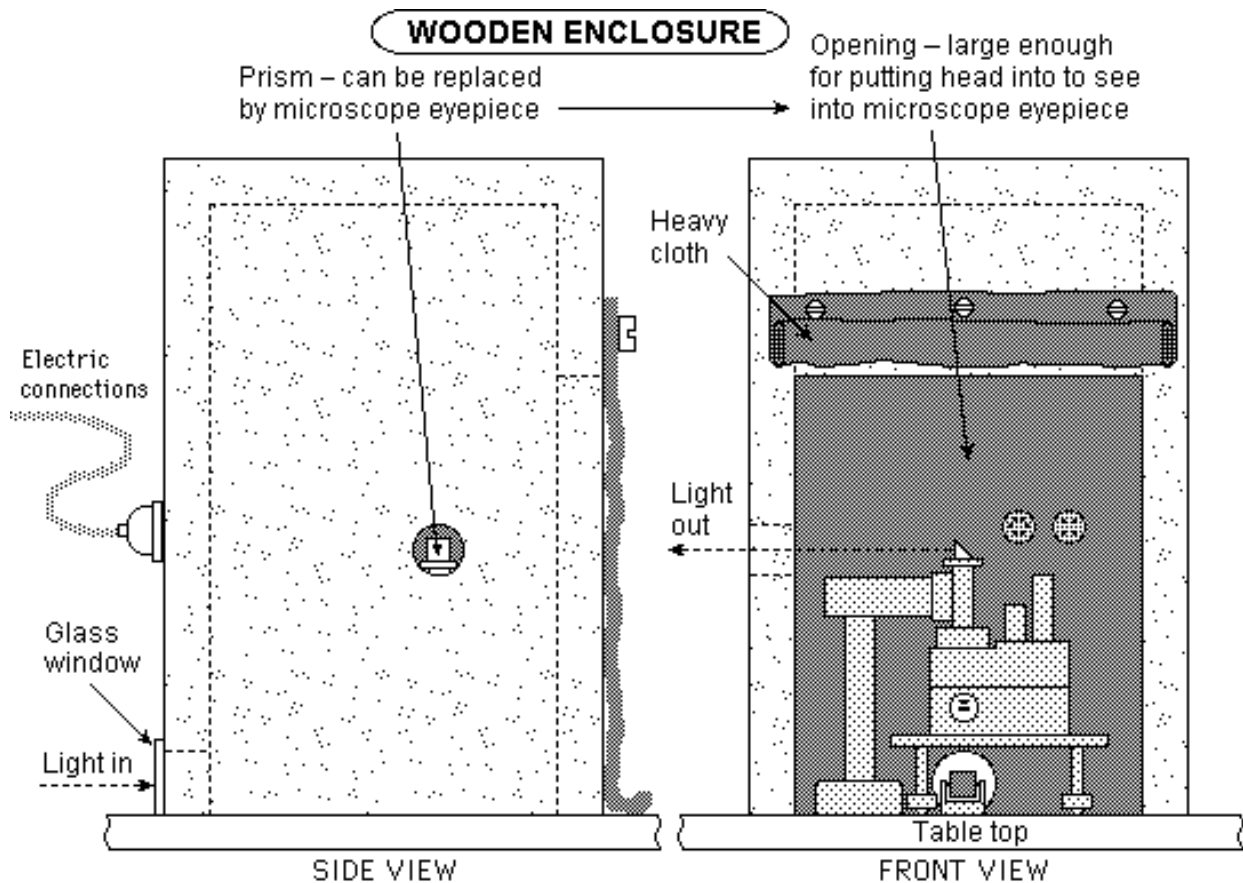


Figure 55

SFA 2000 BASIC UNIT

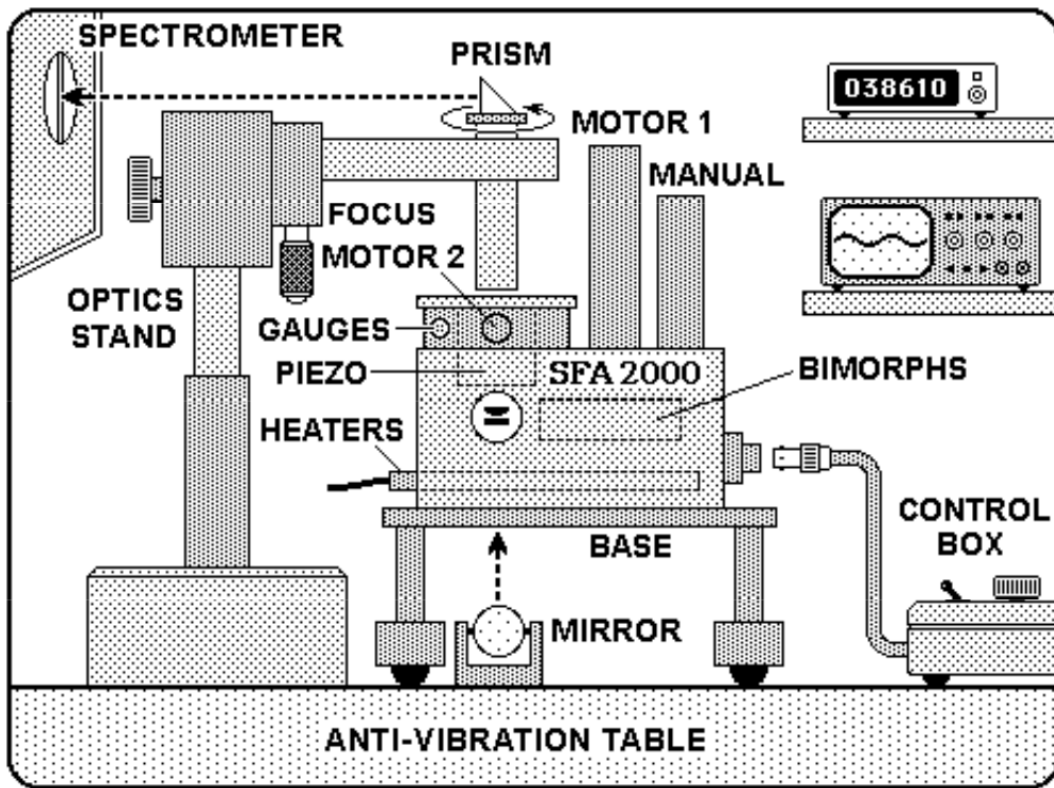


Figure 56. Schematic of SFA 2000 setup, also showing those parts that are controlled by the CONTROL CONSOLE or CONTROL BOX. Recommended horizontal distance from prism to spectrometer entrance slit: 50 cm; vertical distance from prism/slit center to table-top: 30 cm.

The Basic Unit consists of the following items:

- Main chamber**
- Main stage**
- Various internal (lower) mounts**
- Piezo (upper) mount**
- Motor-driven and manual micrometers**
- Base and legs**
- Mirror**
- Optics stand**
- Control console and electric cables**
- Encoder display counters**
- Tool kit (for assembly, handling disks, etc.)**
- Supply box (including spare and replacement parts)**

SUPPLY ITEMS

Kinematic mounts (three, for base legs)
Rubber pads (for Optics Base, Mirror, Control Box)
Belt (for Optics Stand)
Eyepiece (X10 wide-angle, *Nikon CFWE*)
Force-measuring springs (including spare)
Friction Device clamping screws (including spare)
Glass disk for sealing apparatus without using piezo mount and for leak tests
Steel plate for sealing motor 1 opening
Glue (Shell EPON RESIN 1004, 1007 and 1009)
Graticule / reticule with cross-hair (for eyepiece)
Kel-F tubing with Luer connectors at ends; special Luer for Vapor Pressure bath
Luer fittings (2 fem-fem, 2 male-male, 2 fem-male, 3 caps, 2 male ports, 2 female ports, 1 valve, O-rings: various sizes, including -003 for Luer threads, Teflon Luer filter)
Microscope tube with X5 and X10 objectives (one installed)
Needles (for cleaving mica)
Needles (2-3 inches long, 3 flat-ended, for injecting liquid between surfaces)
O-rings (including ~30 spare)
Prism (1 inch, for placing on top of Optics Stand)
Screws (spares, non-standard sizes only)
Self-adhesive vernier scale for motor housing and limit switches (spare strip)
Silica disks: various: 2.5 - 5.0 mm high
Teflon or Kel-F tipped 1.6 mm and 0-80 stainless steel set screws
Spirit level (for placing on Base)
Syringes (for injecting droplets between surfaces)
Thermistor
PTFE (TReflon) shrink tubing for piezo mount
Springs (cantilever and helical, various stiffnesses, including spare)

ELECTRIC CABLES AND CONNECTORS

Check that the Control Console (or Control Box) and Apparatus are electrically earthed or 'grounded' before switching on. The Apparatus should be earthed via the hole on the front of the Base Plate. See comments on avoiding 'earth loops' or 'ground loops' on page 45. On switching on the Power Switch on the Control Console turn lights brightness knob clock-wise to test that the Console is being powered and to adjust the brightness of the panel lights.

All cables supplied are labeled.

Power cable: for connecting Control Box to mains outlet.

Optics cable: from Control Box Optics Output to the Optics Stand.

Motor 1 – distance control (encoder & limit switches): from Control Box Output to Motor 1.

Motor 2 – friction speed control (encoder & limit switches): from Control Box Output to Motor 2.

Display counter cables: for connecting each display counter to power via transformer (supplied).

Encoder cables: from display counters to each motor.

Piezo output BNC-BNC cable: from Control Box to amplifier (Trek).

Piezo input BNC-Lemo cable: from amplifier to piezo mount.

Friction device cable: from Friction Device to Signal Conditioning amplifier, model 2311 or 2310.

Bimorph slider cable: from function generator via amplifier to SFA chamber input on right.

Heater cables: from Heater output to heater rods.

Thermistor cable: Connect thermistor leads to resistance input on multimeter (not supplied).

Earth (ground) lead: Single wire connection from front of Base plate to earth (ground).

Fuses: the Control Box has one 0.5 and 1.0 Amp fast action fuses.

TOOLS

Screw drivers: flat, Philips, 2 nut-drivers, hexagonal (socket head) drivers (straight or Allen keys): 0.9 1.3, 1.5, 2.0, 2.5, 3.0, 4.0 mm, 0.028", 0.035".

Right-angled manual rotating hex driver (for tightening disk set screws).

Tweezers and forceps for handling mica and small parts.

Tweezers – including specially shaped, for picking up round and dove-tailed disks.

Cleaning brushes – for cleaning threaded holes with water or alcohol only.

SFA 2000 BASIC UNIT, ATTACHMENTS AND PARTS

SFA 2000 ASSEMBLY

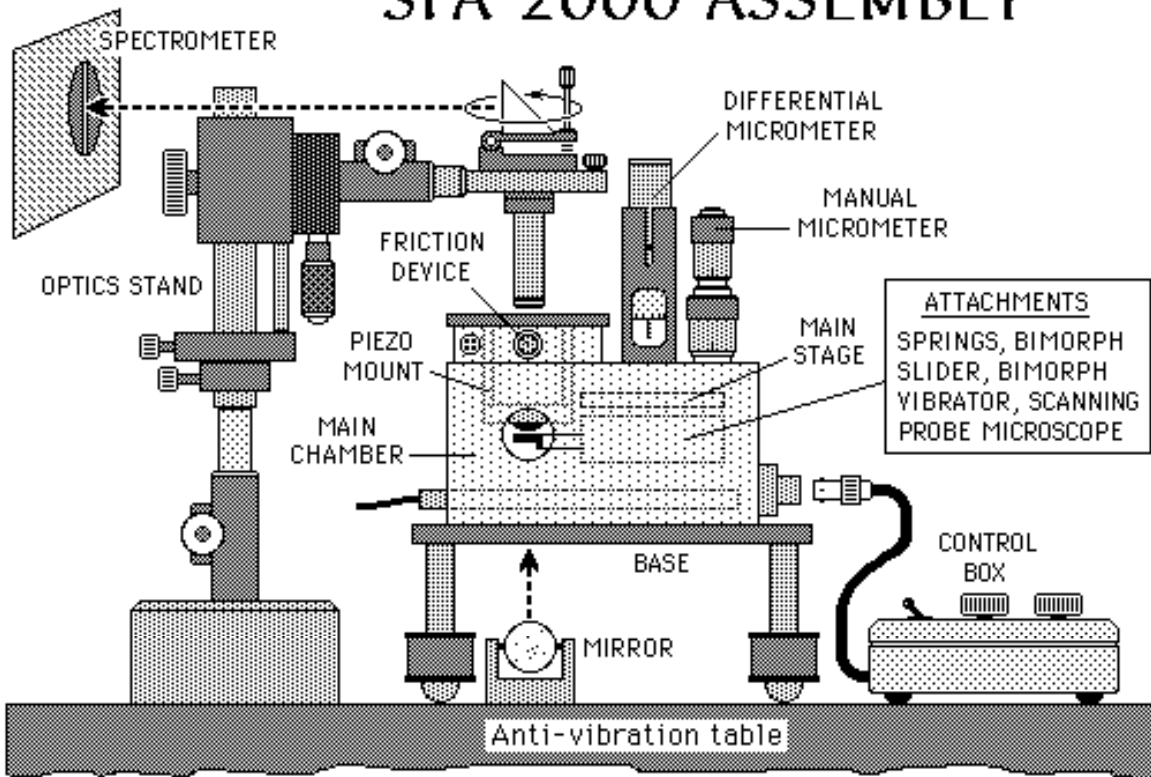


Figure 57. Units and attachments of the SFA 2000.

Introduction to the SFA 2000 and its attachments

The SFA 2000 operates in a similar fashion to the SFA Mk 2 and 3. The main differences between these instruments is that the SFA 2000 was specifically developed for commercialization, that is, for the academic and industrial R&D community. Thus, it has fewer parts, it is easier to fabricate, assemble and operate, and it accepts a variety of new attachments for performing traditionally non-SFA type experiments, such as Scanning Probe Microscopy and Atomic Force Microscopy.

The main reason for the greater simplicity of the SFA 2000 is that it operates on a different mechanical principle from previous SFAs. In the SFA 2000, one central simple-cantilever spring is used for generating both coarse and fine motions over a total range of seven orders of magnitude (from millimeters to ångstroms). This mechanism is described in the section "How it works".

All of the above advantages in cost, time and expertise have not been made at the expense of performance: tests with the SFA 2000 show that it has the same or better performance specifications (e.g., of stability and drift) than the SFA 3 and other SFAs, in addition to being more adaptable. One drawback, however, is that when large compressive forces are being applied using weak springs (requiring large deflections of the springs) there is a small lateral displacement of the surfaces. To avoid this it is recommended to use stiffer 'force-measuring' springs when measuring or applying large forces or pressures.

Specifications of the SFA 2000 Basic Unit:

Coarse control (manual): Differential micrometer, positioning accuracy: ~5000 Å.

Medium control (manual): Differential micrometer, positioning accuracy: ~500 Å.

Fine control (motor 1): Differential spring system, positioning accuracy: ~10 Å.*

Piezo control: Piezo mount, positioning accuracy: <1 Å.

* The positioning accuracy of the fine control depends on the stiffness of the helical spring used. Weaker springs give better control but at the cost of a reduced overall range of travel. Three springs of different stiffnesses have been provided.

Figure 57 shows the different units and attachments that together make up a complete SFA 2000 system (the BASIC UNIT and the various ATTACHMENTS). These are shown in greater detail in Figures 58-70.

BASIC UNIT

- MAIN CHAMBER, MICROMETERS and MOTORS
- MAIN STAGE
- FORCE-MEASURING SPRING & LOWER DISK MOUNT
- PIEZO MOUNT & UPPER DISK MOUNT
- BASE and LEGS
- OPTICS STAND & MIRROR
- CONTROL BOX, ELECTRIC CABLES, CONNECTORS & DISPLAY COUNTERS
- MISCELLANEOUS TOOLS AND ACCESSORIES (e.g., heaters)

In addition, one or more of the following UNITS or ATTACHMENTS may be used for carrying out different types of measurements

- FRICTION DEVICE (for lateral, friction or shearing force measurements)
- BIMORPH SLIDER (for extending the dynamic range of friction force measurements)
- BIMORPH VIBRATOR (for dynamic normal force and thin film rheology measurements)

Each UNIT is composed of a number of machined PARTS, together with special screws, O-rings, electric connections and other small fittings. All of these come together to produce the final assembled apparatus. The BASIC UNIT is normally delivered fully assembled and functional. The other units, will also be pre-assembled before delivery, and mounted into the SFA chamber during the setting up demonstration on delivery (see also vieos). Some parts and supply items do not belong to any obvious unit or are used in a number of different units, these belong to the SUPPLIES & TOOLS category.

The following pages contain figures, assembly drawings and photographs of different units and attachments, and their assembly and use can also be viewed in the videos supplied with your SFA 2000.

MAIN CHAMBER

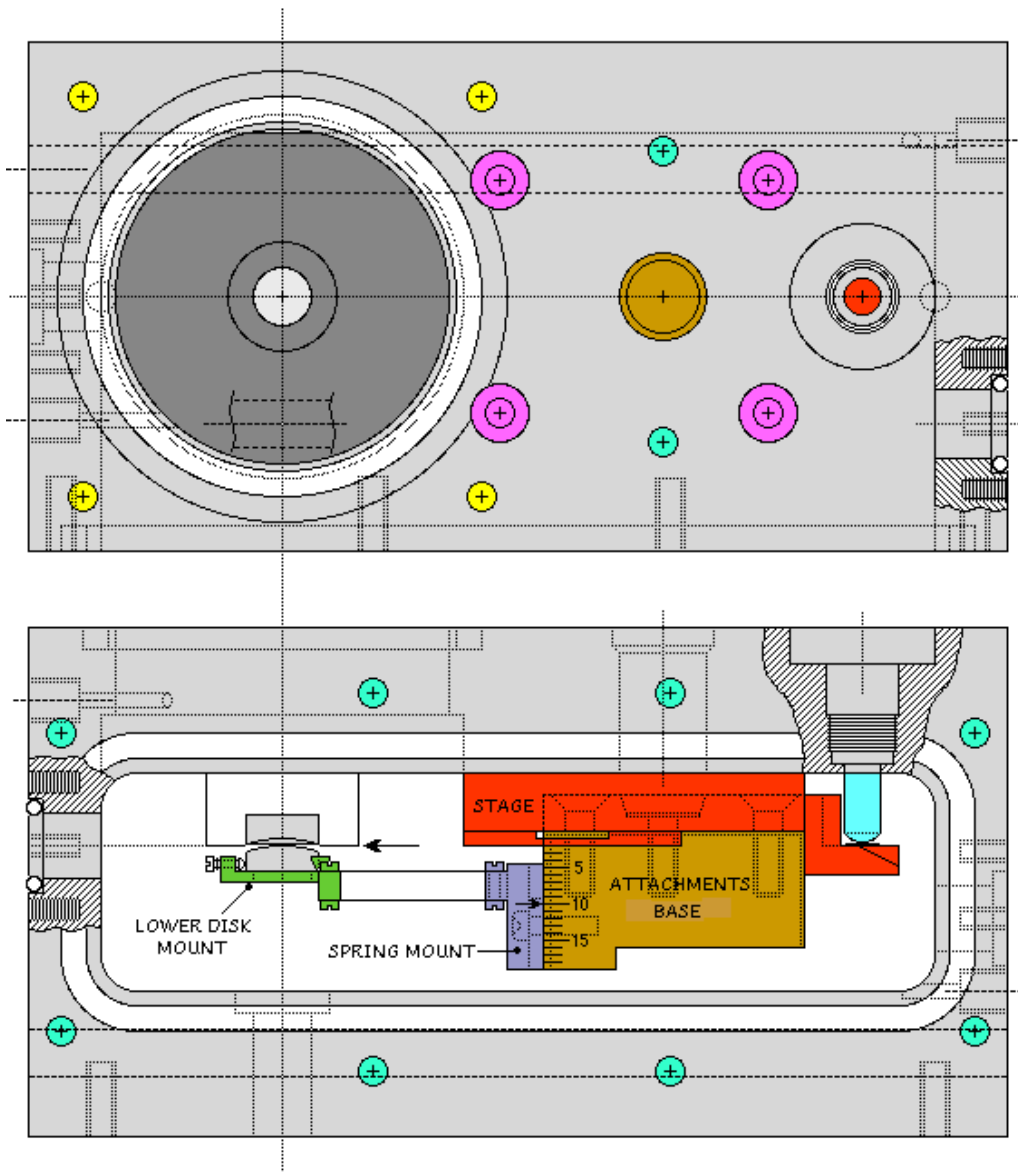


Figure 58 A

SFA 2000

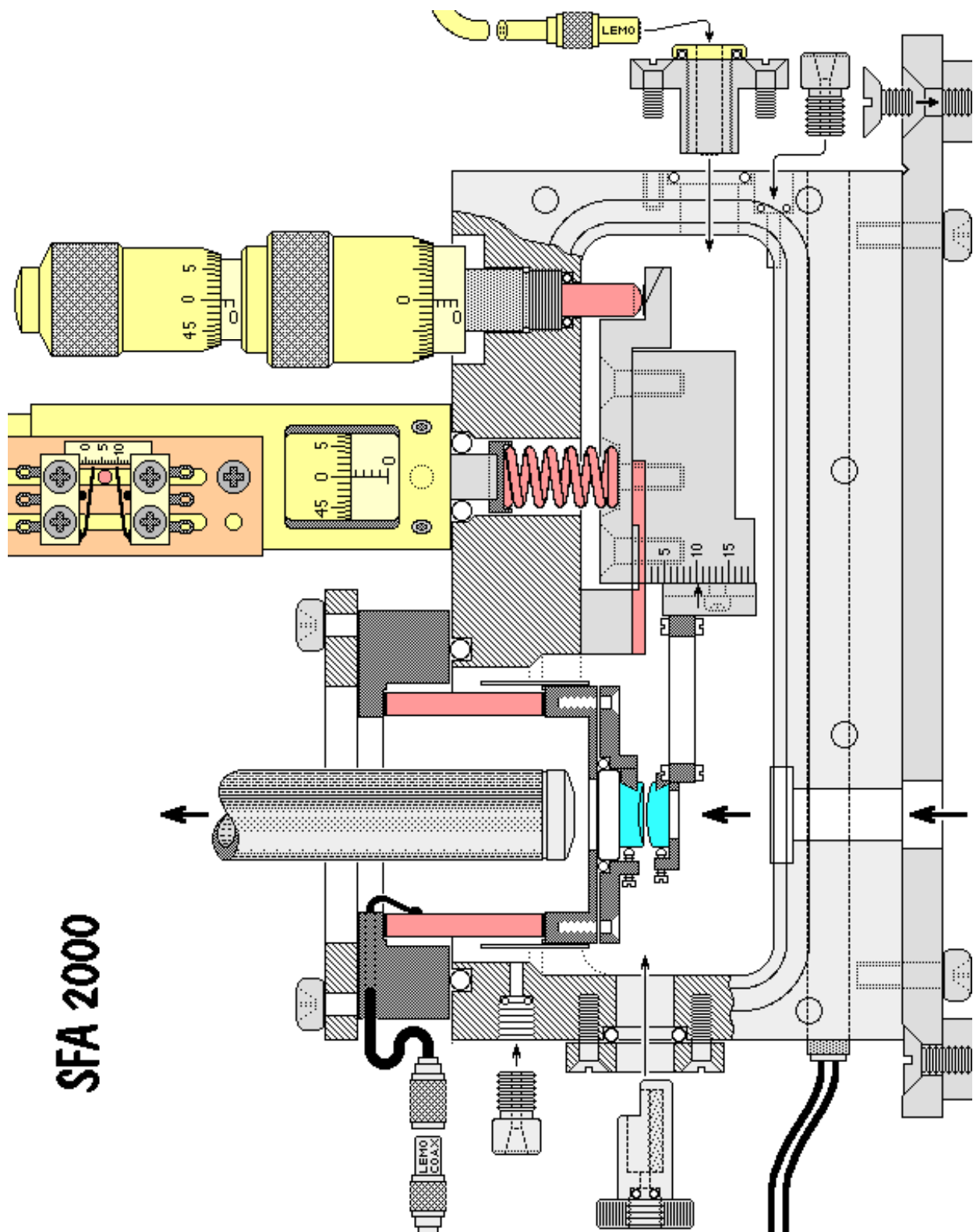


Figure 58 B

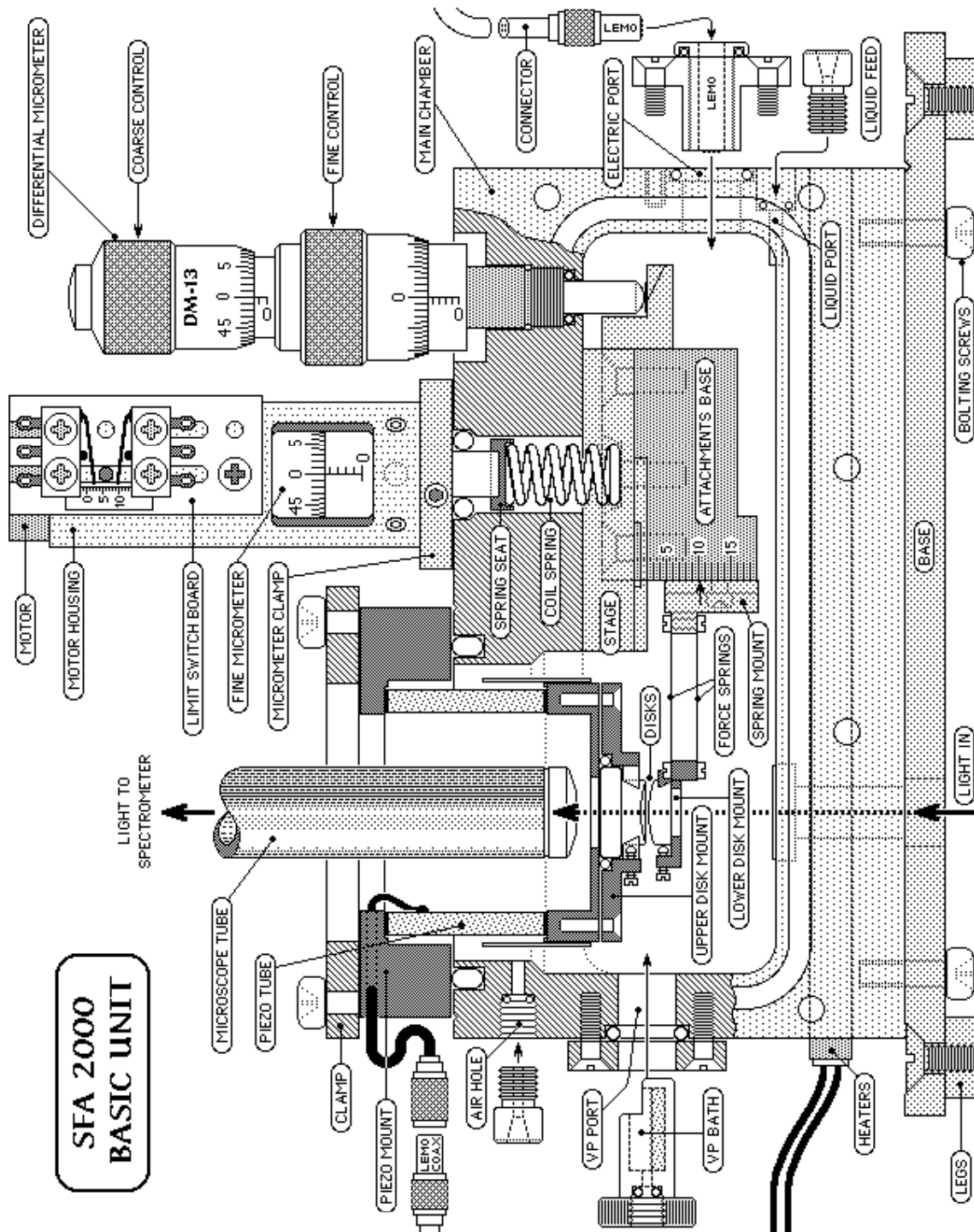


Figure 58 C

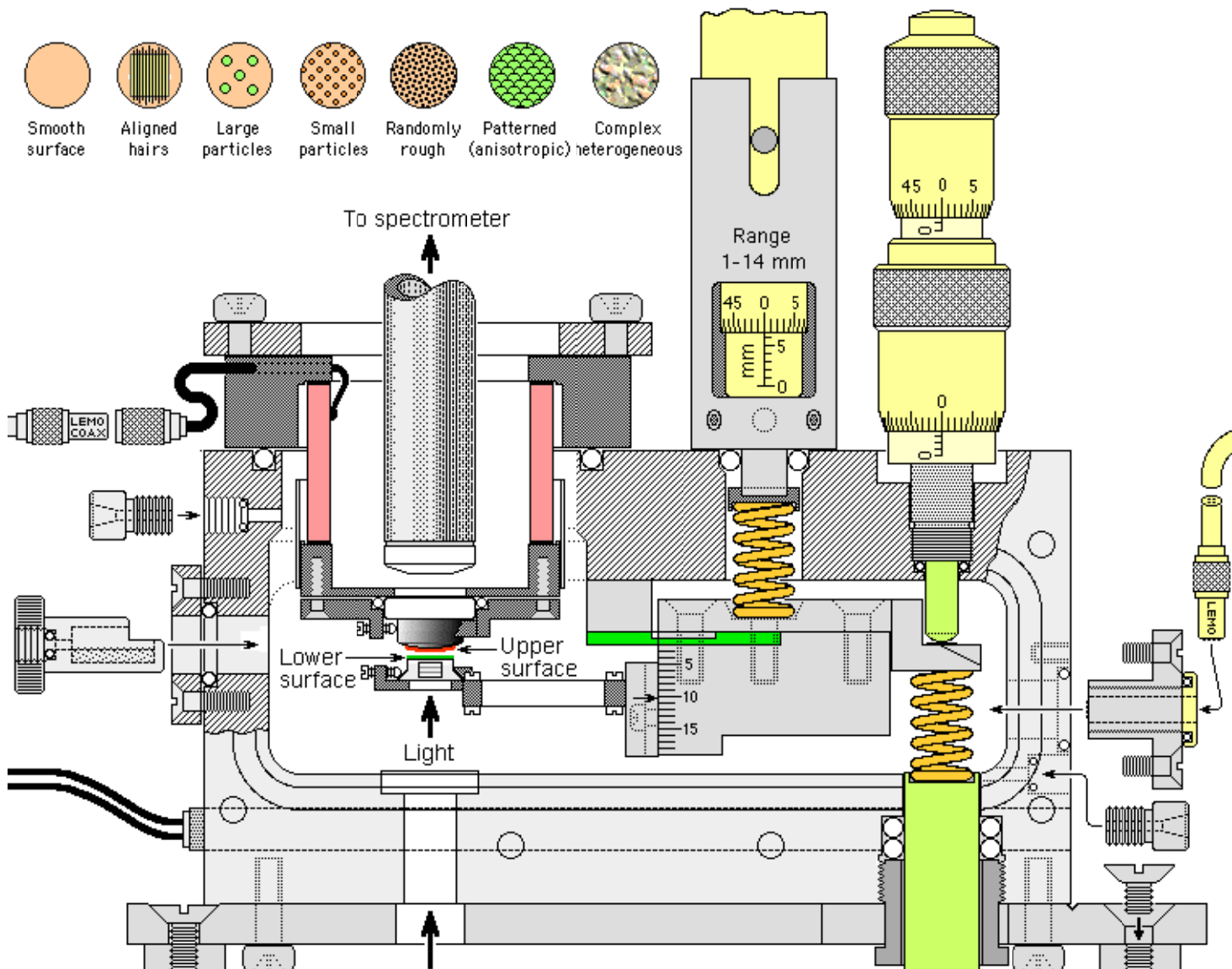


Figure 58 D. Some of the different types of surfaces that can be studied with the SFA 2000.

Figure 58. Three views of the SFA 2000 MAIN CHAMBER, assembled for normal force measurements, showing key parts: location of surfaces, lower support, upper support on piezo mount, base, micrometers, motors, anti-backlash spring, limit switches, electric connections, heaters and vapor pressure bath.

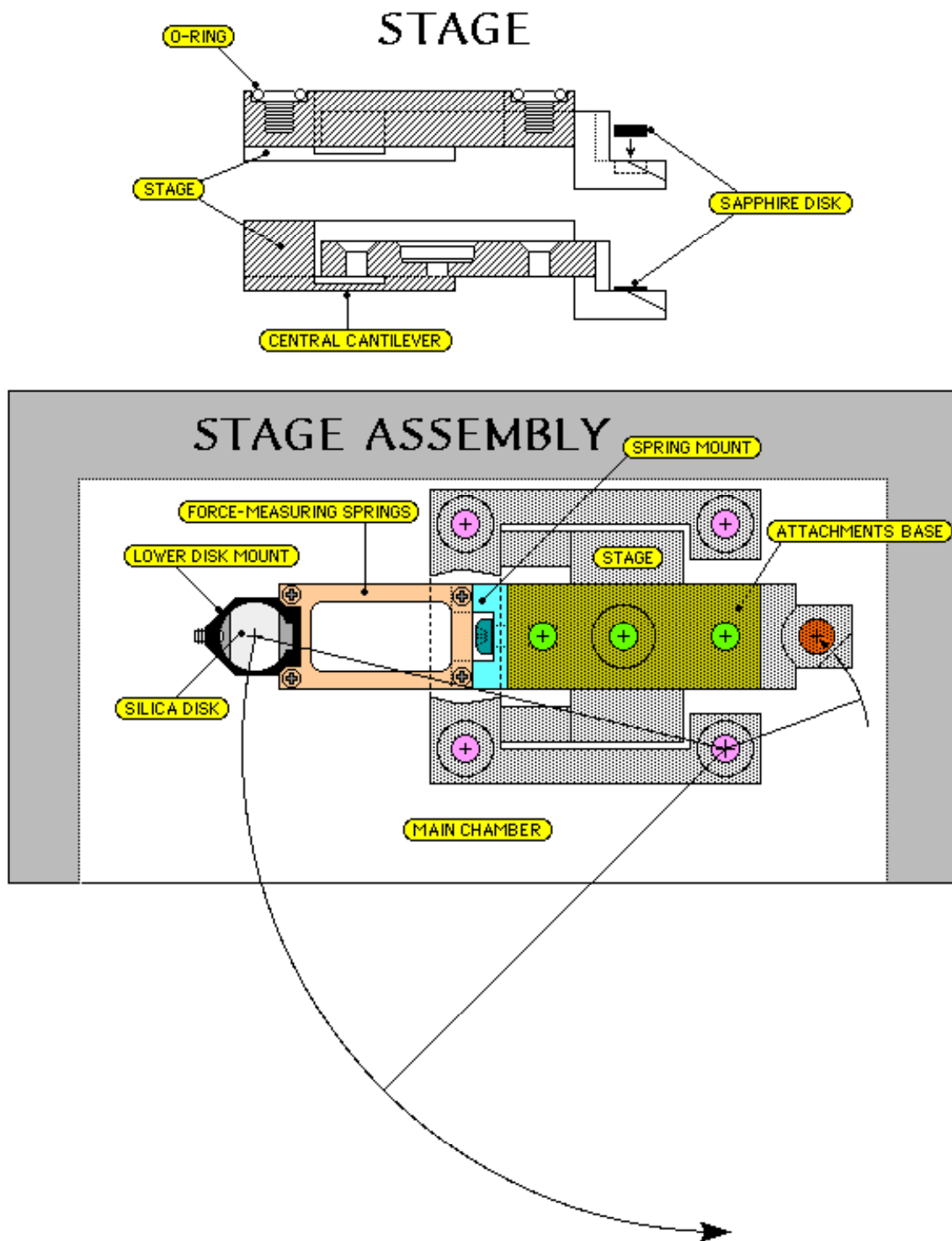


Figure 59. MAIN STAGE. See Fig. 72 for mode of operation of the Central Cantilever spring. Various attachments can be connected to the Main Stage for different types of experiments.

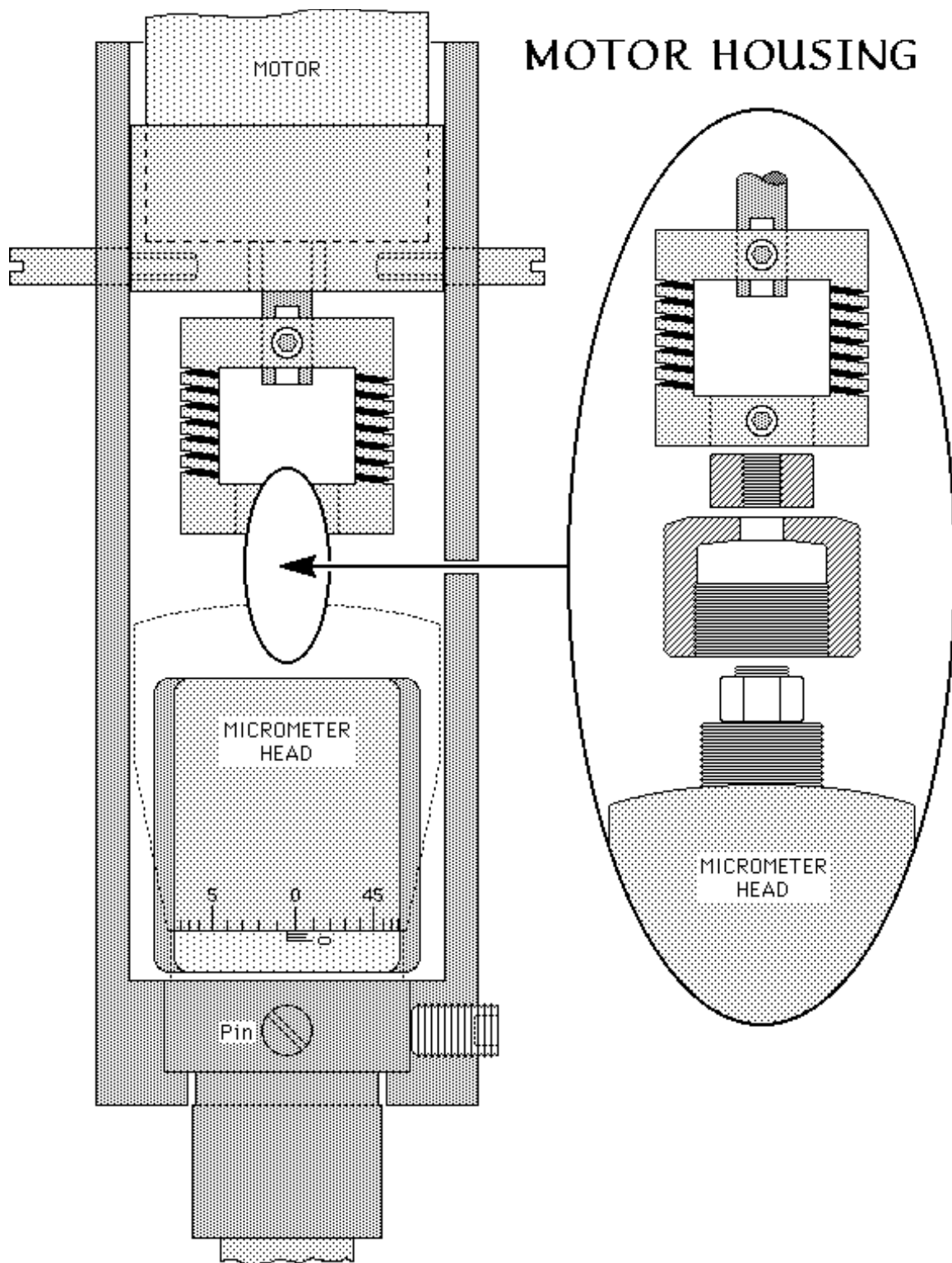


Figure 60. MOTOR HOUSING showing how micrometers are connected to the motor-encoder unit.

LIMIT SWITCHES

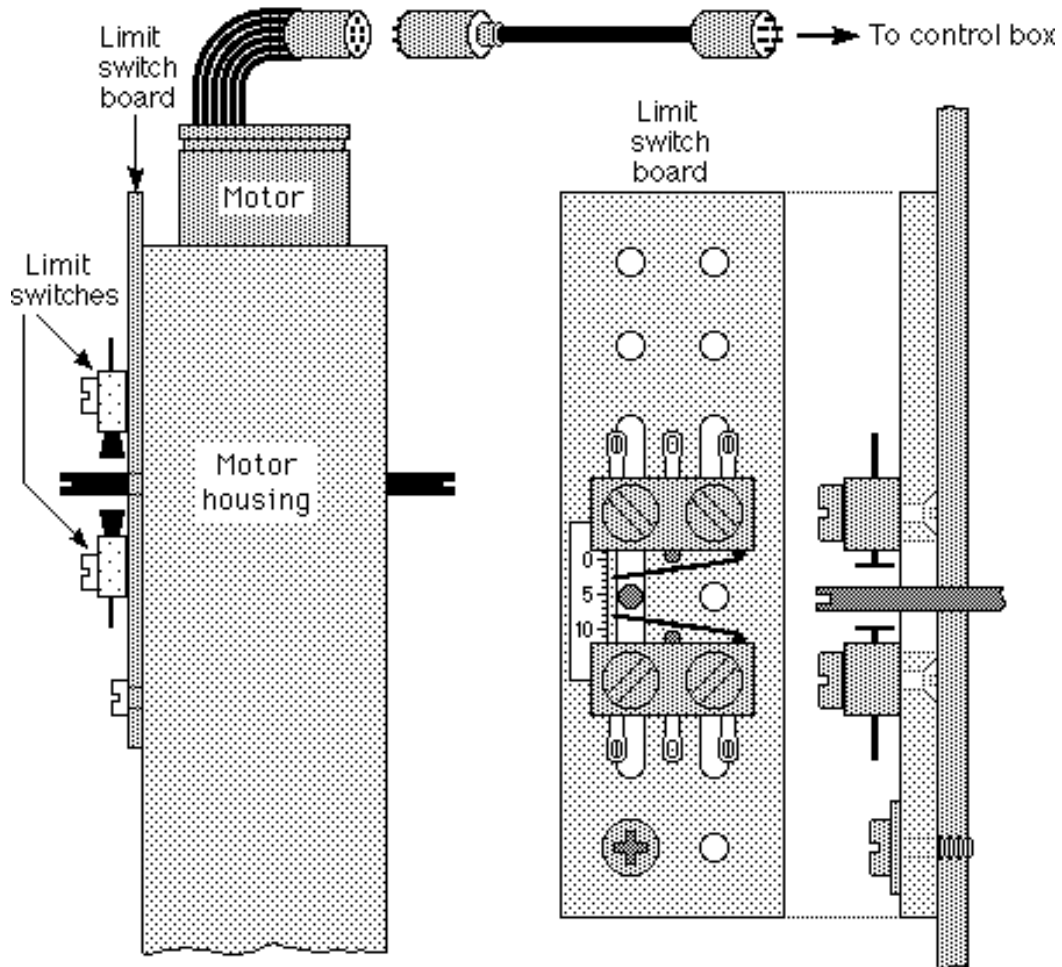


Figure 61. LIMIT SWITCHES on MOTOR HOUSINGS (discontinued).

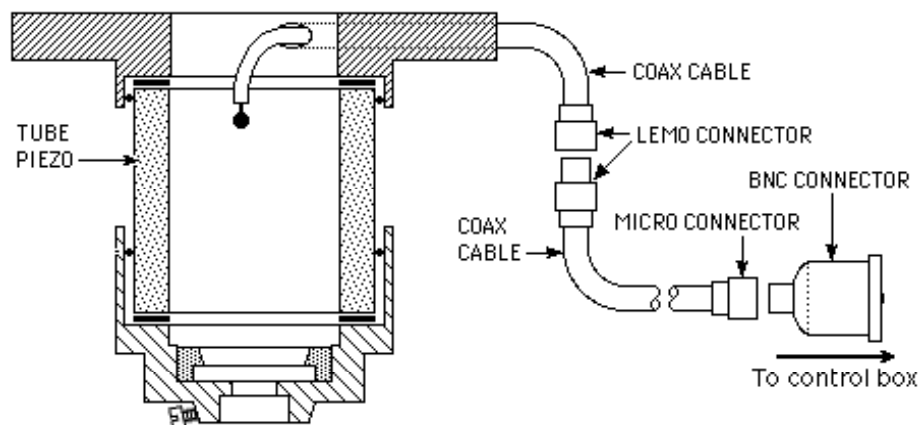


Figure 62. PIEZO MOUNT (fixed type) – one of various designs: other designs have removable/exchangeable disk mounts for both round and dove-tailed disks.

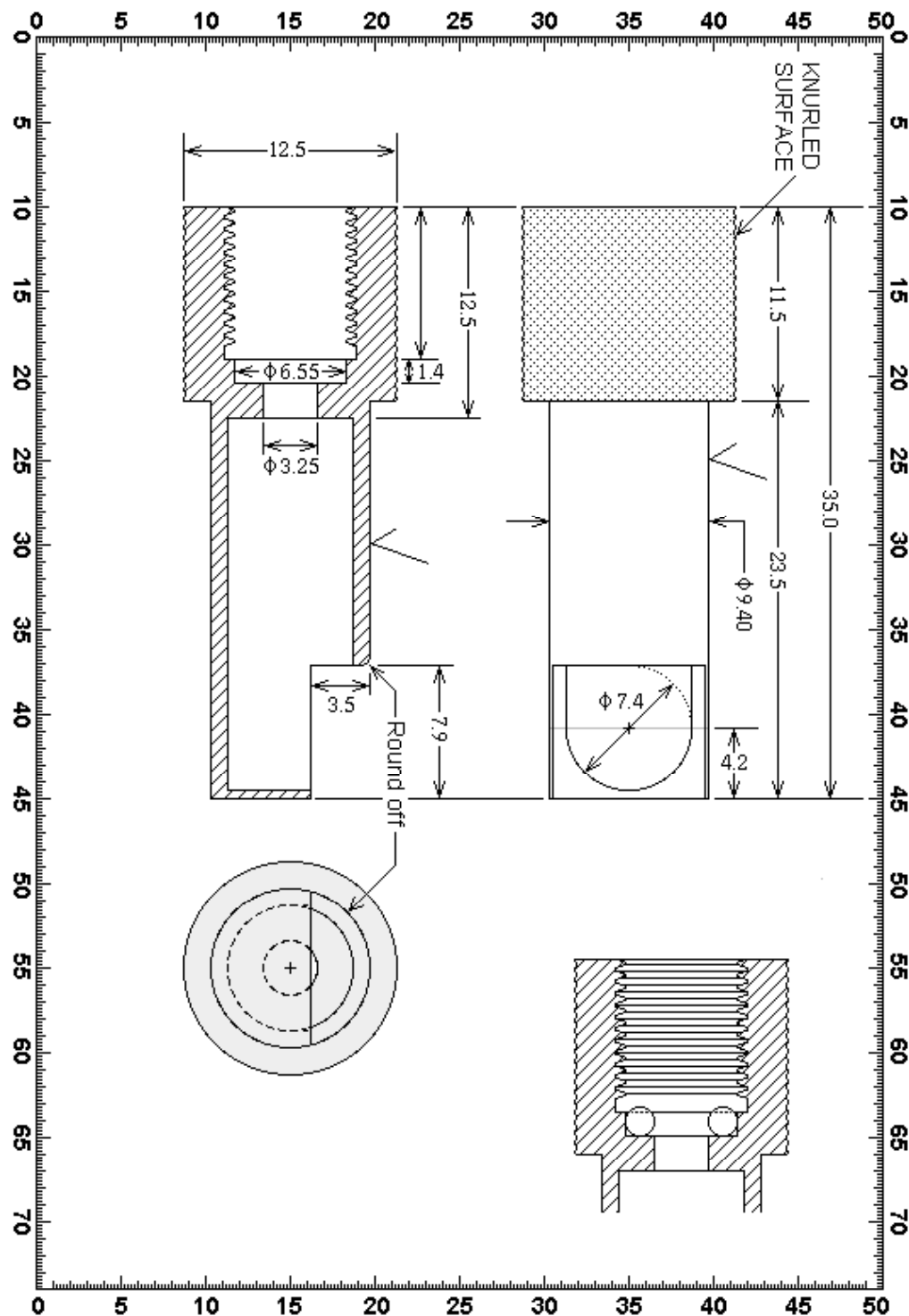


Figure 63. VAPOR PRESSURE (VP) boat/bath for controlling the VP of different liquids in the chamber.

FRONT PLATE

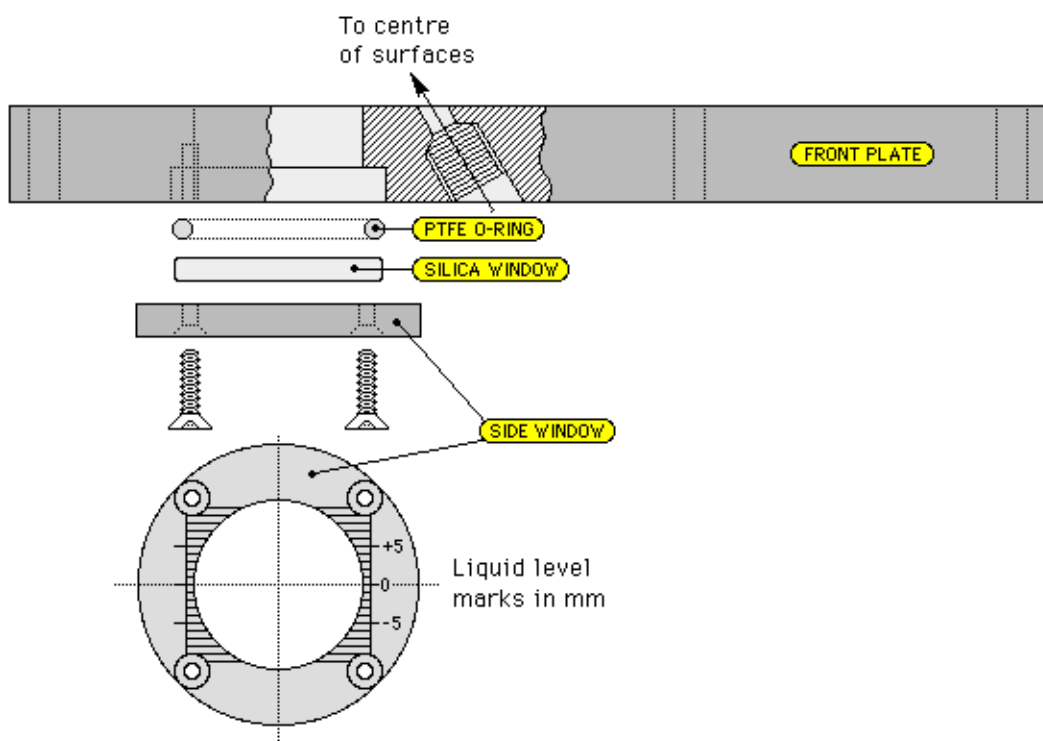
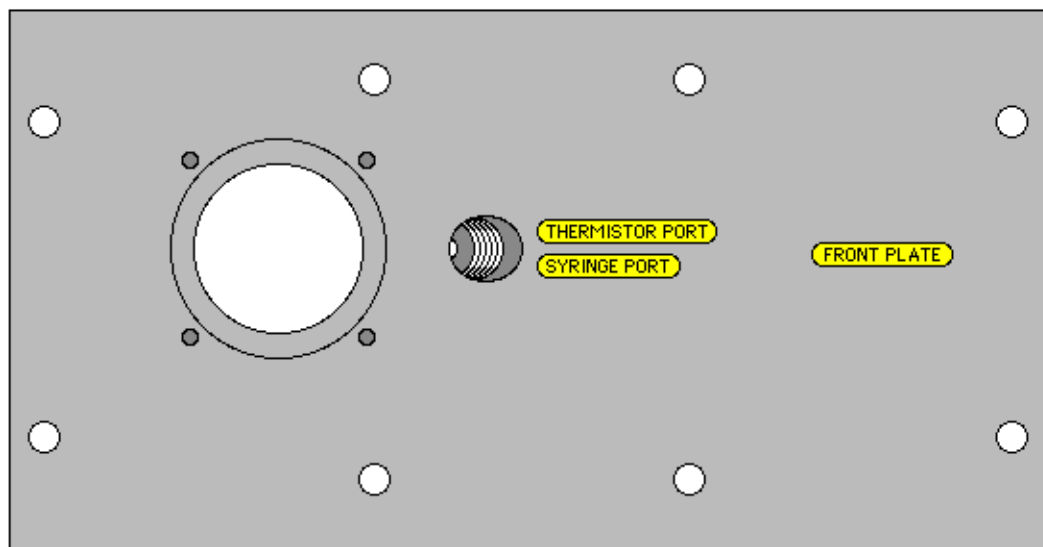
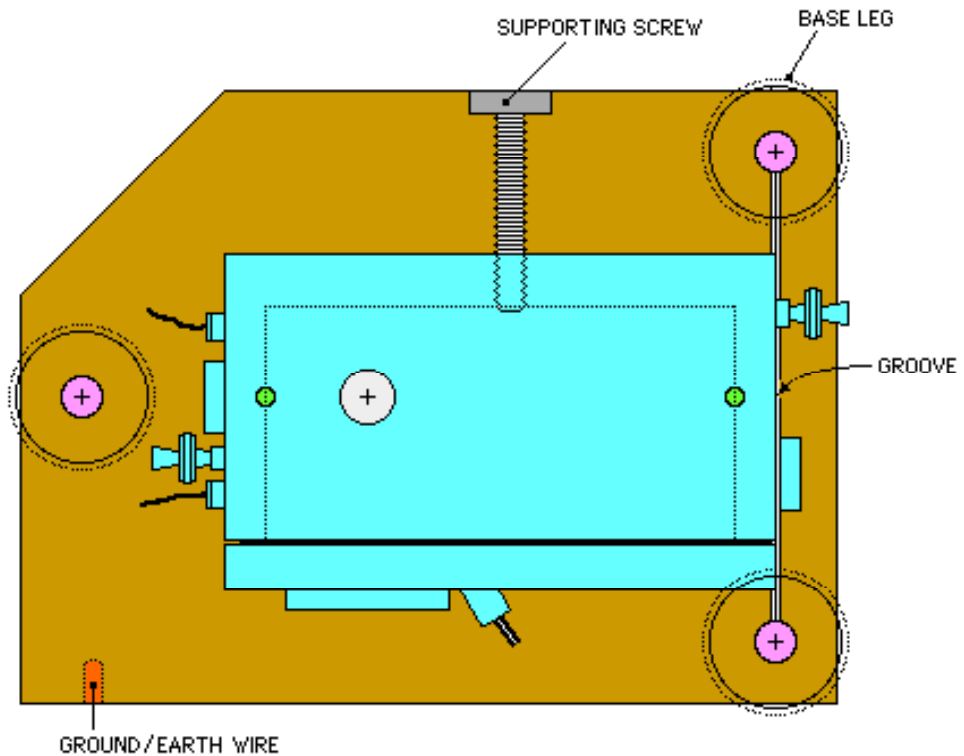
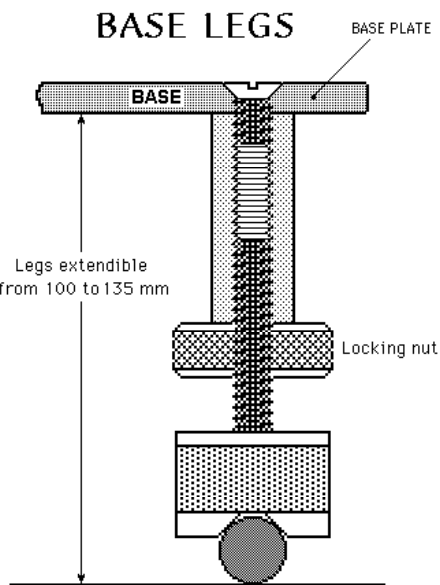


Figure 64. FRONT PLATE with viewing window and thermistor and syringe injection port.

BASE



(A)



(B)

Figure 65. (A) BASE and (B) LEGS. The small screw hole on the front of the base plate is for electrically connecting the apparatus to earth (ground) using the earthing wire supplied.

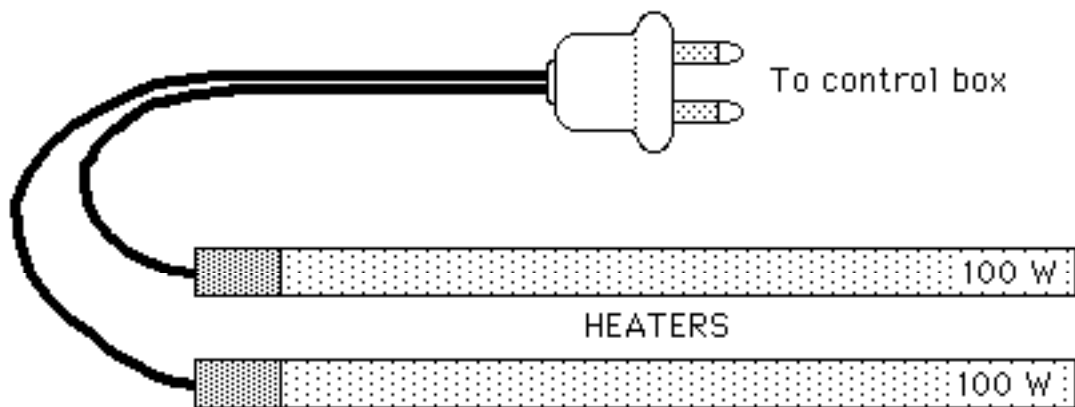


Figure 66. HEATERS for Main Chamber.

OPTICS STAND

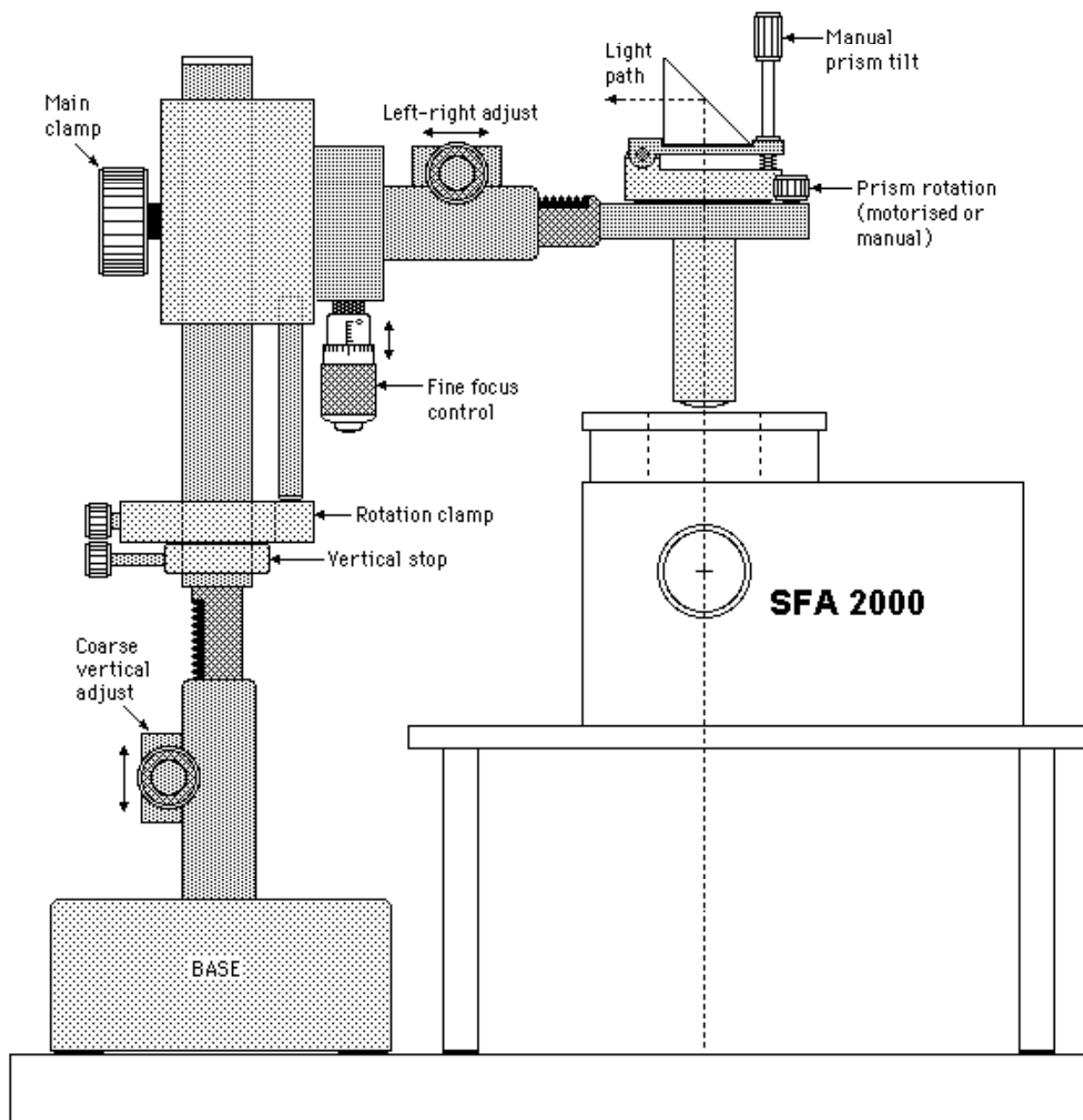


Figure 67. OPTICS STAND.

FRICTION DEVICE

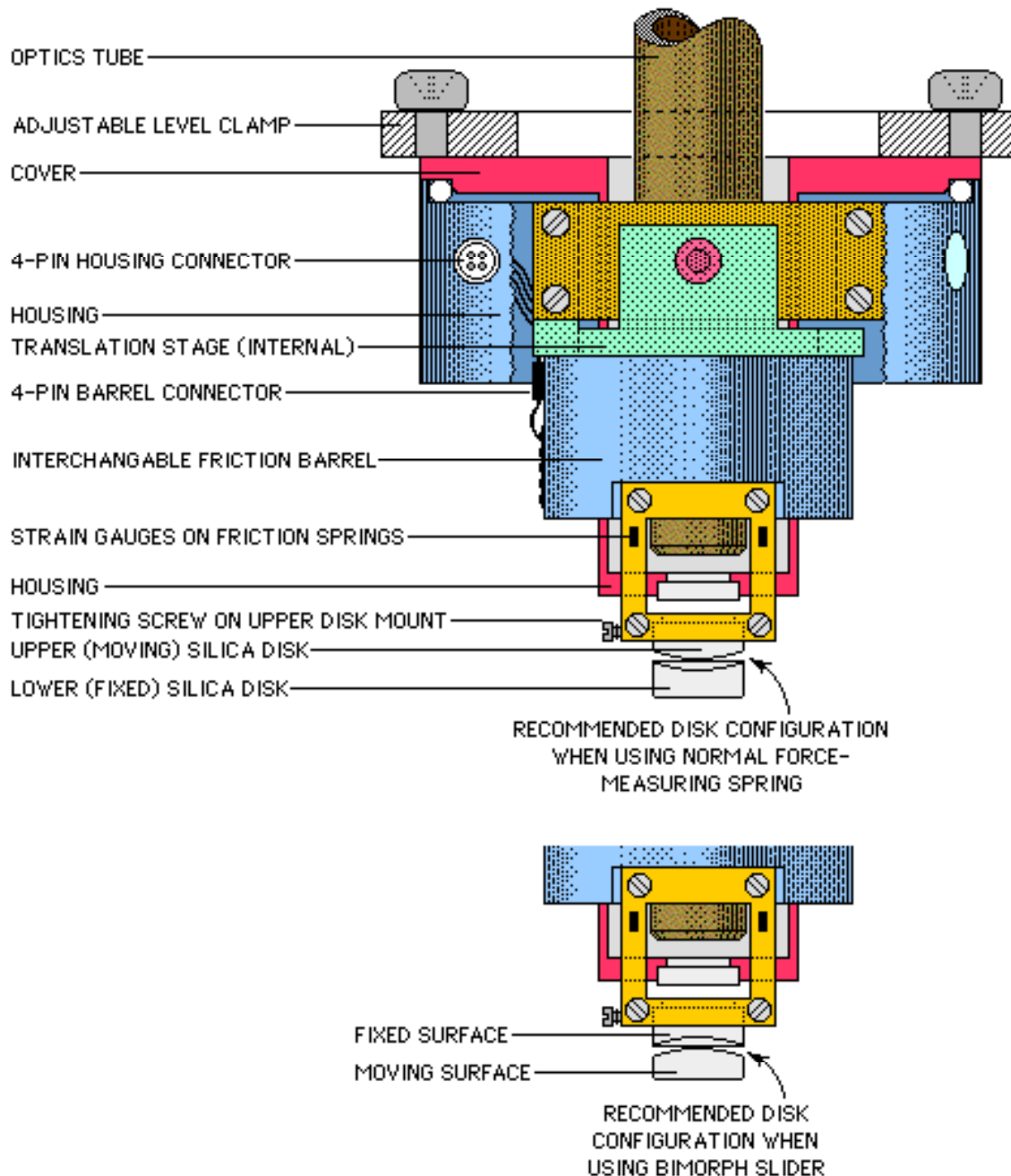


Figure 68 A

**SFA 2000
with FRICTION ATTACHMENT**

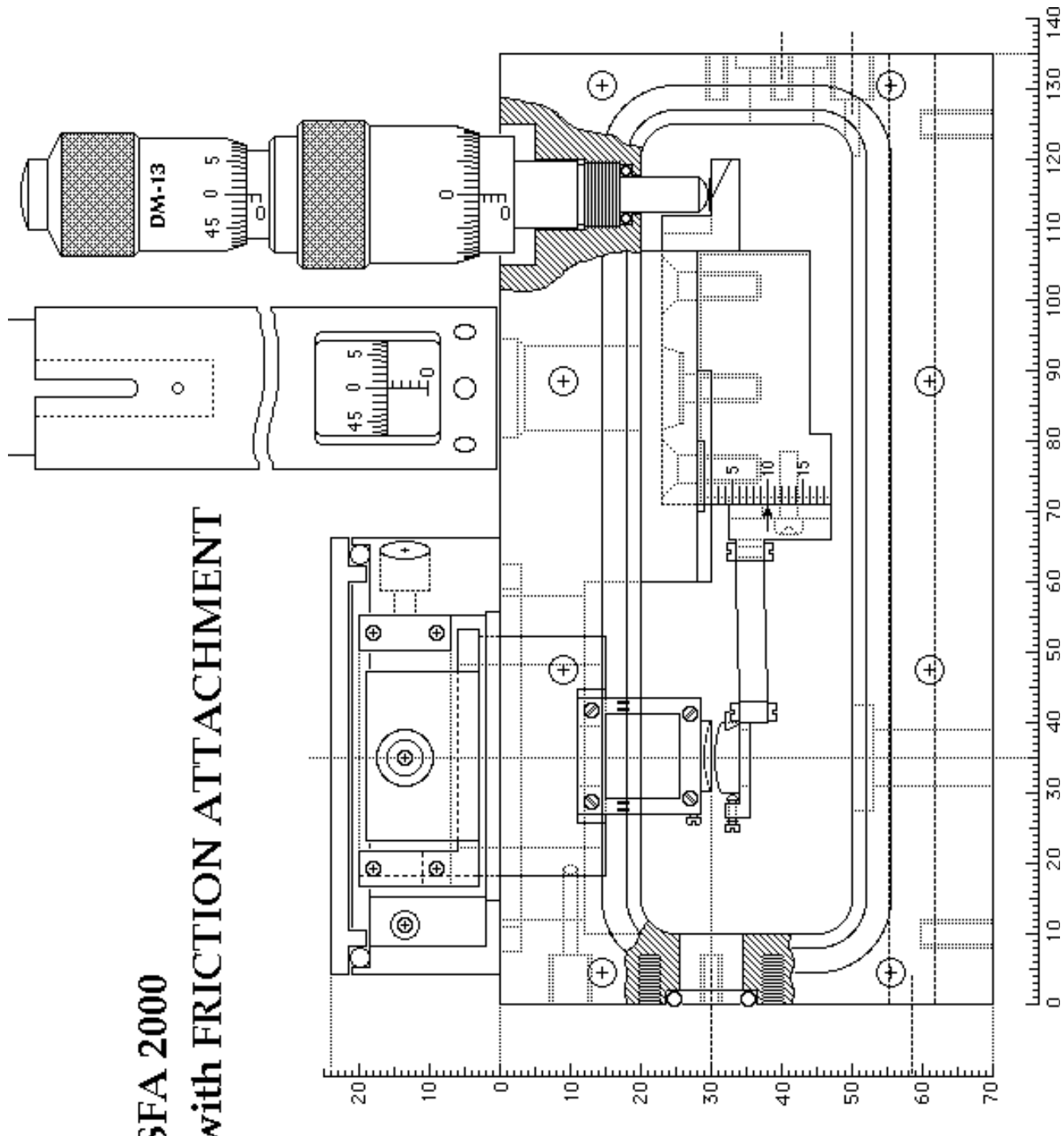


Figure 68 B

Figure 68. Two views of the FRICTION DEVICE. Note the removable/ exchangeable 'barrel' containing the full-bridge strain gauge circuit.

BIMORPH SLIDER 2000

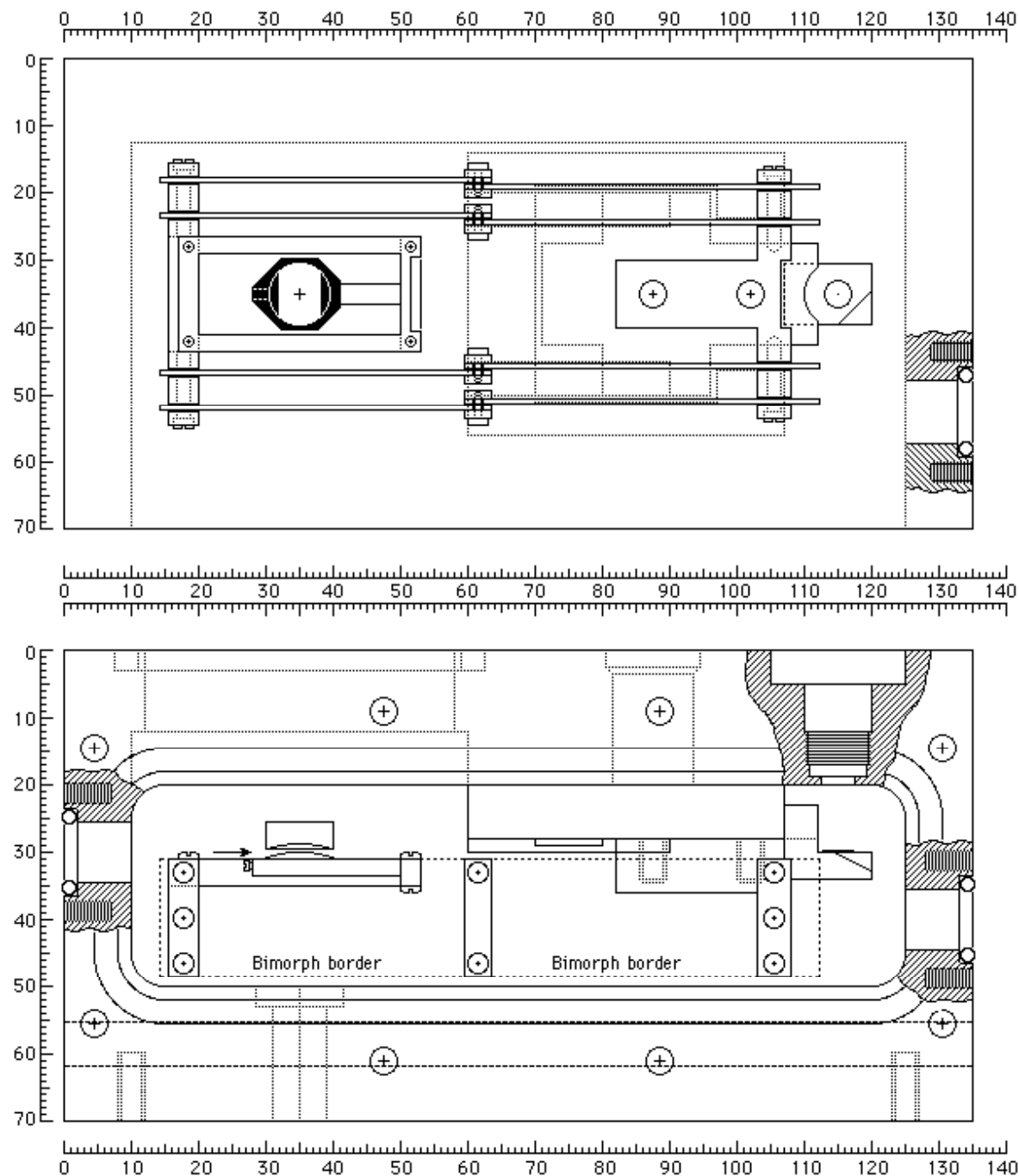


Figure 69 A

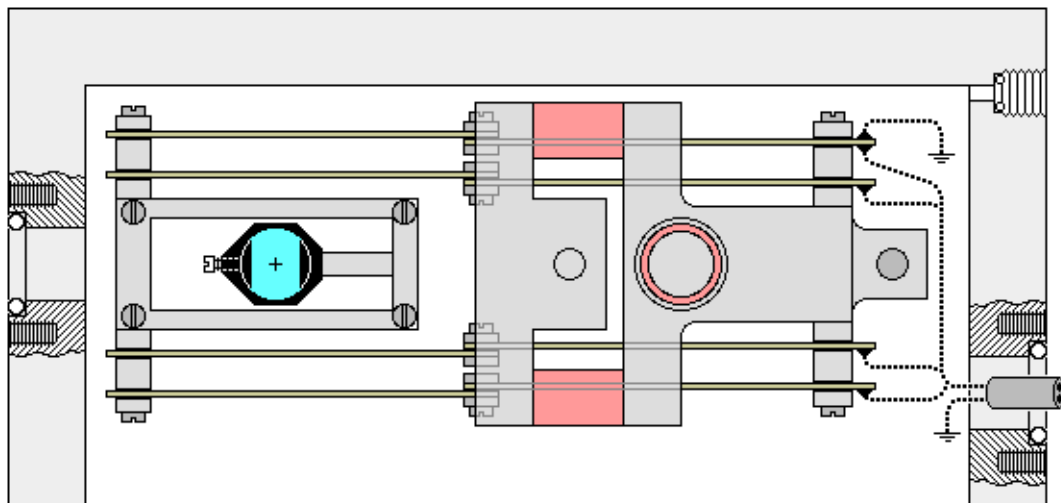
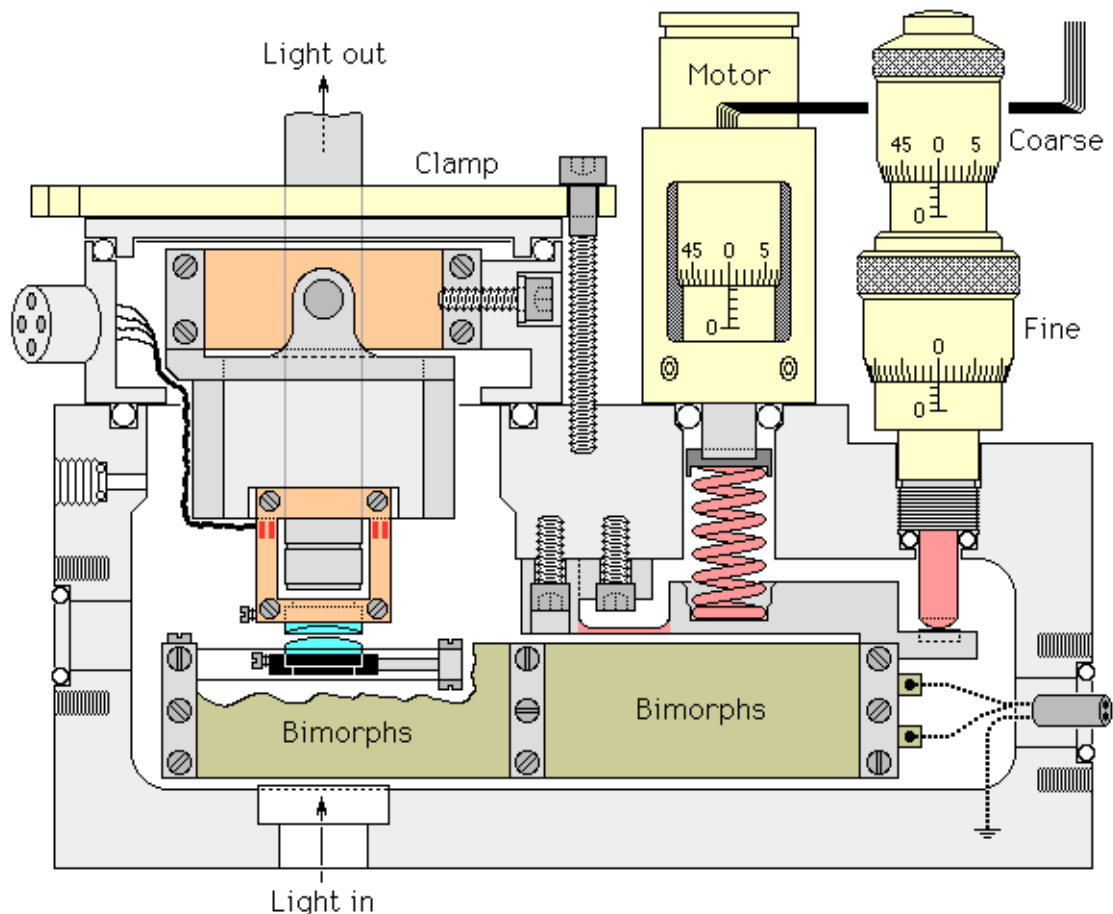


Figure 69 B

Figure 16. Two views of the BIMORPH SLIDER.

BIMORPH VIBRATOR

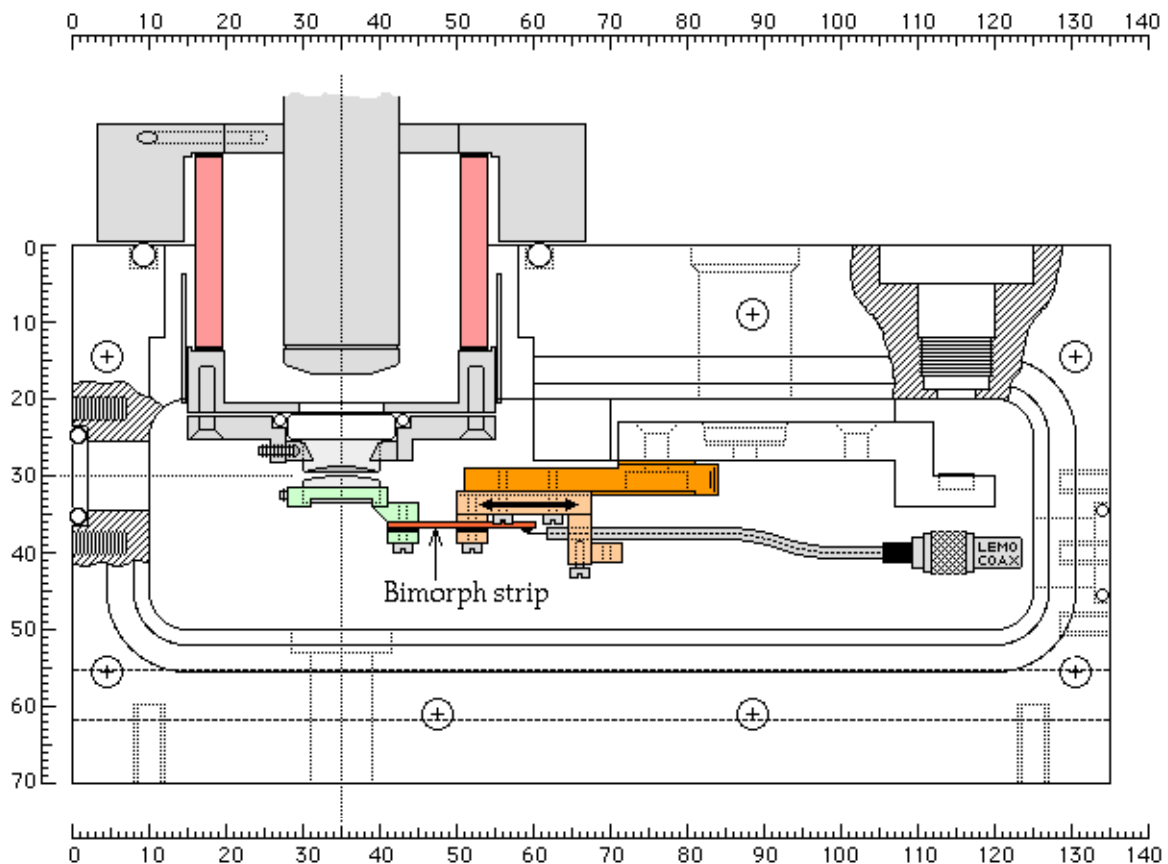
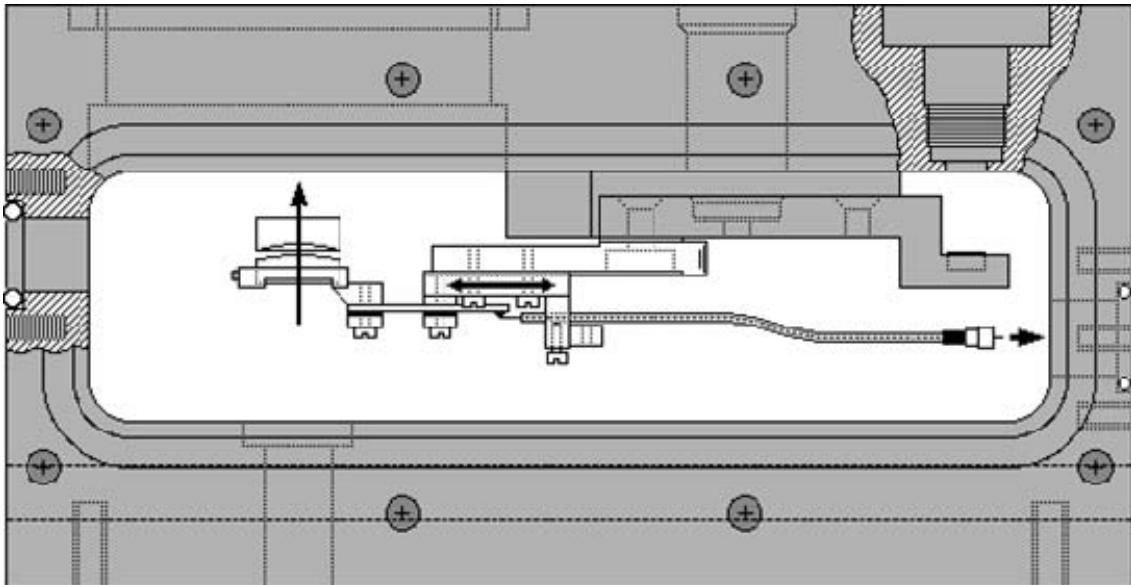


Figure 70 A



BIMORPH VIBRATOR

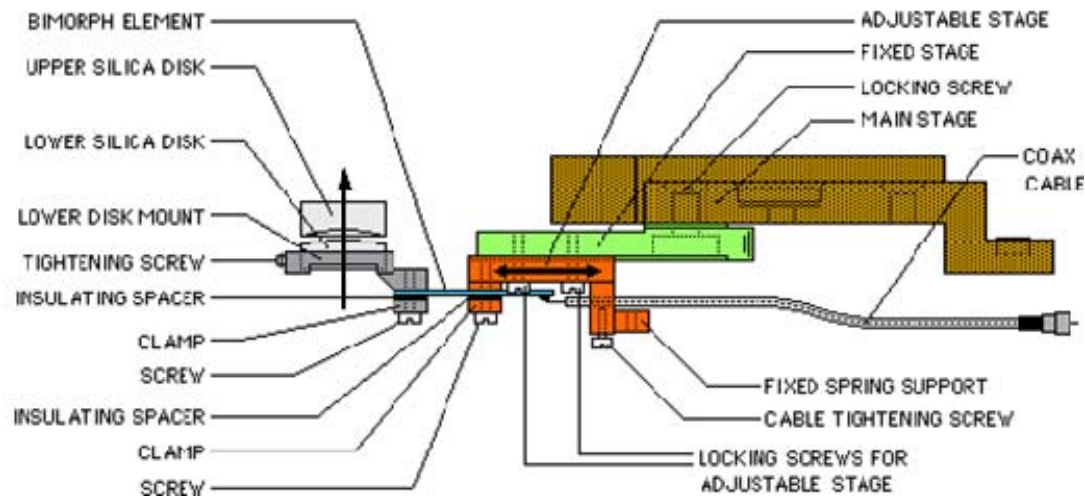


Figure 70 B

Figure 70. Two views of the BIMORPH VIBRATOR.

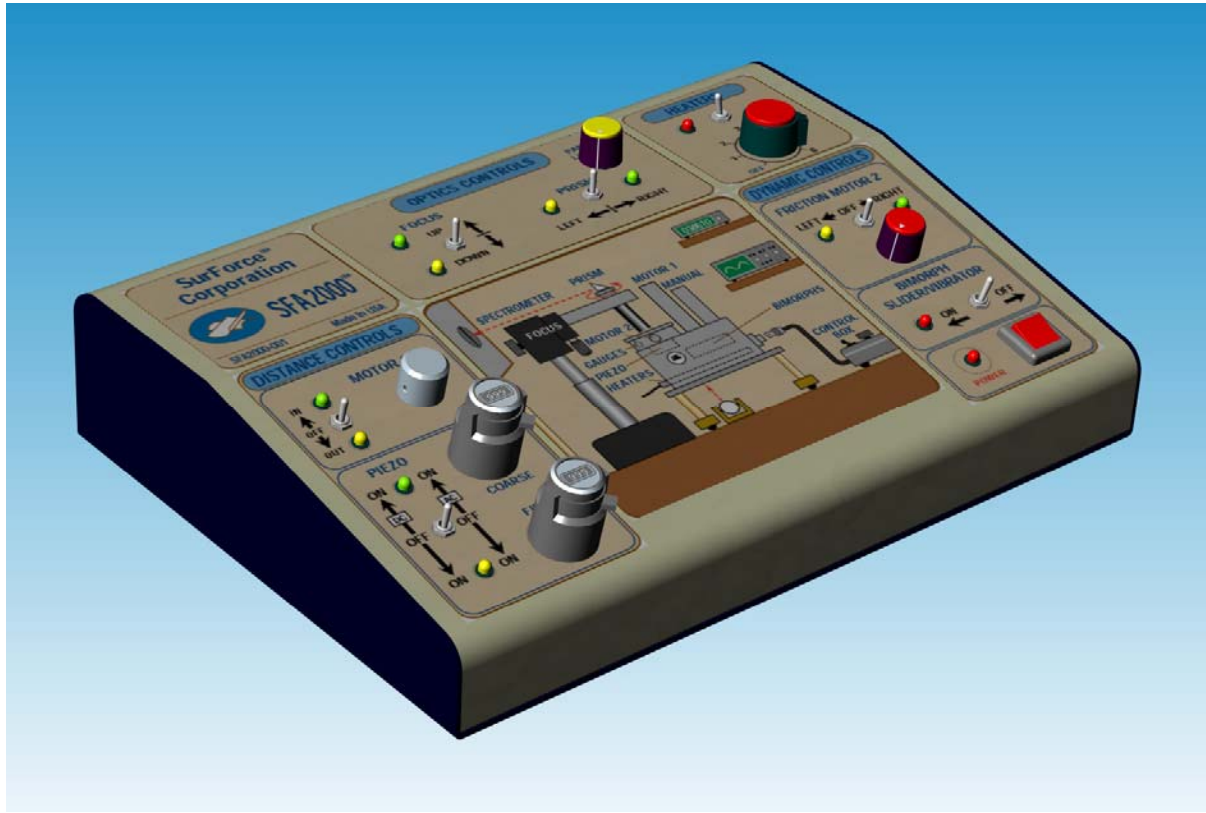


Figure 71 A – CONTROLE BOX / CONSOLE.

Power input and output voltages are 110V @ 60 Hz for the US & Canada, 220V @ 50Hz for Europe, and 100V @ 50 Hz for Japan. Each control box has been adjusted for the local mains voltage supply. See Fig. 71C.

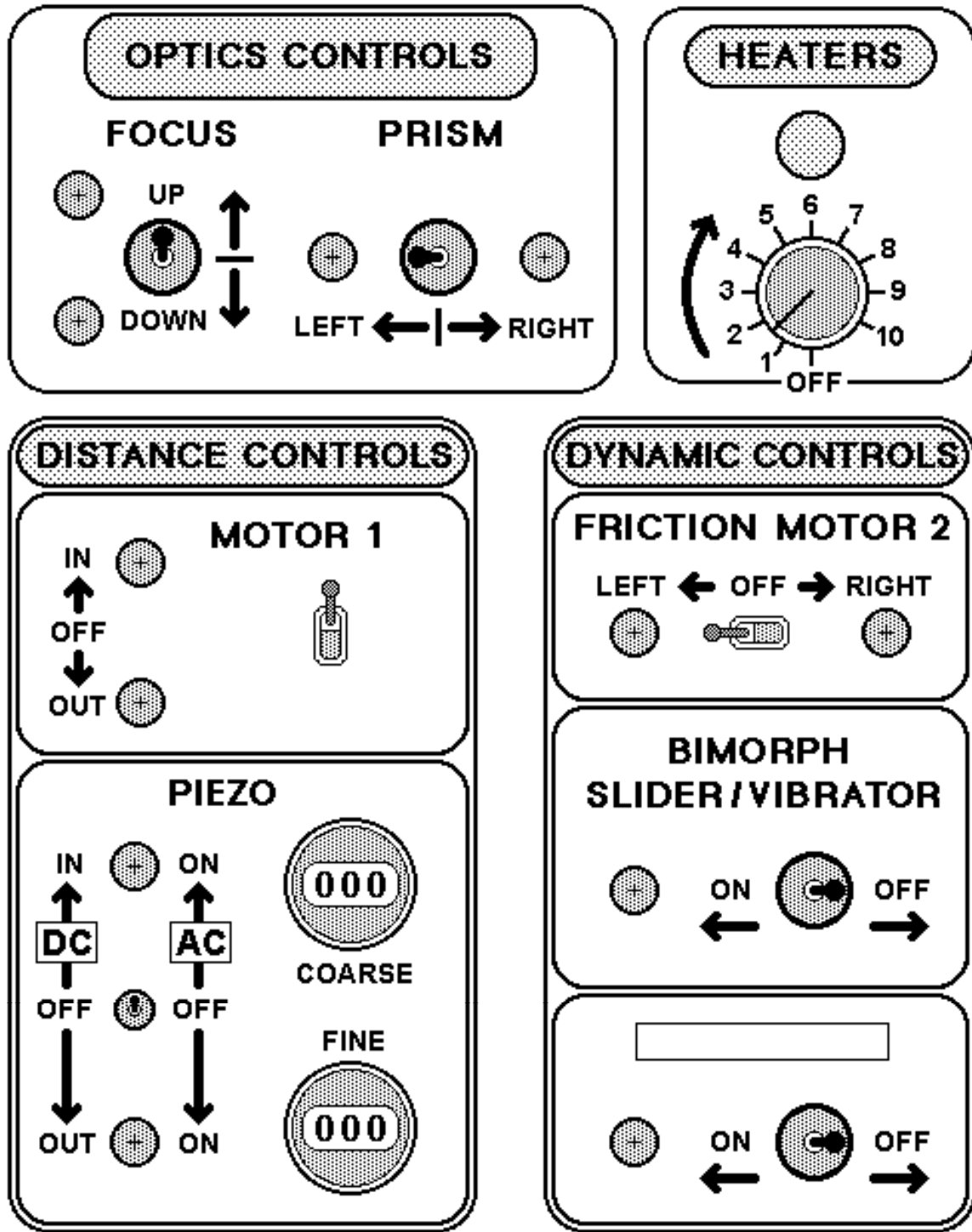


Figure 71B. CONTROL BOX – Front view.

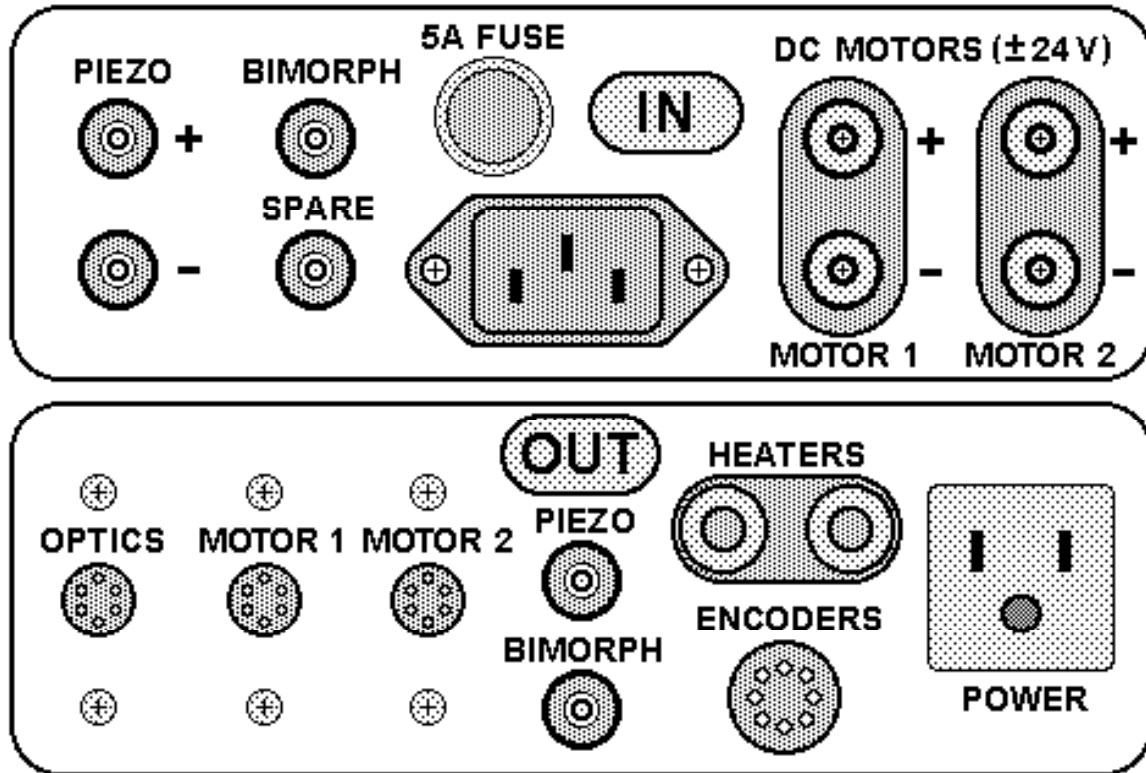


Figure 71C. CONTROL BOX – Back view.

Power input and output voltages are 110V @ 60 Hz for the US & Canada, 220V @ 50Hz for Europe, and 100V @ 50 Hz for Japan. Each control box has been adjusted for the local mains voltage supply.

The SFA 2000 nano-positioning spring system: how it works

The SFA 2000 operates on a different mechanical principle from previous SFAs. In these, two different and independent spring or mechanical translation systems are used in series to produce coarse and fine motion. In the SFA 2000, a single simple-cantilever spring is used for generating both types of motions over a total range of seven orders of magnitude (from millimeters to ångstroms). The crucial element in this design is the short single-cantilever spring on the **Main Stage** (cf. Figs 58, 59 and 72) which allows for two kinds of pivoting motions about the point **P**. When the differential micrometer is moved, the spring **bends** at **P** and the surfaces move by approximately the same amount as the micrometer shaft but in the opposite direction (specifically, the surfaces move by $L\theta$ where L is the distance between the pivot and the surfaces). However, when the **fine micrometer** is used, it compresses the **helical spring** which presses against the **stage**. The right end of the **Stage** remains in contact with the shaft of the **differential micrometer**, and the cantilever spring on the **stage** now **buckles** by a very small amount, **D**, as shown in Fig. 72. The displacement **D** is determined by the ratio of the stiffnesses of the helical and cantilever spring (in buckling mode). The displacement of the surfaces is approximately equal to $2D$. In this way, by sequentially using the **differential** and **fine micrometers**, the surfaces can be moved with an accuracy of $\sim 1\text{\AA}$ over a range of $\sim 5\text{ mm}$. **Helical springs** having different stiffnesses can be used to increase or decrease the distance control resolution of the **fine control micrometer**; however, the finer the movement the shorter is the full range of travel of the surfaces using this micrometer.

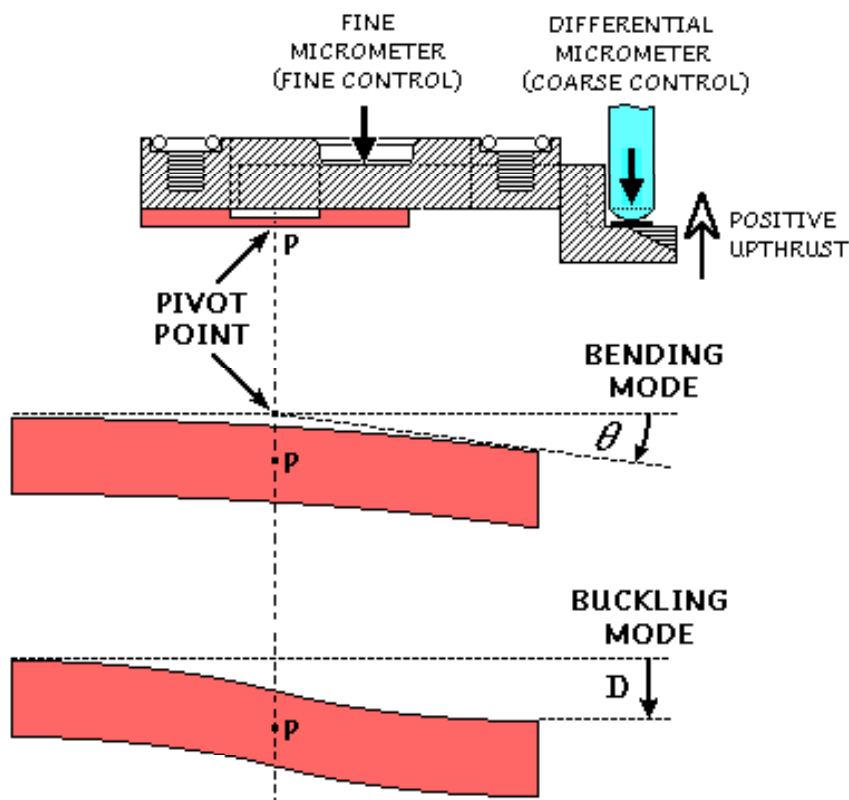


Figure 72. Mode of bending and buckling of the main (Central Cantilever) spring on the Stage (Fig. 59) for controlling the displacement of the lower surface.

ASSEMBLY OF THE BASIC UNIT FOR NORMAL FORCE MEASUREMENTS

This section should be read in conjunction with viewings of the videos describing the assembly and operation of the SFA and its attachments.

Tools required

Depending on which attachments are to be assembled, the following small tools and glassware will be needed for cleaning and assembly. Before proceeding, make sure that all parts and tools are clean and ready for use inside a laminar flow cabinet (see Cleaning section).

SFA 2000 supply items, assembly tools, ‘nuts & bolts’, electric cables.

Luer fittings and stop-cocks for inlets and outlets.

Syringes and needles.

Thermistor.

Micrometers in their housings.

O-rings.

Screws, nuts and washers.

Spatulas (both Teflon-coated and stainless-steel).

Various miniature cleaning brushes (toothbrush-type, pipe-cleaning type).

Screw drivers, including Philips-head, hex-head and nut-head types.

Allen keys: metric and English.

Stainless steel and Teflon-tipped tweezers and forceps – various sizes & types.

Spanners and wrenches.

Ethanol (clean liquid in sealed bottle or squirt bottle). Acetone.

Ethanol gun (pressure rinser).

Air gun: compressed clean dry nitrogen gas gun (compressed gas should come from liquid nitrogen tank, not compressed gas cylinder, and all connecting tubes should be made of clean Teflon tubing or stainless steel).

Beakers: 2 large flat-bottomed (6" or 15 cm diameter).

Beakers: 8 small (100-200 ml).

Petri dishes (can also be used as beaker covers).

Beaker covers for all of the above (petri dishes will do).

Lint-free absorbing tissues.

Make sure that all apparatus parts, assembly tools, O-rings, screws, etc., needed for the assembly are clean, dry and placed ready for handling inside a laminar flow cabinet. Check in advance that you have the right screws for each part (in particular their length and head type – see Fig. 73). Newly machined parts and screws may sometimes be difficult to fit together or screw into. This may be because a small piece of metal (burr) is still lodged in a hole or thread or screw head. Rather than force the parts together, use a small needle file or de-burring tool to remove such pieces of metal until the parts fit together smoothly.

Base and legs (Figure 65)

Attach the three legs into the base plate using the three 4 mm flat-head socket head screws. Screw in hexagonal coupling nuts, circular knurled thumb screws and rubber & ball-ended legs. Place base on flat table and adjust height (checking the level using the spirit level). You may adjust the level and height of the base plate by turning the coupling nuts on the legs and tightening with the circular knurled thumb nuts. Later, clamp or screw in the three ‘kinematic’ mounts to your experimental table using threaded machine screws or wood screws so that the base will always settle at precisely the same place each time you put it down (place mount with round conical hole at far right, the V-grooved mount at middle left, and the flat mount at the near right for the near-right leg). When positioning the SFA chamber and base, place the far-right leg down first, then swing the left leg into place and finally lower the front right leg.

Assembly of SFA main chamber

Figure 58 shows an assembled **Basic Unit** ready for normal force measurements. The following text, figures and photographs describe the assembly and operation of each part. Consult the videos and this manual for visual and more in-depth details of the theory and practice of SFA measurements.

Figure 58 also shows top and side views of the **Main Chamber*** (or simply **Chamber**), where important holes and parts are highlighted in different colors. Before proceeding, it is best to mount the **Chamber** on the **Base**, shown in Fig. 65. First, mount the three **base legs** to the under-side of the **base plate** as shown in Fig. 65B, and tighten the **locking nuts** with the plate height adjusted to be mid-way between maximum and minimum. The **Chamber** can now be placed on top of the **base plate** and bolted securely into place from the under-side with two screws (through the two small green holes in Fig. 65A). Tighten the **supporting screw** into the hole at the back of the **Chamber**, as shown in Fig. 65A. This allows for the whole unit to be placed on its side, which is useful for certain operations, such as filling the chamber up with water. Test this.

Stand the unit upright. Referring to Figs 57 and 59, connect the two **Force-Measuring Springs** to the **Lower Disk Mount** at one end and to the **Spring Mount** at the other (using 4 small screws at each end).

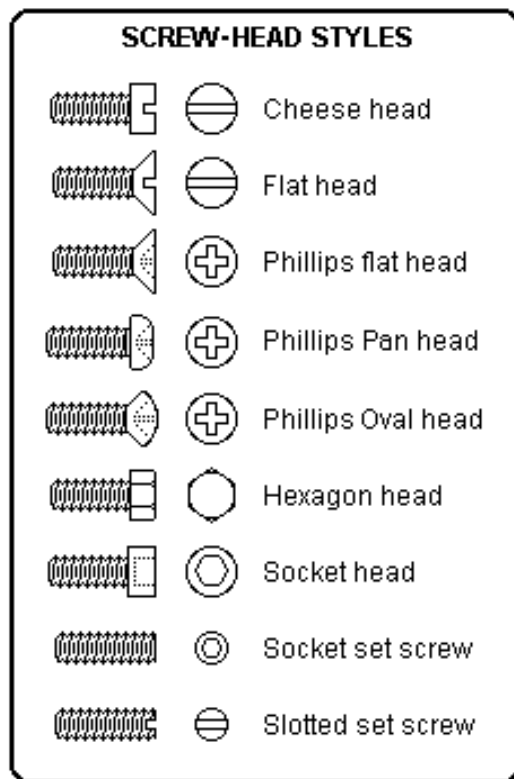


Figure 73. Types of screw heads used in the SFA.

You may adjust the level and height of the base plate by turning the coupling nuts on the legs and tightening with the circular knurled thumb nuts. Later, clamp or screw in the three ‘kinematic’ mounts to your experimental table using threaded machine screws or wood screws so that the base will always settle at precisely the same place each time you put it down (place mount with round conical hole at far right, the V-grooved mount at middle left, and the flat mount at the near right for the near-right leg). When positioning the SFA chamber and base, place the far-right leg down first, then swing the left leg into place and finally lower the front right leg.

* Words in **bold** signify parts or labels that appear in the figures.

Connect the **Spring Mount** to the **Attachments Base** with the arrow at height level 10.0 (using the adjustable screw) as shown in the figure, and the **Attachments Base** to the **Stage** (using 3 screws through the green holes in Fig. 59). Ensure that the **sapphire disk** is in place. Place 4 O-rings in the counter-bored recesses on the **Stage** (purple holes in Fig. 59), and position the whole **stage assembly** inside the **Chamber** with these four threaded holes located under the four purple clearance holes as shown in Fig. 58A. Insert the four screws into these holes and tighten the **stage assembly** in place. Note that by removing three of these screws and loosening the fourth (on the lower right of Fig 58A or 59), the whole assembly can be swung in and out of the **Chamber** as illustrated in Fig. 59. This allows for **silica disks** and certain other **attachments** to be inserted and removed (however, this operation is not necessary for inserting or removing the **lower silica disk**, as will be described later). Figure 59 also shows the path taken by the center of the **silica disk** when the **stage** is swung out of the **Chamber**.

With the stage assembly bolted firmly in place, insert an O-ring into the hole of the **Differential (manual) micrometer** (red hole in Fig. 58A), and screw in the micrometer. Make sure that it is fully inserted, i.e., that it presses against the O-ring. Tighten *gently* by holding it only on the main body near the shaft. Rotate the **coarse control micrometer** (see Fig. 58C) until the **force-measuring spring** is roughly horizontal, and test that it responds to vertical coarse movements of up to 2 mm on either side of this ‘zero’ level (the vertical displacement of the **lower disk mount** should be exactly the same as that of the **differential micrometer**). Test that both the coarse and fine micrometer controls function smoothly, although there may be some ‘running in’ after a new O-ring has been inserted. If the movement appears to be too stiff, causing jerky motion, slightly relieve the micrometer tightness.

Position the **force springs** roughly horizontally. Place a **silica disk** into the **lower disk mount** and secure it in place by tightening the small Kel-F tipped screw using a Philips or hex head screw driver passed through the **Vapor Pressure (VP) Port** hole on the left side of the **Chamber**. Assemble the **Piezo Mount** as indicated, and insert an oval **O-ring** into the deep O-ring groove on top of the **Chamber** (white circular band in Fig. 58A). Insert another **silica disk** into the **upper disk mount** of the **Piezo Mount**, and place the latter through the piezo opening in the **Chamber** so that the two silica disk surfaces come close to contact; avoid actual contact at this stage by ensuring that the disks are not too thick – 3.5 mm should be about right – or by adjusting the level of the lower surface with the **coarse control** of the **differential micrometer**. If necessary, adjust the height of the **spring mount** with the **adjusting screw** so that the **force-springs** are roughly horizontal when the surfaces are just about to touch, i.e., about to come into contact. This adjustment will depend on the heights (thicknesses) of the **silica disks** in the upper and lower mounts. Note the optimum position of the engraved arrow in relation to the thickness of the two disks for future reference.

Cover the **Piezo Mount** with the four-hole **clamp** and tighten the unit in place with 4 screws threaded into the yellow holes of Fig. 58A. Make sure that the tightening process does not force the surfaces into contact. By differently adjusting the tightness of the four screws the angle of the **clamp** and, therefore, the upper surface can be changed by up to 1-2 degrees away from the horizontal along any axis in the x-y plane. This is useful when positioning and aligning the two surfaces, especially prior to a ‘friction run’. Connect the **piezo coax cable** to the **control box**.

Assemble the motorized (left) **fine micrometer** and **limit switches** (Fig. 61). Bolt the micrometer to the **micrometer clamp**, pass an O-ring through the shaft (some units may require a washer before the O-ring), and press the **spring seat** into position at the end. Rotate the **micrometer head** until the **spring seat** is about 7 mm from the O-ring. Press fit a **coil (helical) spring** onto the **spring seat** recess (making sure that the coil is coaxial with the shaft) and insert the unit through the brown hole in the **Chamber** (Fig. 58A). Tighten the **micrometer clamp** (Fig. 58C) in place *gently and evenly* with two screws threaded into the

green holes on the **Chamber** on either side of the brown hole (Fig. 58A). Make sure that it is vertical. Test for ease and smoothness of rotation (this should be done either manually or electrically at each stage of the assembly). Insert the anti-backlash spring shown schematically in Fig. 58D and tighten it by hand at an appropriate height.

The full range of travel of the **fine (motorized) micrometer** is about 15 mm. Test and establish this range in your apparatus, and then position the **limit switches** with the various adjusting screws so that the **motor** cannot be driven beyond this range in either direction. For remote (electric drive) operations of the **fine micrometer**, connect the Motor 1 cable to the **control box** (Fig. 71) and to one of the display counters (the other display counter is for the friction motor drive, Motor 2).

Assemble the **Front Plate** as shown in Fig 64. The threaded hole on the right side of the **window** is both for **syringe injection** and for the **thermistor** temperature sensor. It can also be plugged if not needed. Insert O-ring around thermistor or plug before screwing them on. This hole points towards the center of the surfaces. The **front plate** is attached to the **Chamber** with eight screws bolted into the 8 green holes shown in the lower panel of Fig. 58A.

Before filling the **chamber** with liquid or purging with clean inert gas, make sure that the following holes are closed or sealed:

On the front plate:

- (1) **Main chamber** opening (8 screws with large O-ring).
- (2) **Front viewing window** (4 screws with O-ring).
- (3) **Syringe/thermistor hole** (threaded connector with O-ring).

On the Chamber:

- (4) Vapor Pressure or **VP Port** on left side (insert **VP bath** or plug with O-ring).
- (5) **Electric port** on right side (insert LEMO connector receptacle with O-ring).
- (6) Two **micrometer** ports on top (both should be O-ring sealed).
- (7) The **air hole** on the left side should be open (insert filter and luer plug as shown in Fig. 58C).
- (8) The **liquid port** on the right side should be open for filling (insert liquid feed or filter).
- (9) Lower window for incoming light: tighten O-ring against silica window.

The chamber may be filled with liquid or purged with inert (e.g., nitrogen) gas via the **liquid port**. Fill or purge with the **chamber** either in the horizontal (resting) position or by tilting it about the **groove** on the **base plate** that runs between the two leg screws (see Fig. 65A). Tilting the chamber enables the rising liquid meniscus to sweep rapidly across the two surfaces *at an angle* which avoids air bubbles and contaminants becoming trapped between or on the surfaces. After tilt filling with liquid, plug both the **liquid** and **air ports**, and bolt the **chamber** back on the **base**. Note the liquid level on the graduated scale on the viewing **window**.

The **Optics Stand** (Fig. 57) arrives fully assembled and requires no maintenance and its use is fairly self-explanatory. Place the **Optics Stand** as shown in Figs 1 and 4, and connect the cable to the back of the **control box**. Fine focusing and the prism turntable angle can be controlled from the front panel via the two 'momentary' switches. Familiarize yourself with the following controls, which are self-explanatory (see demonstration video):

Coarse vertical adjusting stage (just above the base).
Vertical stop with lock nut.
Rotation clamp with lock nut.
Main clamp (with lever locking arm).
Left-right adjusting stage with lock nut.
Fine focusing control micrometer (manual or with belt for FOCUS motor drive).
Prism turntable rotation control gear wheel (manual or with PRISM motor drive).
Prism tilting thumb-screw (manual-control).

The standard objective fitted at the end of the optics tube is a modified Ealing Electro-Optics X5 objective. If a higher image magnification is required, a X10 objective (supplied) can be used instead.

Before using the apparatus, you may wish to insert the two **heaters** (Fig. 66) into the lower sides of the chamber. These, too, should be connected to the back of the **control box**.

Insert a small O-ring into each threaded hole (e.g., the **air hole**) before inserting a Kel-F connectors.

USING THE SFA AND ITS ATTACHMENTS

(Refer to this manual and videos for more details)

Control Box / console

Connect the cables provided and familiarize yourself with the various controls: the main power switch, the dimming panel lights control, the variable speed motorized distance control and direction reversing switch (Motor 1), the piezo control (coarse and fine, and direction reversing switch), the prism control, the focus control, the heater, and (when using the friction device) the sliding speed control (Motor 2). Remember to ground/earth the SFA through the cable which should be connected to the left front of the base plate.

Testing a new or newly cleaned apparatus

After an assembly of a newly cleaned and passivated apparatus, with some of the old O-rings replaced, the chamber may be filled with clean ethanol to about three quarters of the way up the front window. Various tests and calibrations could be done at this stage: You may calibrate the liquid volume of your assembled chamber by filling/injecting up to a particular level, as measured from the engraved calibration lines on the front the window, and noting the volume injected. Clamp plain glass disk above piezo entrance hole and cover Motor 1 hole with steel clamp (both parts supplied). Tighten all screws, O-rings and luer fittings. Test for leaks by leaving overnight and noting if the level has dropped; if so, then some ethanol must have evaporated out through a small hole somewhere, in which case you should further tighten all the seals. The apparatus can now be left as it is until it is used.

Filling the SFA chamber with liquid

When filling the chamber with surfaces in them, tilt clockwise with the right lower edge inside the groove there. This will ensure that the rising liquid meniscus passes the surfaces quickly and at an angle rather than horizontally, which can cause contaminants to be deposited and air bubbles to be trapped between the two surfaces.

Friction device attachment

Figure 68A shows the Friction Device attachment, which can be used with the standard normal force-measuring **Spring Mount** (Fig. 68B) or with the **Bimorph Slider** (Fig. 69B). Refer to this manual for further information on the assembly, specifications and operation of the **Friction device**, which also apply to the SFA 2000 device. If the Friction Device strain gauges are going to be exposed to water vapor, it is recommended to first coat their surfaces, and all the wiring connections, with a suitable Humiseal™ coating. This usually increases the friction-force-measuring spring stiffness by 10-15% and reduces the force-measuring sensitivity of the device by a similar amount.

Earth loops / ground loops

Electrical noise can be picked up when making sensitive measurements of weak currents or voltages, as occurs during friction experiments using the strain gauges of the Friction Device. When wiring up the control box and other instruments to the apparatus, one must never earth the apparatus in more than one place or else one is liable to pick up electric noise from "earth loops" or "ground loops" (you may read up on this important phenomenon in any electrical engineering handbook). The earthing contact for the apparatus is a small hole on the front left of the base plate, which should be used as the common terminal for connecting the apparatus and all electric units requiring a ground terminal (piezos, bimorphs, motors, etc.). All bimorphs should have their earthed sides connected to the steel wall of the apparatus and not independently through the outer shield of its coaxial cable.

However, if a power supplier or amplifier is already grounded in such a way that the apparatus is grounded through the cable connecting the supply to the SFA chamber, as could happen with the piezo coax cable, then the apparatus should NOT be separately grounded (since it is already grounded by through this connection). However, do check that the outer surface of the Piezo Mount is indeed earthed through its electric connection to the amplifier you use.

Bimorph slider attachment

Figure 69A shows the **Bimorph Slider** attachment (Fig. 69B shows it together with the **Friction Device**). Because the SFA 2000 Bimorph Slider is about twice as long as the SFA 3 slider, it has a much larger range of travel per volt applied across the conducting electrode surfaces. To compensate for the decreased stiffness of the longer bimorphs, the SFA 2000 slider assembly has two bimorphs at each side, instead of one, and a further three can be added to each side to increase the stiffness even more, if needed. Lateral motion should be about 5-10 $\mu\text{m}/\text{V}$ or about 1 mm per 100 V pk-pk. However, since bimorphs become increasingly non-linear at voltages exceeding 40 V (when deviations from linearity begin to exceed 1%), some calibration of the bimorphs is recommended if the applied displacements are large and need to be known to high accuracy. Refer to the manual for further information and references on the assembly and operation of this attachment. Note, too, that bimorphs can be used in liquids or 'under water' after suitably coating their surfaces, and all the wiring connections, with a suitable coating (ask SurForce LLC for details). This usually increases their stiffness by 10-15% and reduces their sensitivity to movement by a similar amount.

Bimorph vibrator attachment

Figure 60 shows the bimorph vibrator attachment which can be assembled in a number of ways and which can also be used for mounting other fixtures, such as fixed force-measuring springs of different lengths from the standard length. Refer to the manual for further information and literature references on the assembly, operation and specifications of the **Bimorph Vibrator** for dynamic normal force measurements, most of which also apply to the SFA 3. Note, that Vibrator bimorphs can also be used in liquids or 'under water' after suitably coating their surfaces, and all the wiring connections, with a

suitable coating (ask SurForce LLC for details). This usually increases their stiffness by 10-15% and reduces their sensitivity to movement by a similar amount.

MAINTENANCE AND CLEANING

Cleaning of fully disassembled parts before full assembly

The following describes the recommended cleaning procedure of individual parts. All cleaning and drying should be done in a clean air, dust-free atmosphere, e.g., in a laminar flow cabinet.

First, thoroughly clean all glassware and tools (glass beakers, stainless-steel forceps, etc.) with clean ethanol (absolute alcohol). Carefully place all non-electric, non-piezo parts into ethanol-filled glass beakers. The larger parts may all be placed into the 15 cm diameter flat bottomed beaker. The smaller parts, including small screws and O-rings, should be placed into well-marked smaller beakers. You may wish to identify different beakers for the small parts, otherwise you may confuse different screws and O-rings that look similar. Use Teflon-coated tweezers to pick up the parts and carefully place (not drop) them into the beakers. When handling the parts, be particularly careful not to scratch any of the smooth polished surfaces, particularly the O-ring grooves and sealing surfaces. Teflon O-rings need particular care when being handled.

While still immersed in ethanol, scrub metal parts with a *soft* chemically inert brush (fine toothbrush type). Use the miniature pipe-cleaning type brushes to clean inside screw holes. Note that vigorous scrubbing should be avoided since this will remove the protection afforded by the passivation layer causing possible contamination by Cr³⁺ leaching. One by one, remove parts from beaker, squirt ethanol from a hand-held ‘ethanol gun’ directly onto all sides and into holes of each part. Direct the ethanol jet outwards, being careful to ensure that the reflected ethanol spray does not land inside the laminar-flow cabinet or on surfaces that need to remain clean. When all sides of a part have been squirted, place the part in a second ethanol-filled beaker. Cover the beakers, then cover everything with a transparent glass globe (Fig. 74) and leave to ‘soak’ until ready for assembly.

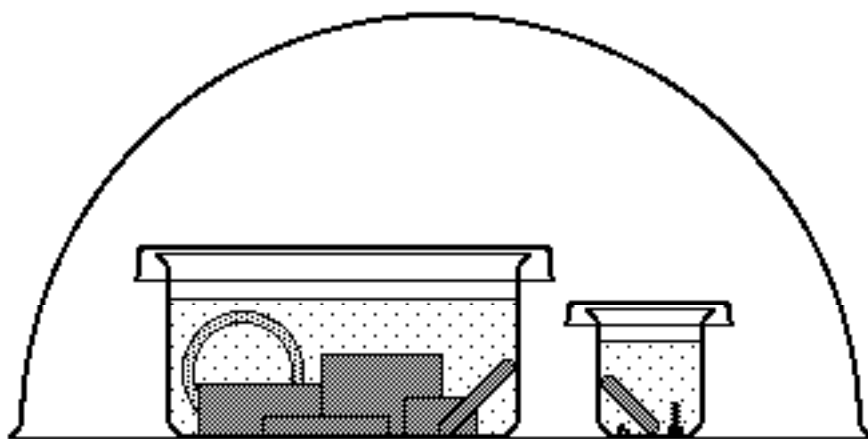


Figure 74. Soaking of metal, glass and Teflon parts in ethanol prior to assembly or between experiments. Round transparent perspex (plexi-glass) DOMES or large beakers are readily available from a number of suppliers (see Table I).

Prior to assembly, remove each part from the beakers, rapidly blow-drying (especially the small holes and threads) with a nitrogen jet as they are taken out. Direct the nitrogen jet outwards, being careful not to blow away small parts. Note: blow drying is essential; if apparatus parts are simply left to dry by allowing the ethanol to evaporate, only the ethanol is removed leaving behind undesirable contaminants.

By blowing the surfaces dry with a pressurized N₂-gun both the ethanol and contaminants are swept away quickly (the pressure rinser by Gelman is recommended; plastic squirt bottles are not since they suck in air contaminants continuously as they are used). Place dry parts on a clean stainless-steel surface or clean Teflon-coated paper sheet inside the laminar flow-cabinet. When all the parts (or units) have been cleaned and dried, proceed with the assembly.

Cleaning between experiments (requiring no disassembly)

The following describes the recommended cleaning procedure between experiments when full disassembly is not required, for example, during a series of experiments using similar liquids. In most cases, it is only necessary to rinse the apparatus a few times with ethanol: each time filling the apparatus then draining, aspirating and blow-drying, following the instructions given in the above paragraphs. For a more thorough cleaning, especially after experiments with polymer and surfactant solutions, a preliminary light scrubbing with soft brushes in ethanol or chloroform (CHCl₃) is recommended followed by soaking in chloroform, depending on the polymer (see above). When all units have been cleaned and dried, proceed with the next experiment (described elsewhere in this manual). Alternatively, fill the chamber with clean ethanol, close the apparatus and all outlets (using the large glass disk instead of the piezo mount, and the rectangular two-hole clamp instead of the motorized micrometer), and leave until required.

Periodic passivation of stainless steel parts

All internal steel parts have already been passivated in 30% conc. HNO₃ and/or electropolished. Passivation of those steel parts whose surfaces come into contact with the experimental solution is recommended every 12 months or more often if experiments routinely involve strong aqueous salt solutions, especially chlorides, or if the internal surfaces have become scratched. To passivate, immerse the stainless steel parts (but *not* any protruding electrical connections such as the piezo crystal) in 30% HNO₃ at 60°C for 30 minutes (note: Kel-F is inert to conc. HNO₃), then remove all excess acid by thorough washing in clean distilled water.

Degreasing, deburring and sonication

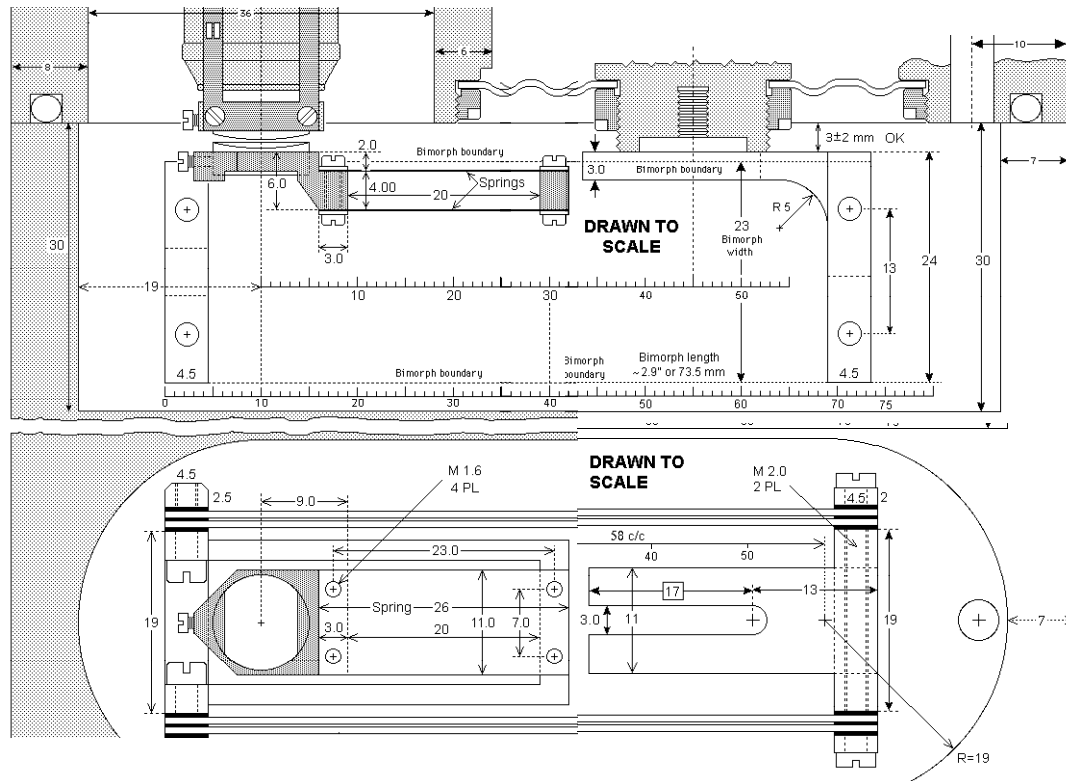
If some parts have become visibly dirty or greasy, for example, if a part has been sent to the machine shop, a degreasing in acetone is recommended. Use small scrubbing brushes if necessary, making sure that the bristles are not dissolved by acetone. This could be followed by sonication, especially if new thread holes have been tapped. All threaded holes and other cavities should have any debris or burr finally removed by air-blasting or squirting ethanol into the holes using an ethanol gun.

Greasing the micrometer threads

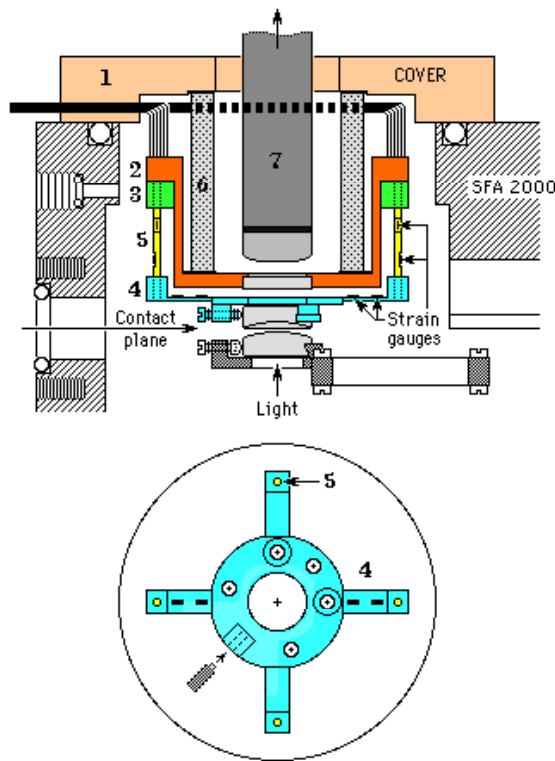
The two micrometers on the Upper Chamber and the one on the Friction Device do not come into contact with the internal chamber and so can be greased with any suitable low VP grease. For greasing the micrometers of motors 1 or 2, remove the motor housing by unscrewing it (you may have to loosen the limit switch board first). Note the position of the protruding shaft and then loosen the two set screws on the housing and gently unscrew the threaded micrometer shaft until it comes away from the housing. Clean the thread by rubbing with acetone or alcohol. Rub some grease between your thumb and index finger, then rub your fingers round the thread only. Reinsert shaft and lock back into place in exactly the same position as before. For greasing the Differential Micrometer, turn the top knob all the way until the small part comes out. Grease both threads separately. Don't over grease and don't use force in any of the above operations. Replace with the inside part in the 'correct' position.

SOME NEW, RECENTLY INTRODUCED ATTACHMENTS OR MODIFICATIONS

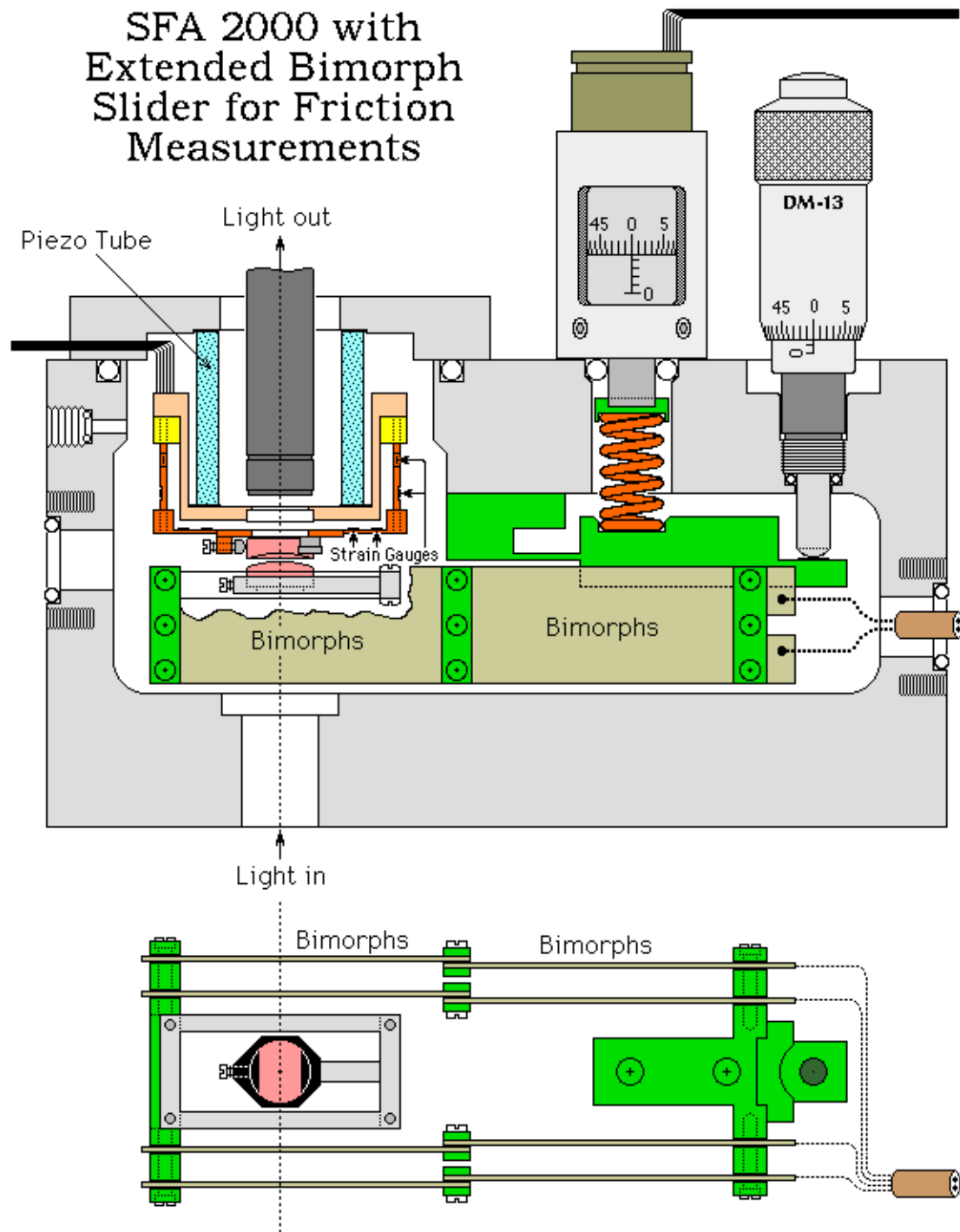
Extended bimorph for the SFA 3



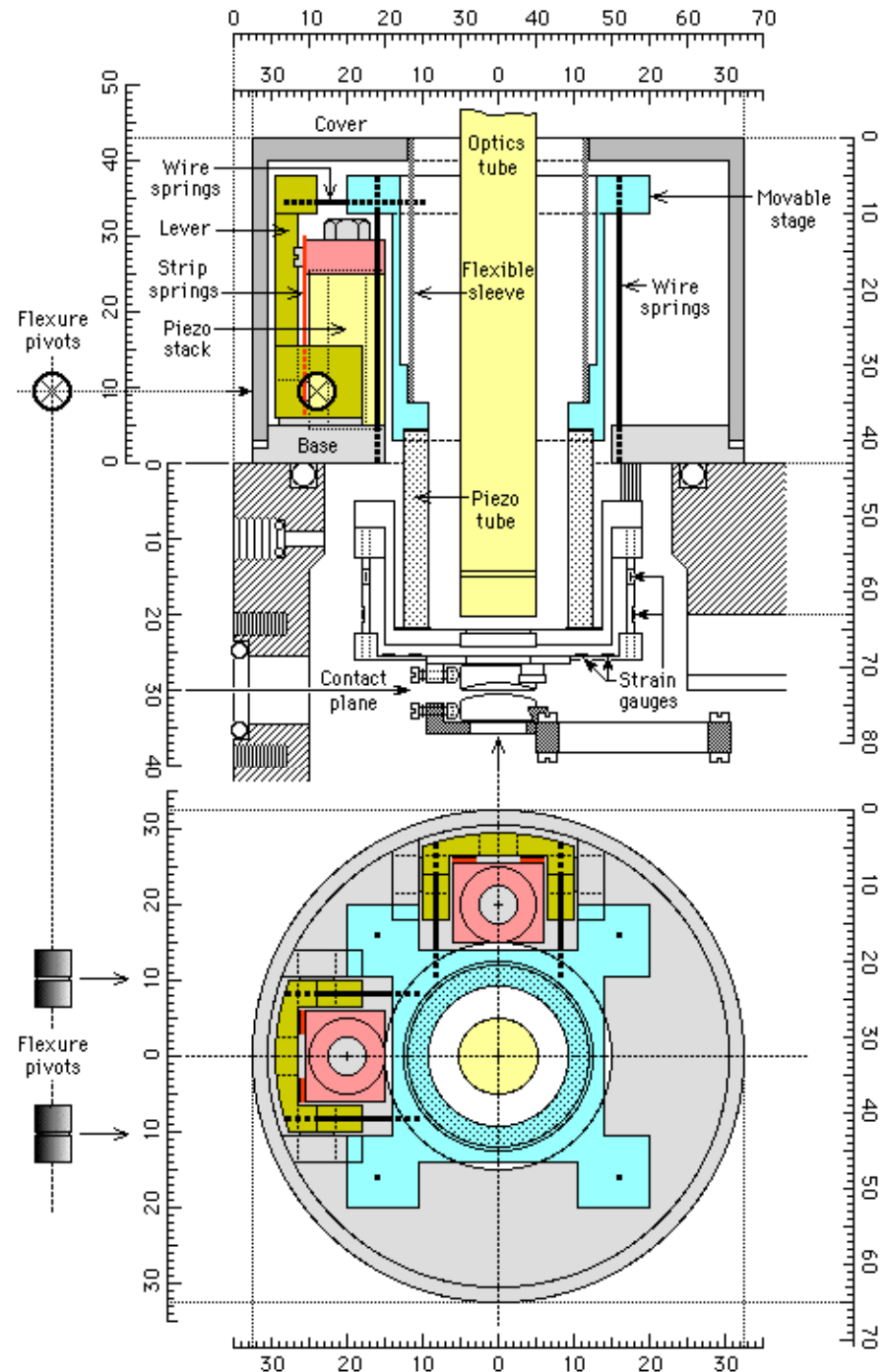
XYZ (3D) displacement sensor



SFA 2000 with extended bimorph slider and XYZ displacement sensor



SFA 2000 with both XYZ (3D) scanner and displacement sensor



Extended bimorph sliders for the SFA 3 and SFA 2000

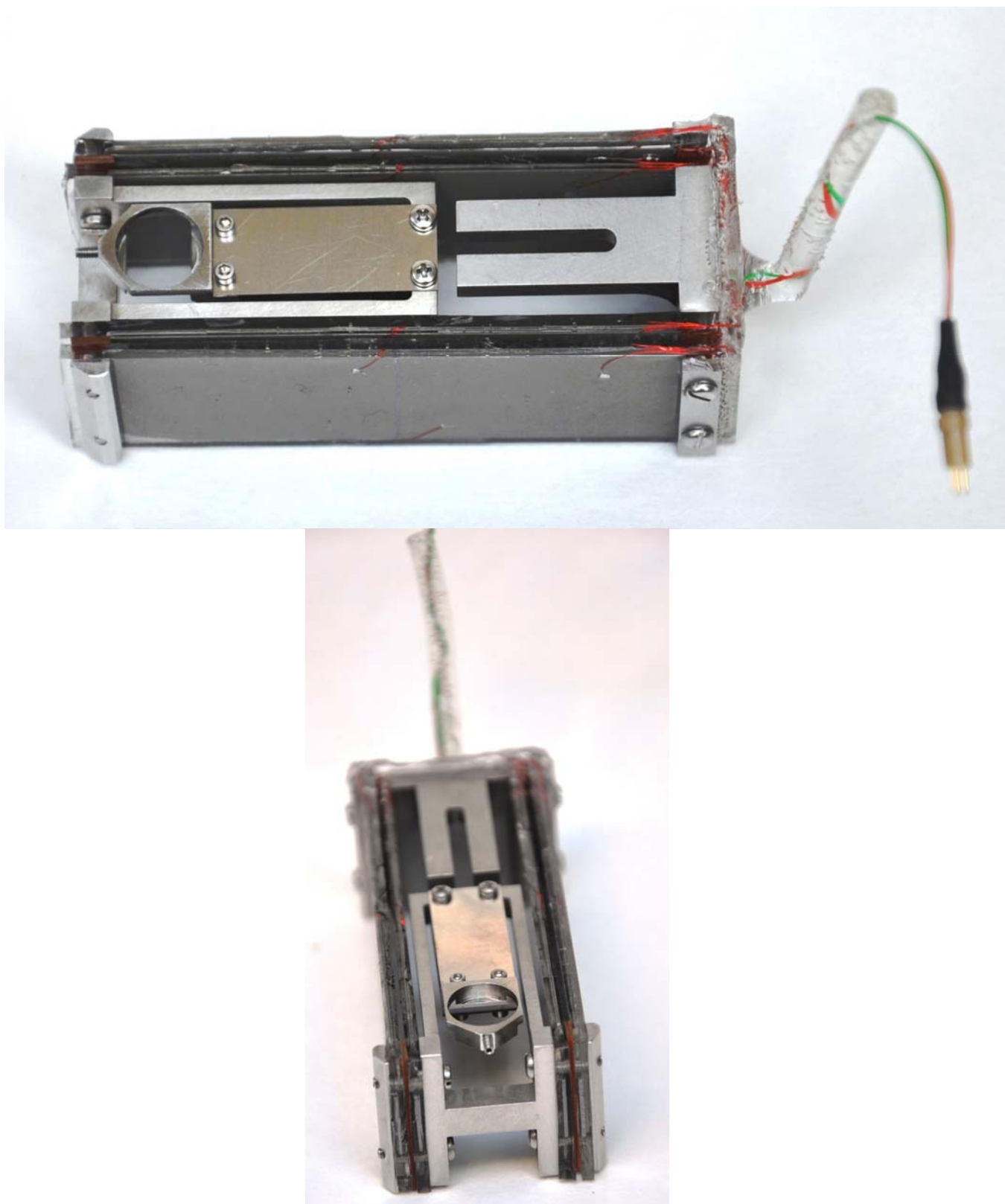


Figure 79

See SurForce LLC website for more of the latest updates.